Methods in Molecular Biology™

VOLUME 199

Liposome Methods and Protocols

Edited by

Subhash C. Basu

Manju Basu

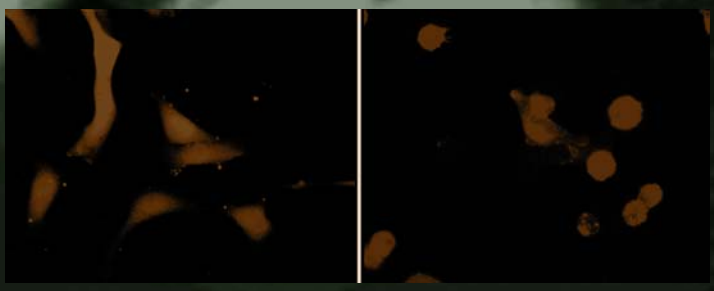

HUMANA PRESS

1

Preparation, Isolation, and Characterization of Liposomes Containing Natural and Synthetic Lipids

Subroto Chatterjee and Dipak K. Banerjee

1. Introduction

The specificity, homogeneity, and availability of large-batch production of liposomes with natural lipids and synthetic lipids have made them an extremely useful tool for the study of diverse cellular phenomena, as well as in medical applications. In many cases, however, the success of the use of liposomes as drug carriers or vaccines and in gene delivery depends entirely on both their formulation and the method of preparation.

Liposomes are synthetic analogues of natural membranes. Consequently, in view of the fact that the lipid composition of the cell membrane is fixed, the general concept in the preparation of liposomes is to modify combinations of these lipid mixtures (to emulate the natural membrane) in the presence or absence of a variety of bioactive molecules with diverse functions. The methods for the preparation, isolation, and characterization of liposomes are as diverse as the applications of these molecules in health and disease. Accordingly, we feel it is a daunting task to cover each and every method that has been described for preparing liposomes. Thus, in this chapter we have focused on the preparation of three classes of liposomes, namely, the multilamellar vesicles (MLVs), small unilamellar vesicles (SUVs), and large unilamellar vesicles (LUVs). Several excellent books on liposome technology and its application in health and disease ***(1–3)*** have been published over the last decade. Readers are suggested to consult these works to obtain more information on an individual method relevant to the needs of their studies.

From: *Methods in Molecular Biology, vol. 199: Liposome Methods and Protocols*
Edited by: S. Basu and M. Basu © Humana Press Inc., Totowa, NJ

2. Materials

1. Cholesterol is commercially available from several sources, for example, Avanti Polar Lipids (Alabaster, AL), Matreya, Inc. (Pleasant Gap, PA).
2. Dicetylphosphate (DCP) is available from KMK Laboratories (Fairview, NJ), Sigma Chemical Co. (St. Louis, MO), and Pierce Biochemicals, (Milwaukee, WI).
3. Dimyristoyl phosphatidylcholine (DMPC) is available from Avanti Polar Lipids, Sigma Chemical Co., CalBiochem-Behring (San Diego, CA), Pierce Biochemicals, and Matreya, Inc. Several other phospholipids and glycosphingolipids are available commercially in high quality from Matreya, Inc. as well. (*see* **Note 1**).
4. Organic solvents, typically chloroform (JT Baker, Phillipsburg, NJ), are used in the solubilization of a variety of lipids. However, often a small amount of methanol is also required to solubilize gangliosides and relatively polar lipids, such as phospholipids. Both chloroform and methanol are available commercially. Because chloroform can deteriorate on storage for more than 1–3 mo, it is a routine practice in many laboratories to redistill chloroform before use in a variety of biochemical experiments but in particular in liposome preparation. Subsequent to distillation, 0.7% ethanol is added as a preservative. Pear-shaped boiling flasks manufactured by Lurex Scientific Inc. (Vineland, NJ) have been recommended by some investigators for use because they have the best shapes for the distillation of organic solvents ***(4)***. Microbeads used for the distillation of solvents are commercially available from Cataphote Division of Ferro Corp. (Cleveland, OH and Jackson, MS).

3. Methods

3.1. Preparation of Multilamellar Liposomes

The strategy for preparation of MLVs is to use well characterized lipids in order to produce well defined liposomes ***(4)***. Equally important is the selection of bilayer components for toxicity and for shelf life optimization. The lipids normally used are the unsaturated egg phosphatidylcholine (PC), phosphatidic acid (PA), phosphatidylglycerol (PG), and the saturated lipids DMPC, dipalmitoyl phosphatidylcholine (DPPC), dipalmitoyl phosphatidic acid (DPPA), and dipalmitoyl phosphatidylglycerol (DMPG). Stearylamine is used when cationic liposomes are preferred; and natural acidic lipids, such as phosphatidylserine (PS), PG, phosphatidylinositol (PI), PA, and cardiolipin (CL) are added when anionic liposomes are desired, while cholesterol is often included to stabilize the bilayer. Small amounts of antioxidants such as α-tocopherol or β-hydroxytoluidine (BHT) are included when polyunsaturated neutral lipids are used. A general protocol to prepare MLV is as follows:

1. Prepare a suitable solution of the lipid component in a pear-shaped flask (lipid concentrations between 5 and 50 m*M* in either chloroform or in chloroform–

methanol (3 : 1, v/v), and filter the mixture to remove minor insoluble components or ultrafilter to reduce or eliminate pyrogens.

2. Employing a rotary evaporator, remove the solvent, while maintaining a temperature of ~40°C in a water bath under negative pressure (*see* **Note 2**). Other methods of drying include spray drying and lyophilization ***(5)***. Traces of organic solvents are removed employing a vacuum pump, normally overnight at pressures below milliTorr (~0.1 Pa). Alternatively, the sample may be dried under a very low vacuum (<50 μmol/mg) for 1–2 h in a dessicator with drierite™ (Fisher Scientific, Malvern, PA).
3. Subsequent to drying, 100 μL of 0.5 mm glass beads are added to the 10-mL flask containing the dried lipid mixture, and hydration fluid (0.308 *M* glucose), which is equal to the final volume of the liposome suspension, is added. Typically, the volume of hydration fluid used is determined by the amount of liposomal phospholipid and is usually in millimolars with respect to the hydration fluid ***(1)***.
4. Vortex mixing the flask for 1–2 min causes all of the dried lipid from the flask to be dispensed into the hydration fluid. Alternative hydration mediums are distilled water, buffer solution, saline, or nonelectrolytes such as a sugar solution. For an in vivo preparation, physiological osmolality (290 mosmol/kg) is recommended and can be achieved using 0.6% saline, 5% dextrose, or 10% sucrose solution. MLVs of tens of micrometers to several tenths of a micrometer are spontaneously formed when an excess volume of aqueous buffer is added to the dry lipid and the flask is agitated.
5. The "dry" lipid mixture is then hydrated in an aqueous medium containing buffers, salts, chelating agents, and the drug to be entrapped (*see* **Note 3**).

3.2. Preparation of Small Unilamellar Liposomes

High-energy sonic fragmentation processes were introduced in the early 1960s ***(6)*** Refinements of these procedures using a high-pressure homogenization device followed ***(7,8)***. SUVs are prepared by the following methodology to disperse phospholipids in water to form optically clear suspensions.

3.2.1. Sonication

Methods for the preparation of sonicated SUVs have been reviewed in detail by Bangham and others ***(8)***. Typically the MLV dispersion is placed in test tubes and sonicated either in a bath sonicator or by tip sonication. Normally a 5–10-min sonication procedure (above T_c) is sufficient to prepare SUVs with radii < 50 nm. With some lipids, radii < 20 nm are also possible while some diacyl cationic lipids (including 1-[2-(oleoyloxy)-ethyl-2-oleoyl-3-(2-hydroxyethyl) imidarolinium chloride (DOIC) and dioctadecylamidoglycylspermine (DOGS) can even form micelles. Dioctadecyl diammonium bromide (DOBAD) neutral lipid liposomes cannot be sized <130 nm (*see* **Note 4**).

3.2.2. Extrusion

Prefiltering the LMV solution through a filter with pores ~1 μm is followed by prefiltering the solution five times through 0.4- and 0.2-μm pores. This is followed by 5–10 extrusions through a filter with a pore size of 100 nm. Allowing the formation of LUVs with diameters slightly above presizes (~110–120 nm). If smaller vesicles are desired, continued filtering through 80- and 50-nm pores is needed. Extrusion through smaller pores (30 nm) or in the case of some more rigid bilayers, 50 nm, does not reduce the size further but rather increases it owing to the imposition of too high a curvature to vesicles. The extrusion method yields the best vesicles with respect to the homogeneity of size distribution and to control the size distribution of vesicles, especially for larger (100–500 nm) diameters.

3.2.3. Homogenization

MLVs are dispersed by forcing them through a small hole at 20,000 psi so they collide into a wall, a small ball, or the tip of the pyramid. The advantages of this method are its simplicity for scaleup, large capacity, and speed (e.g., from 10 mL to hundreds of liters in 1 h). The disadvantages are possible sample degradation and contamination with very small and some large lipid particles. Normally, three to five passages through the interaction chamber are enough to achieve minimal size (*see* **Note 5**).

The following two methods produce relatively uniform unilamellar vesicles with encapsulation efficiencies of 20–45%. Dissolve the lipid mixture solution in diethyl ether and inject it into an aqueous solution of the material to be encapsulated at 55–65°C or under reduced pressure ***(9)***. The vaporization of ether leads to the formation of single-layer vesicles of diameters ranging from 50 to 200 nm. Liposomes with buffered pH were produced to study proton-hydroxyl flux across lipid membranes following this procedure.

Naturally occurring plant lipids in a composition of PC–PA (9 : 1 molar ratio) have also been used (*see* **Note 6**). Another method involves using a fluorocarbon such as Freon 21 (CHFC12) with a boiling point at 9°C at atmospheric pressure that was used to overcome the hazards of diethyl ether. Large unilamellar liposomes are formed when Freon 21 lipid mixtures are injected into an aqueous medium at 37°C ***(10)***.

The principle in this procedure is somewhat different. Here the solvent (ethanol, glycerin, and polyglycols) containing the lipid is diluted by an excess amount of the aqueous phase. As the solvent concentration is reduced, liposomes form. Lipids dissolved in ethanol are rapidly injected through a fine needle into a buffer solution and SUVs are formed instantaneously. The

procedure is simple, rapid, and gentle to both lipids and the material to be entrapped (*see* **Note 7**).

SUVs can be formed from mixed dispersions of PC and PA provided that the molar proportion of PC is 70% or less. The liposomes are formed when the phospholipid mixtures are dispersed either directly in sodium hydroxide at pH ~10 or in water, the pH of which is then rapidly (~1 s) increased ***(11)***. Exposure of the phospholipids to a high pH level is short (<2 min) and during this time no degradation is detectable by thin-layer chromatography (TLC). The size of such liposomes is dependent on the acidic phospholipid used, the molar ratio of acidic phospholipid to PC, the ratio of counter ion to acidic phospholipid in the organic phase, and the rate and extent of the pH change. The technique, however, is limited to charged phospholipids and mixtures of neutral phospholipids.

3.3. Preparation of Large Unilamellar Liposomes

Large unilamellar liposomes refer to vesicles > 100 nm in diameter bounded to a single bilayer membrane. LUVs provide a number of advantages compared to MLVs, including high encapsulation of water-soluble drugs, economy of lipid, and reproducible drug release rates. These liposomes are the most difficult type of liposomes to produce; however, a number of techniques for producing LUVs such as freeze–thaw cycling, slow swelling in nonelectrolytes, dehydration followed by rehydration, and the dilution or dialysis of lipids have been reported. The two primary methods used are one involving detergent dialysis, while the other uses the formation of a water-in-oil emulsion.

Detergents commonly used for this purpose exhibit a relatively high critical micelle concentration (CMC) such as bile salts and octylglucoside. During dialysis, when the detergent is removed, the micelles become progressively richer in phospholipid levels and finally coalesce to form closed, single-bilayer vesicles. Liposomes (100 nm in diameter) are formed within a few hours (*see* **Note 8**).

Uniform single-layered phospholipid vesicles of 100 nm are formed when sonicated, small phospholipid vesicles or dry phospholipid films are mixed with deoxycholate at a molar ratio of 1 : 2. Subsequently, the detergent is removed by passing over a Sephadex G-25 column ***(12)***. This procedure separates 100-nm vesicles from small sonicated vesicles. The phospholipid solution is layered onto a sucrose gradient and subjected to high-speed centrifugation. The SUVs form as a sediment, leaving behind detergent in the supernatant layer.

This procedure involves the removal of a nonionic detergent, Triton X-100, from detergent/phospholipid miceller suspensions. Bio-Beads SM-2 have the

ability to absorb Triton X-100 rapidly and selectively. Following absorption of the detergent, the beads are removed by filtration. The final liposome size depends on the conditions used including lipid composition, buffer composition, temperature, and, most importantly, the amount and the efficacy of the detergent-binding capacity of the beads.

Another procedure to prepare LUVs employs water-in-oil emulsions of phospholipids and buffer in excess. This method is particularly useful to encapsulate a large amount of a water-soluble drug ***(13,14)***. Two phases are usually emulsified by sonication. Removal of the organic solvent under the vacuum causes the phospholipid-coated droplets to coalesce and eventually form a viscous gel. The removal of the final traces of solvent under a high vacuum or mechanical disruption results in the collapse of the gel into a smooth suspension of LUVs.

To prepare reverse phase evaporation vesicle (REV)-type liposomes, the phospholipids are first dissolved in either diethyl ether isopropyl ether or mixtures of two solvents such as isopropyl ether and chloroform. Emulsification is most easily accomplished if the density of the organic phase is ~1. The aqueous phase containing the material to be entrapped is added directly to the phospholipid–solvent mixture, forming a two-phase system. The ratio of aqueous phase to organic phase is maintained as 1:3 for ether and 1:6 for isopropyl ether–chloroform mixtures. The two phases are sonicated for a few minutes, forming a water-in-oil emulsion, and the organic phase is carefully removed on a rotary evaporator at 20–30°C. The removal of the last traces of solvent transforms the gel into large unilamellar liposomes (*see* **Note 9**).

3.4. Characterization of Liposomes

Liposomes prepared by one of the preceding methods must be characterized. The most important parameters of liposome characterization include visual appearance, turbidity, size distribution, lamellarity, concentration, composition, presence of degradation products, and stability.

3.4.1 Visual Appearance

Liposome suspensions can range from translucent to milky, depending on the composition and particle size. If the turbidity has a bluish shade this means that particles in the sample are homogeneous; a flat, gray color indicates the presence of a nonliposomal dispersion and is most likely a disperse inverse hexagonal phase or dispersed microcrystallites. An optical microscope (phase contrast) can detect liposomes > 0.3 μm and contamination with larger particles. A polarizing microscope can reveal lamellarity of liposomes: LMVs are birefringent and display a Maltese cross. A waterlike surface tension, slight

foaming, and quick rising of bubbles are characteristic of liposome solutions. Slow rising of the "entrapped" bubbles, becoming entrapped easily on shaking, or not dewetting the glass quickly are indications of nonliposomal lipid dispersions due to high surface hydrophobicity. Most often these are dispersions of hexagonal II phases. Due to high surface charges, nonliposomal and nonbilayered lipid dispersions or suspensions can be very stable.

3.4.2. Determination of Liposomal Size Distribution

Size distribution is normally measured by dynamic light scattering. This method is reliable for liposomes with relatively homogeneous size distribution. A simple but powerful method is gel exclusion chromatography, in which a truly hydrodynamic radius can be detected. Sephacryl-S1000 can separate liposomes in the size range of 30–300 nm. Sepharose-4B and -2B columns (Amersham, Pharmacia, Piscataway, NJ) can separate SUV from micelles. These columns with positively charged colloidal particles are difficult to operate because of possible electrostatic interactions with the medium (which can have a slightly negative charge). The addition of salt can cause aggregation of the sample and clogging of the column. Many investigators use electron microscopy to measure liposome size. The most widely used methods are negative staining and freeze-fracturing; they are prone to artifacts owing to the changes during sample preparation as well as for geometric reasons. Cryoelectron microscopy, in which a sample is frozen and directly observed in the electron beam without any staining, shadowing, or replica preparation, is much more reliable.

3.4.3. Determination of Lamillarity

The lamellarity of liposomes is measured by electron microscopy or by spectroscopic techniques. Most frequently the nuclear magnetic resonance (NMR) (^{32}P-NMR or ^{19}F-NMR) spectrum of liposomes is recorded with and without the addition of a paramagnetic agent that shifts or bleaches the signal of the observed nuclei on the outer surface of liposomes. Encapsulation efficiency is measured by encapsulating a hydrophilic marker (i.e., radioactive sugar, ion, fluorescent dye, etc.). Electron spin resonance methods allow the determination of the internal volume of preformed vesicles. The surface potential is measured via ζ-potential. Particles migrate in an electric field, and their movement is detected either by the naked eye through a microscope or by laser (Doppler effect). Osmolality is normally checked by vapor pressure osmometer while pH is checked with a standard pH meter. Phase transition and phase separations are measured by fluorescence pH indicators, NMR, fluorescence methods, Raman spectroscopy, and electron spin resonance ***(1–3)***.

3.4.4. Determination of the Lipid Content of Liposomes

The measurement of lipid levels in liposomes is one of the stringent requirements in the characterization of liposomes. **Figure 1** is a summary of the lipid isolation procedure used in our laboratory over the last 2½ decades. The volumes of organic solvents described in **Fig. 1** are for ~1–5 mg of lipid present either in liposomes or in tissues. Various modifications of this method can be made proportionately depending on the anticipated lipid content of the liposome. Further details of these procedures are described in several of the references ***(15,16)***. Typically the liposomes and/or tissue are lyophilized into a powder in a 30-mL Pyrex glass tube. Ten milliliters of chloroform–methanol (2 : 1 v/v) is added and a vigorous extraction in a vortex mixer is carried out. The extract is filtered through a glass fiber filter (Fisher Scientific Products). If any residual protein is subsequently collected on the filter, it is subject to further extraction with another round of 10 mL of chloroform–methanol (2 : 1 v/v) and then with 5 mL of chloroform–methanol (1 : 2 vv). The samples are filtered and the pooled filtrate is then dried under nitrogen at 40°C. The dried lipid sample is then solubilized in 20 mL of chloroform–methanol (2 : 1 v/v) Next, 5 mL of 0.1 *M* KCl is added to the lipid extract, mixed vigorously, and allowed to settle for about 10 min at room temperature. It is then subjected to centrifugation (1500 rpm for 10 min). The upper phase, which contains gangliosides, protein, amino acids, peptides, etc. is saved, and the lower phase is subjected to further partitioning with 5 mL of theoretical upper phase (chloroform, methanol–KCl, 3 : 47 : 48 by vol), mixed, centrifuged, and the upper phase collected. Finally, to the lower phase 5 mL of chloroform–methanol–water (3 : 48 : 47 by vol) is added, vortex-mixed, centrifuged, and the upper phase is withdrawn. The pooled upper phase is dried in a nitrogen atmosphere, resuspended in 2–5 mL of water and subjected to dialysis for 48 h at 4°C against 4 L of distilled water with a change of water every 24 h. Finally, the dialyzed sample is lyophilized (fraction 2 in **Fig. 1**). It consists mostly of gangliosides and is subjected to TLC analyses on HPTLC (Kieselgel-60) plates (EM Science Gibbstown, NJ) employing chloroform–methanol–water (60 : 40 : 9 by vol) containing 0.02% $CaCl_2 \bullet 2H_2O$). Gangliosides are revealed with a resorcinol–HCl reagent ***(16,17)***.

The lower phase is dried in nitrogen, resuspended in 1 mL of chloroform, vortex-mixed vigorously, and applied on a prep-Sep column (Fisher Scientific, Inc.). After the absorption of the lipid extract it is allowed to settle for about 5 min at room temperature. It is then eluted consecutively with 10 mL each of chloroform to collect the neutral lipids, acetone–methanol (9 : 1 v/v) to collect neutral glycolipids, and finally with methanol to collect the phospholipids. The neutral lipids are separated into individual molecular species by TLC on Silica

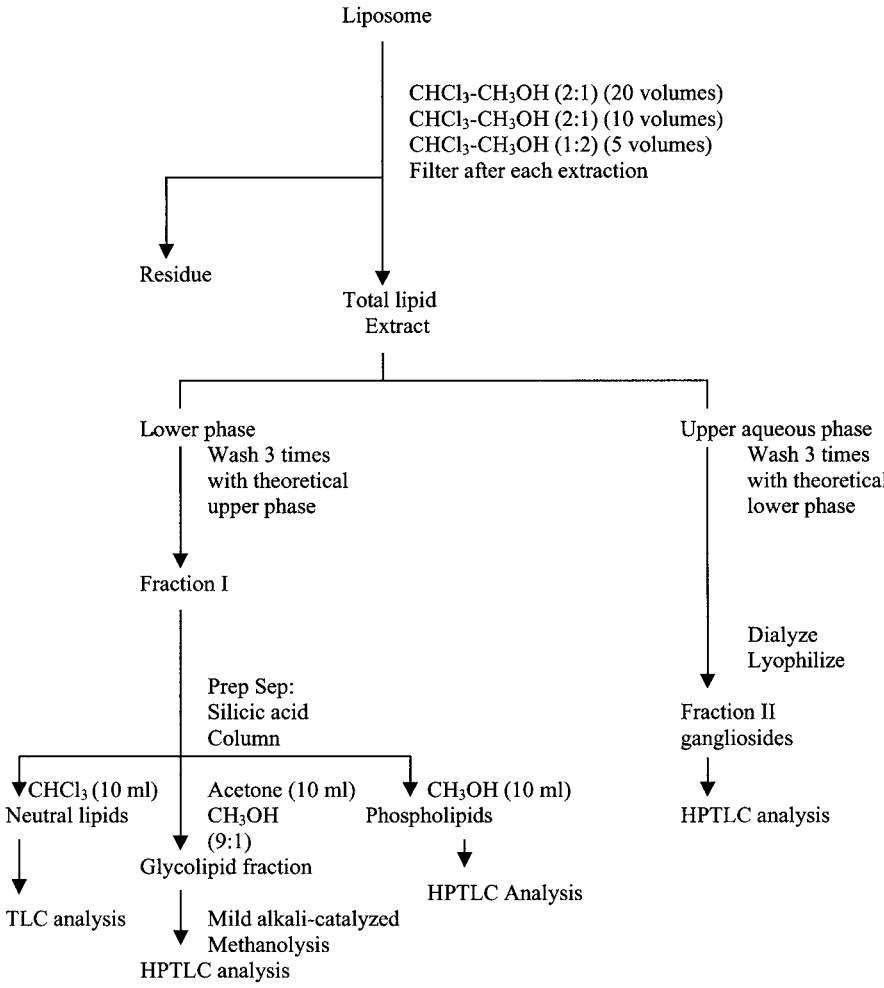

Fig. 1. Summary of lipid isolation procedure.

gel-G coated plates (Fisher Scientific) with heptane–ethyl ether–acetic acid (85 : 15 : 1 by vol) as a developing solvent. The plate is then dried in the air and exposed to iodine vapors and/or sprayed with 50% sulfuric acid in ethanol and heated to 180°C in an oven. The stained bands are then subjected to densitometry scanning and quantitation. Appropriate standard solutions of cholesterol, cholesteryl esters, and triglycerides (10 μg each) are simultaneously applied on the plate. The acetone–methanol fractions containing mostly neutral glycolipids are subjected to mild alkali-catalyzed methanolysis to remove unwanted phospholipids and then subjected to HPTLC analysis employing

chloroform–methanol–water (100:42:6 by vol) as the developing solvent. Glycolipids are detected and quantified by densitometry as described previously. The phospholipid fraction is subjected to TLC analysis on Silica gel-H coated plates, employing chloroform–methanol–formic acid (65:25:4 by vol) as the developing solvent. These plates are subsequently sprayed with molydenium phosphoric acid reagent or exposed to iodine vapors and quantified (*see* **Note 10**).

3.4.5. Liposome Stability

Liposome stability is a complex issue, and consists of physical, chemical, and biological stability. In the pharmaceutical industry and in drug delivery, shelf-life stability is also important. Physical stability indicates mostly the constancy of the size and the ratio of lipid to active agent. The cationic liposomes can be stable at 4°C for a long period of time, if properly sterilized.

Chemical instability primarily indicates hydrolysis and oxidation of lipids. Hydrolysis detaches hydrophobic chains of ester bonds (–CO–O–C–). Oxidation is more likely here owing to the presence of unsaturated chains, but an antioxidant such as BHT can protect them. Biological stability of liposomes is rather limited. Cationic liposomes in plasma often exhibit leakage and are prone to aggregation. In vivo stability is even more compromised because of negatively charged surfaces, colloidal particles in biological systems, and certain serum components. For example, high-density lipoproteins (HDLs) are responsible for the destabilization of liposomes prior to interaction with circulating phagocytic cells such as monocytes ***(18,19)***. A plausible mechanism to explain the phenomenon could involve the exchange of lipids on the interaction of liposomes with HDLs ***(20)***. To circumvent this problem the use of positively charged, stable vesicles containing 60% PC, 30% cholesterol, and 10% stearylamine is recommended ***(21)***. Industrial applications of liposomes require shelf-life stability. Highly charged cationic liposomes can be stable in liquid form in the presence of low salt solutions (at optimal pH) and antioxidants. The addition of cryoprecipitants significantly increases the stability freeze-dried liposomes. For freeze–thawing, 5% dextrose is normally sufficient, while for freeze–drying and rehydration 10% sucrose seems to be the optimal cryoprotectant ***(22)***.

4. Notes

1. Previously several of these commercially available lipids were subject to further purification in the laboratories. Some lipids, particularly cholesterol, were subjected to recrystallization to remove the products of oxidation. However, because of the high quality and availability of liposome grade phospholipids from

commercial sources, at present many investigators do not purify these lipids any further. Instead, they directly use them in the preparation of liposomes. Nevertheless, for quality control purposes, assessment of the purity of lipids prior to liposome preparation is desirable and recommended.

2. Note that as dried lipids deteriorate rapidly they must be discarded if not used within 1 wk.
3. Hydration influences the type of liposomes formed (number of layers, size, and entrapped volume). The nature of the dry lipids, its surface area, and its porosity determine the formation of thin to thick film, flaky to fine powder, granular pellets, etc. Other factors influencing the rate of liposome formation and morphology are the rates at which the aqueous phase is added, temperature, agitation, and ionic conditions. Liposomes produced during hydration are heterogeneous in size but can be downsized by extrusion or mechanical fragmentation. The encapsulated drug can also be removed and recovered by centrifugation, dialysis, or diafiltration. Hydration time, conditions of agitation, temperature, and the thickness of the film can result in markedly different preparations of MLVs, in spite of identical lipid concentrations and compositions and volume of suspending aqueous phase. Most cationic lipids contain dioleoyl or dimyristoyl chains and working at room temperature is sufficient. Charged analogues have lower values of T_c than their phospholipid counterparts. The transition temperature of DODAB is 37°C; hydration therefore should be performed at temperatures above the T_c of the most rigid lipid during vigorous mixing, shaking, or stirring, with the recommendation that it last at least 1 h. Often aging (standing overnight) eases downsizing. Highly charged lipids may swell into very viscous gel when hydrated with low ionic strength solutions. The gel can be broken by the addition of salt or by downsizing the sample. With liposomes that contain more than 20–40% neutral lipid, gel normally does not occur. An alternative hydration method is to dissolve the lipids in either ethanol, isopropanol, or propylene glycol, injecting this solution directly into the aqueous phase while stirring vigorously. This step may require additional dialysis or diafiltration to remove organic solvent, but for topical applications these solvents are normally not removed, as they provide sterile protection.

   One of the major drawbacks of thin-film and powder hydration methods is the relatively poor encapsulation efficiency (5–15%) of water-soluble drugs. Papahadjopoulus and co-workers ***(22)*** have developed a method that begins with a two-phase system consisting of equal volumes of petroleum ether containing a lipid mixture and an aqueous phase. The phases are emulsified by vigorous vortex-mixing and the ether phase is removed by passing a stream of nitrogen gas over the emulsion. A similar method was reported by Gruner et al. ***(23)***, except that the diethyl ether was used as the solvent, sonication was used in place of vortex-mixing, and the aqueous phase was reduced to a relatively small proportion in relation to the organic phase. For example, the lipid dissolved in 5 mL of ether, and 0.3 mL of the aqueous phase to be entrapped is added. The resulting MLVs encapsulate up to 40% of the aqueous phase.

4. Bath sonication is preferred because of better temperature control. The sonicator tip can, during direct sonification, also shed titanium particles, which must be removed by centrifugation. Bath sonication requires small sample volumes (1 mL/tube) and is most suitable for samples that do not swell well or are in jelly form. Tip sonication dissipates more energy and the sample size may vary from 1 to 5 mL.
5. Precautions must be taken not to overdo the homogenization procedure without controlling the temperature well. Otherwise, the lipids with unsaturated dioleoyl chains can oxidize and hydrolyze.
6. The method is relatively simple and applicable to a wide variety of lipid mixtures and aqueous solutions. The primary drawbacks are that the organic solvent used may be harmful to certain classes of solute and the method cannot be used to incorporate proteins into liposomes.
7. Unfortunately, the method is restricted to the production of relatively dilute SUVs. If the final concentration of ethanol exceeds 10–20% by volume, the SUVs either will not form, or they will grow in size soon after formation. The removal of residual ethanol by vacuum distillation also poses a problem. Its partial pressure at low residual concentrations is small compared to that of water; therefore, ultrafiltration represents a suitable alternative. The major disadvantage, however, is that some biologically active macromolecules tend to become inactive in the presence of even low amounts of ethanol. Polyhydric alcohols (such as glycerol, propylene glycol, polyglycerol, and ethylene glycol as well as glyceroesters) are claimed to adequately solubilize lipids and have been used as alternative water-miscible solvents to produce liposomes.
8. Shortcomings of the approach include leakage and dilution of drugs during liposome formation, and the high cost, quality control, and difficulty of removing the last traces of the detergent. Additional methods to remove detergent are column chromatography, centrifugation, and the use of Bio-Beads.
9. The principal disadvantage of this method is exposure to organic solvents and mechanical agitation, which leads to the denaturation of some proteins. The high encapsulation provided by the REV method, however, is a real advantage, and with the development of safer systems, most obstacles can be overcome.
10. Although HPTLC analyses of several lipid species have been shown to be quantitative, it is desirable to pursue vigorous quantitative analyses employing gas–liquid chromatography (GLC) and/or HPLC. For example, cholesterol can be quantified by GLC analyses ***(24)*** and neutral glycolipids can be quantified following perbenzolyation and quantitation by HPLC ***(25,26)***. The phospholipids can be quantified by the measurement of inorganic phosphate ***(26)***. A method to quantify gangliosides employing HPLC has also been developed and is recommended for the quantitation of these novel lipids ***(25)***.

References

1. Gregoriadis, G., ed. (1993) *Liposome Technology*, vols. I, II, III, 2nd edit. CRC Press, Boca Roton, FL.

2. Lasic, D. D. and Paphadjopoulus, D., eds. (1998) *Medical Applications of Liposomes*. Elsevier, New York, NY.
3. Lasic, D. D., ed. (1997) *Liposomes in Gene Delivery*. CRC Press, Boca Raton, FL.
4. Alvin, C. R. and Sivartz, G. M., Jr. (1984) *Liposome Techology*, vol. II. CRC Press, Boca Raton, FL, pp. 55–69.
5. Szoda, F. C. and Papahadjopoulos, D. (1981) Liposomes: preparation and characterization, in *Liposomes: From Physical Structure to Therapeutic Application* (Knight, C. G., ed.), Elsevier, Amsterdam, pp. 51–82.
6. Payne, N. L., Browning, I., and Haynes, C. A. (1986) Characterization of Proliposomes. *J. Pharmaceut. Sci.* **75,** 330–333.
7. Saunders, L., Perrin, J., and Gammack, D. B. (1962) Ultrasonic irradiation of some phospholipids sols. *J. Pharmaceut. Pharmacol.* **14,** 567–572.
8. Huang, C. H. (1969) Studies on phosphatidylcholine vesicles. Formation and physical characteristics. *Biochemistry* **8,** 344–351.
9. Bangham, A. D., Hill, M. W., and Miller, G. A. (1974) Preparation and use of liposomes as models of biological membranes, in *Methods in Membrane Biology* (Korn, E. D., ed.), Plenum. Press, New York, pp.1–68.
10. Deamer, D. and Bangham, A. D. (1976) Large volume liposomes by an ether vaporization method. *Biochim. Biophys. Acta* **443,** 629–634.
11. Cafiso, D. S., Petty, F. R., and McConnell, H. M. (1981) Preparation of unilamellar vesicles at 37°C by vaporization methods. *Biochim. Biophys. Acta* **649,** 129–132.
12. Hauser, H. and Grains, N. (1982) Spontaneous vesiculation of phospholipids: a simple and quick method of forming unilamellar vesicles. *Proc. Natl. Acad. Sci. USA* **79,** 1683–1687.
13. Enouch, H. G. and Strittmatter, P. (1979) Formation and properties of 1000-Ao diameter, single-bilayer phospholipid vesicles. *Proc. Natl. Acad. Sci USA* **76,** 146–149.
14. Hope, M. J., Bally, M. B., Webb, G., and Cullis, P. R. (1985) Production of large unilamellar vesicles by a rapid extrusion procedure: characterization of size distribution and ability to maintain a membrane potential. *Biochim. Biophys. Acta* **812,** 55–65.
15. Chatterjee, S., Sekerk, C. S., and Kwiterovich, P. O. (1982) Increased urinary excretion of glycosphingolipids in familial hypercholesterolemia. *J. Lipid Res.* **23,** 513–522.
16. Esselman, W. J., Laine, R. A., and Sweeley, C. C. (1972) *Methods in Enzymology*, vol. 28, Part B, Academic Press, New York, pp. 140–156.
17. Ledeen, R. W. and Yu, R. K. (1982) *Ganglioside Structure, Isolation and Analysis*. *Methods in Enzymology*, vol. 83, Part D, 139–191.
18. Krupp, L., Chobanian, A. V., and Brecher, J. P. (1976) The in vivo transformation of phospholipid vesicles to a particle resembling HDL in the rat. *Biochem. Biophys. Res. Commun.* **72,** 1251–1258.
19. Senior, J., Gregoriadis G., and Mitropoulous, K. A. (1983) Stability and clearance of small unilamellar liposomes. Studies with normal and lipoprotein-deficient mice. *Biochim. Biophys. Acta* **760,** 111–118.

20. Tall, A. R. and Small, D. M. (1977) Solubilization of phospholipid membranes by human plasma high density lipoproteins. *Nature* (Lond.) **265,** 163–164.
21. Vitas, A. I., Diaz, R., and Gamazo, C. (1996) Effect of composition and method of preparation of liposomes on their stability and interaction with murine monocytes infected with *Brucella abortus*. *Antimicrob. Agents Chemother.* **40,** 146–151.
22. Papahadjopoulos, D. and Watkins, J. C. (1967) Phospholipid model membranes II. Permeability properties of hydrated liquid crystals. *Biochim. Biophys. Acta* **135,** 639–652.
23. Gruner, S. M., Lenk, R. P., Janoff, A. S., and Ostro, M. J. (1985) Novel multilayered lipid vesicles. Comparison of physical characteristics of multilamellar liposomes and stable plurilamellar vesicles. *Biochemistry* **24,** 2833–2842.
24. Chatterjee, S. (1994) Neutral sphingomyelinase action induces signal transduction of tumor necrosis factor in increasing cholesteryl ester synthesis in human fibroblasts. *J. Biol. Chem.* **269,** 879–882.
25. Jungalwala, F. B., Ullman, M. D., and McCluer, R. H. (1987) High performance liquid chromatography of glycosphingolipids in brain disease. *J. Chromatogr.* **32,** 348–377.
26. Chatterjee, S. and Yanni, S. (1987) Analysis of neutral glycosphinoglipids and sulfatides by high performance liquid chromatography. *LC-GC* **5,** 571–574.

2

Preparation and Use of Liposomes for the Study of Sphingolipid Segregation in Membrane Model Systems

Massimo Masserini, Paola Palestini, Marina Pitto, Vanna Chigorno, and Sandro Sonnino

1. Introduction

Several investigations, carried out in either artificial or cellular models and using a variety of techniques ***(1–3)***, confirmed the prediction of Singer and Nicholson ***(4)*** about the presence of domains in biological membranes, that is, of zones where the concentration of the components and the physicochemical properties differ from the surrounding environment. Some domains have been better characterized in terms of the morphological, compositional, and functional aspects. This is the case for caveolae, flask-shaped invaginations of the plasma membrane, characteristically enriched in proteins of the caveolin family ***(5)***. However, the techniques used to isolate caveolae, when applied to cells apparently lacking caveolin, lead to the isolation of membrane fractions (caveolae-like) having characteristics in common with caveolae, such as their peculiar protein and lipid composition ***(6–9)***. In fact, caveolae and caveolae-like domains are enriched with functionally related proteins, suggesting a role of these domains in the mechanisms of signal transduction, cell adhesion, and lipid/protein sorting ***(6)***. Among lipids, sphingolipids (namely glycolipids and sphingomyelin) and cholesterol are characteristically enriched. In particular, GM1 ganglioside ***(10)*** has been proposed as a marker for these membrane structures in cells where this glycolipid is expressed. The peculiar lipid composition has suggested the involvement of glycolipid-enriched domains ("rafts") in lipid/protein sorting at the trans-Golgi network (TGN) level, and, in general, in all cell membranes ***(11)***.

From: *Methods in Molecular Biology, vol. 199: Liposome Methods and Protocols*
Edited by: S. Basu and M. Basu © Humana Press Inc., Totowa, NJ

Preparation of model membranes mimicking the lipid assembly of caveolae and caveolae-like domains is available and is fundamental in order to study the biochemical, functional, and architectural features of domains. In recent years, several investigations clarified the fundamental features of sphingolipid domain formation in model membranes.

In this chapter, preparation of phospholipid vesicles containing sphingolipids in different segregation states is described. For this purpose, some known features affecting their segregation properties are taken into account. First, it is known that glycolipid segregation increases with increasing number of saccharide units ***(1,12,13)***. In this respect, GD1a ganglioside has a strong tendency toward lateral phase separation; and, for this reason, preparation of monolamellar phospholipid vesicles containing GD1a domains is described. Second, the segregation of sphingolipids depends on their ceramide moiety: when ceramide length and unsaturation are different from the membrane environment, glycolipids undergo domain formation. This has been demonstrated in model membranes ***(14)*** and in rabbit brain microsomal membranes ***(14,15)***. For this reason, and given the central role of GM1 ganglioside in caveolae and caveolae-like domains, the preparation of monolamellar phospholipid vesicles containing GM1 ganglioside domains is described. Third, the formation of sphingolipid domains depends on the presence of cholesterol. This occurrence has been reported for a large number of cellular systems ***(16)*** and in model membranes ***(17)***. For this reason, the preparation of monolamellar phospholipid vesicles containing glycolipids, cholesterol, and sphingomyelin domains is described. Starting from these experimental premises, this chapter describes the preparation of monolamellar liposomes of 100 nm diameter, in which different types of domains are realized, simply varying the nature and the proportion among the components.

In brief, after mixing lipids in organic solvent in the preestablished proportions, the solvent is evaporated and a lipid film is formed on the walls of a test tube. Lipids are soaked in buffer at a temperature higher than the gel to liquid-crystalline temperature transition of the lipid mixture. Finally, lipid mixtures are extruded 10 times, always at a temperature above the gel to liquid-crystalline temperature transition, through two stacked filters having controlled pores of 100 nm.

2. Materials

1. Thin-layer chromatography (TLC) plates, RP-8 high-performance liquid chromatography (HPLC) columns, and silica gel 100 for column chromatoghraphy are available from Merck GmbH. Filters (100 nm pore size) can be purchased from Nucleopore (Pleasanton, CA, USA).
2. Deionized water was distilled in a glass apparatus.

3. Phospholipids and cholesterol: Dipalmitoylphosphatidylcholine (DPPC), palmitoylsphingomyelin (SM), and cholesterol are available from Avanti Polar Lipids. All lipids can be stored at –20°C, either in a dried state or in stock solutions in chloroform–methanol (2:1 v/v), and are stable for several months at –20°C under nitrogen.
4. Gangliosides: Gangliosides GM1 and GD1a can be either prepared by fractionation of the total ganglioside mixture extracted from mammal brains by the tetrahydrofuran–phosphate buffer and purified from the glycerolipid contamination by partitioning with diethyl ether ***(18)*** followed by an alkaline treatment ***(19)***, or purchased from suppliers. Ganglioside molecular species of GM1 and GD1a with homogeneous ceramide moieties can be prepared by reversed-phase HPLC. The purity of gangliosides is very important. Spend some time to check for their purity: small impurities can have a large impact on the final result. Purity can be easily checked by TLC. Gangliosides must be stored at –20°C as dried powder.
5. 0.05 *M* Sodium acetate, 1 m*M* $CaCl_2$, pH 5.5.
6. *Clostridium perfringens* sialidase.
7. LiChroprep RP18 column.
8. *p*-Dimethylaminobenzaldehyde.
9. 10% Ammonium sulfate.

3. Methods

3.1. Lipids

3.1.1. Assay and Assessment of Purity of Phospholipids

The assay of phospholipid amount can be carried out spectrophotometrically by assaying the phosphorus content ***(20)***. The purity of phospholipids is very important. Purity can be easily checked by TLC. For this purpose, the TLC plate is overloaded with approx 15 nmol of a single lipid. The plate is developed with chloroform–methanol–water (60:35:4, by vol), and stopped when the solvent is at 0.5 cm from the top of the plate, usually after 20 min. Visualization of the phospholipid is carried out with a spray reagent to detect phosphorus ***(21)***. Only one spot must be visible in the TLC under these conditions.

3.1.2. Preparation of Ganglioside GM1

Ganglioside GM1 is 10–20% (molar) of the total ganglioside mixture from most mammalian brains. The GM1 content can be increased by treatment of the ganglioside mixture with bacterial sialidase. This treatment acting on the ganglioside sialosyl chains transforms the polysialogangliosides into GM1 ***(22)***.

1. The ganglioside mixture is dissolved (40 mg/mL) in prewarmed (36°C) 0.05 *M* sodium acetate, 1 m*M* $CaCl_2$ buffer, pH 5.5.
2. *Clostridium perfringens* sialidase (50 mU/g of ganglioside mixture) is added to the solution every 12 h. Incubation at 36°C is maintained for 2 d while stirring.

3. The sialidase-treated ganglioside mixture is then applied to a LiChroprep RP18 column (3–4 mL gel/g of ganglioside mixture) and, after washing with water to remove salts and free sialic acid, the gangliosides are eluted with methanol.
4. The methanolic solution is dried, dissolved in the minimum volume of chloroform–methanol–water (60:35:8 by vol), and applied to a silica gel 100 column (180–200 mL of gel/g of ganglioside mixture) chromatography, equilibrated, and eluted with the same solvent system; the chromatography elution profile is monitored by TLC (*see* **Subheading 3.1.5.**).
5. Fractions containing GM1 are collected, dried, and the residue dissolved in the minimum volume of propan-1-ol–water (7:3 v/v), and precipitated by adding four volumes of cold acetone.
6. After centrifugation (15,000*g*) the pellet is separated from the acetone and dried under high vacuum. By this procedure GM1 is obtained with homogeneity > 99.9% (assessed by TLC; *see* **Subheading 3.1.5.**). This procedure is suitable for a very large range of ganglioside mixture amounts, from a few milligrams to several grams.

3.1.3. Preparation of Ganglioside GD1a

GD1a is the main ganglioside of the ganglioside mixtures from mammalian brains, covering 30–45% as molar fraction of the total ganglioside mixture.

1. The ganglioside mixture is dissolved in the minimum volume of chloroform–methanol–water (60:35:8 by vol) and applied to a silica gel 100 column chromatography (300–320 mL of gel/g of ganglioside mixture), equilibrated, and eluted with the same solvent system; the chromatography elution profile is monitored by TLC (*see* **Subheading 3.1.5.**).
2. Fractions containing GD1a are collected, dried, and the residue subjected to a further chromatographic purification using the same conditions described in the preceding.
3. Fractions containing only GD1a are collected, dried, and the residue dissolved in the minimum volume of propan-1-ol:water (7:3 v/v), and precipitated by adding four volumes of cold acetone.
4. After centrifugation (15,000*g*) the pellet is separated from the acetone and dried under high vacuum. By this procedure GD1a with homogeneity > 99.9% is prepared (by TLC analysis; *see* **Subheading 3.1.5.**). This procedure is suitable to be adapted to a very large range of ganglioside mixture amounts.

3.1.4. Preparation of GM1 and GD1a Ganglioside Species Homogeneous in the Lipid Portions

Gangliosides GM1 and GD1a purified from brain gangliosides are characterized by a high content of stearic acid (> 90% of the total fatty acid content) and by the presence of both the molecular species containing C_{18}- and C_{20}-sphingosine (94–96% of the total species). Thus, by reversed-phase HPLC,

each ganglioside homogeneous in the oligosaccharide chain is fractionated mainly into two species containing stearic acid and C_{18}- or C_{20}-sphingosine ***(18,23)***. Reversed-phase chromatographic columns show very high resolution in separating the ganglioside species differing in the length of sphingosine, only when a small amount of ganglioside is loaded. We suggest to load a 25×4 cm column with a quantity of 5–6 µmol of ganglioside.

1. Five-micromole portions of GM1 or GD1a are dissolved in 1 mL of acetonitrile–water (1:1 v/v), and applied to a reversed-phase LiChrosphere RP8 column, 25×4 cm internal diameter, 5 µm average particle diameter (Merck, Darmstadt, FRG) through a syringe-loading sample injector equipped with a 1-mL loop.
2. Chromatography is carried out at 20°C with the solvent mixtures: acetonitrile–5 m*M* phosphate buffer, pH 7.0, in the ratio of 3:2 and 1:1 for GM1 and GD1a, respectively. The flow rate is 13 mL/min and the elution profile is monitored by flow-through detection of UV absorbance at 195 nm. The overall procedure requires about 90 min.

3.1.5. Ganglioside Homogeneity

1. Twenty to thirty micrograms of GM1 or GD1a, heterogeneous in the ceramide moiety, are applied for a width of 3–4 mm on silica gel HPTLC plates, then developed with the solvent system chloroform–methanol–0.2% aqueous $CaCl_2$ (50:42:11 by vol).
2. Twenty to thirty micrograms of GM1 or GD1a species, homogeneous in the ceramide moiety and containing C_{18}- or C_{20}-sphingosine, are applied as a 3–4 mm line on reversed-phase RP18-HPTLC plates, then developed 2 times with the solvent system methanol–acetonitrile–water (18:6:1 by vol).
3. After TLC, the gangliosides are made visible by treatment with an anisaldehyde reagent followed by heating at 140°C for 15 min ***(24)***, with a *p*-dimethylamino-benzaldehyde reagent followed by heating at 120°C for 20 min ***(25)***, and with 10% ammonium sulfate followed by heating up to 160°C. Quantification of the ganglioside spots is performed with a densitometer.

3.1.6. Ganglioside Assay

Ganglioside concentrations can be assessed using the sialic acid Svennerholm's assay ***(26)***.

3.1.7. Preparation of Stock Solutions of Lipids

Separate stock solutions are prepared in chloroform–methanol (2:1 v/v) containing 100 µmol/mL of one of the following lipids: DPPC, SM, or cholesterol. Prepare stock solutions of gangliosides containing 10 µmol/mL in chloroform–methanol (2:1 v/v).

3.2. Liposomes

3.2.1. Liposomes Composed of DPPC, Containing GD1a Ganglioside Domains

The main characteristics of these liposomes are the following: size 100 nm (1000 Å); shape monolamellar; gel to liquid-crystalline temperature transition (T_m) 42.5°C, determined by high-sensitivity differential scanning calorimetry. Therefore, the physical state up to this temperature is gel, and this feature should be taken into account anytime the physical state is important for the particular experiment to be performed.

For the preparation of these liposomes, containing 10% molar ganglioside, mix 90 µL of the stock solution of DPPC with 100 µL of the stock solution of GD1a ganglioside and proceed as described in **Subheading 3.3.** The approximate final concentration of liposomes is 9 µmol of phospholipid/mL, 1 µmol of ganglioside/mL. The exact final concentration should be checked by phospholipid and sialic acid assay. The reference temperature for this mixture, important for the preparation of liposomes, is 45°C.

3.2.2. Liposomes of DPPC, Containing Domains of GM1 Ganglioside

For the preparation of liposomes carrying such domains, the use of the molecular species of GM1 ganglioside carrying C_{20}-sphingosine is required, as formation of domains is dependent on the phospholipid environment. The main characteristics of these liposomes are the following: size 100 nm (1000 Å); shape monolamellar; gel to liquid-crystalline temperature transition (T_m) 41.5°C, determined by high-sensitivity differential scanning calorimetry. Therefore, the liposomes are in the physical state of gel up to this temperature, and this feature should be taken into accout anytime the physical state is important for the particular experiment to be performed.

For the preparation of these liposomes containing 10% molar ganglioside, mix 90 µL of the stock solution of DPPC with 100 µL of the stock solution of C_{20}-sphingosine GM1 ganglioside. The approximate final concentration of liposomes is 9 µmol of phospholipid/mL, 1 µmol of ganglioside/mL. The exact final concentration should be checked by phospholipid and sialic acid assay.

3.2.3. Liposomes Composed of SM, Containing Domains of Cholesterol and of GM1 Ganglioside

In these liposomes, distinct SM/cholesterol and SM/ganglioside domains coexist. The main characteristics of these liposomes are the following: size 100 nm (1000 Å); shape monolamellar; gel to liquid-crystalline temperature transition (T_m) 38°C, determined by high-sensitivity differential scanning

calorimetry. Therefore, the liposomes are in the physical state of gel up to this temperature, and this feature should be taken into account anytime the physical state is important for the particular experiment. For the preparation of these liposomes containing 10% molar ganglioside, mix 80 μL of the stock solution of SM with 100 μL of the stock solution of GM1 ganglioside and with 10 μL of the stock solution of cholesterol. The approximate final concentration of liposomes is 8 μmol of phospholipid/mL, 1 μmol of ganglioside/mL, 1 μmol of cholesterol/mL. The exact final concentration should be checked by phospholipid, cholesterol, and sialic acid assay. The reference temperature for this mixture important for the preparation of liposomes is 45°C.

3.2.4. Liposomes of DPPC, Containing GM1 Ganglioside Carrying C_{18}-Sphingosine, Not Forming Domains in This Phospholipid

For the preparation of these liposomes containing 10% molar ganglioside, 90 μL of the stock solution of DPPC is mixed with 100 μL of the stock solution of ganglioside. The approximate final concentration of liposomes is 9 μmol of phospholipid/mL, 1 μmol of ganglioside/mL. The exact final concentration should be checked by phospholipid and sialic acid assay. The reference temperature for this mixture, which will be important for the preparation of liposomes, is 45°C.

3.2.5. Liposomes Having Different Proportions Among the Components

Liposomes containing domains of GM1 or GD1a ganglioside, in proportions different from those described in the preceding in the standard procedure can be prepared, simply varying the amount of ganglioside in the standard recipe. Up to 20% molar percent GM1 ganglioside and up to 15% GD1a can be utilized. At higher molar percentages the stability of liposomes decreases while increasing their tendency to form mixed micelles instead of bilayers.

For SM/cholesterol/GM1 ganglioside liposomes, molar percentages can be varied up to 30% for cholesterol and up to 20% for ganglioside.

3.3. Preparation of Liposomes

3.3.1. Preparation of the Lipid Film

This step must be carried out the day before the actual preparation of liposomes. Usually, it is advisable to perform this first step in the afternoon and the subsequent steps on the following day.

1. Lipids are mixed in a vacuum-fitting test tube of 5 mL total volume, withdrawing proper amounts of each lipid from the stock solutions, in the proportions described in the preceding for the various types of liposomes.

2. Chloroform–methanol (2 : 1 v/v) is added to obtain a total volume of 400 μL. The solvent is slowly evaporated using a gentle stream of nitrogen, under the hood. During this step, the test tube must be kept inclined and continuously rotated. This can be achieved or rotating the test tube by hand or, better, fitting it to a rotating mechanical device (at about 60 rpm). Removal of solvent will produce the deposition of lipids as a film on the bottom and on the walls of the test tube. The removal must be slow (it should take about 5 min) in order to allow the proper mixing among the components. Alternatively, use a rotatory evaporator. In this case, be careful that no drops are ejected from the solution. Fit the tube to a lyophilizer and lyophilize overnight. Lyophilization overnight is recommended. If limited time is available, the lyophilization time can be reduced to 3 h, but this is not recommended. The presence of traces of solvent is deleterious for the assembly of domains.

3.3.2. Use of the Extruder

The extruder is assembled as specified by the manufacturer (Lipoprep). Two overlaying Nucleopore filters are placed in the extruder, handling them only with a flat-tip tweezers. The filters must be placed in the extruder maintaining the same orientation (up/down) as they are taken from their box.

The connected circulating bath is turned on and the temperature inside the extruder is set to reach is the reference temperature indicated for each type of liposomes. If the setting temperature is not known, the procedure is as follows: 1 mL of buffer, preheated at the reference temperature, is placed inside the extruder, then wait 10 min. The temperature of the buffer inside the extruder is measured until the reference temperature is reached. The circulating bath is run for about 30 min before proceeding with the following steps.

The extruder is loaded with 1.5 mL of distilled water using a Pasteur pipet. After 10 min the water is extruded. The pressure from the extruder is released and replaced. All the water at this point shall be removed. This is repeated two times.

To condition the filters, 1.5 mL of the buffer to be utilized for the preparation of liposomes needs to be extruded two times. Using a Pasteur pipet, 1.5 mL buffer is loaded. After a 10-min extrusion, pressure removal and repressurization are carried out. All the buffer will be removed after this step.

A tube containing about 3 mL of buffer, the tube containing the lipid film, and a glass pipet are placed in an oven at the temperature given below for the various types of liposomes. After thermostating for 20 min, 1 mL of buffer is withdrawn with the pipet. A propipet is used when hot. The buffer is added to the lipid film and vortex-mixed for 1 min. This is put in the oven for 5 min and vortex-mixed again for 1 min. The suspension is maintained at the reference temperature.

3.3.3. Extrusion of Liposomes

The extruder is loaded with the lipid suspension. Wait 5 min to ensure thermostatting. The suspension is extruded and collected in a test tube maintained at the reference temperature. The liposomes are extruded again, ten times, and collected in different test tubes each time, always thermostatted at the reference temperature.

4. Notes

Please consider the following points for a correct preparation of liposomes.

1. The final lipid concentration of liposomes is much lower than expected. Possible causes are: (a) the temperature of the solution in the extruder is lower than the reference temperature indicated for each type of liposomes (check the temperature inside the extruder as described in the preceding); (b) the concentration of stock solutions is not correct (assay the lipid concentration of stock solutions).
2. Liposomes are not coming out from the extruder. Possible causes are: (a) the temperature is not adequate (too low: adjust the temperature of the circulating bath); (b) the filters are clogged (raise the temperature and the pressure: if no effect is noticed, withdraw the lipid suspension from the extruder and replace the filters).
3. Liposomes are coming out too fast from the extruder or the lipid suspension is not becoming clearer after some extrusion steps. This occurs if the filters have been damaged. Commonly this is due to misuse of the Pasteur pipet used to load the extruder, or the tweezers used to handle the filters. Withdraw the lipid suspension from the extruder and replace the filters. Be careful not to touch the filters with the Pasteur pipet. Check the tweezers.

Acknowledgments

This work was supported by Consiglio Nazionale delle Ricerche (CNR), Italy (Target Project: Biotechnology) to S. S. and MURST (Rome, Italy, Cofinanziamento 1998) to M. M.

References

1. Thompson, T. E. and Tillack, T. W. (1985) Organization of glycosphingolipids in bilayers and plasma membranes of mammalian cells. *Annu. Rev. Biophys. Chem.* **14,** 361–386.
2. Tocanne, J. F., Dupou-Cezanne, L., Lopez, A., and Tournier, J. F. (1989) Lipid lateral diffusion and membrane organization. *FEBS Lett.* **257,** 10–16.
3. Welti, R. and Glaser, M. (1994) Lipid domains in model and biological membranes. *Chem. Phys. Lipids* **73,** 121–137.
4. Singer, S. J. and Nicholson, G. L. (1972) The fluid mosaic model of the structure of cell membranes. *Science* **75,** 720–731.

5. Harder, T. and Simons, K. (1997) Caveolae, DIGs, and the dynamics of sphingolipid-cholesterol microdomains. *Curr. Opin. Cell Biol.* **9,** 534–542.
6. Simons, K. and Ikonen, E. (1997) Functional rafts in cell membranes. *Nature* **387,** 569–572.
7. Verkade, P. and Simons, K. (1997) Lipid microdomains and membrane trafficking in mammalian cells. *Histochem. Cell Biol.* **108,** 211–220.
8. Gorodinsky, A. and Harris, D. A. (1995) Glycolipid-anchored proteins in neuroblastoma cells form detergent-resistant complexes without caveolin. *J. Cell Biol.* **129,** 619–627.
9. Wu, C., Butz, S., Ying, Y., and Anderson, R. G. (1997) Tyrosine kinase receptors concentrated in caveolae-like domains from neuronal plasma membrane. *J. Biol. Chem.* **272,** 3554–3559.
10. Parton, R. G. (1994) Ultrastructural localization of gangliosides; GM1 is concentrated in caveolae. *J. Histochem. Cytochem.* **42,** 155–166.
11. Simons, K. and Van Meer, G. (1988) Lipid sorting in epithelial cells. *Biochemistry* **27,** 6197–6202.
12. Masserini, M., Palestini, P., and Freire, E. (1989) Influence of glycolipid oligosaccharide and long-chain base composition on the thermotropic properties of dipalmitoylphosphatidylcholine large unilamellar vesicles containing gangliosides *Biochemistry* **28,** 5029–5039.
13. Terzaghi, A., Tettamanti, G., and Masserini, M. (1993) Interaction of glycosphingolipids and glycoproteins: thermotropic properties of model membranes containing GM1 ganglioside and glycophorin. *Biochemistry* **32,** 9722–9725.
14. Masserini, M. and Freire, E. (1986) Thermotropic characterization of phosphatidylcholine vesicles containing ganglioside GM1 with homogeneous ceramide chain length. *Biochemistry* **25,** 1043–1049.
15. Palestini, P., Masserini, M., Fiorilli, A., Calappi, E., and Tettamanti, G. (1991) Evidence for nonrandom distribution of GD1a ganglioside in rabbit brain microsomal membranes. *J. Neurochem.* **57,** 748–753.
16. Brown, D. and Rose, J. K. (1992) Sorting of GPI-anchored proteins to glycolipid-enriched membrane subdomains during transport to the apical cell surface. *Cell* **68,** 533–544.
17. Ferraretto, A., Pitto, M., Palestini, P., and Masserini, M. (1997) Lipid domains in the membrane: thermotropic properties of sphingomyelin vesicles containing GM1 ganglioside and cholesterol. *Biochemistry* **36,** 9232–9236.
18. Tettamanti, G., Bonali, F., Marchesini, S., and Zambotti, V. (1970) A new procedure for the extraction, purification and fractionation of brain gangliosides. *Biochim. Biophys. Acta* **296,** 160–170.
19. Ledeen, R. W., Yu, R. K., and Eng, L. F. (1973) Gangliosides of human myelin: sialosylgalactosylceramide (G7) as a major component. *J. Neurochem.* **21,** 829–839.
20. Bartlett, G. R. (1959) Phosphorus assay in column chromatography. *J. Biol. Chem.* **234,** 466–468.

21. Vaskovsky, V. E. and Kostetsky, E. Y. (1968) Modified spray for the detection of phospholipids on thin-layer chromatograms. *J. Lipid Res.* **9,** 396.
22. Acquotti, D., Cantù, L., Ragg, E., and Sonnino, S. (1994) Geometrical and conformational properties of ganglioside GalNAc-GD1a, IV^{4}GalNAcIV^{3}Neu5AcII^{3}Neu5AcGgOse$_4$Cer. *Eur. J. Biochem.* **225,** 271–288.
23. Sonnino, S., Ghidoni, R., Gazzotti, G., Kirscherner, G., Galli, G., and Tettamanti, G. (1984) High performance liquid chromatography preparation of the molecular species of GM1 and GD1a gangliosides with homogeneous fatty acid and long chain composition. *J. Lipid Res.* **25,** 620–629.
24. Stahl, E. (1962) Anisaldehyd-Schw Efelsaure fur Steroide, Terpene, In: Zucker, U. N. P. so W. M. Dunnschicht, eds. Chromatographie, Springer-Verlag, Berlin, p. 498.
25. Partridge, S. M. (1948) Filter-paper partition chromatography of sugars. I: General description and application to the qualitative analysis of sugars in apple juice, egg white and fetal blood of sheep. *Biochem. J.* **42,** 238–248.
26. Svennerholm, L. (1957) Quantitative estimation of sialic acid. II. A colorimetric resorcinol-hydrochloric acid methods. *Biochim. Biophys. Acta* **24,** 604–611.

3

Peptide-Induced Fusion of Liposomes

Eve-Isabelle Pécheur and Dick Hoekstra

1. Introduction

Current experimental evidence suggests that the merging of two closely apposed lipid bilayers to form one continuum is mediated by specific fusion proteins. The dissection of the molecular pathways eventually leading to membrane merging can be accomplished by various approaches, including genetic, immunological, biochemical, or biophysical technology. However, our understanding of the mechanisms of biological membrane fusion is still rudimentary, and in this context, the use of artificial membranes such as liposomes and model peptide systems is of great value to simulate protein-induced fusion.

Until now, most studies on peptide-induced fusion have employed synthetic peptides corresponding to the putative fusion domains of fusogenic proteins which are added to the liposome suspension as free monomers. Fusion is then monitored by following the mixing of membranes and that of liposomal aqueous contents, using a variety of fluorescence assays. These peptides usually induce efficient lipid mixing but cause extensive content leakage, reflecting poor control of the fusion event.

We therefore aimed to design a simplified membrane system, consisting of a liposome-anchored short fusogenic peptide, that allowed for studying the regulation of fusion. Peptide–lipid and peptide–peptide interactions on the pathway of peptide-induced fusion were studied by employing techniques based on the use of fluorescent probes, after covalent attachment of the peptide to the liposomal surface.

In this chapter, we present and comment on our strategy to design a peptide model system and show some applications of this model to the molecular study

From: *Methods in Molecular Biology, vol. 199: Liposome Methods and Protocols*
Edited by: S. Basu and M. Basu © Humana Press Inc., Totowa, NJ

of peptide-induced fusion. The assays commonly used to monitor fusion are briefly described.

2. Materials

1. Sigma and Avanti Polar Lipids were the sources of lipids used for the fabrication of liposomes. Lipids were checked regularly by thin-layer chromatography (TLC) on silica gel plates for oxidation products and purity (*see* **Subheading 3.**). Common lipids from both sources gave very similar results in terms of quality. Phospholipid standards and molybdenum blue spray reagent were obtained from Sigma.
2. Fluorescent lipid probes *N*-(7-nitro-2,1,3-benzoxadiazol-4-yl)phosphatidyl ethanolamine (*N*-NBD-PE) and *N*-(lissamine rhodamine B sulfonyl)-dihexadecanoyl-*sn*-glycero-3-phosphoethanolamine *(N*-Rh-PE) were obtained either from Avanti Polar Lipids (Alabaster, AL) or from Molecular Probes (Eugene, OR).
3. Polyunsaturated phosphatidylcholine species were exclusively purchased from Avanti Polar Lipids (and used within 3 mo). *N*-Succinimidyl-3-(2-pyridyldithio) propionate (SPDP) and dipicolinic acid were from Sigma, and Boc-Lys-Boc-OSu was from Bachem Fine Chemicals (Bubendorf, Switzerland).
4. $TbCl_3$•$6H_2O$ was from Acros Organics (Geel, Belgium).
5. Aminonaphthalenetrisulfonic acid (ANTS) and *p*-xylylene *bis*(pyridinium) bromide (DPX) were from Molecular Probes (Eugene, OR).
6. Silica-coated sheets for TLC were from Riedel-de Haën (Seelze, Germany).
7. Silica for gel filtration chromatography (Kieselgel 60, 70–230 mesh) was from Merck (Darmstadt, Germany).
8. Preswollen microgranular carboxymethylcellulose CM52 was from Whatman Biosystems Ltd. (Maidstone, England).

3. Methods

3.1. Liposome Preparation and Handling

3.1.1. Lipid Handling

The quality and purity of the lipids used in the assays described herein are of major importance. Lipids are regularly checked for oxidation and hydrolysis by ultraviolet (UV) spectrophotometry and TLC on silica-coated plates. Natural phospholipids contain nonadjacent double bonds that give rise to a UV absorbance peak at short wavelengths in ethanol (200–210 nm). Oxidation products, as a result of a free radical chain mechanism (to which double bonds are most susceptible), appear as additional peaks in the UV spectrum: the presence of dienes is indicated by a peak around 230 nm, and trienes give rise to an additional peak around 270 nm. The degree of oxidation

can be calculated from the OD reading at 233 nm (molar extinction coefficient for dienes = 30,000 M^{-1} cm^{-1}), according to the following formula:

$$\% \text{ oxidation} = ([\text{diene}] / [\text{phosphate}]) \times 100$$

The phosphate concentration is determined according to the method of Bartlett ***(1)***. We wish to refer the reader to **ref. *2*** for further details on the chemistry of the reaction and on the experimental protocol.

Minor amounts (~1%) of oxidation products (dienes) were routinely found in freshly opened ampules of natural phospholipids (e.g., egg yolk phosphatidylcholine, phosphatidylserine or phosphatidylethanolamine from bovine brain, phosphatidylinositol from bovine liver). However, heavily oxidized batches (> 5%) are discarded as these oxidation products can affect the fusion properties of liposomes (*see* **Subheading 3.3.**). The purity of lipid batches is also readily revealed by TLC on silica-coated sheets. By this technique, any contamination by other lipid species and the presence of hydrolysis products can be detected. Lipid standards are used as reference spots, and lipid samples are spotted from chloroform or chloroform–methanol solutions (≥ 5 µmol of lipid). The plates are run with a solvent such as chloroform–methanol–water (65 : 25 : 4 by vol), until the solvent front is ~0.5 cm from the top of the plate. Phospholipids and lysophospholipids can be revealed as blue spots by spraying a molybdenum blue reagent on the dried plate. Under these conditions, lysolipids typically run to positions below the phospholipid spots, and quantitation can be performed after scanning of the plate and densitometric analysis (e.g., with the program Scion Image© for Windows).

3.1.2. Synthesis of PE-PDP

L-α-Dipalmitoyl phosphatidylethanolamine (DPPE) is derivatized by SPDP, to yield PE-PDP ***(3)*** which serves as a lipid anchor for the peptide (*see* **Subheading 3.2.**), thus allowing its coupling to a liposomal surface.

1. Typically, 20 µmol of DPPE (dissolved in chloroform at $T \geq 50°C$) is mixed with 30 µmol SPDP in ethanol and 30 µmol of triethylamine.
2. The mixture (1 mL final in a sealed tube) is incubated in the dark for 3 h at room temperature under agitation and an argon atmosphere.
3. The final reaction mixture is analyzed by TLC (with chloroform–methanol–acetic acid as solvent, 60 : 30 : 3), and PE-PDP appears as a spot running faster than DPPE.
4. Elimination of unreacted compounds is achieved by adding Tris-buffered saline, pH 7.4, to the chloroform solution (ratio organic [O]/aqueous [A] phase, 1 : 4 v/v), followed by centrifugation for 10 min at 900*g* at room temperature.

5. The organic phase and interface are collected, and the emulsion formed with water (ratio O/A, 1:3 v/v) is centrifuged twice for 5 min at 900*g*.
6. Finally, the organic phase is collected and, if necessary, methanol is added to eliminate the emulsion. The PE-PDP sample is concentrated by evaporation under a stream of nitrogen at room temperature, and assayed for phosphate ***(1)***.
7. The lipid derivative is stable up to 6 mo on storage in glass ampules under argon at –50°C. Before use, the presence of hydrolysis products should be checked by TLC.

3.1.3. Synthesis of PE-Lys

In some of our fusion experiments, L-lysine-derivatized DPPE was used ***(4)*** as a means to allow vesicle aggregation between the (negatively charged) peptide exposing vesicles and (positively charged) PE-Lys-containing target vesicles.

1. DPPE (200 µmol) dissolved in a hot chloroform–ethanol (1:1) mixture is incubated for 12 h at 50–60°C with 600 µmol of Boc-Lys(Boc)-OSu (protected L-lysine) in the presence of triethylamine as a catalyst. TLC is employed to reveal the quantitative conversion of DPPE into a faster running compound (with chloroform–methanol–water, 65:25:4 as a solvent).
2. The sample is concentrated under reduced pressure and applied to a 10-mL silica gel column (Kieselgel 60) presoaked in chloroform. Elution is accomplished with two volumes of 15 mL of chloroform, two volumes each of 80:20, 60:40, and 40:60 chloroform–ethanol mixtures, and finally twice with 15 mL of ethanol. The phosphate-containing fractions are pooled and concentrated under reduced pressure.
3. The deprotection of the lysine residue is performed in 4 mL of a 20:80 chloroform–trifluoroacetic acid mixture, for 3 h at room temperature. After concentration under reduced pressure, successive washings with chloroform are performed until no acidic vapors are released. A TLC is run with chloroform–methanol–NH_4OH, 60:35:6.5, as a solvent; free amine residues are revealed by ninhydrin spraying (0.25 g of ninhydrin in 100 mL of acetone–lutidine, 9:1 v/v), and phosphate by molybdenum blue reagent spraying. PE-Lys gives a spot which is running slower than DPPE (R_f values 0.45 and 0.56, respectively).
4. The sample is further purified by gel chromatography on carboxymethylcellulose (CM52), washed extensively in phosphate- or Tris-buffered saline, pH 7.4. The column is then rinsed three times with chloroform before loading the sample. Elution is done with 30 mL of chloroform, followed by 90:10, 80:20, and 70:30 chloroform–methanol mixtures. Ninhydrin- and phosphate-positive fractions are pooled and evaporated to dryness. PE-Lys, as a dry powder, is stored at –20°C up to 6 mo without detectable degradation.

3.1.4. Preparation of Liposomes

Three techniques were used to obtain unilamellar vesicles of ~150 nm that are subsequently used in the fusion assay; all three techniques gave similar results in terms of fusion.

3.1.4.1. Freeze–Thaw and Extrusion The lipid film is obtained by mixing appropriate amounts of lipids in chloroform. The organic solvent is removed by evaporating under a stream of nitrogen. After resuspension by vigorous vortex-mixing in the desired aqueous buffer, the liposome suspension undergoes a cycle of freezings in liquid nitrogen followed by thawing in a 40°C water bath, carried out 10 times. Liposomes are then extruded through a polycarbonate membrane with a pore size of 0.1 μm (Nucleopore Corp.), yielding particles with a diameter of ~ 150 nm, as determined by electron microscopy and dynamic light scattering in a Coulter N4S submicron particle analyzer.

3.1.4.2. Sonication and Extrusion The liposome suspension obtained by vortex-mixing (*see* **Subheading 3.1.4.1.**) is submitted to sonication for 30 min with a 50% active cycle on a VibraCell (Bioblock) at 4°C. The sonicated suspension is then extruded as described in **Subheading 3.1.4.1.**

3.1.4.3. Reversed-Phase Evaporation and Extrusion The lipid film is redissolved in 3 mL of diethyl ether, and the aqueous buffer (1 mL) is added by rapid injection with a syringe. After a 10-s sonication burst with the VibraCell probe (to form a fine inverted emulsion), ether is evaporated slowly under reduced pressure until a gel phase is formed. At that stage, the vacuum is released and the gel is disrupted manually by vigorous agitation. This procedure yields liposomes with a diameter of ~ 400 nm. The suspension is subsequently sized to ~150 nm by extrusion. For further details about the principle of this technique, the reader is referred to **ref. *5***.

Donor liposomes are defined as the liposomes to which the peptide is coupled and that contain the fluorescence probes for monitoring lipid mixing (*see* **Subheding 3.3.1.**). Typically, they are composed of egg yolk phosphatidylcholine (EYPC), cholesterol (chol), PE-PDP, *N*-NBD-PE, and *N*-Rh-PE (molar ratios 3.5 : 1.5 : 0.25 : 0.05 : 0.05, respectively). In some cases, they also contain *N*-biotinoyl-phosphatidylethanolamine (biotinPE). Target liposomes consist of natural or synthetic phosphatidylcholines, cholesterol, and PE-Lys (molar ratio 11 : 6 : 3), or, in some, experiments, natural or synthetic phosphatidylserine (PS) and phosphatidylethanolamine (PE) (*see* **Subheding 3.3.1.**).

Liposomes are freshly prepared and used within 3 d. Liposomes prepared with polyunsaturated PC species are used within 1 d and kept in the dark at all times.

3.2. Fusogenic Peptide: Handling and Coupling to Liposomes

Based on the structural features known to date of fusion peptides present in (membrane-linked) fusion glycoproteins of viruses or cells, and in an attempt to convey fusogenic properties to the peptide only after its membrane anchorage, we developed a model peptide: (1) rich in alanine residues, highly abundant

in sequences of fusion peptides from various viruses ***(6)***; (2) exhibiting a segregated distribution between hydrophobic and hydrophilic residues when modeled as a theoretical α-helix, and possessing a hydrophobicity index > 0.5, both parameters thought to be relevant for fusion ***(7)***; (3) short, that is, fewer than 20 residues, to avoid spanning the target lipid bilayer, and thus to avoid a major uncontrolled membrane destabilization; (4) containing a cysteine (Cys) residue to allow its covalent coupling to the liposomal surface via formation of a disulfide bridge with PE-PDP; and (5) containing a N-terminal tryptophan (Trp) residue to allow for monitoring of the interaction of the N-terminus with the target membrane ***(8)***.

Importantly, the possibility to anchor the peptide covalently to liposomes, thereby dictating geometrical constraints, is of great value to closely simulate membrane fusion induced by a membrane-bound protein, as structural and orientational features of the peptide are implicitly taken into account.

3.2.1. Handling of the Peptide

The peptide, N-Trp-Ala-Glu-Ser-Leu-Gly-Glu-Ala-Leu-Glu-Cys-OH (or N-WAESLGEALEC-OH) (WAE), was synthesized and purified to > 95% purity by Synt:em SA (Nîmes, France). Before use, an aliquot is dissolved into a 20 m*M* ammonium bicarbonate solution that has been argon-flushed to minimize the risks of oxidation of the Cys and Trp residues. Concentrations of peptide stock solutions are quantitated spectrophotometrically at 280 nm (molar extinction coefficient of the Trp residue = 5600 $M^{-1}cm^{-1}$). The working solution is stored at –20°C, and assayed for Cys dimerization from time to time according to the method of Gailit ***(9)***. Dry sodium borohydride (NaBH4) is added to an aliquot of peptide in solution, to reduce the disulfide bonds and restore free sulfhydryl groups. The number of free thiol groups is assayed by the Ellman's reagent (5,5′-dithiobis (2-nitrobenzoic acid), or DTNB [10]), before and after reduction by $NaBH_4$.

3.2.2. Coupling to Liposomes

Donor liposomes (EYPC–chol–PE-PDP, 3.5:1.5:0.25) are incubated overnight at 4°C on a rolling device with peptide in solution, in a PE-PDP/peptide molar ratio of 1:5. The reaction shown at top of next page takes place.

The only means to detach the peptide from the donor membrane is by treatment with 50 m*M* dithiothreitol (DTT), pH 8. The reaction can be followed by measuring spectrophotometrically at 343 nm released 2-thiopyridone ***(3)***; typically, the coupling efficiency of the *added peptide fraction* is 10–20%, implying that at a density of 5 mol% PE-PDP and a PE-PDP/peptide ratio of 1:5, at least half of the PE-PDP molecules contain coupled peptide.

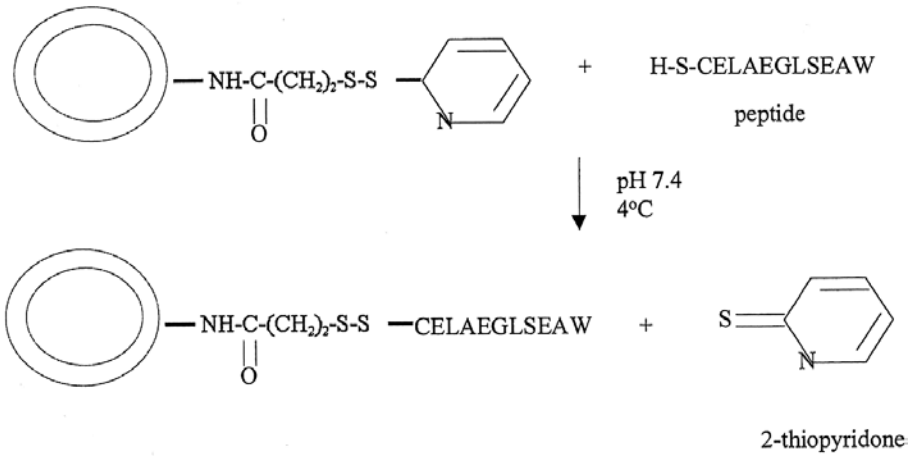

Reproducibility of the coupling yield can be also checked by Fourier transform infrared spectroscopy, by comparing the relative intensities of the coupled peptide and lipid bands, measured between 1680 and 1600 cm^{-1}, and between 1770 and 1700 cm^{-1}, respectively ***(11)***. In addition, information about structural and orientational features of the peptide can be obtained by this technique. This is beyond the scope of the present chapter, but the reader is referred to recently published work ***(12)***.

Uncoupled peptide is eliminated by gel filtration on a Sephadex G-25 column (PD-10, Pharmacia, Sweden), and the lipid phosphorus content is measured ***(1)***.

3.3. Fusion Assays: Lipid Mixing, Internal Contents Mixing, Leakage Measurements

The process of membrane fusion consists of several subsequent stages– aggregation and close apposition of the membranes about to fuse, followed by membrane destabilization and mixing of lipid components, and then by coalescence of the aqueous contents of the membrane-bounded compartments. By definition, this process is controlled; that is, it does not lead to content leakage or to lysis of the vesicles involved in fusion. These steps must be kept in mind when determining if a peptide, polypeptide, or protein has fusogenic properties. Indeed, aggregation between particles can be a fairly nonspecific phenomenon, driven, for example, by electrostatic interactions between cations in the buffer and negatively charged phospholipids. This could eventually lead to membrane destabilization and lipid mixing, although this process could not be called membrane fusion. Also extensive perturbation of membranes can translate into lipid and content mixing but accompanied by extensive contents

leakage. Therefore, a crucial question to ask when studying the fusogenic properties of a protein or a peptide by these assays is, Is the fusion event accomplished in a controlled way? Yet, a good indication of such a control would reside in a similarity of the kinetics of lipid and contents mixing.

Membrane fusion can be monitored by a large number of techniques. In the following subheadings, we briefly describe several assays frequently used in our laboratory and that rely on the mixing of lipids and the mixing of contents. For further details of these procedures, the reader is referred to several reviews on this topic ***(13–15)***.

3.3.1. Lipid Mixing

One of the most widely used and most reliable assays relies on the use of resonance energy transfer between two lipidic probes, *N*-NBD-PE, the energy donor, and *N*-Rh-PE, the energy acceptor. When both are present in vesicles at a ratio not exceeding 1 mol% of the total lipids, an efficient energy transfer between *N*-NBD-PE and *N*-Rh-PE occurs, corresponding to a minimal fluorescence intensity of the energy donor when monitored at its excitation and emission wavelengths. During the process of membrane merging between fluorescent-labeled and unlabeled vesicles, the distance separating both fluorophores will increase as their surface density decreases, which translates into a decrease in the efficiency of the energy transfer and consequently an increase in the fluorescence intensity of the NBD moiety.

From an experimental point of view, donor liposomes consisting of EYPC/chol/PE-PDP/*N*-NBD-PE/*N*-Rh-PE (3.5 : 1.5 : 0.25 : 0.05 : 0.05), to which WAE has been coupled, are equilibrated under agitation to the desired temperature in a quartz cuvette for 1 min. Their fluorescence intensity, thus measured, is taken as 0% fluorescence (λ_{exc} = 460 nm; λ_{em} = 534 nm). An aliquot of target liposomes ("acceptors"; PC/chol/PE-Lys 11 : 6 : 3) is added in a molar donor/acceptor ratio of 1 : 6 (final lipid concentration not exceeding 100 μ*M* to avoid light scattering and inner filter effects), and the kinetics of NBD fluorescence increase are monitored in a continuous fashion. After a plateau is reached, vesicles are lysed by addition of Triton X-100 (0.1% final concentration) to the suspension. The value thus obtained is multiplied by 1.54, to take into account the effect of the detergent on NBD fluorescence, and is set to 100% fluorescence ***(16)***. This value can also be obtained by measuring the fluorescence intensity of a mock fusion product labeled with 0.07 mol% each of *N*-NBD-PE and *N*-Rh-PE, that is, the density reached when all vesicles would fuse, at a 1 : 6 ratio of donor over acceptor. The percentage of fusion can then be calculated according to

$$F(t) = [(F(t) - F_o) / (F_{max} - F_o)] \times 100 \quad (1)$$

where $F(t)$ is the fluorescence intensity at time t, F_o the initial fluorescence of the labeled liposomes, and F_{max} the maximal level of fusion reached. Full details of this technique can be found in **ref. *17***.

Although this assay reflects the mixing of membranes, it does not allow for discriminating which leaflet of the membrane is involved. To address this point more specifically, fluorescently and symetrically labeled liposomes can be treated with sodium dithionite (20 m*M* for 20 min at 37°C), a specific and nonpermeant quencher of NBD fluorescence. This treatment extinguishes exclusively the fluorescence of the outer leaflet. In this way, any increase in the fluorescence signal of NBD will mean that the inner leaflet of the bilayer participates in the membrane mixing process ***(18)***. This approach is sometimes taken, for example, when content mixing cannot be carried out, to support the occurrence of genuine fusion reported by the lipid mixing assay, rather than lipid exchange or transfer. However, whenever possible, contents mixing is preferred as an additional means to rigorously demonstrate the fusion event.

3.3.2. Internal Contents Mixing

Fluorescence assays monitoring the coalescence of the aqueous compartments of vesicles rely on the use of molecules encapsulated into the liposomes.

3.3.2.1. Terbium/Dipicolinic Acid Assay. This assay relies on the formation of a chelation complex between $TbCl_3$, initially (weakly) complexed with citrate anions and encapsulated into the peptide-coupled liposomes, and dipicolinic acid (DPA, as a sodium salt) encapsulated into the target vesicles. Tb^{3+} ions *per se* are weakly fluorescent at λ_{exc} = 276 nm and λ_{em} = 545 nm; at these wavelengths, DPA absorbs but does not fluoresce. When the aqueous contents of donor and target liposomes mix, the strongly fluorescent $Tb(DPA)_3^{3-}$ high-affinity complex is formed, corresponding to a 10^4-fold increase in the fluorescence of Tb^{3+}.

1. The lipid film of donor vesicles is resuspended in 2.5 m*M* $TbCl_3$ buffered in 50 m*M* sodium citrate, 10 m*M* 4-(2-hydroxyethyl)-1-piperazineethanesulfonic acid (HEPES), pH 7.4, vortex-mixed, and processed as described ***(9,14)***. The coupling with WAE is performed overnight, and the unbound peptide and unencapsulated Tb are removed in one step by gel filtration on a PD-10 column with a 10 m*M* Hepes, 100 m*M* NaCl, 1 m*M* EDTA buffer at pH 7.4.
2. The lipid film of target vesicles (PC/chol/PE-Lys) is resuspended in 50 m*M* DPA buffered in 20 m*M* NaCl, 10 m*M* HEPES, pH 7.4. Elimination of unencapsulated material is similarly performed by gel filtration.

3. Note that (a) these concentrations of Tb and DPA are to be encapsulated in large unilamellar liposomes (diameter ~ 100 nm), and not in small vesicles < 50 nm in diameter; (b) adjusting the pH of the DPA solution should be done carefully, as solvation is slow and the pH can be easily overshot while titrating; and (c) DPA is in our model encapsulated into target liposomes because it is not expected to electrostatically react with the PE-Lys present in the membranes, in contrast to the Tb^{3+} cations.
4. The fusion assay is performed under similar conditions as those described for the lipid mixing assay, in buffer consisting of 10 m*M* HEPES, 100 m*M* NaCl, 1 m*M* EDTA, pH 7.4 at the desired temperature. EDTA is included because it chelates Tb that would leak from the donor liposomes, thereby eliminating any contribution to the fluorescence signal derived from the outside medium where it might complex with leaked DPA. It is essential to equilibrate the Tb-loaded vesicles at the recording temperature before adding the target liposomes, so as to avoid artificial, temperature-dependent variations in the fluorescence signal. In the WAE system, the kinetics of content mixing appear as a continuous increase in the Tb fluorescence signal.
5. The initial fluorescence intensity of the peptide-coupled Tb-loaded liposomes is taken as the 0% fluorescence. The 100% is obtained as follows: Tb-loaded vesicles (equivalent to the amount of Tb vesicles used in the actual assay) are lysed by sonication in the presence of 0.5% (w/v) Na cholate or 0.8 m*M* $C_{12}E_8$ (Calbiochem, San Diego, CA), in a solution containing 20 μ*M* free DPA, in the HEPES buffer *without EDTA*. The percentage of fluorescence is calculated according to Eq. (1). Full details of this assay can be found in **ref. *19***.

3.3.2.2. Aminonaphthalenetrisulfonic Acid (ANTS) / p-Xylylene bis(Pyridinium) Bromide (DPX) Assay

An alternative to the Tb/DPA content mixing assay is an assay that relies on mixing of ANTS and DPX. Changes in fluorescence on contents mixing in this assay rely on collisional quenching instead of fluorescent complex formation as is the case for Tb and DPA. Indeed, ANTS, encapsulated in the peptide-coupled population of vesicles, is highly fluorescent (λ_{exc} = 360 nm; $\lambda_{em} \geq$ 530 nm). Mixing of contents with DPX-loaded target vesicles leads to the quenching of ANTS fluorescence by DPX (owing to its pyridinium moiety which can form charge-transfer complexes). Coalescence of internal compartments is thus visualized as a decrease in the fluorescence of ANTS as a function of time.

1. The donor lipid film is resuspended in 25 m*M* ANTS solubilized in 40 m*M* NaCl, 10 m*M* HEPES, pH 7.4, while the target liposomes are made by resuspending the lipids in 90 m*M* DPX, 10 m*M* HEPES, pH 7.4.
2. Removal of nonencapsulated compounds is performed by gel filtration chromatography on a PD-10 column. Fusion was monitored at λ_{exc} = 360 nm and λ_{em} = 530 nm, and, for calibration, the 100% and 0% of fluorescence are taken

as the initial fluorescence of the ANTS-loaded peptide-coupled vesicles and the fluorescence of ANTS/DPX-loaded liposomes (1 : 1 mixture of the solutions described in the preceding), respectively ***(14)***.

3.3.3. Leakage Measurements

As mentioned earlier, fusion reactions can lead to undesired leakage of internal contents, which could already be suspected when the kinetics of internal contents and lipid mixing are dissimilar (in terms of initial rates and/or extent). This leakage can be directly monitored by techniques based on the use of the same fluorescent pairs as described earlier for internal content mixing, except that to allow for monitoring leakage, the molecules are encapsulated in the same population of liposomes as 1 : 1 mixtures (*see* **Subheadings 3.3.2.1.** and **3.3.2.2.** for composition of the solutions).

For the Tb–DPA complex, leakage is registered as a decrease in the fluorescence intensity of the complex, owing to dissociation of the complex outside the vesicles by EDTA. The 100% fluorescence corresponds to the initial fluorescence of the Tb–DPA-containing target vesicles, and the 0% is obtained after lysis of the vesicle mixture (Tb–DPA-loaded target and peptide-coupled vesicles, ratio 6 : 1) by 0.8 m*M* $C_{12}E_8$, and measurement of the remaining fluorescence in the presence of EDTA.

Conversely, leakage as measured with the ANTS–DPX pair will appear as an increase in the fluorescence signal of ANTS as a function of time, owing to relief of the quenching effect of DPX on ANTS owing to infinite dilution in the extravesicular volume. The 100% fluorescence is obtained after lysis of the suspension of ANTS–DPX target liposomes and peptide-coupled vesicles by 0.1%Triton X-100 or 0.8 m*M* $C_{12}E_8$. The 0% corresponds to the initial fluorescence of the ANTS–DPX-loaded target vesicles alone ***(20)***.

For our peptide model system, leakage was found to be negligible using either assay, implying that the membrane-anchored WAE peptide induces genuine and, in terms of membrane integrity, a carefully controlled fusion process.

3.4. Insight into the Structure–Function Relationship of the Membrane-Anchored Peptide

The membrane-anchored WAE peptide model system we developed offers the unique opportunity to study the molecular relationship between structural and functional features at the level of a fusion peptide. Indeed, conformational studies of similar fusion domains as they occur in their membrane-anchored protein environment are far from being resolved, owing to technical limitations including resolution. Structural features of WAE have been assessed by Fourier transform infrared spectroscopy, a technique particularly well suited

to the study of membrane-associated peptides in their lipid environment. This technique requires only small amounts of peptide (10–100 μg), unlike other biophysical techniques such as X-ray diffraction or nuclear magnetic resonance ***(21)***.

We have shown that the anchorage of WAE to a liposomal surface is an absolute prerequisite for its ability to exert its fusogenic properties ***(8)***. This can be translated in terms of conformational changes: indeed, when free in solution, the peptide adopts mainly a β-structure, and is fusion incompetent. However, when covalently attached to liposomes, it folds into an amphipathic α-helix ***(11)***. As a consequence, the peptide-coupled liposomes fuse with target membranes as revealed by both the mixing of lipids and aqueous contents. Insight into orientational features of the peptide toward its own membrane and the target membrane can also be obtained with this model system, as the geometric constraints of a fusion peptide in its membrane-bound context are implicitly taken into account. This study was performed with target liposomes consisting of PS/PE (molar ratio 10 : 3) as Fourier-transform infrared spectroscopy (FTIR) measurements with target membranes containing PE-Lys are precluded owing to an overlap in the signals of the amide band of the peptide and those of the lysine residue of PE-Lys. Aggregation between donor and target vesicles was brought about by the addition of Ca^{2+}. We were able to determine that the WAE peptide inserted into the target membrane as a sided α-helix, with an angle perpendicular to the surface of the membrane ***(12)***.

4. Notes

The pivotal and critical stage of our peptide model system is the coupling of the peptide to the liposomal surface. Careful attention must be paid to the quality of the coupling lipid PE-PDP, and it is essential to check its integrity by TLC before use. Careful attention must also be paid to the state of oligomerization of the peptide as in case of dimerization through the Cys residues, its potential to couple to liposomes is considerably reduced if not totally impaired. However, having considered these parameters, it must be noted that the coupling procedure *per se* is extremely reproducible, as confirmed by evaluating the coupling yield by infrared spectroscopy. Also the stability of the coupling is excellent over a period of 1 wk, even in diluted suspension of liposomes (lipid concentration < 1 m*M*), provided that the peptide-coupled vesicles are stored in the dark at 4°C. This applies to both the peptide/lipid ratio and the amounts of various secondary structures associated with the peptide, which remain constant over that time period. Indeed, the peptide/lipid ratio was found to be 1 : 40 and the amount of α-helical structures ~50% the day of preparation and 7 d later. This stability allows concentration of the liposome

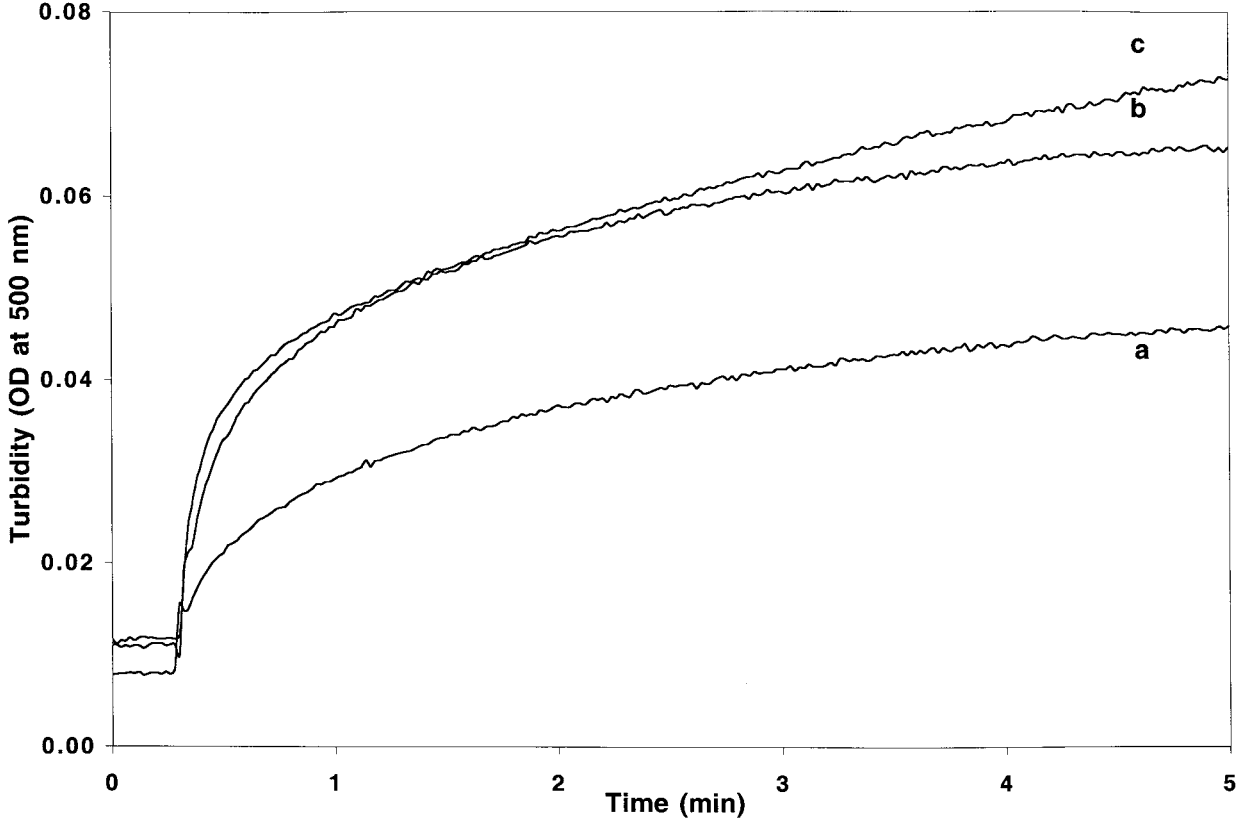

Fig. 1. Time course of vesicle aggregation between positively charged and peptide-coupled liposomes at neutral pH. Aggregation was followed by measuring the turbidity of the suspensions at 500 nm. **a**, **c**: Cationic vesicles vs WAE-liposomes without **(a)** or with 6 mol% **(c)** biotinPE. **b**: Cationic vesicles vs peptide-free liposomes with 6 mol% biotinPE. The total lipid concentration was 70 μ*M*, and experiments were carried out in 10 m*M* Tris, 150 m*M* NaCl, pH 7.4.

sample after gel filtration by Airfuge™ or SpeedVac™ (although this latter technique may lead to an undesired increase in the salt concentration, which may result in the swelling of liposomes when placed into a large volume of isotonic buffer).

The WAE system or analogous systems employing different peptides offer the possibility to dissect at the molecular level the different steps of a fusion process. Indeed, aggregation between donor and target vesicles can be driven by the WAE peptide itself, via electrostatic interactions with a positively charged lipid incorporated in the target membrane, such as PE-lys (**Fig. 1**, *curve a*) ***(8)***. But it can also be driven by biotinPE incorporated into the donor peptide-coupled membranes, and interacting with either PE-PDP-anchored avidin or PE-Lys itself on the target membrane. By this means, the WAE peptide is relieved from its aggregation function and serves merely as a fusogen in the system (**Fig. 1**, *curves b* and *c*), which allows for higher rates and extents of lipid mixing (**Fig. 2A**) and content mixing (**Fig. 2B**) ***(8)***.

Owing to the presence of a Trp residue, the interactions of the peptide with the target membrane, but also with its own membrane, can be monitored by following changes in the Trp intrinsic fluorescence (λ_{exc} = 280 nm; emission scan). An increase in the quantum yield and a shift of the spectral maximum below 350 nm (the maximum observed in a hydrophilic environment) is indicative of a migration of the Trp residue to a more hydrophobic environment. Concomitantly, the accessibility of Trp to aqueous and nonmembrane permeant quenchers of fluorescence can be monitored. Quenching of the Trp fluorescence thus indicates that the residue senses the quencher, and is therefore in the aqueous phase surrounding the vesicles. Conversely, a lack of quenching indicates that the Trp is shielded from the quencher, and is therefore likely inserted into the membrane as a mimic of what is observed for viral fusion peptides in their protein environment at the surface of the virus ***(22)***.

Subsequently, the fusion properties of the peptide can be assessed as described in **Subheading 3**. It is important to verify whether the presence of a peptide at the surface of liposomes does not interfere with the fluorescence assays. Such controls have been carried out for the WAE system and were shown to be negative. Indeed the initial values of fluorescence of *N*-NBD-PE/*N*-Rh-PE-labeled liposomes and that of Tb-loaded liposomes containing PE-PDP are similar, irrespective of the presence of coupled peptide. Neither does the WAE peptide induce a destabilization/leakage of the liposomes to which it is coupled as verified by measuring the fluorescence of Tb–DPA-loaded peptide-coupled vesicles as a function of time. Temperature is a critical point in these experiments because it affects both the quantum yield of fluorescence and the fusogenic properties of the peptide; it is thus important when performing an experiment as a function of temperature to allow the peptide-coupled liposomes

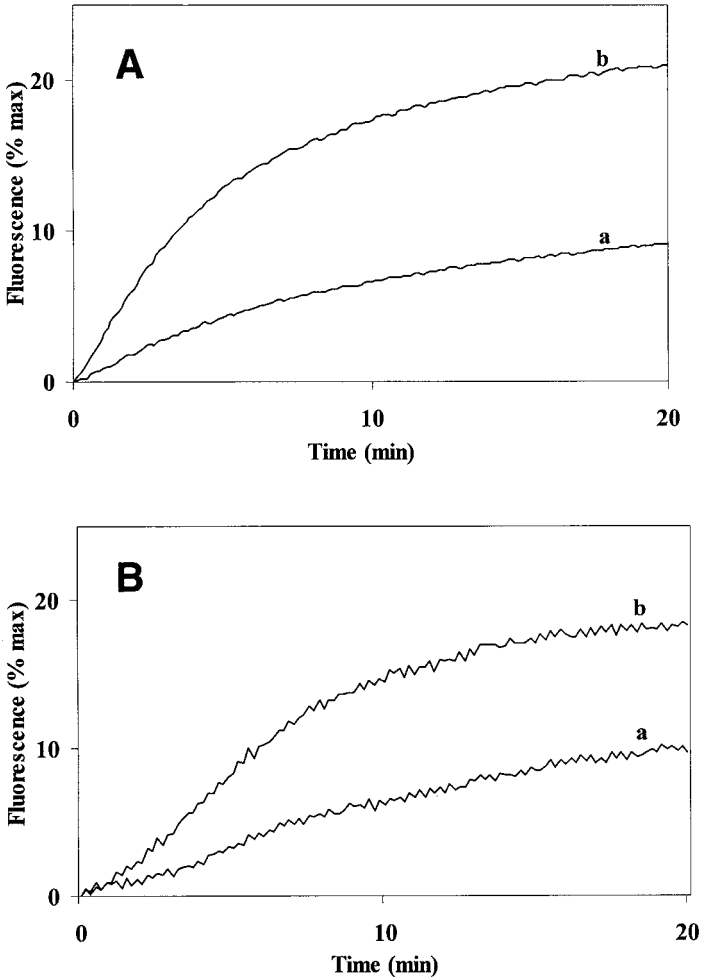

Fig. 2. Time course of lipid and internal contents mixing on interaction of positively charged target and peptide-coupled liposomes at neutral pH. **A**: Lipid mixing; WAE-coupled liposomes labeled with 1 mol% each of *N*-NBD-PE and *N*-Rh-PE were added to PE-Lys vesicles (PE-Lys at 15 mol%) in a lipid molar ratio of 1:6 (total lipid concentration 70 μ*M*). The buffer was 10 m*M* Tris, 150 m*M* NaCl, pH 7.4. The increase in *N*-NBD-PE fluorescence was recorded continuously. **B**: Internal contents mixing; WAE-coupled liposomes containing $TbCl_3$ were added to DPA-loaded PE-Lys vesicles in the same molar ratio as for the lipid mixing assay, in 10 m*M* HEPES, 100 m*M* NaCl, 1 m*M* EDTA, pH 7.4. In both assays: **(a)** liposomes without biotinPE; **(b)** liposomes with 6 mol% biotinPE.

to equilibrate for at least 1 min at the temperature of the buffer. Indeed, WAE-induced fusion, like fusion induced by viral fusion peptides or proteins, is impaired at temperatures below 10–12°C and is maximal around 37°C.

The simplicity of this peptide model system allows its use in a number of applications, from gaining molecular insight into the mechanisms of membrane fusion at the level of the fusion peptide to its use, for example, as a fusogenic "drug-delivery system" for encapsulated material into cells. The encapsulated material can be of varying nature and size because the size of the peptide-coupled liposomes can be easily modulated to the desired diameter at the extrusion stage. It must be noted at this point that the coupling reaction and yield are totally independent of the vesicle size and thus allow for a great flexibility in terms of applications. From a fundamental point of view, this model system appears of great value, as the fusogenic properties of the peptide are brought about by its membrane anchorage. This makes it closely resemble the properties of fusion peptides as present in their membrane-anchored glycoprotein environment at the surface of viruses or cells ***(8)***.

Such an approach could be applied to other peptides, polypeptides, or protein fragments derived from membrane-bound proteins, in an attempt to analyze their lipid-interacting properties in a context resembling their biological environment. Indeed, this approach respects key features of a biological medium: (1) the three-dimensional context, the model system relying on the use of liposomes in aqueous suspensions; (2) the lipid composition of the liposomes and the pH of the buffer used, modulated according to the medium studied; and (3) the covalent membrane anchorage of a protein-derived fragment, and more specifically of a fusion peptide or a fusion domain, by the geometrical constraints it induces which closely simulates orientational features as observed on the biological membrane from which they originate.

References

1. Bartlett, G. R. (1959) Phosphorus assay in column chromatography. *J. Biol. Chem.* **234,** 466–468.
2. New, R. R. C. (1990) Characterization of liposomes, in *Liposomes: A Practical Approach* (New, R. R. C., ed.), IRL Press, Oxford, pp. 105–162.
3. Martin, F. J., Hubbell, W. L., and Papahadjopoulos, D. (1981) Immunospecific targeting of liposomes to cells: a novel and efficient method for covalent attachment of Fab′ fragments via disulfide bonds. *Biochemistry* **20,** 4229–4238.
4. Puyal, C., Milhaud, P., Bienvenue, A., and Philippot, J. R. (1995) A new cationic liposome encapsulating genetic material. A potential delivery system for polynucleotides. *Eur. J. Biochem.* **228,** 697–703.

5. Szoka, F., Jr. and Papahadjopoulos, D. (1978) Procedure for preparation of liposomes with large internal aqueous space and high capture by reverse-phase evaporation. *Proc. Natl. Acad. Sci. USA* **75,** 4194–4198.
6. Pécheur, E. I., Sainte-Marie, J., Bienvenüe, A., and Hoekstra, D. (1999) Peptides and membrane fusion: towards an understanding of the molecular mechanism of protein-induced fusion. *J. Membr. Biol.* **167,** 1–17.
7. White, J. M. (1992) Membrane fusion. *Science* **258,** 917–924.
8. Pécheur, E. I., Hoekstra, D., Sainte-Marie, J., Maurin, L., Bienvenüe, A., and Philippot, J. R. (1997) Membrane anchorage brings about fusogenic properties in a short synthetic peptide. *Biochemistry* **36,** 3773–3781.
9. Gailit, J. (1993) Restoring free sulfhydryl groups in synthetic peptides. *Analyt. Biochem.* **214,** 334–335.
10. Gergel, D. and Cederbaum, A. I. (1997) Interaction of nitric oxide with 2-thio-5-nitrobenzoic acid: implications for the determination of free sulfhydryl groups by Ellman's reagent. *Arch. Biochem. Biophys.* **347,** 282–288.
11. Pécheur, E. I., Martin, I., Ruysschaert, J. M., Bienvenüe, A., and Hoekstra, D. (1998) Membrane fusion induced by 11-mer anionic and cationic peptides: a structure–function study. *Biochemistry* **37,** 2361–2371.
12. Martin, I., Pécheur, E. I., Ruysschaert, J. M., and Hoekstra, D. (1999) Membrane fusion induced by a short fusogenic peptide is assessed by its insertion and orientation into target bilayers. *Biochemistry* **38,** 9337–9347.
13. Kok, J. W. and Hoekstra, D. (1999) Fluorescent lipid analogues: applications in cell and membrane biology, in *Fluorescent and Luminescent Probes for Biological Activity*, 2nd ed. (Mason, W. T., ed.), Academic Press, London, pp. 136–155.
14. Düzgünes, N. and Wilschut, J. (1993) Fusion assays monitoring intermixing of aqueous contents. *Methods Enzymol.* **220,** part A, 3–14.
15. Hoekstra, D. and Düzgünes, N. (1993) Lipid mixing assays to determine fusion in liposome systems. *Methods Enzymol.* **220,** part A, 15–32.
16. Nichols, J. W. and Pagano, R. (1981) Kinetics of soluble lipid monomer diffusion between vesicles. *Biochemistry* **20,** 2783–2789.
17. Struck, D., Hoekstra, D., and Pagano, R. E. (1981) Use of resonance energy transfer to monitor membrane fusion. *Biochemistry* **20,** 4093–4099.
18. Hoekstra, D., Buist-Arkema, R., Klappe K., and Reutelingsperger, C. P. M. (1993) Interaction of annexins with membranes: the N-terminus as a governing parameter as revealed with a chimeric annexin. *Biochemistry* **32,** 14194–14202.
19. Wilschut, J., Düzgünes, N., Fraley, R., and Papahadjopoulos, D. (1980) Studies on the mechanism of membrane fusion: kinetics of calcium ion induced fusion of phosphatidylserine vesicles followed by a new assay for mixing of aqueous vesicle contents. *Biochemistry* **19,** 6011–6021.
20. Düzgünes, N., Allen, T. M., Fedor, J., and Papahadjopoulos, D. (1987) Lipid mixing during membrane aggregation and fusion: why fusion assays disagree. *Biochemistry* **26,** 8435–8442.

21. Goormaghtigh, E., Cabiaux, V., and Ruysschaert, J. M. (1990) Secondary structure and dosage of soluble and membrane proteins by attenuated total reflection Fourier-transform infrared spectroscopy on hydrated films. *Eur. J. Biochem.* **193,** 409–420.
22. Novick, S. L. and Hoekstra, D. (1988) Membrane penetration of Sendai virus glycoproteins during the early stages of fusion with liposomes as determined by hydrophobic photoaffinity labeling. *Proc. Natl. Acad. Sci. USA* **85,** 7433–7437.

4

Liposomes

Applications in Protein–Lipid Interaction Studies

Sujoy Ghosh and Robert Bell

1. Introduction

Liposomes are synthetic mimics of cellular membranes and represent an experimental system widely used for more than 30 yr in the field of biochemical research involving lipids. Liposomes typify a hallmark in the reductionist's approach to biology: by controlling the nature and mole fraction of the lipids composing the liposomes, the investigator is able to precisely determine the effects of such lipids on the biological process under study. With few exceptions, lipids are generally hydrophobic in nature, a property traditionally making them difficult to study. Liposomes provide a way around the solubility problem and consequently make it feasible to study the roles of lipids in various cellular processes. The application of liposomes in biological and biochemical research today can be broadly classified into the following five categories:

1. Studies on protein–lipid interactions.
2. Studies on the regulation of protein function by lipids.
3. Studies on membrane dynamics.
4. Structural studies on membrane associated proteins.
5. Delivery systems for biomolecules and small molecules into cells.

1.1. Studies on Protein–Lipid Interactions

Several proteins translocate to cellular membranes in response to intracellular and extracellular signals. This movement of the proteins from one location in the cell (cytosol) to another (a membrane surface) is often necessary for normal functioning of the protein. Translocation to cell membranes is often

From: *Methods in Molecular Biology, vol. 199: Liposome Methods and Protocols*
Edited by: S. Basu and M. Basu © Humana Press Inc., Totowa, NJ

achieved by an interaction of the protein with the lipids constituting the membrane, through specific domains within the protein. Understanding the details of such protein–lipid interactions is crucial to signal transduction research, especially for cell signaling pathways originating at cell membranes. With the aid of molecular biological methods such as recombinant DNA technology, deletion and site-directed mutagenesis, and by using liposomes of a defined physical and chemical composition, it is now possible to map the association of cell signaling proteins with membrane lipids in great detail, enhancing our understanding of signal transduction processes. Indeed, such an approach has greatly contributed to our understanding of the lipid-association properties of critical cell signaling proteins such as protein kinase C ***(1–3)***, Raf-1 kinase ***(4,5)***, the G-α subunit of heterotrimeric G proteins ***(6)***, Vac1p, Vps 27p ***(7)***, and the human immunodeficiency virus type 1 matrix protein, p17MA ***(8)***, to name a few.

1.2. Studies on the Regulation of Protein Function by Lipids

Besides functioning as important structural elements of the cell membrane, many lipids also play a regulatory role in cellular metabolism by stimulating or inhibiting specific enzyme activities. Lipids affecting signal transduction pathways by influencing the activity of key cell signaling molecules have come to be known as lipid second messengers; examples of this class of lipids include diacylglycerol, sphingosine, ceramide, arachidonic acid, among others. Proteins shown to be regulated by lipids include specific isoforms of protein kinase C which are activated on binding one molecule of the neutral lipid diacylglycerol in the presence of an acidic phospholipid such as phosphatidylserine ***(9,10)*** and the Ral-GDP dissociation stimulator protein (Ral GDS), a downstream effector of Ras that is inhibited by acidic phospholipids such as phosphatidylinositol or phosphatidylserine ***(11)***.

1.3. Studies on Membrane Dynamics

Liposomes behave as model membrane systems and, as such, may be used for investigating membrane dynamics in response to specific stimuli, in vitro. Changes in the physical and chemical properties of membranes provide an integral part of cell behavior and lie at the core of several cell-signaling pathways originating in the plasma membrane. For example, liposomes have been used to demonstrate the presence of membrane microdomains, known as DIGEM (Detergent Insoluble Glycosphingolipid Enriched Microdomains), which are enriched in clustered glycosphingolipids and where signaling proteins such as Ras, Rho, c-Src, and Fak are also found to colocalize ***(12)***. In another example, when vesicles containing an equimolar mixture of sphingomyelin, phosphatidylcholine, phosphatidylethanolamine, and cholesterol are

coincubated with phospholipase C and sphingomyelinase, the joint hydrolytic activities of the two enzymes result in vesicle fusion; the aggregation is not observed when only one enzyme activity is included ***(13)***. In another study, phosphatidylserine-containing liposomes have been shown to increase the stimulus-induced (induced by formylmethionyl-leucyl-phenylalanine) generation of reactive oxygen species in neutrophils, suggesting the role of a phosphatidylserine-containing membrane surface in the process ***(14)***.

1.4. Structural Studies on Membrane-Associated Proteins

Liposomes have been widely used as model systems for structural studies on membrane-associated proteins and peptides through various methods including nuclear magnetic resonance (NMR), Fourier-transform infrared spectroscopy (FTIR) spectroscopy, circular dichroism, and so forth. These studies enable one to ascertain how neighboring lipid molecules can affect the structure of the protein or peptide. Examples of the application of liposomes in this area include a study determining the effects of neutral and acidic phospholipids on the structure of a lipid-binding domain of Raf-1 kinase by 2D-NMR ***(15)***. In another study, ^{2}H-NMR has been employed to assess the orientation and motion of a peptide fragment of the human EGF receptor in a bilayer environment constituted with liposomes containing 1-palmitoyl-2- oleoylphosphatidylcholine (POPC) and cholesterol ***(16)***.

1.5. Delivery of Biomolecules and Small Molecules into Cells

Specially formulated cationic liposomes have been developed and are now widely used for the delivery of biomolecules (nucleic acids, peptides, antibodies, etc.) and small molecules (drugs, chemically synthesized inhibitors/activators of intracellular enzymes, etc.) in cultured cells ***(17,18)***. Cationic liposomes often offer an experimental advantage in delivery efficiency over other existing methods such as calcium phosphate transfection, scrape loading, etc. These liposomes are now commercially available from several vendors.

The focus of the present chapter is on the application of liposomes toward understanding protein–lipid interactions. (*See* **Note 1**.) Our experience with protein–lipid interaction is built on studies performed with protein kinase C and Raf-1 kinase. These studies have led to the identification of specific domains within the two proteins and critical amino acid residues within the domains that mediate interaction with specific lipids. The experimental procedures involved in these studies are based on the following steps:

1. Experimental design, selection of controls.
2. Expression and affinity purification of recombinant proteins from *E. coli*.
3. Preparation of liposomes.

4. Incubation of proteins with liposomes in solution.
5. Precipitation of liposome-bound protein and separation from unbound protein.
6. Preparation of precipitated protein for sodium dodecyl sulfate-polyacrylamide gel electrophoresis (SDS-PAGE).
7. PAGE of liposome-bound protein.
8. Staining and quantification of electrophoresed proteins by scanning densitometry.

The major focus of the following subheadings will be on the application of liposomes for experimental studies employed in our laboratory for invesigating the interaction of protein kinase C-γ and Raf-1 kinase with phospholipids. The majority of the methods described are incorporated in previous publications ***(19,20)***. These studies were conducted with protein fragments (corresponding to full-length or specific domains of protein kinase C and Raf-1 kinase) overexpressed in *E. coli* using standard molecular biological procedures ***(21)*** and purified by affinity chromatography. All studies were done in vitro, where purified proteins of interest were incubated with freshly prepared liposomes of varying phospholipid composition for a given period of time and the degree of association of the proteins with the liposomes subsequently assessed by gel electrophoretic methods.

2. Materials

1. L-[^{14}C]-α-Dioleoyl phosphatidylcholine (120 mCi / mmol) was from DuPont-New England Nuclear.
2. All phospholipids used were from Avanti Polar Lipids, Inc., with the exception of *bis*-phosphatidic acid, cardiolipin, and bovine brain phosphatidylserine, which were from Serdary.
3. Prestained protein molecular weight standards were from Bio-Rad.
4. Glutathione–agarose matrix (sulfur-linked) and phosphate-buffered saline (PBS) were from Sigma.
5. pGEX-2T prokaryotic expression vector was from Pharmacia-LKB Biotechnology Inc.
6. Competent DH5α strain of cells was from Life Technologies Inc.
7. Competent BL-21 strain of cells was from Novagen. All aqueous buffers used in the liposome association experiments were prepared fresh.
8. Extraction buffer: 50 m*M* 4-(2-hydroxyethyl)-1-piperazineethanesulfonic acid (HEPES), pH 8.0, 1 m*M* dithiothreitol (DTT), 0.1% Triton X-100, 10% ethylene glycol, 1 m*M* phenylmethylsulfonyl fluoride, 0.01 mg/mL of benzamidine, 0.02 mg/mL of antipain, and 0.01 mg/mL of leupeptin.
9. Lysis buffer: PBS, pH 7.3, 1 m*M* EDTA, 2 m*M* DTT, 0.5–1% Nonidet P-40, 0.01 mg/mL of benzamidine, 0.02 mg/mL of antipain, and 0.01 mg/mL of leupeptin.
10. Elution buffer: 50 m*M* HEPES, pH 8.0, 10% ethylene glycol, 2 m*M* DTT, 5 m*M* reduced glutathione, 0.01% Nonidet P-40.

11. Resuspension buffer: 50 m*M* Tris-HCl, pH 7.5, 10 m*M* $MgCl_2$, 0.1 m*M* DTT, 0.05 mg/mL of butylated hydroxytoluene, 0.1 m*M* diethylenetriamine pentaacetic acid, and either 1 m*M* $CaCl_2$ or EGTA.

All phospholipids were stored in glass tubes with Teflon-coated caps at –20 °C. Competent *E. coli* cells were stored at –80°C. All fusion proteins used in the study were also stored at –80°C.

3. Methods

The design of the liposome association experiments can be divided into three sections. If it is known from prior studies that a specific lipid binds to a full-length protein, then one aspect of the experimental design is to determine the region or regions within the protein that mediate such association. In this case, liposome binding studies are designed such that the composition of the liposomes, containing the lipid of interest, remains constant while several fragments of the protein of interest are used at a fixed concentration to determine which fragment or fragments are capable of associating with liposomes. Such studies, for example, have led to the identification of a cysteine-rich region in protein kinase C and Raf-1 kinase that interacts with liposomes containing acidic phospholipids such as phosphatidylserine ***(20,22)***. In the second case, if it is suspected that a protein or protein domain may be capable of lipid binding, then the domain may be tested for association with liposomes containing a variety of lipids in different molar ratios to determine the lipid binding profile ***(4)***. Finally, the dependence of association of a protein to a particular lipid may be determined by comparing the degree of association of the protein to liposomes containing the lipid of interest at increasing molar concentrations. In all examples, it is important to consider control experiments to avoid incorrect inferences based on experimental artifacts. One such control is determining the amount of protein recovered after precipitation (*see* **Subheading 3.5.**) in the absence of liposomes and in the presence of liposomes not containing the lipid of interest (if already known). Another control is to test different fragments from the same protein for binding to the liposomes; only the lipid-associating fragments should show significant binding. When recombinant fusion proteins are used for the assay (such as glutathione-*S*-transferase [GST]-fusion proteins), it is important to determine the association of the fusion tag (GST for example) with the liposomes under study. Nonspecific binding of any kind should be subtracted from total binding to estimate the specific binding of a protein to a liposome preparation. For reproducibility, each liposome association experiment should be repeated at least three times and the average of the protein association values be calculated to determine binding.

3.1. Expression and Purification of Proteins

3.1.1. Protein Expression

1. In all experiments, the proteins or protein fragments of interest (from protein kinase Cs and Raf-1 kinase) are fused to GST and overexpressed in *E. coli*. The GST-fusion proteins are generated by ligating a DNA sequence corresponding to the protein fragment of interest to the pGEX-2T prokaryotic expression vector.
2. The DNA sequences are obtained by polymerase chain reaction (PCR) from a template sequence using appropriate forward and reverse primers containing unique restriction sites (*BamH*1 and *EcoR*1 for Raf-1 fragments, for example). Typically, the PCR is carried out at 94°C for 5 min followed by 30–40 cycles each at 94°C for 1 min, 55°C for 1 min, and 72°C for 2 min.
3. The products obtained by PCR are digested with both restriction enzymes (corresponding to the unique restriction sites designed on the forward and reverse primers), purified on a low-melting agarose gel such as 2% low-melt SeaPlaque agarose (FMC Bioproducts), and then directionally subcloned into the appropriately digested plasmid vector, pGEX-2T.
4. The recombinant DNA plasmids are transfected initially into DH5α cells. Some protein fragments (such as full-length Raf-1) are degraded when expressed in DH5α cells; they are retransfected into the BL-21 strain of *E. coli* (Novagen, deficient in the *lon* and *ompT* proteases) for protein expression.
5. *E. coli* with plasmids containing the required inserts are grown in Luria–Bertiani broth overnight at 37°C under ampicillin selection (0.05 mg/mL of ampicillin) until the stationary phase is reached. A fresh culture is inoculated at 37°C with these cells (1–2 mL cells per 100 mL of Luria–Bertiani broth) and grown to an absorbance of 0.5–0.6 measured at 600 nm.
6. At that density the cells are transferred to 20°C and allowed to grow to an absorbance of 0.7–0.8, when protein expression is induced by addition of isopropyl-β-D-thiogalactopyranoside (IPTG; 50 mg/mL stock solution) to a final concentration of 0.02 m*M*. The culture medium is also fortified at this stage with 0.01 m*M* $ZnCl_2$ (*see* **Note 2**). Depending on the proteins expressed, the cells are harvested between 1 and 16 hours post induction, centrifuged to remove supernatant, and the pellets frozen at –70°C until further use.

3.1.2. Protein Purification by Method A

1. To recover the GST-fusion proteins from the frozen cell pellets, the pellets are lysed by cavitation (French press) in extraction buffer at a ratio of 1 mL of buffer per cell pellet from 15 mL of *E. coli* culture medium. Insoluble cell debris is removed by centrifugation at 15,000*g* for 10 min at 4°C.
2. The supernatant is applied to an equal volume of glutathione–agarose (Sigma) matrix preequilibrated in phosphate buffer, pH 7.3 (1 m*M* sodium phosphate, 15 m*M* NaCl). After the resin is washed with 10 column volumes of phosphate buffer to remove nonspecifically bound proteins, the GST-fusion proteins are

then specifically eluted with 5 m*M* reduced glutathione (*see* **Note 3**) in 50 m*M* HEPES, pH 8.0, with 10% ethylene glycol.

3. The eluted proteins are characterized on 10–12.5% minigels by SDS-PAGE. The purified proteins are stored at –70°C in elution buffer. Under these conditions the proteins were stable for > 2 yr.

3.1.3. Protein Purification by Method B

1. The frozen cell pellet is lysed in lysis buffer at a ratio of 10 mL of buffer per 100 mL of *E.coli* culture medium. The resuspended cell pellet is sonicated using a probe sonicator (three times for 15 s each, keeping the tubes in ice water at all times).
2. The lysate is then centrifuged at 15,000*g* for 10 min at 4°C and the pellet discarded.
3. The supernatant is then applied to 0.1 volume of glutathione–agarose resin that had been prewashed in PBS (1 mL of resin for 10 mL of supernatant, for example) in a 50-mL centrifuge tube. The tube is rotated gently for 15–20 min at room temperature and then poured into a 10-mL plastic disposable column (Bio-Rad). The column is washed first with 10 column volumes of lysis buffer followed by 10 column volumes of lysis buffer with 0.01% Nonidet P-40.
4. Following the washes, the GST-fusion proteins are eluted in elution buffer, characterized by SDS-PAGE, and stored at –70°C.

3.2. Preparation of Liposomes

Liposomes contain more than one phospholipid in varying ratios (expressed as mole fractions) and are prepared such that the total lipid concentration is 0.5 mg/mL (*see* **Note 4**).

1. Liposomes are prepared by first drying down the stock solutions of phospholipids (in chloroform or ethanol) under a stream of nitrogen in glass tubes.
2. The dried-down lipids are then suspended in resuspension buffer by sonication in a bath sonicator. Sonication is repeated three times for 15 s each with intermittent cooling on ice for 30 s each.
3. Following sonication, liposome preparations are stored on ice and used within 1 h. For the determination of lipid recovery in precipitated liposomes, trace amounts (< 10% of total phospholipids) of ^{14}C-labeled phosphatidylcholine may be used.

3.3. Incubating Proteins with Liposomes in Solution

Reactions are carried out in Beckman ultracentrifuge tubes suitable for use in a Beckman TL-100 ultracentrifuge as follows:

1. Dilute liposome solutions fivefold in resuspension buffer to a final lipid concentration of 0.1 mg/mL (e.g., add 0.4 mL of buffer to 0.1 mL of liposome solution).

2. Add other reagents (e.g., phorbol esters, diacylglycerol, etc.) at desired concentrations as necessary.
3. Add proteins at desired concentrations and incubate at 25°C for 30 min.

3.4. Precipitation of Liposomes (See Note 5)

1. At the end of incubation in **Subheading 3.3., step 3**), centrifuge the tubes at 500,000*g* for 15 min at 4°C in a Beckman TL-100 ultracentrifuge.
2. At the end of centrifugation, place the samples immediately on ice. Remove and discard supernatant.
3. Solubilize the pellets in 0.1 mL of EDTA buffer (10 m*M* Tris-HCl, pH 7.5–8.0, 1 m*M* EDTA) containing 10% Triton X-100 detergent.
4. Measure lipid recovery for each pellet by determining the [^{14}C]phosphatidylcholine radiolabel in a 0.01-mL aliquot of the resolubilized pellet.
5. Process remainder of the samples for SDS-PAGE analysis.

3.5. Preparation of Precipitated Protein for SDS-PAGE Analysis (19)

Resolubilized protein sample from **Subheading 3.4., step 5** is transferred to a microcentrifuge tube and treated as follows:

1. Add four volumes of methanol to the protein sample (0.4 mL of methanol to 0.1 mL of protein sample, for example).
2. Vortex-mix and centrifuge for 10 s at 9000*g* at room temperature in a microcentrifuge.
3. Add chloroform equal to two volumes of protein sample (0.2 mL of chloroform for 0.1 mL of protein), vortex-mix, and centrifuge again for 10 s at 9000*g* at room temperature.
4. Add 0.35 mL of water to the centrifuged samples (for phase separation), vortex-mix the samples vigorously for 1 min, and then centrifuge for 1 min at 9000*g* at room temperature.
5. Carefully remove and discard the upper phase. Precipitated proteins are present in the interphase. Take care not to disturb the interphase.
6. Add 0.35 mL of methanol to lower phase, vortex-mix, and centrifuge for 2 min at 9000*g* to pellet the proteins.
7. Remove and discard supernatant and air-dry the protein pellet. Resuspend the pellet in SDS-PAGE sample buffer and proceed to electrophoresis.

3.6. PAGE of Liposome-Bound Protein

1. Following chloroform/methanol precipitation (**Subheading 3.5., step 6**), the pelleted protein is resuspended in SDS-PAGE sample buffer ***(20)***.
2. Proteins are analyzed on 10% or 12.5% polyacrylamide minigels (the percentage of the minigel is chosen based on the size of the protein fragment to be

analyzed) using Bio-Rad or Novagen electrophoresis units and by following the manufacturer's directions.
3. To determine "percent association" (explained in **Subheading 3.7.**), run a sample of the total amount of protein used per incubation.

3.7. Staining and Quantification of Electrophoresed Proteins by Scanning Densitometry

1. The electrophoresed protein samples are visualized by staining with Coomassie Brilliant Blue stain ***(20)***.
2. The protein band intensities are quantified by scanning densitometry (Photometrics Ltd., Tucson, AZ) used in conjunction with the NIH Image image processing software.
3. The intensity of a protein band recovered after incubation with liposomes, expressed relative to the intensity determined for the total amount of protein used in each assay, is referred to as the "percent association." These values, corrected with the lipid recovery factor determined from ^{14}C-radiolabeled phosphatidylcholine recovery, may be plotted as a function of the concentration of the test lipid in the liposomes (expressed as mole percent of total lipid) to determine the affinity of the protein fragment studied for the lipid of interest.

4. Notes

1. In addition to liposomes, two other related methods for studying protein–lipid interactions were developed in our laboratory and are briefly mentioned here. One of them employs "mixed micelles" of detergents and lipids in place of liposomes to investigate the binding and regulation of enzymes by specific phospholipids. By controlling the composition of the mixed micelles, one is able to vary the number of lipid molecules per micelle. This technique has been employed to determine the number of diacylglycerol and PS molecules that bind and activate protein kinase C ***(27)*** and to identify phospholipid activators of yeast cholinephosphotransferase ***(28)***. The second method, known as the "enzyme-linked immunosorbent assay (ELISA) format assay," is based on a solid-phase binding assay in which lipid mixtures of choice are bound to polystyrene plates and incubated with proteins or protein fragments of interest. Unbound proteins are washed off and proteins that bind lipids are detected immunologically by an antibody directed against an epitope of the protein. In our example, an antibody to GST was used to determine the domains of Raf-1 kinase, all expressed as GST-fusion proteins, that bind PS and PA ***(5)***. Details of these methods are given in the relevant publications.
2. The inclusion of 1 m*M* $ZnCl_2$ in the *E. coli* culture medium is to ensure that enough Zn atoms are available for coordination to the Zn-binding cysteine-rich domains of the overexpressed proteins (protein kinase Cs or Raf-1 kinase).
3. It is important to remember to use reduced glutathione for elution of the GST-fusion proteins from the glutathione–agarose affinity matrix. Nonreduced

glutathione, which is also commercially available, will result in a greatly decreased elution efficiency of the GST-fusion proteins.

4. Liposomes containing phosphatidylserine (PS) are always prepared in the presence of phosphatidylcholine (PC): PC is known not to interact with protein kinase C or Raf-1 kinase. The reason for the inclusion of PC is the following. Many experiments employing liposomes contain divalent cations (such as calcium in conjunction with PS liposomes) which can cause sonicated PS vesicles to aggregate ***(23)***, leading to experimental difficulties. However, when vesicles are prepared using a PS/PC mixture, stable bilayers are generated, reducing the problem of aggregation in the presence of cations ***(24,25)***. This led us to always incorporate PC in liposomes containing PS.
5. To ensure quantitative precipitation of liposomes, we include 10 m*M* $MgCl_2$ in the liposome resuspension buffer. This addition is based on the observation that PS/PC vesicle preparations can be sedimented quantitatively in the presence of magnesium ions ***(26)***.

References

1. Kishimoto, A., Takai, Y., Mori, T., Kikkawa, U., and Nishizuka, Y. (1980) Activation of calcium and phospholipid-dependent protein kinase by diacylglycerol, its possible relation to phosphatidylinositol turnover. *J. Biol. Chem.* **255,** 2273–2276.
2. Jimenez-Monreal, A. M., Aranda, F. J., Micol, V., Sanchez-Pinera, P., de Godos, A., and Gomez-Fernandez, J. C. (1999) Influence of the physical state of the membrane on the enzymatic activity and energy of activation of protein kinase C alpha. *Biochemistry* **38,** 7747–7754.
3. Quest, A. F., Ghosh, S., Xie, W. Q., and Bell, R. M. (1997) DAG second messengers: molecular switches and growth control. *Adv. Exp. Biol.* **400A,** 297–303.
4. Ghosh, S., Strum, J. C., Sciorra, V. A., Daniel, L., and Bell, R. M. (1996) Raf-1 kinase possesses distinct binding domains for phosphatidylserine and phosphatidic acid. *J. Biol. Chem.* **271,** 8472–8480.
5. Ghosh, S. and Bell, R. M. (1997) Regulation of Raf-1 kinase by interaction with the lipid second messenger, phosphatidic acid. *Biochem. Soc. Trans.* **25,** 561–565.
6. Escriba, P. V., Ozaita, A., Ribas, C., Miralles, A., Fodor, E., Farkas, T., and Garcia-Sevilla, J. A. (1997) Role of lipid polymorphism in G protein-membrane interactions: nonlamellar-prone phospholipids and peripheral protein binding to membranes. *Proc. Natl. Acad. Sci. USA* **94,** 11375–11380.
7. Burd, C. G. and Emr, S. D. (1998) Phosphatidylinositol(3)-phosphate signaling mediated by specific binding to RING FYVE domains. *Mol. Cell* **2,** 157–162
8. Zhou, W. and Resh, M. D. (1996) Differential membrane binding of the human immunodeficiency virus type 1 matrix protein. *J. Virol.* **70,** 8540–8548.
9. Konig, B., DiNitto, P. A., and Blumberg, P. M. (1985) Stoichiometric binding of diacylglycerol to the phorbol ester receptor. *J. Cell. Biochem.* **29,** 37–44.
10. Kaibuchi, K., Takai, Y., and Nishizuka, Y. (1981) Cooperative roles of various membrane phospholipids in the activation of calcium-activated, phospholipid-dependent protein kinase. *J. Biol. Chem.* **256,** 7146–7149.

11. Kishida, S., Koyama, S., Matsubara, K., Kishida, M., Matsura, Y., and Kikuchi, A. (1997) Colocalization of Ras and Ral on the membrane is required for Ras-dependent Ral activation through Ral GDP dissociation stimulator. *Oncogene* **15,** 2899–2907.
12. Hakomori, S., Yamamura, S., and Handa, A. K. (1998) Signal transduction through glyco (sphingo)lipids. Introduction and recent studies on glyco(sphingo)lipid-enriched microdomains. *Ann. NY Acad. Sci.* **845,** 1–10.
13. Ruiz-Arguello, M. B., Goni, F. M., and Alonso, A. (1998) Vesicle membrane fusion induced by the concerted activities of sphingomyelinase and phospholipase C. *J. Biol. Chem.* **273,** 22977–22982.
14. Takahashi, M., Ikeda, H., Sato, E. F., Akimura, K., Edamatsu, R., Inoue, M., and Utsumi, K. (1992) Stimulus-specific enhancement of luminol chemiluminescence in neutrophils by phosphatidylserine liposomes. *Arch. Biochem. Biophys.* **298,** 43–48.
15. Xu, R. X., Pawelczyk, T., Xia, T. H., and Brown, S. C. (1997) NMR structure of a protein kinase C-gamma phorbol-binding domain and study of protein–lipid micelle interactions. *Biochemistry* **36,** 10709–10717.
16. Jones, D. H., Barber, K. R.,VanDerLoo, E. W., and Grant, C. W. (1998) Epidermal growth factor receptor transmembrane domain: 2H NMR implications for orientation and motion in a bilayer environment. *Biochemistry* **37,** 16780–16787.
17. Hayashida, W., Horiuchi, M., and Dzau, V. J. (1996) Intracellular third loop domain of angiotensin II type-2 receptor. Role in mediating signal transduction and cellular function. *J. Biol. Chem.* **271,** 21985–21992.
18. Ohta, S., Mizuno, M., Takaoka, T., and Yoshida, J. (1997) Augmentation of anti-Fas antibody-mediated apoptosis on human glioma cells by liposomes associated with the antibody. *J. Neurooncol.* **35,** 7–11.
19. Quest, A. F. G., Bardes, E. S. G., and Bell, R. M. (1994) A phorbol ester binding domain of protein kinase Cγ. *J. Biol. Chem.* **269,** 2953–2960.
20. Ghosh, S., Xie, W. Q., Quest, A. F. G., Mabrouk, G. M., Strum, J. C., and Bell, R. M. (1994) The Cysteine-rich region of Raf-1 kinase contains zinc, translocates to liposomes, and is adjacent to a segment that binds GTP-Ras. *J. Biol. Chem.* **269,** 10000–10007.
21. Sambrook, J., Fritsch, E. F., and Maniatis, T. (1989) *Molecular Cloning: A Laboratory Manual*, Cold Spring Harbor Laboratory Press, Cold Spring Harbor, NY.
22. Quest, A. F. G. and Bell, R. M. (1994) The regulatory region of protein kinase Cγ. *J. Biol. Chem.* **269,** 20000–20012.
23. Duzgunes, N., Wilschut, J., Fraley, R., and Papahadjopoulos, D. (1981) Studies on the mechanism of membrane fusion. Role of head-group composition in calcium- and magnesium-induced fusion of mixed phospholipid vesicles. *Biochim. Biophys. Acta* **642,** 182–195.
24. Hui, S., Stewart, T. P., and Boni, L. T. (1983) The nature of lipidic particles and their roles in polymorphic transitions. *Chem. Phys. Lipids* **33,** 113–126.
25. Boni, L. T. and Rando, R. R. (1985) The nature of protein kinase C activation by physically defined phospholipid vesicles and diacylglycerols. *J. Biol. Chem.* **260,** 10819–10825.

26. Sossin, W. S. and Schwartz, J. H. (1992) Selective activation of Ca^{2+} activated PKCs in *Aplysia* neurons by 5-HT. *J. Neurosci.* **12,** 1160–1168.
27. Bell, R. M., Hannun, Y., and Loomis, C. (1986) Mixed micelle assay of protein kinase C. *Methods Enzymol.* **124,** 353–359.
28. McMaster, C. R., Morash, S. C., and Bell, R. M. (1996) Phospholipid and cation activation of chimaeric choline/ethanolamine phosphotransferases. *Biochem. J.* **313,** 729–735.

5

Lipids in Viral Fusion

Anu Puri, Maite Paternostre, and Robert Blumenthal

1. Introduction

1.1. Viral Fusion Process

Enveloped animal viruses infect host cells by fusion of viral and target membranes. This crucial fusion event occurs either with the plasma membrane of the host cells or with the endosomal membranes ***(1)***. Fusion is triggered by specific glycoproteins in the virus membrane ***(2)*** and involves a range of steps before the final merging of membranes occurs. These steps include molecular processes, such as envelope protein conformational changes; aggregation of envelope protein; lipid–envelope protein interactions; and fusion pore formation and pore widening (*see* **Fig. 1**) ***(3,4)***. The reader is referred to a number of reviews on viral glycoprotein-mediated membrane fusion ***(5–9)***.

Because lipids are integral elements in the membrane fusion process, a number of key issues concerning the role of lipids deserve thorough examination.

1.2. Contribution of Physicochemical Properties of Various Membrane Lipids to Promote Fusion

The ability of membrane lipids to bend into curved structures is a crucial property in the fusion process. Chernomordik and co-workers ***(10)*** have shown that addition of amphiphiles to the outer monolayer that promote (e.g., oleic acid) or inhibit (e.g., lysophosphatidylcholine [lysoPC]) negative curvature respectively, will promote or inhibit the formation of the initial lipid junction. Conversely, amphiphiles added to the inner monolayer that promote positive curvature (e.g., lysoPC) will promote the formation of the fusion pore.

From: *Methods in Molecular Biology, vol. 199: Liposome Methods and Protocols*
Edited by: S. Basu and M. Basu © Humana Press Inc., Totowa, NJ

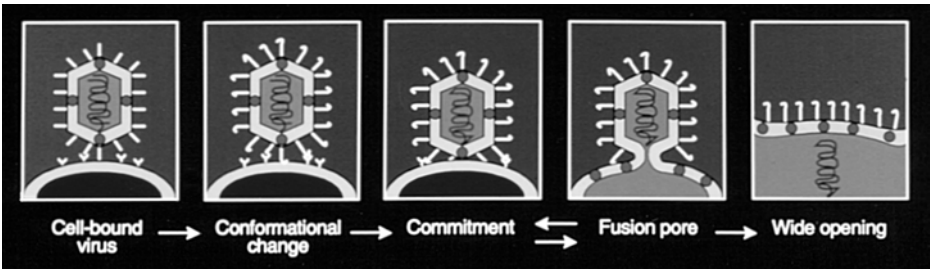

Fig. 1. A cartoon depicting various fusion intermediates following structural changes in viral proteins. This cartoon taken from Blumenthal et al. ***(3)*** shows fusion intermediates after virus binds to the target cells.

1.3. Effects of Target Membrane Lipid Asymmetry on Viral Fusion

The human erythrocyte plasma membrane is the most highly characterized system with respect to lipid asymmetry. In the human erythrocyte membrane, the aminophospholipids phosphatidylserine (PS) and phosphatidylethanolamine (PE) are preferentially located on the inner monolayer, while zwitterionic lipids such as PC and sphingomyelin (SM) are on the outer layer. Human erythrocyte ghosts can be manipulated such that their lipids are distributed either asymmetrically or symmetrically between inner and outer monolayers ***(11)***. We found that fusion of vesicular stomatitis virus (VSV) with lipid-symmetric erythrocyte ghosts was rapid at low pH and 37°C, whereas little or no fusion was observed with lipid-asymmetric ghosts. Biophysical studies indicate that the susceptibility to VSV fusion is not dependent on any particular phospholipid but is rather related to packing characteristics of the outer leaflet of the target membrane ***(11)***.

1.4. Requirement of Specific Lipids as Viral Receptors/Fusogens in Viral Fusion

A good example is Semliki Forest virus (SFV), which requires both cholesterol ***(12)*** and sphingomyelin ***(13)***. Cholesterol is required for binding, whereas SM acts as a cofactor, possibly through activation of the viral fusion protein ***(14)***. Specific glycosphingolipids (GSLs) are also known to serve as receptors for viruses such as influenza ***(15)*** and Sendai ***(16)***.

1.5. Modulation of Fusion by GSLs in the Target Membrane

Evidence for this concept is based on the fact that inhibitors of GSL biosynthesis affect human immunodeficiency virus type 1 (HIV-1) infection and fusion, and that fusion activity can be recovered following addition of

purified GSLs to the fusion-impaired cells ***(17,18)***. Studies in reconstituted monolayers of purified GSL at the air–water interface showed evidence for CD4-induced interactions between HIV-1 gp120 and certain GSLs (Gb3 and GM3) ***(19,20)***.

1.6. Methods to Study the Role of Membrane Lipids in Viral Fusion

The study of the role of lipids in fusion is not as straightforward as that of viral envelope glycoproteins and their protein receptors. Once the proteins have been cloned they can readily be expressed on the cell surface and their structure and function can be studied in the context of the fusion reaction. To examine the role of viral lipids more elaborate strategies have been developed. They include:

1. Amphiphiles (e.g., lysoPC, fatty acids) can be directly added to target membranes, or target membranes can be modified with phospholipases to produce these amphiphiles *in situ* ***(21)***. Although these methods have been successful in studying the role of membrane curvature in viral fusion, issues of partitioning, metabolism, and amount incorporated into the membrane have to be carefully examined ***(22)***.
2. Liposomes with defined lipid (phospholipid, cholesterol, and/or sphingolipid) composition can be used as targets for membrane fusion. However, in lipid mixing assays, nonspecific effects (unrelated to the known behavior of the viral envelope glycoprotein) have been noted ***(23)***. A number of low-pH fusing viruses (such as influenza, SFV, VSV) have been shown to fuse efficiently with liposomes with appropriate controls. A neutral pH fusing virus, Sendai fuses with liposomes, but has also been shown to fuse with greater efficiency with biological targets ***(24)***. Attempts to monitor viral envelope glycoprotein-specific fusion of other neutral pH-fusing viruses such as murine leukemia virus (MuLV) and HIV with liposomes have been unsuccessful.
3. Cholesterol levels in biological membranes have been altered by using agents such as methyl-β-cyclodextrin ***(25)***. Cell lines have also been selected with defective mobilization of cholesterol from the plasma membrane to the endoplasmic reticulum ***(26)***. Recent experiments from our laboratory indicate that cholesterol removal from target membranes significantly reduces their susceptibility to HIV-1 envelope glycoprotein-mediated fusion (M. Viard et al., *unpublished observations*). It is also possible to alter target membrane GSL levels by treatment of cells with inhibitors of GSL biosynthesis ***(18,37)***.

During the past few years, we have developed assays to monitor viral fusion in lipid-modified biological membranes. We describe in detail the following two methods of lipid addition to biological targets: (1) lipid incorporation into plasma membrane vesicles (PMVs) by detergent solubilization methods; (2) addition of GSL to nucleated cells by influenza hemagglutinin (HA)-mediated

fusion of liposomes containing specific GSLs. We also describe ways to monitor fusion of lipid-modified targets with viral envelope-glycoprotein-expressing cells. Finally we discuss the technical limitations encountered to incorporate natural lipids to the membranes of cells and possible experimental approaches to overcome these difficulties.

2. Materials

1. Fluorescent probes were from Molecular Probes (Eugene, OR).
2. Phospholipids were purchased from Avanti Polar Lipids (Alabaster, AL).
3. 10× Trypsin–EDTA: 0.5% Trypsin, 5.3 m*M* EDTA 4Na.
4. 100× Penn-Strep: 10,000 U/mL of penicillin G, 10,000 µg/mL of streptomycin sulfate in 0.85% saline.
5. 100× Penn-Strep-Gln: 10,000 U/mL of penicillin G sodium,10,000 µg/mL of streptomycin sulfate, and 29.2 mg of L-glutamine/mL in 0.85% saline.
6. Fetal bovine serum (FBS): Heat inactivated, mycoplasma tested (Life Technologies, cat. no. 16140-055).
7. RPMI: RPMI-1640 + L-glutamine (1×).
8. DMEM: Dulbecco's modified Eagle medium with 4.5 g of glucose per liter, without glutamine.
9. Phosphate-buffered saline (PBS): 137 m*M* NaCl, 2.7 m*M* KCl, 8.1 m*M* Na_2HPO_4, 1.5 m*M* KH_2PO_4, pH 7.4 (Life Technologies, cat. no. 14190-144).
10. D-PBS: Dulbecco's PBS containing 2 m*M* Ca^{2+} and 2 m*M* Mg^{2+}.
11. D2: DMEM containing 2% FBS.
12. D10: DMEM supplemented with 10% heat-inactivated FBS, 100 U/mL of penicillin, 100 µg/mL of streptomycin (Life Technologies, Custom Formula number 84-0199AJ).
13. D5: 500 mL of DMEM containing 10 mL of G418 sulfate solution (50 mg/mL GENETICIN aqueous solution, Life Technologies cat. no. 10131-027), 25 mL of FBS, and 5 mL of Penn-Strep-Gln.
14. R10: 500 mL of RPMI-1640 containing 50 mL of FBS and 5 mL of Penn-Strep solution.
15. HEPES-NaCl buffer: 10 m*M* 4-(2-Hydroxyethyl)-1-piperazineethanesulfonic acid (HEPES), 145 m*M* NaCl, pH 7.4, filter sterile through a 0.2-µm filter.
16. 1× Trypsin–EDTA: 20 mL of trypsin–EDTA (10×) is diluted with 180 mL of PBS. It is recommended to prepare the solution as needed but it can be stored at 4°C for about 2 wk.
17. Homogenization buffer: The quantities are given for 1-L solution. 1.42 g (10 m*M*, mol wt 142) Na_2HPO_4, 203 mg (1 m*M*, mol wt 203) $MgCl_2 \cdot 6H_2O$, 1.753 g (30 m*M*, mol wt 58.44) NaCl, 154 mg (1 m*M*, mol wt 154) dithiothreitol (DTT), 0.87 mg (0.005 m*M*, mol wt 174.2) phenylmethylsulfonyl fluoride (PMSF); 200 mg (0.02%) NaN_3. NaN_3 may be omitted depending on the experimental set up. Addition of a few micrograms of DNase is recommended to avoid precipitation

of DNA during the homogenization step. Homogenization buffer is filtered sterile through a 0.22-μm filter and stored at 4°C.

18. Mink-CD4 cells ***(27)***, a gift from Dr. Paul Clapham, Chester Beatty Institute, London, were grown in D5.
19. TF228.1.16 cells that constitutively express HIV-1 gp120-gp41 ***(28)*** (from Zdenka L. Jonak, Smithkline Beecham Pharmaceuticals, PA) were grown in R10.
20. Vero cells (an African green monkey kidney cell line) and HeLa cells (a human cervix epitheloid carcinoma cell line) were obtained from American Type Culture Collection (Rockville, MD) and grown in D10.
21. Purified VSV (Indiana serotype) was prepared by J. Brown and B. Newcomb at the University of Virginia as described ***(29)***.
22. Influenza virus (A/PR8/34/H1N1 strain) was grown in 11-d embryonated eggs as described previously ***(30)***. One-milliliter aliquots of influenza virus (allantoic fluid) were stored at –70°C.
23. PD10 column (Pharmacia)
24. Trypsin: 1 mg/mL stock in PBS. Use tissue culture tested (Sigma).

3. Methods

3.1. Incorporation of Cardiolipin into the PMVs

*3.1.1. Preparation of PMVs **(35)***

1. Vero cells are grown in D10 to nearly 90% confluency in six to eight T150 tissue culture flasks.
2. The cells are harvested using 1× trypsin–EDTA. Each flask is treated as follows: culture medium is removed, and 15 mL of 1× trypsin–EDTA solution is added, rinsed, and trypsin solution is aspirated. This step is repeated and 4 mL of 1× trypsin–EDTA solution is added to the flask and incubated at 37°C for 8–12 min. The cells should be detached from the flask as seen under a microscope. Sixteen milliliters of D10 medium is added to the cells, mixed by pipetting several times, and transferred to a 50-mL centrifuge tube. The cells are pelleted by centrifugation at 800–1200 rpm for 5–10 min at 4°C.
3. The cell pellets are combined into a 50-mL centrifuge tube and washed by resuspending in 30–40 mL of PBS, followed by centrifugation as described in **step 2**. The supernatant is removed and this step is repeated again. The cell numbers are counted at this step using a cell counting chamber.
4. The cells are centrifuged and the pellet is resuspended in cold homogenization buffer at a concentration of 1–2 × 10^8 cells/mL and homogenized using an ice bath by means of a precooled Teflon-coated homogenizer (10–15-mL capacity). Usually 10–30 strokes are sufficient for complete lysis of cells.
5. An aliquot is tested for efficient lysis of cells as follows: 20 μL of lysed cells are mixed with an equal volume of Trypan blue (0.4% solution in sterile PBS,

stored at room temperature) and observed under the microscope. Maximum lysis is determined by uptake of dye by the cells. (Any dye that can stain live/dead cells can be used at this step.)

6. The nuclei are removed by centrifugation at 500*g* for 10 min at 4°C. The supernatant (which contains PMV) is transferred to another tube, adjusting the volume to 3 mL by addition of cold homogenization buffer.
7. One milliliter of 41% sucrose solution (prepared in sterile distilled water) is placed in a 4-mL capacity centrifuge tube (for Beckman Rotor SW60), 3 mL of supernatant (from **step 6**) is gently layered on the 1-mL 41% sucrose cushion, and the solution centrifuged at 100,000*g* for 1 h at 4°C.
8. The tubes are carefully removed from the rotor buckets. A cloudy layer of PMV should be visible above the 41% sucrose layer. The clear supernatant just above the PMV layer is discarded using a pasteur pipet. The PMVs are collected and carefully transferred to a 1-mL tube (volume of PMV at this step is approx 0.5 mL). The samples are dialyzed for 6–8 h at 4°C against 100–200 volumes of cold PBS to remove most of the sucrose from the PMV preparation. The protein content of PMV is determined using the Protein-BCA reagent kit (Pierce, Rockford, IL). Typically, a yield of 2.0–2.5 mg of PMV protein is obtained. The yield depends on the type of cells used for preparing the PMVs. At this step PMVs can be aliquoted and stored at –20°C.

3.1.2. Solubilization and Reconstitution of PMV (Reconstituted PMV [R-PMV] and Cardiolipin Incorporated Reconstituted PMV [CL-R-PMV])

The solubilization process by detergents consists in the progressive disruption of the membrane in favor of mixed micellar structure. Detergents are soluble amphiphiles that form soluble aggregates (micelles) when their total concentration is higher than their critical micellar concentration (CMC). The solubilization process depends on choice of detergent, the temperature, ionic strength of the solution, as well as nature and concentration of the lipids and the proteins present in the membrane ***(31–33)***. Therefore, it is important to control these parameters to determine the exact detergent concentration required for solubilization. The simplest way to monitor the solubilization process is to record the evolution of the turbidity of an initial membrane suspension on detergent addition. Indeed, this process is characterized by a change in the organization of the amphiphiles, which leads to important changes in the size and shape of the amphiphile aggregates. Natural membranes such as PMV consist of "big" aggregates of a few hundred nanometers whereas mixed micelles of detergents, lipids, and proteins consist of "small" aggregates of about few tens of nanometers. Therefore, these aggregates scatter light differently (i.e., membranes scatter light much more than mixed micelles) and the solubilization process can be visualized by a sharp drop in turbidity ***(31,34)***.

3.1.2.1. Turbidity Measurements

1. PMV (from **Subheading 3.1.1., step 8**) is resuspended at a typical concentration of 1.3 mg/mL in PBS for the protein, which corresponds to 1.0 mg/mL for the lipids based on a published analysis of the plasma membrane fraction ***(35)***.
2. A 200 m*M* solution of octyl glucoside (OG, mol wt 292.4) is prepared in PBS. OG solution can be stored at 4°C for at least a month.
3. For the turbidity experiment, any spectrophotometer (UV-Visible or spectrofluorimeter) can be used to measure the optical density of the sample. To record turbidity changes during solubilization the wavelengths are chosen in a range in which no light absorption is recorded (e.g., at 450 nm for the PMV). A quartz cuvette (1 cm optical length) is placed in the spectrofuorimeter (SLM8000) ex/em 450 nm) and 0.4 mL of PMVs + 1.6 mL of PBS are added to the cuvette to final PMV protein and lipid concentrations of approx 0.26 mg/mL and 0.2 mg/mL, respectively.
4. The sample is maintained at 25°C and stirred continuously with a Teflon-coated stir bar (2 × 7 mm). Small aliquots (10 µL) of the OG solution are added to the PMV suspension and after each OG addition, the signal is recorded until it is completely stable. (This stabilization may take a few seconds or a few minutes depending on the concentration.) In this experiment, 20–26 m*M* final OG concentration was sufficient for complete solubilization of PMVs. It is recommended to optimize the choice and the concentration of the detergent for any protein–lipid mixture to be solubilized.
5. The solubilization curve is then obtained by plotting the turbidity of the suspension after each detergent addition and after stabilization as a function of the total detergent concentration in the cuvette (**Fig. 2**).
6. To remove insoluble material, the sample is transferred from the quartz cuvette to a centrifuge tube and centrifuged in a Beckman Ti50 rotor, 60 min, 4ºC at 30,000 rpm.
7. After centrifugation, *the supernatant is collected and saved for detergent removal* without or with addition of exogeneous lipid, cardiolipin (*see* below). The turbidity of the supernatant after centrifugation is about 10 times lower than the turbidity recorded at the end of the solubilization experiment, indicating that some insoluble materials have been eliminated from the sample by centrifugation.

3.1.2.2. Generation of R-PMV by Detergent Removal Using Bio Beads

The PMVs are reconstituted by removal of detergent. This can be easily achieved by using Bio Beads SM2 (BB SM2, cat. no. 152-3920, Bio-Rad, Hercules, CA). BB SM2 are small hydrophobic beads, with a high surface capacity, that absorb any amphiphilic molecules, particularly detergents. One must be careful, however, because some of the solubilized lipids and proteins can also be removed by using this technique ***(31,32,36)***. Therefore, successive

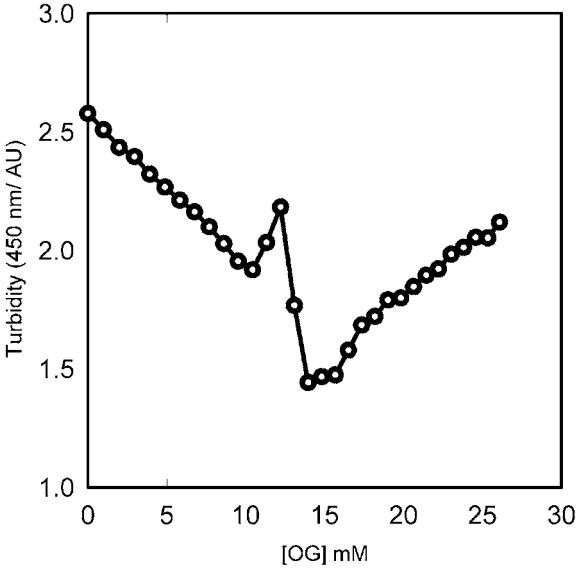

Fig. 2. Determination of OG concentration to solubilize PMVs.

steps using small quantities of BB SM2 are preferred for detergent elimination. For each 200 µg vesicle lipid sample, the following steps are used:

1. Ten glass vials (3–5 mL capacity) with caps containing 2 × 5 mm stir bars are prepared and labeled as 1–10. Twenty milligrams of BB SM2 (wet wt) are placed in each vial and 1 mL of PBS is added.
2. PBS is removed from vial 1 (containing BB SM2) and 1 mL of solubilized PMV supernatant (from **Subheading 3.1.1., step 8**) is added. The sample is incubated with BB SM2 for 12 min at 25°C under gentle magnetic stirring. At the end of incubation, stirring is stopped to allow the BB SM2 to sediment. The PBS from vial 2 is removed and the sample from vial 1 is transferred to vial 2. This process is repeated for the remaining vials for complete detergent removal.

3.1.2.3. Incorporation of Exogeneous Lipid Cardiolipin into PMV (CL-R-PMV)

1. Fifty micrograms of cardiolipin (CL, Avanti Polar Lipids, cat. no. 840012) is dried in a 5-mL glass tube under a stream of N_2 and the tube is placed in a vacuum desiccator for 12–24 h to ensure removal of traces of solvent.
2. One milliliter of solubilized PMV supernatant (from **Subheading 3.1.1., step 8**) is added to the tube containing CL.
3. The samples are incubated at room temperature with gentle shaking for 30–60 min to allow complete solubilization of CL.

We use a ratio of 50 µg CL for 200 µg plasma membrane lipid in our reconstitution procedure. This ratio can be modified and any exogeneous lipid can be reconstituted in PMVs at this step. Control samples are prepared in the same manner except that CL is omitted. Removal of detergent using Bio Beads is performed as described in **Subheading 3.1.2.2.**

3.1.2.4. Labeling of PMV with Octadecyl Rhodamine. The method described is this subheading is used for octadecyl rhodamine (R18) labeling of PMV, R-PMV, or CL-R-PMV.

1. A stock solution of R18 (cat. no. 0-246, Molecular Probes, Eugene, OR) is prepared in absolute alcohol in a glass vial at 1 mg/mL and stored at –20°C in small aliquots.
2. Ten to fifty microliters of R18 is added to 1 mL of PMV preparation (containing approx 200 µg of vesicle protein from **Subheadings 3.1.1., step 8**; **3.1.2., step 2**; or **3.1.2., step 3**) using a Hamilton Syringe under constant vortex mixing and the mixture is incubated for 30 min at room temperature in the dark.
3. R18-labeled PMVs are centrifuged on a 10–41% sucrose gradient at 100,000*g* for 60 min at 4°C as described in **Subheading 3.3.1.**
4. R18-labeled PMVs are collected from the 41% sucrose layer. This step is crucial as it eliminates any unincorprated R18 on the 10% sucrose layer which can lead to nonspecific effects in fusion assays.
5. R18-labeled PMV are passed through a PD10 column using D-PBS as an eluant. Fluorescent PMVs are collected in a total volume of 1 mL.
6. R18-labeled PMV obtained at this step are used as targets to monitor fusion with VSV-G expressing cells (*see* **Subheading 3.3.1.**).

3.2. Incorporation of GSLs into the Membranes of Mink-CD4 Cells

We have described the method of GSL transfer for GSL extracted from human (GSL-Hu) or bovine erythrocytes (GSL-Bov)***(17)***. The method for GSL transfer is applicable to a number of commercially available GSL ***(18,37)***.

3.2.1. Preparation of GSL-Containing Liposomes

1. The following components are mixed in a 7-mL glass tube: 3.0 mg of egg PC (0.6 mL, from a 5 mg/mL stock in $CHCl_3$, Avanti Polar Lipids, cat. no. 840051), 1.5 mg of egg PE (0.3 mL, from a 5 mg/mL stock in $CHCl_3$, Avanti Polar Lipids, cat. no. 840021), 1.0 mg of GSL (1 mL, from a 1 mg/mL stock in $CHCl_3$–methanol (2:1).
2. The solvents are removed under a stream of N_2 and a thin lipid film is formed on the wall of the glass tube. The lipid film is dried in a vacuum desiccator for 12–24 h.
3. Three milliliters of sterile PBS is added to the tube and vortex-mixed intermittently for 5–10 min at room temperature. This step results in the formation of multilamellar vesicles (MLVs).

4. An additional 3 mL of PBS is added to the MLVs, bringing the final volume to 6.0 mL (0.9 mg of lipid/mL). The lipid composition is PC–PE–GSL (4.5 : 2.25 : 1.5, by wt).
6. The MLVs are transferred to a 15-mL tube (round-bottom polypropylene, Falcon cat. no. 2059) and subjected to at least five freeze–thaw cycles to generate a homogeneous preparation of MLVs. At this step, MLVs can be aliquoted and stored at –20°C until further use.
7. To generate unilamellar liposomes, MLVs are extruded through a 0.2-μm filter using an Extruder (Lipex Biomembranes, Inc., Vancouver, BC) to yield vesicles with a diameter of about 200 nm. The extrusion process is repeated at least three to five times. Resulting liposomes stored at 4°C can be used within 24–36 h.

3.2.2. Influenza (PR/8) Infection of Mink-CD4 Cells and Fusion with GSL-Liposomes

Efficiency of influenza infection depends on the cell type and the strain of influenza used. Therefore, it is recommended to determine efficiency of influenza infection when a new virus preparation or a different cell line is used.

1. Mink-CD4 cells are plated on microwells (10^5 per dish, 14 mm coverslips no. 0, MatTek Corp., Ashland, MA) overnight at 37°C.
2. The influenza virus is thawed, diluted (50 μL of PR/8 allantoic fluid/mL of D2) and vortex-mixed briefly to remove any virus aggregates.
3. Diluted influenza virus is added to the coverslip (0.5 mL/dish) and incubated 1–2 h at 37°C. Unbound virus is removed, 1 mL of D5 is added, and the mixture incubated 5–6 h at 37°C.

3.2.2.1. Activation of Influenza HAo to Fusion Active HA by Trypsin Treatment

Because HA is expressed on the surface of cells as an uncleaved precursor (HAo), the cells are treated with 5 μg/mL of trypsin for 5 min at room temperature to convert HAo to fusogenic HA. This procedure involves the following steps ***(38)***:

1. Trypsin, 1 mg/mL stock in PBS (or water), is prepared and stored in small aliquots at –20°C. A working dilution 1 : 200 in D-PBS is made to a final concentration of 5 μg of trypsin/mL.
2. Each dish is washed three times with D-PBS (1 mL each time) to completely remove D5 from the wells.
3. One milliliter of diluted trypsin is added to each dish and the dish is incubated 5 min at room temperature. The cells are checked after 3 min; if they look healthy, incubation is continued 2 min more; otherwise trypsin is removed at this point and 1 mL of D5 is added. Control wells are treated in parallel except trypsin is omitted from the incubation mixture. Controls are designated as HA_0 controls.

3.2.2.2. Liposome Binding

1. Wheat germ agglutinin (WGA) stock at 1 mg/mL in PBS is prepared and stored at –20°C in small aliquots. A working solution is prepared by adding 160 µL of WGA solution to 4 mL with D-PBS to a final concentration of 40 µg/mL of WGA.
2. Medium is removed from the wells. Twenty-five microliters of diluted WGA solution is layered into the central well of each microwell.
3. Two hundred microliters of unilamellar liposomes (*see* **Subheading 3.2.1.**) are added to the center of the microwell and incubated 20–30 min at room temperature to promote binding of liposomes to the cells.
4. Liposome solution is aspirated from the central well, 1 mL of **prewarmed** PBS (preadjusted to pH 5.1) is added, and the solution is incubated at 37°C for *only* 1–2 min.
5. The PBS, pH 5.1, is aspirated immediately and replaced with 1 mL of D10, pH 7.4. Incubation is continued in the culture medium at pH 7.4 for 20–30 min at room temperature. GSL-supplemented cells are used for fusion with TF228 cells (*see* **Subheading 3.3.2.**

3.3. Fusion of Lipid-Supplemented Biological Targets with Viral Envelope Glycoprotein Expressing Cells

3.3.1. Kinetics of Fusion of R18-Labeled PMVs with VSV-G Expressing HeLa Cells

3.3.1.1. Infection of HeLa cells with VSV

1. 3×10^6 HeLa cells are plated in a T75 tissue culture flask 1 d prior to infection with VSV.
2. VSV is diluted it into 2.0 mL of D-PBS (at 6 multiplicity of infection) and mixed well.
3. Medium is removed from the flask and diluted VSV is added to HeLa cells on T75 flasks. Virus and cells are incubated for 30–45 min at 37°C.
4. Unbound virus is removed, 10 mL of D10 added, and incubation continued at 37°C for 6 h. Infection for 6–8 h results in high expression of VSV-G on the cell surface. At the end of the incubation, the cells are scraped off the flask, and suspended cells are transferred to a 15-mL polypropylene centrifuge tube.
5. The cells are pelleted by centrifugation at 800–1200 rpm for 5 min. The pellet is resuspended in 0.3 mL of D-PBS (approx 10^6 cells/100 µL), and 100 µL aliquots are transferred in to a 15-mL tube (×3).

3.3.1.2. Binding of R18-Labeled PMV to VSV-G Expressing Cells

1. One milliliter of R18-labeled PMV preparation (approx 100 µg of vesicle protein, from **Subheading 3.1.2.4**) is added to 100 µL of cells (from **Subheading 3.3.1.1., step 5**) and the cells–PMV mixture is placed on ice and incubated for 30–40 min with shaking in the dark.

2. After incubation, 10 mL of PBS is added to the tubes and the cells are pelleted. The supernatant is discarded and cell pellet is resuspended in 100 µL of PBS.

3.3.1.3. Kinetics of Fusion

1. Kinetics of fusion is monitored with an SLM8000 spectrofluorimeter. A cuvette (all sides clear, suitable for fluorescence spectroscopy) containing a 2 × 7 mm stir bar is placed into the fluorimeter; 2 mL of HEPES-NaCl buffer, pH 7.4 or at desired preadjusted pH value, is added; the solution is equilibrated at the desired temperature using a circulating water bath equipped with the fluorimenter ***(39)***.
2. Twenty to fifty microliters of vesicle-cell suspension is added to the cuvette and fluorescence is measured at ex/em 560/590 nm with a 560 nm cutoff filter at the emission.
3. For preset pH values, measurement is continued for the desired time.
4. For samples at pH 7.4, 10–100 µL of 0.5 *M* 4-morpholino ethanesulfonic acid (MES) is added using a Hamilton syringe at 20 s to lower the pH. The amount of MES required to obtain a desired pH is calibrated beforehand.
5. At the end of the run, 10 µL of an aqueous Triton X-100 (10% w/v solution is added and fluorescence measurement is continued to until a steady signal is achieved (usually 20–50 s).
6. Percentage of dequenching is calculated according to:

$$\% \text{ dequenching} = 100 \times (F - F_o)/(F_t - F_o), \quad (1)$$

where F, F_o, and F_t are fluorescence values at a given time, at zero time, and after total dequenching by addition of Triton X-100 (0.05% final concentration), respectively.

Figure 3 (top panel) shows fusion of R-PMV with VSV-G-expressing HeLa cells at 37°C. Fusion was monitored at the preset pH 6.66 for the indicated time period and additional MES was added to lower the pH to 5.6 (indicated by arrow). As can be seen, VSV-G-induced fusion kinetics of R18-labeled R-PMV is similar to that previously observed with R18-labeled PMV ***(39)***. A slight decrease in fusion observed with the samples preincubated at pH 6.66 (250 s) was consistent with previously observed inactivation of fusion activity of intact VSV ***(40)***. Therefore, treatment of PMV with OG does not impair fusion with VSV-G-expressing cells. R-PMV display characteristics similar to intact cells as targets for VSV-G mediated fusion. To ascertain incorporation of additional components in OG-solubilized PMV, we tested the ability of a fusogenic lipid CL to enhance fusion of R-PMV. **Figure 3** (lower panel) shows fusion of R18-labeled CL-R-PMV with VSV-G-expressing HeLa cells. As PMV fuse efficiently with VSV-G-expressing cells at 37°C, pH 6.3 ***(39)***, we monitored fusion of CL-R-PMV at the subthreshold temperature 32°C. Data presented in

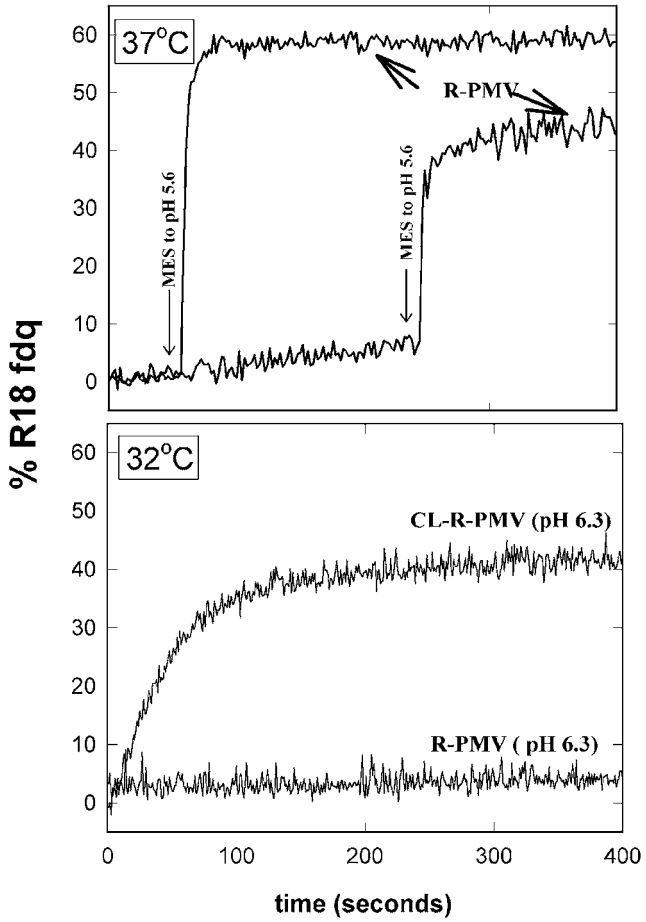

Fig. 3. Fusion of VSV-G expressing HeLa cells with R18-labeled PMVs. Cells were infected with VSV at 6 m.o.i. for 6 h. R18-labeled PMVs were bound to cells at 4°C at pH 7.4 and unbound PMVs were removed by centrifugation. The vesicle-cell suspension was added to preequilibrated buffer at various pH values. At the end of the incubation, Triton X-100 was added and percentage fusion was calculated as described in **Subheading 3.** **(Top)** Fusion of VSV-G expressing HeLa cells with R18-labeled R-PMV at 37°C. The vesicle-cell suspension was added to preequilibrated buffer at pH 6.66. 0.5 *M* MES (50–70 µL) was added (indicated by *arrow*) to bring the pH of the samples to 5.6. **(Bottom)** Fusion of VSV-G expressing HeLa cells with R18-labeled CL-R-PMV at 32°C at pH 6.3.

Fig. 3 (lower panel) show that incorporation of CL into R-PMV enhanced fusion of PMV with VSV-G-expressing cells. Observed fluorescence dequenching was specific, as we did not see any dequenching at pH 6.8 and neutral pH (data not shown).

3.3.2. Fusion of GSL-Supplemented Mink-CD4 Cells with HIV-1 Envelope Glycoprotein Expression Cells

3.3.2.1. Labeling of Mink-CD4 Cells with CMFDA

1. The cytoplasmic fluorescent probe 5-chloromethylfluorescein diacetate (CMFDA; Molecular Probes cat. no. C-7025, ex/em 492/516 nm) is solubilized at 10 m*M* concentration in dimethyl sulfoxide (DMSO), aliquoted into a 10- or 20-µL volume, and stored at –20°C. A working dilution of CMFDA (1:500) is prepared in D10.
2. Medium is removed from GSL-containing mink-CD4 cells on microwells (from **Subheading 3.2.2.**), 1 mL of diluted CMFDA solution is layered, and samples are incubated at 37°C for 45–60 min. Dye solution is replaced with 1 mL of D10 and incubation continued for additional 15–30 min.

3.3.2.2. Labeling of TF228 Cells with 1,1′-Dioctadecyl-DiI

1. DiI (Molecular Probes cat. no. D282, ex/em 550/565 nm) is solubilized in 10 m*M* DMSO, divided into small aliquots and stored at –20°C. Five microliters of 3,3,3′,3′-tetramethylindo-carbocyanine perchlorate (DiI) solution is added to 0.1 mL of Diluent C (Sigma, cat. no. CGL-DIL) in a 1.5-mL Eppendorf tube and vortex-mixed (the dye solution should be clear solution without any insoluble material).
2. TF228 cells (5×10^6) are pelleted by centrifugation at 1000 rpm, and the pellet resuspended in 10 mL of PBS and centrifuged again. The cell pellet is resuspended in 0.5 mL of PBS.
3. One-half milliliter of cells (from **step 2**) are added to the DiI solution and mixed quickly. The mixture is transferred to a fresh Eppendorf tube and incubated for 2–5 min at room temperature.
4. One milliliter of R10 is added to the mixture and the sample is centrifuged for 30 s in a microfuge. The supernatant is discarded and the cells resuspended in 5 mL of R10 and incubated at room temperature for 5 min.
5. The cells are pelleted and washed three times with PBS (5 mL each wash), then resuspended at 10^5/mL in R10.

3.3.2.3. Cell–Cell Fusion

1. Two milliliters of DiI-labeled TF228 cells (from **Subheading 3.3.2.2., step 5**) are added to CMFDA-labeled mink-CD4 cells and the two cell populations incubated for 3–5 h at 37°C.

2. At the end of incubations, medium is replaced with 1 mL of D-PBS and the phase and fluorescence images are acquired at room temperature using an Olympus IX70 inverted microscope with a 40× oil immersion UPlanApo objective (1.0 NA). We routinely use the cooled charge coupled device (CCD) camera (Princeton Instruments, Trenton, NJ), and the Metamorph image analysis software package for image acquisition (Universal Imaging, West Chester, PA) which allows average intensities to be determined within user-defined regions of an image.
   U-MNG filter cube (530–550 nm ex, 570 nm dichroic mirror, 590 nm high pass em) is used for DiI observation and the U-MNIBA filter cube (470–490 nm ex, 505 nm dichroic mirror, 515–550 nm em) to visualize CMFDA fluorescence. Images are collected randomly from 6–10 different selected fields for each sample.
3. The data are analyzed using Metamorph software (Universal Imaging Inc.) by overlaying and counting the images. The total number of cells positive for CMFDA are counted. Then the number of cells positive for both fluorescent probes are scored. Bright field images are used to distinguish false-positives where labeled cells were lying over one another but had not actually fused.
4. Percent fusion is calculated as

$$\% \text{ fusion} = 100 \times \frac{[\text{number of cells positive for both dyes}]}{[\text{total number of target cells}]}$$

Figure 4 shows fusion of GSL-supplemented mink-CD4 cells with TF228 cells. The data presented in **Fig. 4** show that addition of only human GSL to mink-CD4 cells resulted in subsequent fusion with TF228 cells. Lack of fusion with bovine GSL-supplemented mink-CD4 showed that recovery of fusion was specific. Percentage fusion from one such experiment was as follows: GSL-Hu-mink-CD4 cells, 35–40%; GSL-Bov-mink-CD4 cells, 8–10%; mink-CD4 cells without GSL addition, 8–10%.

3.4. Discussion

We have described here two methods to incorporate lipids into biological targets. We will briefly discuss the rationale behind the two approaches and compare the limitations and benefits of these two methods.

Previous experiments from our laboratory have shown that time-resolved kinetics of cell-to-cell fusion based on R18 dequenching can be successfully monitored for viruses that utilize erythrocytes as targets ***(41,42)***. Erythrocytes possess the advantage that their membranes can be labeled with R18 at quenched concentrations without internalization of the dye, in contrast to other biological membranes (viz. cultured cells). In an attempt to develop a versatile assay to monitor the fusion kinetics of viral envelope proteins expressed in

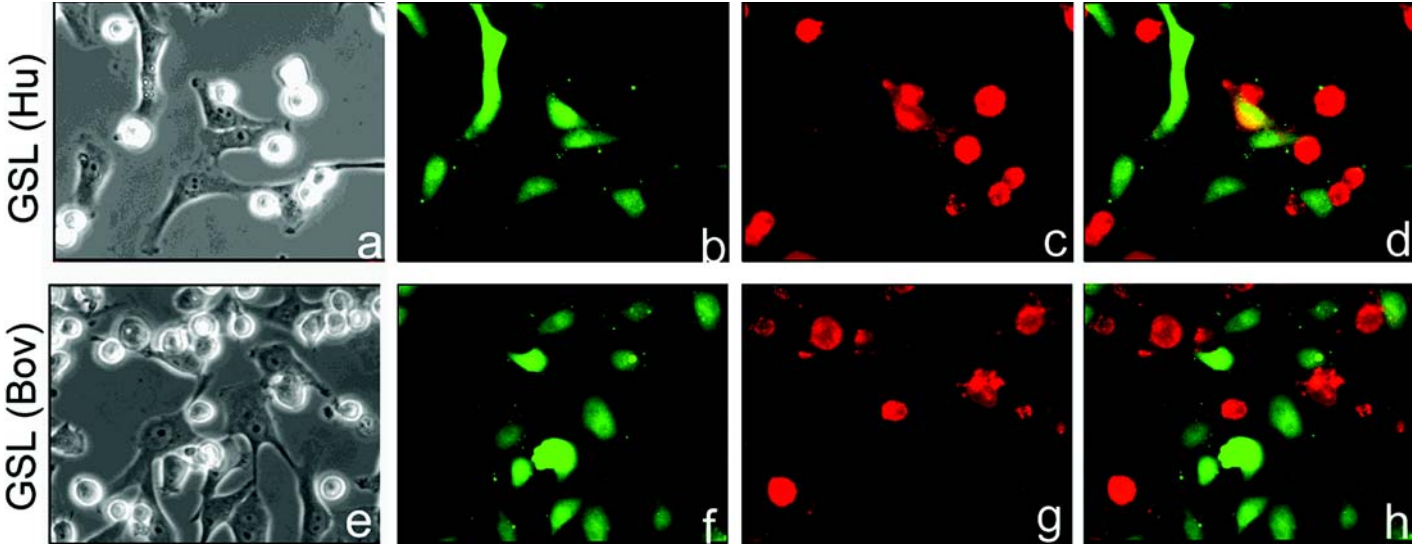

Fig. 4. GSLs from human erythrocytes mediate fusion between mink-CD4 and gp120-gp41-expressing cells. HA was expressed on the surface of mink-CD4 cells and activated by trypsin as described in **Subheading 3.** GSLs were transferred via liposomes as described in **Subheading 3.** GSL-modified mink-CD4 cells were labeled with CMFDA and cocultured with DiI-labeled TF228 cells for 4 h at 37°C. Images were acquired for phase **(a**,**e)**, CMFDA, green **(b**,**f)**, and DiI, red **(c**,**g)** fluorescence. Red and green images were overlayed **(d**,**h)** using Metamorph software as described in the text. GSL-Hu-modified mink-CD4 cells **(a–d)** and GSL-Bov-modified mink-CD4 cells **(e–h)**. Positive fusion events are indicated by orange-yellow color in the overlays **(d)**.

cultured cells, we generated PMVs from appropriate target cells and labeled them with R18 at quenched concentrations. Because PMVs can be prepared from any appropriate membrane ***(39)***, this approach can also be used to study a wide variety of wild-type and mutant envelope proteins expressed in different cells. Furthermore, the role of other viral proteins such as the matrix protein of VSV and the effect of the density of viral proteins on kinetics of fusion can be analyzed. We have previously shown that CD4 bearing plasma membrane vesicles (CD4-PMVs) were potent inhibitors of HIV-1–mediated fusion whereas those exhibited very poor fusogenic activity ***(43)***. In an attempt to enhance the fusogenic activity of these vesicles, we incorporated CL (a natural fusogenic phospholipid) into PMVs by reconstitution using OG followed by removal of detergent with Bio Beads. Efficient solublization of membrane lipids and/or proteins is dependent on the choice of the detergent employed (*see* **Subheading 3.**). Our results show that incorporation of CL in R-PMV (CL-R-PMV) significantly enhances its fusion with VSV-G expressing cells. In control experiments in which CL-R-PMV were incubated with the uninfected HeLa cells, no R18 dequenching was observed at low or neutral pHs (data not shown). Therefore our method of incorporation of CL enhances specific fusion activity of reconstituted vesicles. Using a similar protocol, we incorporated CL into CD4-PMV (generated from $CD4^+$ cells). However, fusion of these vesicles with HIV-1 envelope glycoprotein-expressing cells was limited. Our unsuccessful attempts to utilize PMV to study fusion with HIV-1 envelope glycoprotein-expressing cells prompted us to explore alternative methods to incorporate lipids (specifically GSL) into the membranes of cultured cells.

Our inital attempts to supplement GSL into the membranes of target cells by incubation with a suspension of GSLs in the culture medium did not result in recovery of fusion, presumably due to insufficient incorporation, incorrect orientation of GSL molecules in the membrane, and/or GSL recycling from the surface of target cells. We also attempted to incorporate GSL using polyethylene glycol following a previously described procedure ***(44)***. Although GSL were incorporated by polyethylene glycol-induced fusion of GSL-containing liposomes with $CD4^+$ cells, recovery of HIV-1 fusion with GSL-supplemented cells by this method was not achieved. Therefore, we developed an alternative method to incorporate lipids that relies on influenza HA-mediated low pH fusion of GSL-containing liposomes with the target cells ***(17)***. The assay allows relative quantitation of transfer of liposomal lipids as compared to direct incorporation of lipids to cultured cells ***(17)***. This method, however, is limited to study fusion of only neutral pH fusing viral envelope glycoproteins (*see* **Table 1**). We have shown here that GSL-mink-CD4 cells become susceptible to HIV-1 fusion (**Fig. 4**). We have also reported recently that one of the

Table 1
Viral Envelope Glycoprotein-Mediated Fusion with Lipid-Modified Targets

Lipid transfer	Advantages	Limitations	Viral proteins studied
Direct addition	Minimum manipulation	Poor incorporation, internalization of lipids	HIV-1, HIV-2
Reconstitution of PMV	Any target cell can be used	Study restricted to low-pH fusing viruses	VSV, influenza HIV-1, Sendai
HA-mediated transfer	Correct orientation of incorporated molecules, efficient and quantitative incorporation	Only neutral pH viral proteins can be studied; influenza infection of cells required	HIV-1, HIV-2

fractions in the human erythrocyte GSL mixture (globotriosylceramide, Gb3) is the active component that confers susceptibility to HIV-1 fusion ***(18,37)***.

Acknowledgments

We thank Dr. Paul Clapham for the mink-CD4 cells and Dr. Zdenka L. Jonak for the TF228.1.16 cells. We also thank Drs. A. Dimitrov, M. Viard, and Han-Ming J. Lin for critical reading of the manuscript. This work was supported by the NIH Intramural AIDS Targeted Antiviral Program.

References

1. White, J., Matlin, K., and Helenius, A. (1981) Cell fusion by Semliki Forest, influenza, and vesicular stomatitis viruses. *J. Cell Biol.* **89,** 674–679.
2. White, J. M. (1992) Membrane fusion. *Science* **258,** 917–924.
3. Blumenthal, R., Schoch, C., Puri, A., and Clague, M. J. (1991) A dissection of steps leading to viral envelope protein-mediated membrane fusion. *Ann. NY Acad. Sci.* **635,** 285–296.
4. Blumenthal, R., Pak, C. C., Krumbiegel, M., Lowy, R. J., Puri, A., Elson, H. F., and Dimitrov, D. S. (1994) How viral envelope glycoproteins negotiate the entry of genetic material into the cell, in *Biotechnology Today* (Verna, R. and Shamoo, A., eds.), Ares-Serono Symposia Publications, Rome, pp. 151–173.
5. Blumenthal, R., Puri, A., Sarkar, D. P., Chen, Y., Eidelman, O., and Morris, S. J. (1989) Membrane fusion mediated by viral spike glycoproteins, in *Cell Biology*

of Virus Entry, Replication and Pathogenesis (Helenius, A., Compans, R., and Oldstone, M., eds.), Alan R. Liss, New York, pp. 197–217.
6. Chan, D. C. and Kim, P. S. (1998) HIV entry and its inhibition. *Cell* **93,** 681–684.
7. Dimitrov, D. S. (1997) How do viruses enter cells? The HIV coreceptors teach us a lesson of complexity. *Cell* **91,** 721–730.
8. Hughson, F. M. (1997) Enveloped viruses: a common mode of membrane fusion? *Curr. Biol.* **7,** R565–R569.
9. White, J. M. (1995) Membrane fusion: the influenza paradigm. *Cold Spring Harbor Symp. Quant. Biol.* **60,** 581–588.
10. Melikyan, G. B. and Chernomordik, L. V. (1997) Membrane rearrangements in fusion mediated by viral proteins. *Trends Microbiol.* **5,** 349–355.
11. Herrmann, A., Clague, M. J., Puri, A., Morris, S. J., Blumenthal, R., and Grimaldi, S. (1990) Effect of erythrocyte transbilayer phospholipid distribution on fusion with vesicular stomatitis virus. *Biochemistry* **29,** 4054–4058.
12. Kielian, M. C. and Helenius, A. (1984) Role of cholesterol in fusion of Semliki Forest virus with membranes. *J. Virol.* **52,** 281–283.
13. Nieva, J. L., Bron, R., Corver, J., and Wilschut, J. (1994) Membrane fusion of Semliki Forest virus requires sphingolipids in the target membrane. *EMBO J.* **13,** 2797–2804.
14. Wilschut, J., Corver, J., Nieva, J. L., Bron, R., Moesby, L., Reddy, K. C., and Bittman, R. (1995) Fusion of Semliki Forest virus with cholesterol-containing liposomes at low pH: a specific requirement for sphingolipids. *Mol. Membr. Biol.* **12,** 143–149.
15. Rogers, G. N., Paulson, J. C., Daniels, R. S., Skehel, J. J., Wilson, I. A., and Wiley, D. C. (1983) Single amino acid substitutions in influenza haemagglutinin change receptor binding specificity. *Nature* **304,** 76–78.
16. Suzuki, Y., Suzuki, T., Matsunaga, M., and Matsumoto, M. (1985) Gangliosides as paramyxovirus receptor. Structural requirement of sialo-oligosaccharides in receptors for hemagglutinating virus of Japan (Sendai virus) and Newcastle disease virus. *J. Biochem.* (Tokyo) **97,** 1189–1199.
17. Puri, A., Hug, P., Munoz-Barroso, I., and Blumenthal, R. (1998) Human erythrocyte glycolipids promote HIV-1 envelope glycoprotein-mediated fusion of CD4+ cells. *Biochem. Biophys. Res. Commun.* **242,** 219–225.
18. Puri, A., Hug, P., Jernigan, K., Barchi, J., Kim, H. Y., Hamilton, J., et al. (1998) The neutral glycosphingolipid globotriaosylceramide promotes fusion mediated by a CD4-dependent CXCR4-utilizing HIV type 1 envelope glycoprotein. *Proc. Natl. Acad. Sci. USA* **95,** 14435–14440.
19. Hammache, D., Yahi, N., Maresca, M., Pieroni, G., and Fantini, J. (1999) Human erythrocyte glycosphingolipids as alternative cofactors for human immunodeficiency virus type 1 (HIV-1) entry: evidence for CD4-induced interactions between HIV-1 gp120 and reconstituted membrane microdomains of glycosphingolipids (Gb3 and GM3). *J. Virol.* **73,** 5244–5248.
20. Puri, A., Hug, P., Jernigan, K., Rose, P., and Blumenthal, R. (1999) Role of glycosphingolipids in HIV-1 entry: requirement of globotriaosylceramide (Gb3) in CD4/CXCR4-dependent fusion. *Biosci. Rep.* **19,** 317–325.

21. Chernomordik, L., Kozlov, M. M., and Zimmerberg, J. (1995) Lipids in biological membrane fusion. *J. Membr. Biol.* **146,** 1–14.
22. Gunther-Ausborn, S., Praetor, A., and Stegmann, T. (1995) Inhibition of influenza-induced membrane fusion by lysophosphatidylcholine. *J. Biol. Chem.* **270,** 29279–29285.
23. Loyter, A., Citovsky, V., and Blumenthal, R. (1988) The use of fluorescence dequenching measurements to follow viral membrane fusion events. *Methods Biochem. Anal.* **33,** 129–164.
24. Sarkar, D. P. and Blumenthal, R. (1987) The role of the target membrane structure in fusion with Sendai virus. *Membr. Biochem.* **7,** 231–247.
25. Scheiffele, P., Rietveld, A., Wilk, T., and Simons, K. (1999) Influenza viruses select ordered lipid domains during budding from the plasma membrane. *J. Biol. Chem.* **274,** 2038–2044.
26. Jacobs, N. L., Andemariam, B., Underwood, K. W., Panchalingam, K., Sternberg, D., Kielian, M., and Liscum, L. (1997) Analysis of a Chinese hamster ovary cell mutant with defective mobilization of cholesterol from the plasma membrane to the endoplasmic reticulum. *J. Lipid Res.* **38,** 1973–1987.
27. Clapham, P. R., Blanc, D., and Weiss, R. A. (1991) Specific cell surface requirements for the infection of CD4-positive cells by human immunodeficiency virus types 1 and 2 and by Simian immunodeficiency virus. *Virology* **181,** 703–715.
28. Jonak, Z. L., Clark, R. K., Matour, D., Trulli, S., Craig, R., Henri, E., et al. (1993) A human lymphoid recombinant cell line with functional human immunodeficiency virus type 1 envelope. *AIDS Res. Hum. Retrovir.* **9,** 23–32.
29. Thomas, D., Newcomb, W. W., Brown, J. C., Wall, J. S., Hainfeld, J. F., Trus, B. L., and Steven, A. C. (1985) Mass and molecular composition of vesicular stomatitis virus: a scanning transmission electron microscopy analysis. *J. Virol.* **54,** 598–607.
30. Pak, C. C., Krumbiegel, M., and Blumenthal, R. (1994) Intermediates in influenza PR/8 hemagglutinin-induced membrane fusion. *J. Gen. Virol.* **75,** 395–399.
31. Paternostre, M., Viard, M., Meyer, O., Ghanan, M., Ollivon, M., and Blumenthal, R. (1997) Solubilization and reconstitution of vesicular stomatitis virus envelope using octylglucoside. *Biophys. J.* **72,** 1683–1694.
32. Paternostre, M. T., Lowy, R. J., and Blumenthal, R. (1989) pH-dependent fusion of reconstituted vesicular stomatitis virus envelopes with Vero cells. Measurement by dequenching of fluorescence. *FEBS Lett.* **243,** 251–258.
33. da Graca, M., Eidelman, O., Ollivon, M., and Walter, A. (1989) Temperature dependence of the vesicle-micelle transition of egg phosphatidylcholine and octyl glucoside. *Biochemistry* **28,** 8921–8928.
34. Meyer, O., Ollivon, M., and Paternostre, M. T. (1992) Solubilization steps of dark-adapted purple membrane by Triton X-100. A spectroscopic study. *FEBS Lett.* **305,** 249–253.
35. Allan, D. and Crumpton, M. J. (1970) Preparation and characterization of the plasma membrane of pig lymphocytes. *Biochem. J.* **120,** 133–143.

36. Levy, D., Bluzat, A., Seigneuret, M., and Rigaud, J. L. (1990) A systematic study of liposome and proteoliposome reconstitution involving Bio-Bead-mediated Triton X-100 removal. *Biochim. Biophys. Acta* **1025,** 179–190.
37. Hug, P., Lin, H. M., Korte, T., Xiao, X., Dimitrov, D. S., Wang, J. M., et al. (2000) Glycosphingolipids promote entry of a broad range of human immunodeficiency virus type 1 isolates into cell lines expressing CD4, CXCR4, and/or CCR5. *J. Virol.* **74,** 6377–6385.
38. Klenk, H. D., Rott, R., Orlich, M., and Blodorn, J. (1975) Activation of influenza A viruses by trypsin treatment. *Virology* **68,** 426–439.
39. Puri, A., Krumbiegel, M., Dimitrov, D., and Blumenthal, R. (1993) A new approach to measure fusion activity of cloned viral envelope proteins: fluorescence dequenching of octadecylrhodamine-labeled plasma membrane vesicles fusing with cells expressing vesicular stomatitis virus glycoprotein. *Virology* **195,** 855–858.
40. Clague, M. J., Schoch, C., Zech, L., and Blumenthal, R. (1990) Gating kinetics of pH-activated membrane fusion of vesicular stomatitis virus with cells: stopped flow measurements by dequenching of octadecylrhodamine fluorescence. *Biochemistry* **29,** 1303–1308.
41. Kaplan, D., Zimmerberg, J., Puri, A., Sarkar, D. P., and Blumenthal, R. (1991) Single cell fusion events induced by influenza hemagglutinin: studies with rapid-flow, quantitative fluorescence microscopy. *Exp. Cell Res.* **195,** 137–144.
42. Morris, S. J., Sarkar, D. P., White, J. M., and Blumenthal, R. (1989) Kinetics of pH-dependent fusion between 3T3 fibroblasts expressing influenza hemagglutinin and red blood cells. Measurement by dequenching of fluorescence. *J. Biol. Chem.* **264,** 3972–3978.
43. Puri, A., Dimitrov, D. S., Golding, H., and Blumenthal, R. (1992) Interactions of CD4+ plasma membrane vesicles with HIV-1 and HIV-1 envelope glycoprotein-expressing cells. *J. AIDS* **5,** 915–920.
44. Jacewicz, M. S., Mobassaleh, M., Gross, S. K., Balasubramanian, K. A., Daniel, P. F., Raghavan, S., et al. (1994) Pathogenesis of Shigella diarrhea: XVII. A mammalian cell membrane glycolipid, Gb3, is required but not sufficient to confer sensitivity to Shiga toxin. *J. Infect. Dis.* **169,** 538–546.

6

Liposome-Mediated, Fluorescence-Based Studies of Sphingolipid Metabolism in Intact Cells

Shimon Gatt, Tama Dinur, and Arie Dagan

1. Introduction

Our laboratory has been engaged in studies of lipid hydrolases since the early 1960s. In the course of these studies the following enzymes have been isolated and partially purified: ceramidase ***(1–3)***; two sphingomyelinases: the lysosomal, with an acidic pH optimum ***(4)*** and a neutral, magnesium-dependent ***(5–7)*** enzyme; β-glucosidase and α- or β-galactosidase ***(8–11)***; *N*-acetyl hexosaminidase ***(12–14)***; neuraminidase ***(15)***; phospholipase A_1 ***(16,17)***, lysophospholipase ***(18–20)***, and brain lipase ***(21–23)***. For assaying these enzymes we labeled the respective substrates with tritium (^3H) or ^{14}C and developed procedures for separating the hydrolytic products from the, as yet, nondegraded substrates. In the late 1970s we began synthesizing colored and fluorescent derivatives of lipids. In 1981 in *Methods in Enzymology*, vol. 72 ***(24–32)***, we presented a comprehensive description of the assay procedures using sphingolipids to which we linked trinitrophenol as a colored, yellow marker and the fluorescent probes anthracene, N-(7-nitrobenz-2-oxa-1,3-diazol-4-yl (NBD), pyrene, carbazole, and dansyl. More recently we replaced these with the more polar fluorescent probe, lissamine rhodamine (LR), or with Bodipy; these probes were linked to the sphingolipids via a 12-carbon spacer (LR12 and Bod12) and were used for assaying lipid hydrolases in vitro ***(33–39)***. The availability of fluorescent lipids opened for us a new approach, that is, their administration into intact cells in culture and following their intracellular metabolism ***(40–47)***. In most cases our interest was in their enzymatic hydrolysis within the intact lysosomes of the living cells, normal or derived from patients with lipid storage disorders (sphingolipidoses).

From: *Methods in Molecular Biology, vol. 199: Liposome Methods and Protocols*
Edited by: S. Basu and M. Basu © Humana Press Inc., Totowa, NJ

This approach provided a fluorescence-based evaluation of the intracellular metabolism of the respective sphingolipids and permitted diagnosis of the lipidoses in the intact, living cells and, in some cases, in the culture medium ***(48)***. It also led to the development of a novel procedure for selecting lipidotic cells that have been corrected by transduction with a retroviral vector containing the cDNA encoding the normal gene ***(46,49–51)***. The latter approach was developed in collaboration with Dr. E. H. Schuchman of the Mount Sinai Medical Center in New York City. The present chapter describes the synthesis and use of liposomal dispersions of sphingolipids, labeled with the nonpolar fluorescent probe, pyrene, for administration into cultured cells and their lysosomes, intralysosomal hydrolysis, and the procedure for analyzing and quantifying the metabolic products. For a parallel description of sphingolipids, labeled with the more polar probes, LR or Bodipy (which are administered into the cells as nonliposomal dispersions), the reader is referred to **ref. *52***. A previous article on the use of liposomes for administering and studying the metabolism of fluorescent lipids has also been published ***(53)***.

2. Materials

1. Pyrene dodeconic acid (P12).
2. P12 sphingomyelin (P12 SPM).
3. P12 glucosylceramide (P12 GC)
4. P12 ceramide.
5. P12 dihexosylceramide (P12 CDH).
6. P12 trihexosylceramide (P12 THC).
7. Bromoconduritol B-epoxide (BrCBE).
8. Acid sphingomyelinase (ASM).
9. Sphingomyelin (SPM) (Sigma).

3. Methods

3.1. Synthesis of Pyrene Dodecanoyl Sphingomyelin (P12-SPC)

Forty-three micromoles of sphingosyl phosphorylcholine (SPC, Sigma) were dissolved in 10 mL of a solution of dichloromethane–methanol (CH_2Cl_2–MeOH, 2:1) in a 25-mL Erlenmeyer flask protected from light. Fifty micro-

moles of pyrene dodecanoic acid (P12, Molecular Probes) were added and the mixture was magnetically stirred for 10 min. One hundred micromoles of dicyclohexylcarbodiimide (DCC, Aldrich) were added followed by 40 μL of triethylamine. The mixture was stirred for 24 h protected from light, then evaporated to dryness. The residue was dissolved in a minimal amount of CH_2Cl_2–MeOH (2:1) and applied to a preparative silica gel thin-layer chromatography (TLC) plate. The TLC plate was developed in $CHCl_3$–MeOH–H_2O (65:35:5). The pyrene dodecanoyl SPM band was visualized using a long-wavelength (UVA) lamp. The band was scraped, introduced into a small glass column, and the product, P12-SPM, was eluted with CH_2Cl_2–MeOH–H_2O (1:2:1).

The synthesis of other pyrene sphingolipids followed the aforementioned procedure with minor modifications as summarized in **Table 1**.

3.2. Administration of Pyrene Lipids into Cultured Cells

Our main interest was the degradation of sphingolipids, i.e., glycosphingolipids and sphingomyelin, by lysosomal hydrolases. For assaying the activities in vitro, using cell extracts or purified enzymes, the respective lipids were labeled with a radioactive, colored, or fluorescent probe, and dispersed as a mixed micelle in a detergent or mixture of detergents. The most commonly used detergent for assaying sphingolipid hydrolase is Triton X-100 or a mixture of this nonionic detergent and an anionic one, for example, sodium taurocholate. A suitable buffer (at an acidic pH for assaying lysosomal hydrolases) was added and the reaction mixture incubated at 37°C. The product was then separated from the, as yet, nonhydrolyzed substrate by solvent partitioning or TLC and its radioactivity, absorption (for a colored product), or fluorescence quantified. Such assays provided an evaluation of the activities of sphingolipid hydrolases in extracts of normal cells and of their lipidotic counterparts. Examples of such "in vitro" assays can be found in refs. ***1–34***, ***36–39***.

We then became interested in utilization of the fluorescent sphingolipids for studying and comparing their intracellular catabolism in normal and lipidotic cells. For this purpose we began searching for modes of administration of the respective fluorescent sphingolipids into intact cells grown in tissue culture. A basic requirement for our studies was that the respective fluorescent sphingolipid would be transported across the plasma membrane, trafficked to and taken up by the lysosomes where it would be hydrolyzed. The fluorescent product could remain in the lysosome, be translocated into other compartments of the cell, or even exocytosed to the culture medium (for the latter *see* **ref. *48***). We expected that in lipidotic cells the uptake and trafficking to the lysosomes would not be affected, but because of the genetic effect the intralysosomal

Table 1
Synthesis of Pyrene Sphingolipids

Pyrene-sphingolipid synthesized	Starting material	Fluorescent compound	Solvent	Coupling agent	TLC solvent
Sphingomyelin	Sphingosylphosphocholine[c]	Pl2[a]	CH_2Cl_2–MeOH,[e] 2:1	DCC[f]	$CHCl_3$–MeOH–H_2O (65:35:5)
″	″	PSA-11[b]	″	″	″
Ceramide	Sphingosine[c]	P12	″	″	$CHCl_3$–MeOH–H_2O (95:5:0.5)
″	″	PSA-11	″	″	″
Sulfatide	Lysosulfatide[c]	P12	″	″	$CHCl_3$–MeOH-H_2O (80:20:2)
″	″	PSA-11	″	″	″
Ceramide β-glucose	Lyso Cer-β-glc[c]	P12	CH_2Cl_2	EDAC[g]	$CHCl_3$–MeOH–H_2O (90:10:1)
Ceramide β-galactose	Lyso Cer β-gal[c]	P12	″	″	″
Ceramide β-glucose	Lyso Cer β-glc[c]	PSA-11	″	DCC	″
Ceramide β-galactose	Lyso Cer β-gal[c]	PSA-11	″	″	″
Dihexosylceramide	Lysodihexosylceramide[d]	P12	CH_2Cl_2–MeOH, 1:1	EDAC	$CHCl_3$–MeOH–H_2O (80:20:2)
Trihexosylceramide	Lysotrihexosylceramide[d]	P12	″	″	$CHCl_3$–MeOH–H_2O (75:25:4)
GM1-ganglioside	Lyso GM1-ganglioside[c]	P12	″	″	$CHCl_3$–MeOH–H_2O (60:35:6)

[a]Pyrenedodecanoic acid.
[b]Pyrene sulfonylamido undecanoic acid.
[c]Available in Sigma catalog.
[d]Prepared as per **ref. *55***.
[e]CH_2Cl_2 (dichloromethane); MeOH (methanol).
[f]DCC (dicyclohexylcarbodiimide)—Aldrich.
[g]EDAC (1-ethyl-3-(3-dimethylaminopropyl carbodiimide)—Aldrich.

hydrolysis would decrease considerably. This would result in less product and higher accumulation of the fluorescent sphingolipids within the cells.

The mode of administration of the respective fluorescent sphingolipids into the cells in culture depended on the polarity of the probe linked to it. Thus, when using sphingolipids to which a polar probe was linked (e.g., LR, sulforhodamine, or even Bodipy), the respective lipid could be added as a solution in ethanol or dimethyl sulfoxide (DMSO) to the culture medium ***(52)***. When a nonpolar probe (e.g., pyrene or anthracene) was linked to the sphingolipids, we needed to search for a mode of dispersion that would result in uptake by the cells, transport across the plasma membrane, followed by trafficking to and internalization in the lysosomes. The respective sphingolipids could be divided into two groups: those that bind to albumin (fatty acids, monohexosylceramides, and sulfatide), and those that probably do not (oligohexoside ceramides and sphingomyelin). As most media contain serum albumin at a final concentration of 0.4%, the first group could be added directly to the culture medium. However, formation of a complex with albumin did not provide a means of uptake and trafficking to the lysosomes.

We tried several modes of dispersion, such as preforming a complex with albumin; incorporation into serum lipoproteins; complexing with the envelope of a virus utilizing the receptors of the viral glycoproteins on the plasma membranes of the cells for uptake; dispersion as liposomes (multilamellar) or dispersion as small unilamellar vesicles (SUVs); and adding apolipoprotein E (apo E). As is shown in **Table 2** and **Fig. 1**, the latter was the most efficient both for uptake and degradation of the respective sphingolipids. The assumption is that the apo E-coated SUVs link to the low-density lipoprotein (LDL) receptor on the plasma membrane are internalized by receptor-mediated endocytosis, trafficked to, and internalized into the lysosomes.

For preparation of an apo E-coated liposome, a chloroform–methanol solution of the respective pyrene-lipid was mixed in a glass tube with a four- or eightfold excess of lecithin (phosphatidylcholine from egg or soybean) or, less frequently, of sphingomyelin, in the same solvent mixture. The solvent was evaporated under a stream of nitrogen and, to ascertain the complete evaporation of the solvent, the tube was further kept under vacuum for periods up to 30 min. Saline was added and SUVs (i.e., liposomes) were prepared by ultrasonic irradiation. In our laboratory in Jerusalem, we usually used a sonicator of Microson Heat Systems, Ultrasonics, Farmingdale, NY, at 40% output for 3–4 min. But any other probe sonicator could be used or even a bath sonicator. A solution of apo E was added (a gift from Biotechnology General Inc., Nes-Ziona, Israel but also available commercially from Calbiochem, cat. no. 178475). The quantity of apo E varied, but we used about 1 μg of apo E

Table 2
Uptake and Degradation of Six P12-Sphingolipids

	A. Cosonication with serum		B. Apo E-coated SPM-SUV	
Substrate	Uptake (nmol)	Degradation (% of total)	Uptake (nmol)	Degradation (% of total)
P12-SPM	5.0	29	13.0	51
P12-GM1	0.6	11	2.6	20
P12-CS	3.9	20	9.8	38
P12-gal-Cer	3.4	16	12.6	33
P12-THC	1.6	23	10.2	47
P12-GC	5.8	39	15.6	58

In Mode A, a solution of 100 nmol of P12-lipid in 5 μL of DMSO was mixed with 1 mL of fetal calf serum and, following sonication for 15 min in a bath sonicator, combined with 9 mL of medium, and incubated in a 75-cm^2 flask for 2 d with skin fibroblasts.

In Mode B, 30 nmol of P12-lipid and 120 nmol of SPM were irradiated in a probe sonicator. Thirty micrograms of apo E were added, and after 15 min the liposomes were added to the culture medium and incubated as in Mode A.

per 1 nmol of pyrene lipid. The apo E–SUV suspension was usually kept for 15–30 min at room temperature and added to the culture medium.

We used a large variety of cells in culture. Some adhered to the dish (skin fibroblasts, macrophages, lymphoblasts, embryonic cells, Chinese hamster ovary cells, COS, cancer cells, e.g., breast cancer wild-type MCF-7-NCi and their drug-resistant MCF-7-AdrR) while others were grown in suspension (HL60 and P388 cancer cells). For each cell type a specific culture medium was used. The cells were grown in six-well dishes or in falcons of varying sizes, and the volume of the culture medium varied accordingly.

3.3. Incubation of Pyrene-Lipids with Cells

Depending on the respective experiments, two modes of incubation were used, a "pulse" and "pulse–chase." In the former, the fluorescent lipid was incubated with the cells for the period required and the reaction was terminated. For a "pulse–chase" the fluorescent lipid was incubated with the cells for the period required (pulse). The medium was then removed, the cells washed with sterile saline, fresh medium devoid of fluorescent lipid added, and the incubation continued for the chase period required.

For termination, cells in suspension are sedimented and washed twice with phosphate-buffered saline (PBS). For adherent cells, the medium is removed, the

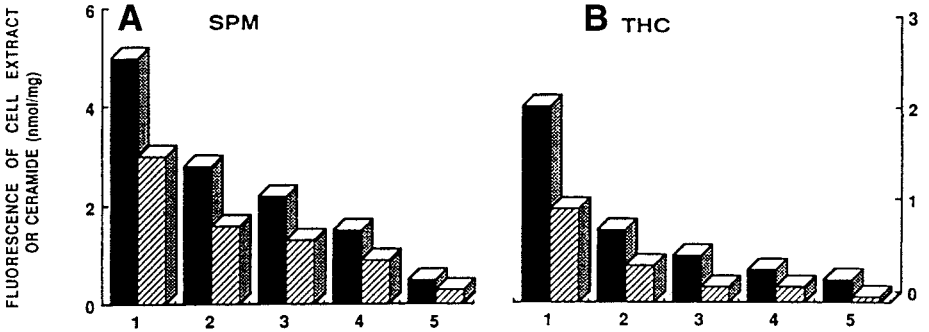

Fig. 1. Effect of the mode of dispersion on the uptake and intracellular degradation of P12-sphingomyelin **(A)** and P12-trihexosylceramide **(B)**. The respective dispersions were incubated with skin fibroblasts for 24 h and the cells processed as described in the text. **(A)** *(1)* SUVs of P12-SPM (40 nmol) and apo E (60 μg). *(2)* P12-SPM (40 nmol) in 20 μL of DMSO was mixed with 0.5 mL of fetal calf serum (FCS), the mixture was cosonicated for 20 min in a bath sonicator, and 4.5 mL minimum essential medium (MEM) was added. *(3)* FCS (0.5 mL) containing 40 nmol of P12-SPM was lyophilized and 5 mL MEM was added. *(4)* P12-SPM SUV (40 nmol) were prepared and added to the medium. *(5)* P12-SPM (40 nmol) was incorporated into LDLs. **(B)** *(1)* Apo E (60 μg) was added to P12-THC-SPM (50 and 116 nmol, respectively). *(2)* P12-THC (50 nmol) in 20 μL of DMSO was mixed with 0.5 mL of FCS and the mixture was sonicated for 20 min in a bath sonicator. *(3)* Same as (**B**, **2**) except that the mixture was dispersed in a probe sonicator. *(4)* SUVs of P12-THC-SPM (50 and 116 nmol, respectively). *(5)* FCS (0.5 mL) of containing 50 nmol of P12-THC was lyophilized and 5 mL of MEM was added. *Solid bars*, cell extract; *thatched bars*, ceramide ***(42)***.

cells washed once with PBS, and a solution of trypsin–EDTA added for 1 min. The liquid is removed and the dish incubated for 2–3 min at 37°C. One to two milliliters of PBS is added and the cells, now in suspension, are transferred to an Eppendorf tube, centrifuged, and the pellet suspended in 200–500 μL of PBS and sonicated in a probe sonicator up to 10 s. An aliquot of 5–10 μL is removed for protein determination (Bradford procedure, Sigma). The rest is transferred to a glass tube or dram vial, water is added to a volume of 1 mL followed by 1.0 mL of methanol containing 2% acetic acid, and the tube is vortex-mixed. One milliliter of chloroform is added and, following vortex-mixing, the tubes are centrifuged and two phases are obtained, the protein being at the interface. The lower, organic phase is pipetted into a dram vial and evaporated to dryness. One hundred microliters of chloroform–methanol (2 : 1) are added and a portion is applied to a TLC plate.

3.4. Analysis of Fluorescence

3.4.1. In Intact Cells

The fluorescence of intact cells can be viewed by fluorescence microscopy or by computerized fluorescence microscopy (also called imaging or microspectrofluorometry). The latter permits quantifying the fluorescence in a single cell and its intracellular components. For quantifying the fluorescence of intact cells, a suspension of the cells is introduced into a cuvette and its fluorescence recorded in a spectrofluorometer. The exitation of pyrene is at 343 nm and the monomolecular emission is at 378 nm. In intact cells frequently an excimeric emission is observed with a peak emission at 475 nm. The latter is a consequence of an "excited state dimers" which are formed when the pyrene residues come to close a proximity of about 10 (and the emission of the pyrene shifts to a higher wavelength (475 nm). Thus, appearance of the excimeric emission and its magnitude relative to that of the monomeric (at 378 nm) indicates the closeness of "packing" of the pyrene molecules within the cell and its compartments. In contrast to the preceding, the extracted cell lipids whose fluorescence is recorded as a solution in an organic solvent (usually chloroform–methanol mixtures) is fully monomeric, that is, an emission only at 378 nm.

3.4.2. In Cell Extracts

The lower, organic phase of the extracted, cellular lipids contains the original fluorescent lipid as well as a variety of its metabolic products. The latter can be hydrolytic products or, alternatively, synthetic ones. Analysis can be done by column chromatography or TLC or by high-performance liquid chromatography (HPLC). For TLC, an aliquot of the lipid extract is applied to a suitable plate which, in most cases, is coated with silica, but plates coated with aluminum oxide or a reverse-phase material can also be used. The plate is then developed in a closed container using a suitable solvent system. The composition of the latter depends on the polarity of the lipids to be separated. Nonpolar lipids are separated in mixtures of hexane–diethyl ether–acetic acid (80:20:1). The more polar lipids are separated using mixtures of chloroform, methanol, and water, 85:15:1.5 for cerebrosides, 75:25:4 for oligohexoside ceramides or sulfatide, 65:35:3.5 for sphingomyelin, and 50:50:10 (or even 1:2:1) for highly polar lipids such as gangliosides. The spots of the respective lipids are identified using suitable fluorescent markers. It should be emphasized that in in vitro studies a lipid is hydrolyzed by its specific hydrolase and produces only one product; for example, sphingomyelin, glucosylceramide, and galactosylceramide are hydrolyzed to ceramide; sulfatide to galactosylceramide; galactosyl-galactosyl-glucosyl ceramide (trihexasylceramide, THC) to DHC, and the various gangliosides to their respective products. This is not so

for an *in situ* (in cell) study. Because the lysosome of a normal cell contains the entire set of hydrolases, usually more than one product is observed. To exemplify, THC is hydrolyzed in vitro by an α-galactosidase to dihexosylceramide (DHC). But in intact cells DHC can be degraded by a β-galactosidase to glucosylceramide, the latter to ceramide, and even this "end product" of all sphingolipids can be further degraded by ceramidase to sphingosine and fatty acid. Therefore, a suitable set of all the respective pyrene lipids should be available. For analysis of the respective fluorescent spots, two modes can be used. In the first, the silica of the respective fluorescent spot, identified by illuminating the TLC plate with an ultraviolet lamp in a dark room, is scraped off the plate, and introduced into a glass tube. One or two milliliters of chloroform–methanol (1 : 2 v/v) are added. The test tube is covered with a thin nylon sheet, heated for 10 min at 55°C, centrifuged, the supernatant transferred to a glass cuvette, and the fluorescence recorded in a spectrofluorometer. To relate the fluorescence to the cell protein, the latter is determined by a Bradford reagent (Sigma B6916) and the fluorescence per milligram calculated.

In the second mode of analysis the TLC plate (or sheet) is scanned in a fluorescence plate scanner (e.g., Fluor-S^{IM}-MultiImager Bio-Rad, Hercules, CA 94547) and the fluorescence of the respective spots is quantified.

It should be emphasized that the fluorescence of intact cells and their intracellular distribution can be quantified by confocal, computerized fluorescence microscopy (imaging), and cell populations with varying fluorescence can be sorted as a suspension on the basis of their respective fluorescence emission in the fluorescence activated cell sorter (FACS). The FACS also permits separation of cell populations with differing fluorescence and collection, under sterile conditions, for regrowing in culture. (For an example, *see* **ref. *51***.)

3.5. Examples of Experimental Results

1. **Table 2** compares the uptake of six sphingolipids that have been deacylated and, subsequently, the fluorescent probe pyrene has been linked via a 12-carbon spacer (P12). The compounds are SPM (sphingomyelin), GM1 (ganglioside GM1), CS (sulfatide), gal Cer (ceramide β-galactose), THC (trihexosylceramide: ceramide-β-glucosyl-β-galactosyl-α-galactose), and GC (ceramide-β-glucose). Two modes of dispersion are compared: cosonication with fetal calf serum and apo E-coated small unilamellar vesicles. In this experiment, bovine brain sphingomyelin was used for liposomal dispersion. It is evident from the data that the liposomes were considerably more taken up by the cells and degraded to ceramide than the sonicates.
2. **Figure 1** compares the effects of five modes of dispersion on the uptake and degradation (to ceramide) of two sphingolipids, a P12-phospholipid (SPM-sphingomyelin) and a P12-glycolipid (THC). With either substrate the greatest uptake and degradation occurred with the apo E-coated SUV.

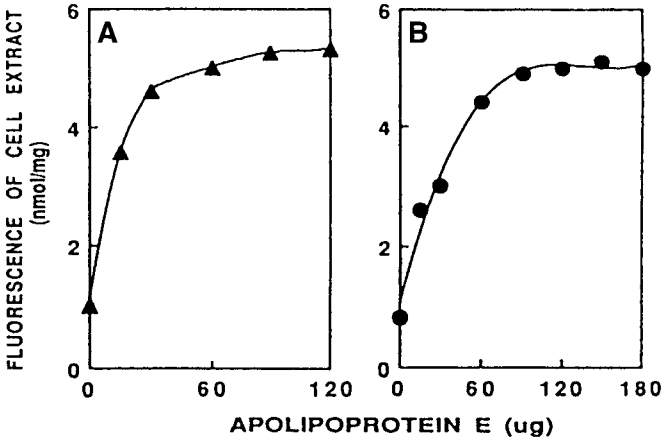

Fig. 2. Effect of increasing concentrations of apo E on uptake of P12-SPM or P12-THC. **(A)** Forty nanomoles of P12-SPM was sonically dispersed as SUVs, increasing concentrations of apo E were added, and the liposomes were incubated with the cells for 24 h in 4 mL of medium. **(B)** Conditions were as in **Fig. 1A**, except a mixture of 50 nmol of P12-THC and 116 nmol of SPM was used *(42)*.

3. **Figure 2** shows the effect on increasing concentrations of apo E on the uptake of P12-SPM (in **2A**) or P12-THC (in **2B**). Optimal uptake was at about 50 μg of apo E.
4. **Figure 3** shows the effect of increasing concentrations of liposomes of P12-SPM **(3A)** and P12-THC **(3B)** mixed with a fixed concentration (60 μg) of apo E.
5. **Figure 4** shows time curves of the fluorescence emission of a suspension of cells incubated with P12-THC-SPM apo E-coated SUV **(4A)** as well as their lipid extract and the product (P12-ceramide, **4B**). Thus, while the emission of the cell suspension increases in hyperbolic mode, that of the extracted lipids is in a straight line.
6. **Figure 5** shows the fluorescence of the extracts of cells that have been incubated for 1 d (pulse), the medium removed, cells washed, and incubation continued for another week (chase). The figure indicates the increase of fluorescence during the pulse and decrease of activity during the chase period.
7. **Figure 6A** describes, during a 9-d chase period the decrease of the fluorescence of extracts of cells preincubated with four lipids labeled with P12. **Figure 6B** describes, similarly, the decrease in the fluorescence of the end product (P12-ceramide).
8. **Figure 7** describes the fluorescence of P12-substrate (P12-THC) and product (glucosylceramide, P12-GC) in cells incubated with apo E-coated liposomes of the substrates. These cell types are compared: normal, heterozygous, and

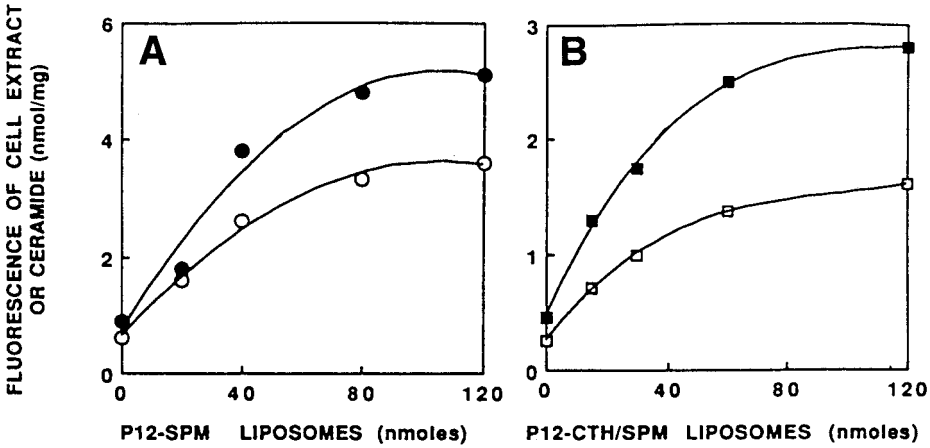

Fig. 3. Effect of increasing concentrations of P12-SPM or P12-THC-SPM liposomes on their uptake and degradation. SUVs of P12-SPM **(A)** or P12-THC-SPM (3:7, *M/M*) **(B)** at increasing concentrations were mixed with 60 μg of apo E and incubated with the cells for 24 h. ●, ■, Fluorescence of the extracted lipids; ○, ❑, Fluorescence of the ceramide ***(42)***.

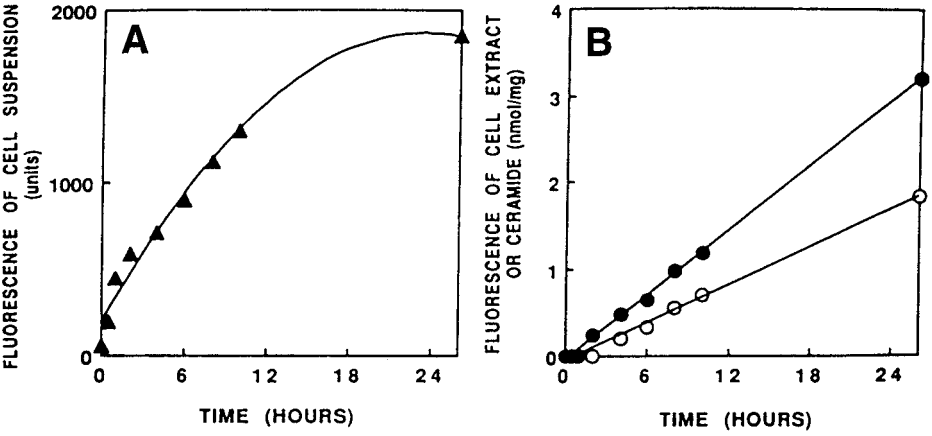

Fig. 4. Effect of incubation time on uptake and degradation of P12-THC. Conditions were as in **Fig. 2B**, except that the incubation time was varied. **(A)** Fluorescence of a suspension of the cells. **(B)** Fluorescence of the extracted lipids (●) or of ceramide (○) ***(42)***.

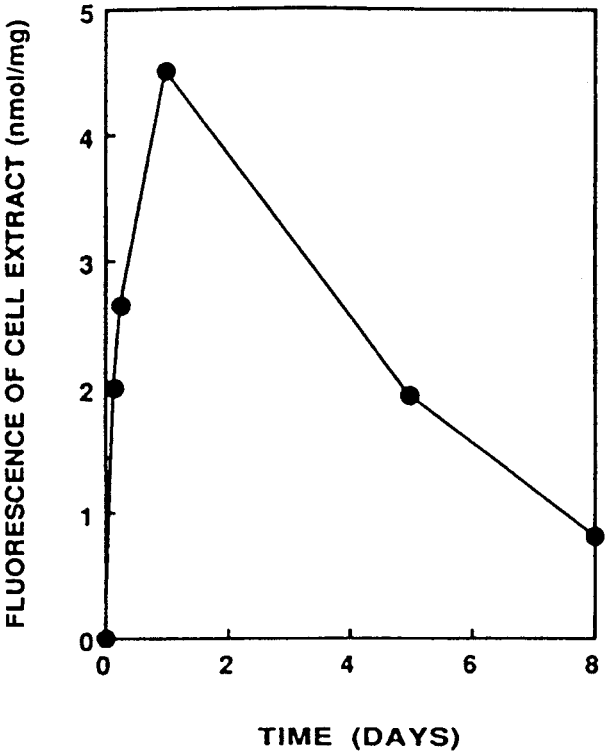

Fig. 5. "Pulse-chase" of cells incubated with P12-SPM-apo E liposomes. P12-SPM-apo E liposomes were prepared as described in the caption to **Fig. 2A** and incubated with cells for periods of up to 24 h ("pulse"); for the "chase," incubation was continued for 7 more days in medium devoid of P12-SPM ***(42)***.

homozygous for a lipid storage disease in which the lysosomal α-galactosidase is deficient (Fabry disease). It is evident that because of this deficiency in the diseased cells, the substrate (P12-THC) is not degraded, and the fluorescence of the substrate is high and that of the product is low. In the normal cells, in which the substrate is hydrolyzed by the normal enzyme, the fluorescence of the product is high and of the substrate low. In the heterozygous cells the values are intermediate between the above two cell types.

9. In a study aimed at working out a fluorescence-based procedure for preventing infants from being born with a lipid storage disease, we reasoned as follows ***(54)***. Semen and ova of heterozygous parents will be coupled, and the resulting embryonal cell grown, in vitro, to the stage of 8–16 cells. One embryonal cell will then be removed, a fluorescent substrate administered, and, if not degraded, a high fluorescence will persist. This will define the embryo as being lipidotic and it should not be implanted. Because ethically human embryos cannot be

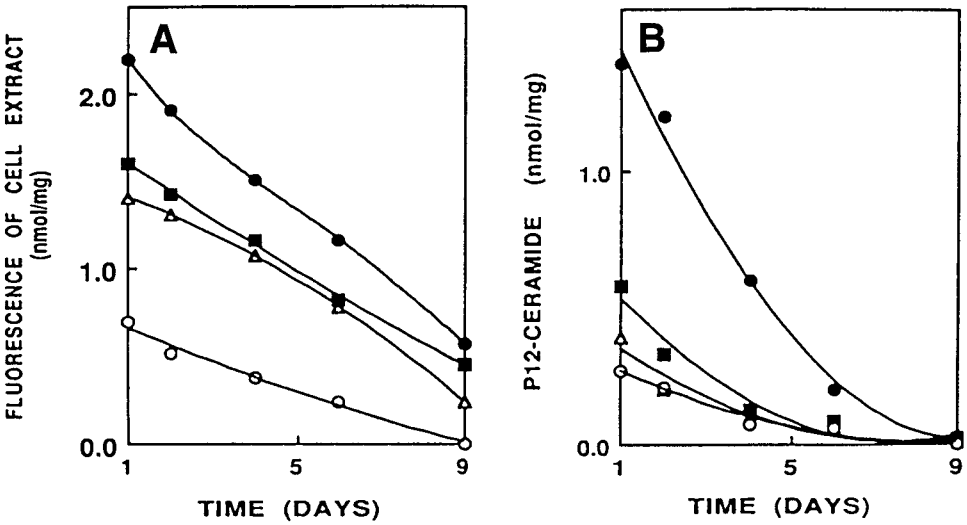

Fig. 6. Decrease of the fluorescence of administered lipids during a prolonged "chase." One hundred nanomoles of each of the P12 derivatives of ceramide (●), glucosylceramide (■), and dihexosyl (Δ), or trihexosyl (○) ceramide were cosonicated with 240 nmol of SPM, and 90 μg of apo E were added. After the mixture was incubated for 48 h with the cells, the cells were collected, dispersed in fresh medium, divided into five equal portions, and further incubated for periods as indicated on the abscissa. **(A)** Fluorescence of the extracted lipids. **(B)** Fluorescence of P12-ceramide ***(42)***.

handled for biological research, murine embryos were used as a model. We set up a model for Gaucher disease, the most prevalent genetic disorder in the Ashkenazi-Jewish population, by incubating the embryos with an inhibitor of the enzyme involved in this disease, β-glucosidase. In a preliminary study we needed to determine whether murine embryos have an LDL receptor (for uptake of apo E-coated liposomes). For this purpose murine embryos were incubated with P12-SPM SUV without and with apo E. **Figure 8** indicates an increased fluorescence (which was analyzed and quantified by computerized fluorescence microscopy in an ACAS 570 interactive laser cytometer) in the presence of apo E, indicating the presence of an LDL receptor on the murine embryo.

In **Fig. 9** a murine model of the lipid storage disorder Gaucher's disease was created. For this purpose murine embryos were incubated with bromoconduritol B-epoxide (Br-CBE), an inhibitor of β-glucosidase. P12-THC in SPM-SUV was then administered and, following a pulse of 2 h and an overnight chase, the fluorescence of the embryo was analyzed. It was expected that in the embryo not treated with Br-CBE, the P12-THC will be degraded to P12-lactosyl ceramide (by α-galactosidase) and the latter to P12-ceramide by β-glucosidase. Further metabolism of this P12-ceramide will result in clearance of the pyrene fluores-

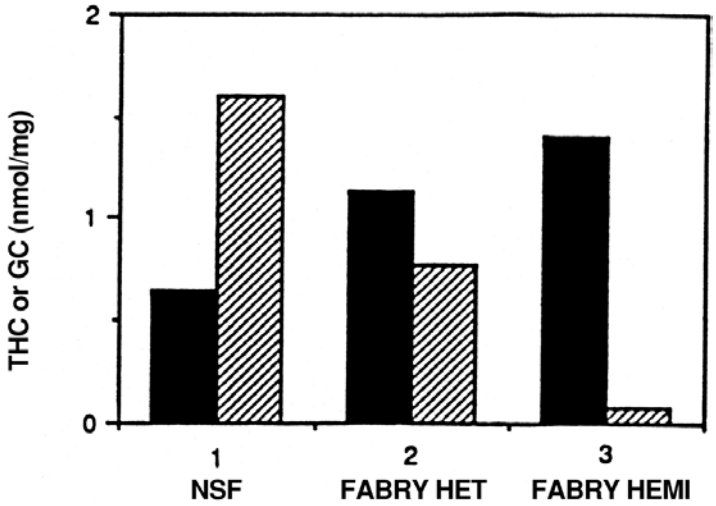

Fig. 7. Intracellular hydrolysis in normal and lipidotic cells: 125 nmol of P12-THC and 375 nmol of SPM in PBS were cosonicated, combined with 75 μg of apo E, and incubated with the respective cells for 4 d. Bromoconduritol B-epoxide (Br-CBE, 20 nmol/mL), a β-glucosidase inhibitor, was included in the medium to stop the chain of hydrolysis at the glucosylceramide step. *Black bars*, fluorescence of trihexosyl ceramide; *hatched bars*, fluorescence of glucosylceramide.

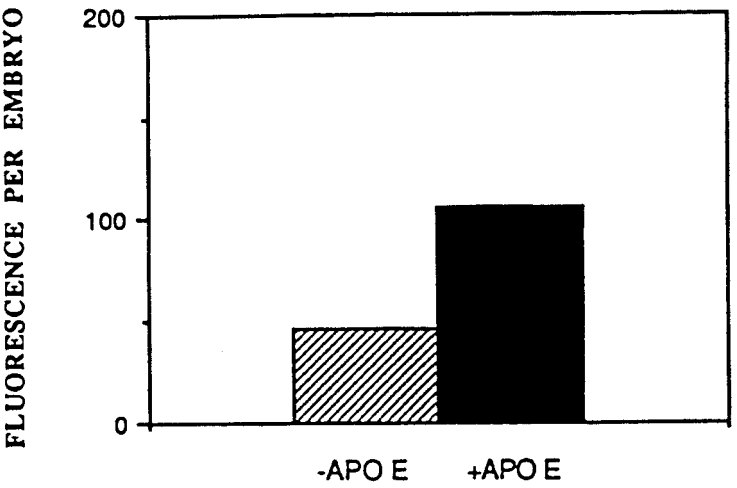

Fig. 8. Fluorescence of murine embryos following administration of P12-SPM in the absence (–) or presence (+) of apo E.

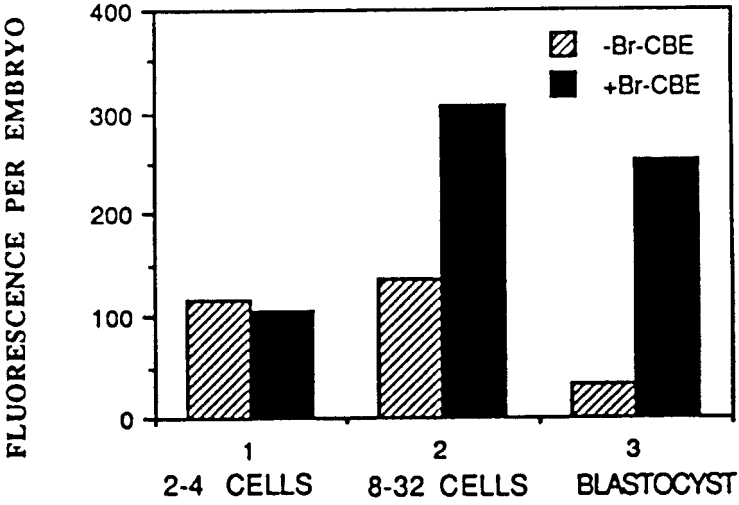

Fig. 9. Expression of fluorescence in murine embryos at varying developmental stages following administration of pyrene dodecanoyl trihexosylceramide (P12-THC) in presence or absence of bromoconduritol B epoxide (Br-CBE): Liposomes of P12-THC-SPM (20:80, mol/mol) were prepared, combined with 20 μg of apo E, and incubated for 90 min with murine embryos at the following stages: two to four cells (1), eight cells to morula (2), and blastocysts (3), without (*hatched*) and with (*solid*) the β-glucosidase inhibitor Br-CBE (20 μ*M*). The respective embryos were then transferred to fresh medium devoid of P12-THC, but with or without Br-CBE, and incubated overnight. The embryos were scanned in the ACAS 570.

cence from the embryo. In contrast, in the embryo treated with Br-CBE and consequently having no β-glucosidase activity, catabolism of the precursor P12-THC will proceed to the stage of P12-glucosylceramide; the latter compound will become an end product and will not be secreted; and high embryo florescence will persist. *Column 3* of **Fig. 9** indicated this is indeed the case. Thus, this experiment represents a model for human embryos that, due to the presence of a mutant sphingolipid hydrolase (homozygous for a lipid storage disease), cannot degrade the fluorescent lipid (a direct or indirect substrate, in this case P12-GC or P12-THC, respectively).

Figure 9 also shows that the same approach could be utilized for studying the developmental pattern of the enzyme β-glucosidase. Thus, in *column 1* of **Fig. 10**, in which two-cell embryos were used, there is no difference between embryos that had or had not been treated with Br-CBE. This indicates this enzyme has not yet been expressed. In *column 2* of **Fig. 9** (morula), and even more so in *column 3* (blastocyst), the difference between the two respective embryos is expressed. Thus,

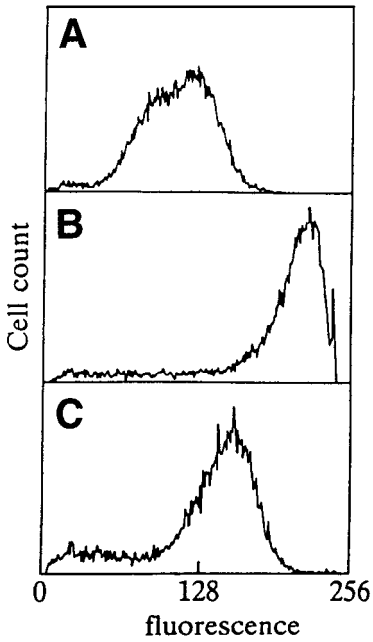

Fig. 10. Sorting of gene-corrected Niemann–Pick disease cells by flow cytometric analysis. Normal **(A)**, NPD **(B)**, and NPD cells transduced with the pBC-1 ASM retroviral vector **(C)** were incubated with apo E-coated P12-SPM liposomes for 48 h in serum-free medium. The medium was then replaced, and the cells were incubated without P12-SPM for 24 h. Cells were harvested and analyzed by using a FACS-440 flow cytometer ***(49)***.

in the absence of Br-CBE, the fluorescence per embryo is considerably lower than in their counterparts that had been incubated with this β-glucosidase inhibitor.

10. **Figure 10** shows the selection of lipidotic cells normalized by gene infection ***(49,50)***: This figure presents an experiment for selection of cells having a defective enzyme, and its counterpart in which this defect has been corrected by administering a gene that encodes for the normal enzyme. This study was done in collaboration with Drs. E. H. Schuchman, R. J. Desnick, M. Suchi, and L. Pereira of the Department of Human Genetics at the Mount Sinai School of Medicine in New York. For this purpose a retroviral construct having the cDNA that encodes for the lysosomal sphingomyelinase (ASM) was administered into fibroblasts of a Niemann–Pick type A (NPD) patient. Those cells that have incorporated the ASM-cDNA into their genome produced normal ASM, which degraded the administered P12-SPM, resulting in decreased fluorescence. The latter cells can be sorted and separated from the noncorrected lipidotic cells using a FACS. **Figure 10** shows the difference in fluorescence, as recorded in the FACS of normal, NPD, and the normalized cells.

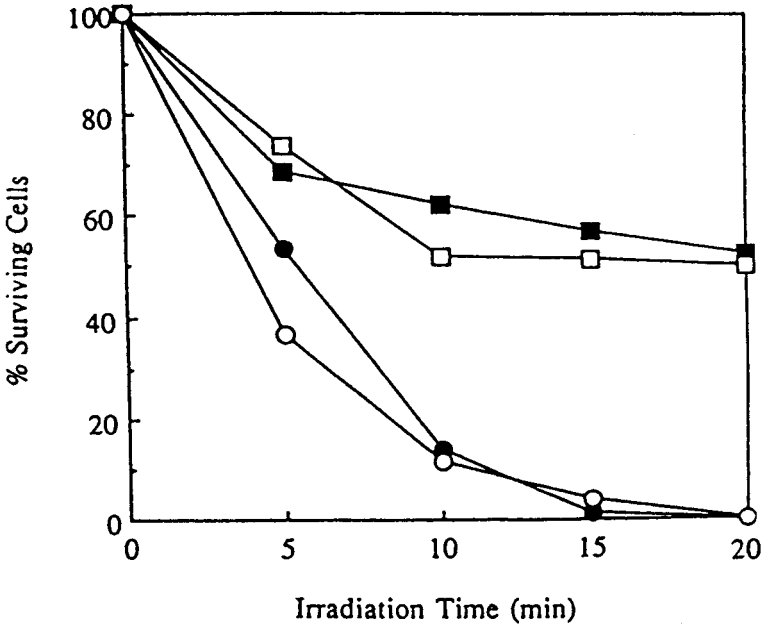

Fig. 11. Photosensitization and selective survival of gene-corrected Niemann–Pick disease cells. Cells were incubated with apo E-coated P12-SPM liposomes for 48 h, suspended in medium, and photoirradiated for 0–20 min. ■, Normal skin fibroblasts (NSF); ❑, type A NPD cell line transduced with pBC-1 retroviral construct (RF-s); ●, nontransduced type A NPD cell line (RF); ○, type A NPD cell line infected with ASM antisense retroviral construct (RF-As) ***(49)***.

11. Selective killing of cells by photosensitization ***(49)***: The fluorescent probe pyrene, used in the above studies, is also a photosensitizer. Thus, when excited at 343 nm, it emits photoactive energy that converts oxygen to singlet oxygen, which is toxic and results in cell killing. The quantity of singlet oxygen, and consequently cell killing, will depend on the quantity of pyrene present within the cell. **Figure 11** exemplifies this approach. In this figure, Niemann–Pick disease cells (lacking the lysosomal acid sphingomyelinase) and their gene corrected counterparts (which express this enzyme) were incubated with P12-SPM and, following pulse and chase periods, illuminated with a long wavelength ultraviolet light source. The Niemann–Pick disease cells were completely killed following a 20-min illumination, whereas normal, or Niemann–Pick disease cells that were "normalized" by gene correction, survived.

3.6. Conclusions

In this chapter we reviewed studies carried out in our laboratory and, in some cases, in collaboration with colleagues from other laboratories. In these selected

studies the nonpolar fluorescent probe pyrene was linked via a 12-carbon chain to phospho- and glycosphingolipids. Samples of these prospective compounds were mixed with sphingomyelin or lecithin and sonicated to form SUVs. Apo E was added to these liposomal dispersions, resulting in linkage of the apo E-SUVs to the LDL receptors on the plasma membrane, and their internalization by receptor-mediated endocytosis. Subsequently, they were trafficked to the lysosomes where they were degraded by hydrolysis in normal but not lipidotic cells.

This chapter describes in detail the synthesis of the respective pyrene lipids; various modes of administration into cells in culture; modes of incubation of the apo E-SUVs with cells; and modes of analysis of fluorescence in cells and their lipid extracts. Finally, 10 examples of application of the preceding are described.

We wish to emphasize that the studies described herein represent only a part of our cell-biological fluorescence-based studies. For such studies using other, more polar fluorescent probes, the reader is referred to our publications and reviews.

Acknowledgments

We wish to thank Biotechnology General, Inc. (Nes-Ziona, Israel) for a generous gift of apo E. Studies of S. Gatt reported in this publication were supported in part by the March of Dimes Birth Defect Foundation, USA, Israel Ministry of Health; US–Israel Binational Scientific Foundation; National Institutes of Health; Israel Academy of Sciences; Ministry of Science and Arts; Niedersachsen, FRG; and Deutsche Forschungs Gemeinschaft.

References

1. Gatt, S. (1963) Enzymatic hydrolysis and synthesis of ceramides. *J. Biol. Chem.* **238,** 3131–3133.
2. Gatt, S. (1966) Enzymatic hydrolysis of sphingolipids. I. Hydrolysis and synthesis of ceramides by an enzyme from rat brain. *J. Biol. Chem.* **241,** 3724–3730.
3. Yavin, Y. and Gatt, S. (1969) Further purification and properties of rat brain ceramidase. *Biochemistry* **8,** 1692–1698.
4. Barenholz, Y., Roitman, A., and Gatt, S. (1966) Enzymatic hydrolysis of sphingolipids. II. Hydrolysis of sphingomyelin by an enzyme from rat brain. *J. Biol. Chem.* **241,** 3731–3737.
5. Gatt, S. (1976) Magnesium-dependent sphingomyelinase. *Biochem. Biophys. Res. Commun.* **68,** 235–242.
6. Gatt, S., Dinur, T., and Kopolovic, J. (1978) Niemann–Pick disease: presence of the magnesium dependent sphingomyelinase in brain of the infantile form of the disease. *J. Neurochem.* **31,** 547–550.

7. Gatt, S., Dinur, T., and Leibovitz-Ben Gershon, Z. (1978) Magnesium dependent sphingomyelinase of infantile brain. Effect of detergents and a heat stable factor. *Biochim. Biophys. Acta* **531,** 206–214.
8. Gatt, S. and Rapport, M. M. (1966) Isolation of β-galactosidase and β-glucosidase from brain. *Biochim. Biophys. Acta* **113,** 567–576.
9. Gatt, S. and Rapport, M. M. (1966) Enzymatic hydrolysis of sphingolipids. Hydrolysis of ceramide lactoside by an enzyme from rat brain. *Biochem. J.* **101,** 680–686.
10. Gatt, S. (1966) Enzymatic hydrolysis of sphingolipids. Hydrolysis of ceramide glucoside by an enzyme from ox brain. *Biochem. J.* **101,** 687–691.
11. Gatt, S. and Baker, E. A. (1970) Purification and separation of α- and β-galactosidases from spinach leaves. *Biochim. Biophys. Acta* **206,** 125–135.
12. Frohwein, Y. Z. and Gatt, S. (1966) Separation of β-*N*-acetylglucosaminidase and β-*N*-acetylgalactosaminidase from calf brain cytoplasm. *Biochim. Biophys. Acta* **128,** 216–218.
13. Frohwein, Y. Z. and Gatt, S. (1967) Isolation of β-*N*-acetylhexosaminidase, β-*N*-acetylglucosaminidase and β-*N*-acetylgalactosaminidase from calf brain. *Biochemistry* **6,** 2775–2782.
14. Frohwein, Y. Z. and Gatt, S. (1967) Enzymatic hydrolysis of sphingolipids. VI. Hydrolysis of ceramide glycosides by calf brain β-*N*-acetylhexosaminidase. *Biochemistry* **6,** 2783–2787.
15. Leibovitz, Z. and Gatt, S. (1968) Enzymatic hydrolysis of sphingolipids. VII. Hydrolysis of gangliosides by a neuraminidase from calf brain. *Biochim. Biophys. Acta* **152,** 136–143.
16. Gatt, S., Barenholz, Y., and Roitman, A. (1966) Isolation of rat brain lecithinase-A_1 specific for the α′-position of lecithin. *Biochem. Biophys. Res. Commun.* **24,** 169–172.
17. Gatt, S. (1968) Purification and properties of phospholipase A_1 from rat and calf brain. *Biochim. Biophys. Acta* **159,** 304–316.
18. Leibovitz, Z. and Gatt, S. (1968) Isolation of lysophospholipase, free of phospholipase activity, from rat brain. *Biochim. Biophys. Acta* **164,** 439–441.
19. Leibovitz-Ben Gershon, Z., Kobiler, I., and Gatt, S. (1972) Lysophospholipases of rat brain. *J. Biol. Chem.* **247,** 6840–6847.
20. Leibovitz-Ben Gershon, Z. and Gatt, S. (1974) Lysolecithinase of rat brain. Further analysis of the effect of the substrate on the particulate and microsomal enzymes. *J. Biol. Chem.* **249,** 1525–1529.
21. Cabot, M. C. and Gatt, S. (1976) Hydrolysis of neutral glycerides by lipase of rat brain microsomes. *Biochim. Biophys. Acta* **431,** 105–111.
22. Cabot, M. C. and Gatt, S. (1977) Hydrolysis of endogenous diacylglycerol and monoacylglycerol by lipases in rat brain microsomes. *Biochemistry* **16,** 2330–2334.
23. Cabot, M. C. and Gatt, S. (1978) The hydrolysis of triacylglycerol and diacylglycerol by a rat brain microsomal lipase with an acidic pH optimum. *Biochim. Biophys. Acta* **530,** 508–512.
24. Gatt, S., Barenholz, Y., Goldberg, R., Dinur, T., Besley, G., Leibovitz-Ben Gershon, Z., et al. (1981) Assay of enzymes of lipid metabolism with colored

and fluorescent derivatives of natural lipids (Lowenstein, J. M., ed.), *Methods Enzymol.* **72,** 351–375.
25. Goldberg, R., Barenholz, Y., and Gatt, S. (1981) Assay of lipase using TNPAL glycerides. *Methods Enzymol.* **72,** 351–354.
26. Gatt, S., Dinur, T., and Barenholz, Y (1981) Assay of sphingomyelinase using fluorescent derivatives of sphingomyelin. *Methods Enzymol.*, **72,** 356–360.
27. Besley, G. and Gatt, S. (1981) Assay of galactosyl cerebroside β-galactosidase using TNPAL-galactosyl sphingosine. *Methods Enzymol.*, **72,** 360–362.
28. Besley, G. and Gatt, S. (1981) Assay of galactosyl cerebroside β-galactosidase using a fluorescent derivative of galactosyl cerebroside. *Methods Enzymol.*, **72,** 362–364.
29. Leibovitz-Ben Gershon, Z., Dinur, T., Barenholz, Y., and Gatt, S. (1981) Assay of glucosyl cerebroside β-glucosidase using TNPAL-glucosyl sphingosine. *Methods Enzymol.*, **72,** 364–367.
30. Gatt, S., Dinur, T., Barenholz, Y., Leibovitz-Ben Gershon, Z., Rosenthal, J., Devine, E. A., et al. (1981) Assay of glucosyl cerebroside β-glucosidase using fluorescent derivatives of glucocerebroside. *Methods Enzymol.*, **72,** 367–372.
31. Gatt, S. and Tsuruki, F. (1981) Assay of phospholipase A_2 using TNPAL phosphatidylcholine. *Methods Enzymol.*, **72,** 372–373.
32. Gatt, S. and Tsururki, F. (1981) Assay of phospholipase A_2 using fluorescent derivatives of phosphatidylcholine. *Methods Enzymol.*, **72,** 373–375.
33. Dinur, T., Grabowski, G. A., Desnick, J. R., and Gatt, S. (1984) Synthesis of a fluorescent derivative of glucosyl ceramide for the sensitive determination of glucocerebrosidase activity. *Analyt. Biochem.* **136,** 223–234.
34. Salvayre, R. and Gatt, S. (1985) Use of mixed dispersions of fluorescent galactosylceramide and sodium dodecylsulfate for assaying galactocylceramide-galactosidase and diagnosing Krabbe disease. *Enzyme* **33,** 175–180.
35. Bach, G., Dagan, A., Herz, B., and Gatt, S. (1987) Diagnosis of arylsulfatase-A deficiency in intact cultured cells using a fluorescent derivative of cerebroside sulfate. *Clin. Genet.* **31,** 211–217.
36. Klar, R., Levade, T., and Gatt, S. (1988) Synthesis of pyrene sulfonylamidosphingomyelin and its use as substrate for determining sphingomyelinase activity and diagnosing Niemann–Pick disease. *Clin. Chim. Acta* **176,** 259–268.
37. Marchesini, S., Viani, P., Cestaro, B., and Gatt, S. (1989) Synthesis of pyrene derivatives of cerebroside sulfate and their use for determining arylsulfatase A activity. *Biochim. Biophys. Acta* **1002,** 14–19.
38. Negre, A., Dagan, A., and Gatt, S. (1989) Pyrene-methyl lauryl ester, a new fluorescent substrate for lipases: use for diagnosis of acid lipase deficiency in Wolman's and cholesteryl ester storage diseases. *Enzyme* **42,** 110–117.
39. Negre, A., Salvayre, R., Dagan, A., and Gatt, S. (1989) Pyrene methyl laurate, a new fluorescent substrate for continuous kinetic determination of lipase activity. *Biochim. Biophys. Acta* **1006,** 84–88.
40. Levade, T., Gatt, S., and Salvayre, R. (1991) Uptake and degradation of several pyrene-sphingomyelins by human skin fibroblasts from controls and Niemann–

Pick disease: effect of the structure of the fluorescent fatty acyl residue. *Biochem. J.* **275,** 211–218.
41. Levade, T., Gatt, S., Maret, A., and Salvayre, R. (1991) Different pathways of uptake and degradation of sphingomyelin by lymphoblastoid cells and the potential participation of the neutral sphingomyelinase. *J. Biol. Chem.* **266,** 13519–13529.
42. Agmon, V., Dinur, T., Cerbu, S., Dagan, A., and Gatt, S. (1991) Administration of pyrene lipids by receptor-mediated endocytosis and their degradation in skin fibroblasts. *Exp. Cell Res.* **196,** 151–157.
43. Negre-Salvayre, A., Dagan, A., Gatt, S., and Salvayre, R. (1993) Use of pyrene methyl laurate for fluorescence-based determination of lipase activity in intact living lymphoblastoid cells and diagnosing acid lipase deficiency. *Biochem. J.* **294,** 885–891.
44. Levade, T., Vidal, F., Gatt, S., Vermeersch, S., Andieu, N., and Salvayre, R. (1995) Degradation of fluorescent and radiolabelled sphingomyelins in intact cells by a non-lysosomal pathway. *Biochim. Biophys. Acta* **1258,** 277–287.
45. Agmon, V., Khosravi, R., Marchesini, S., Dinur, T., Dagan, A., Gatt, S., and Navon, R. (1996) Intracellular degradation of sulforhodamine-GM1: use for a fluorescence-based determination of GM2 gangliosidosis variants in fibroblasts and white blood cells. *Clin. Chim. Acta* **247,** 105–120.
46. Erlich, S., Miranda, S. R. P., Visser, J. W. M., Dagan, A., Gatt, S., and Schuchman, E. H. (1999) Fluorescence-based selection of gene-corrected hemapoietic stem and progenitor cells from acid sphingomyelinase-deficient mice: implications to Niemann–Pick disease gene therapy and the development of improved stem cell gene transfer procedures. *Blood* **93,** 80–86.
47. Chatelut, M., Leruth, M., Harzer, K., Dagan, A., Marchesini, S., Gatt, S., et al. (1998) Natural ceramide is unable to escape the lysosome in contrast to a fluorescent analogue. *FEBS Lett.* **426,** 102–106.
48. Agmon, V., Monti, E., Dagan, A., Preti, A., Marchesini, S., and Gatt, S. (1993) Diagnosis of lipid storage diseases using the culture medium of skin fibroblasts. *Clin. Chim. Acta* **218,** 139–147.
49. Suchi, M., Dinur, T., Desnick, R. J., Gatt, S., Pereira, L., Gilboa, E., and Schuchman, H. (1992) Retroviral-mediated transfer of the human acid sphingomyelinase cDNA: correction of the metabolic defect in cultured Niemann–Pick disease cells. *Proc. Natl. Acad. Sci. USA* **89,** 3227–3231.
50. Dinur, T., Schuchman, E. H., Fibach, E., Dagan, A., Suchi, M., Desnick, R. J., and Gatt, S. (1992) Toward gene therapy for Niemann–Pick disease (NPD): separation of retroviral corrected and non-corrected NPD fibroblasts using a novel fluorescent sphingomyelin. *Hum. Gene Ther.* **3,** 633–699.
51. Yeyati, P. L., Agmon, V., Dinur, T., Fillat, C., Dagan, A., Desnick, R. J., et al. (1995) Preparative isolation of metabolically-corrected Niemann–Pick disease cells for gene therapy: evidence for bystander correction of transduced cells. *Hum. Gene Ther.* **6,** 975–983.

52. Dagan, A., Agmon, V., Gatt, S., and Dinur, T. (1999) Synthesis of fluorescent substrates and their application to the study of sphingolipid metabolism, *in vitro* and in intact cells, *Methods Enzymol.* **312,** 293–304.
53. Gatt, S., Dinur, T., Cerbu-Karabat, S., Dagan, A., and Agmon, V. (1995) Use of liposomes for administering fluorescent lipids and studying their metabolism in normal and lipidotic cells, in *Handbook of Non-Medical Application of Liposomes: Models for Biological Phenomena*, vol. II (Barenholz, Y. and Lasic, D. D., eds.), Academic Press, San Diego, pp. 137–152.
54. Epstein, M., Avital, Y., Agmon, V., Dinur, T., Fibach, E., Gatt, S., and Laufer, N. (1993) Use of fluorescence for diagnosing a murine embryo of Gaucher disease. *Hum. Reprod.* **8,** 302–309.
55. Suzuki, Y., Hirabayashi, Y., and Matsumoto, M. (1984) Hydrozinolysis of glycosphingolipids. A new method for preparation of *N*-deacylated (lyso) glycolipids. *J. Biochem.* **95,** 1219–1222.

7

Micelles and Liposomes in Metabolic Enzyme and Glycolipid Glycosyltransferase Assays

Manju Basu and Subhash Basu

1. Introduction

The use of liposomes has long been in practice for various biochemical purposes including liposome–enzyme targeting into different organelles ***(1–5)***. Different aspects of liposome uses are discussed in this book. This chapter is a general review on the use of liposomes in the enzyme assay with emphasis on glycolipid:glycosyltransferases.

1.1. Use of Liposomes in Enzyme Assays

Liposomes or vesicles have been used for stabilization of solubilized enzymes ***(6–10)***. Enzyme replacement via liposomes has been studied using liposmes with varying lipid compositions to investigate its integrity in biological fluids. Biological fluids disrupt the liposome-constituent balance very rapidly, and studies have indicated that cholesterol and sphingomyelin both enhances liposome integrity in the presence of serum and plasma ***(11)***. The effect of cholesterol on viral and vesicle membranes has been studied using cholesterol oxidase ***(12)***. Modulation of membrane acetylcholinesterase activity by lipids has been studied to demonstrate lipid–protein interaction ***(13)***. The change in catalytic properties of erythrocyte acetylcholinesterase after binding to lecithin liposome has also been studied ***(14)***. Binding of the enzyme to lecithin not only abolishes excess substrate inhibition of the enzyme but also decreases the pH optima of the reaction, increases resistance to heat denaturation of the enzyme, and reduces the extent of calcium activation. The role of phospholipids in restoration of catalytic activity of detergent-solubilized adenylate cyclase was also studied ***(15)***.

From: *Methods in Molecular Biology, vol. 199: Liposome Methods and Protocols*
Edited by: S. Basu and M. Basu © Humana Press Inc., Totowa, NJ

1.2. AcetylCoA-Cholesterol Acyltransferase

Studies on reconstitution of solubilized acetylCoA-cholesterol acyltransferase (ACAT) into liposomes using various phospholipids had shown the reconstituted enzymatic activity to be dependent on cholesterol concentration in the reconstitution mixture *(16)*. The reconstitution was also shown to vary with change in phospholipid head group. Based on results using a solubilized and reconstituted rat liver ACAT preparation, it was hypothesized that the substrate supply and the fluidity of the membrane contribute to the regulation of the rate of cholesterol ester formation *(17)*. This view was further supported by work from other groups with purified ACAT from tumor as well as from Chinese hamster ovary cells *(18,19)*. Studies with human plasma lecithin : cholesterol acyltransferase (LCAT) indicated that high-density lipoprotein (HDL) was a considerably better substrate for LCAT than phosphatidylcholine : cholesterol liposome *(20)*.

1.3. ATPase

Studies with cholate-solubilized Mg^{2+}-ATPase of calf brain clathrin-coated vesicles indicated that the solubilized ATPase could be reconstituted into phospholipid vesicles when combined with a 100,000*g* pellet, which displayed ATP-dependent proton uptake *(21)*. In another study, the Ca^{2+}/Mg^{2+}-ATPase was purified after solubilization by cholate and then reconstituted into a sealed phospholipid vesicle after removal of detergent *(22)*. Ca^{2+} accumulation in these vesicles increased with increasing amount of phospholipids used for reconstitution, independent of the phosphate concentration. This relative effect of phospholipid concentration on Ca^{2+} accumulation had been suggested to be result of an effect of ATPase-mediated Ca^{2+} efflux rate *(22)*. Biochemical characterization of the yeast Golgi derived vesicles accumulated in a mutant defective in secretory enzyme acid phosphatase has indicated that plasma membrane ATPase and secretory acid phosphatase are transported in a single vesicle species. The coordinated process of secretion and plasma membrane assembly, as noted during the fusion of the vesicles with the bud membrane, comprise the yeast cell surface growth *(23)*. Kinetic studies were performed with yeast plasma membrane H^+-ATPase in detergent (Zwittergent TM^{14})/lipid/enzyme micelles (isolated) and proteoliposomes (reconstituted enzyme). It was concluded from these studies that detergent reversibly interacts with the enzyme and all ATP binding sites are directed to the outside of the reconstituted vesicles *(24)*. Studies were continued to investigate the mechanism of membrane enzyme solubilization using ionic and nonionic detergent for solubilization of liposome and plasma membrane enzymes. It was observed that nonionic detergents interact with lipid component of Ca^{2+}-ATPase

membranes below the critical micellar concentration (CMC) whereas charged detergents such as sodium dodecyl sulfate (SDS) extracts the enzyme before solubilization of the lipid. It was suggested that detergent solubilization proceeds by combination of a transbilayer attack by detergent followed by direct extraction of the membrane component by detergent micelles ***(25)***.

1.4. Alkaline Phosphatase

Various groups using different solvent systems have studied alkaline phosphatase activity in reverse micelle. It had been concluded that the shift in the optimum pH of the enzymatic activity in reverse micelles might have resulted from the pH-dependent change in enzyme conformation. This shift is accompanied by exposure or masking of an anchor group providing the interaction of alkaline phosphatase with the reverse micelle matrix ***(26,27)***. Lipid–protein interaction studies with purified rat intestinal alkaline phosphatase showed that the polar head groups are not directly involved in the binding of the enzyme to the membrane ***(28)***. The enzymatic activity was lost by treatment with phospholipase D but could be restored with free choline or choline-containing phospholipid. A hydrophobic interaction with membrane phospholipids was suggested that initiates the activation of the membranous alkaline phosphatase followed by a secondary interaction with choline that protects the active site of the enzyme from inhibition by membrane phosphate groups ***(28)***. A separate investigation with rat tissue specific (intestinal) and tissue nonspecific (kidney) alkaline phosphatase resulted in the finding that although both enzymes are bound to their respective membrane phospholipids by hydrophobic anchor peptides, their sensitivities toward phospholipids are different ***(29)***. Further studies indicated that alterations in cholesterol content and cholesterol/phospholipid ratio of the microvillus membrane could modulate rat proximal small intestinal microvillus membrane alkaline phosphatase ***(30)***.

1.5. Phospholipases

Detailed studies on the mechanism of action of cobra venom phospholipase A_2 (PLA_2) proposed the reaction to proceed via two steps toward the lipid–water interface. The phenomena of surface dilution and activation by certain lipids activate the enzyme at various lipid–water interfaces ***(31)***. Kinetic studies using unilamellar vesicle of egg lecithin showed that PLA_2 has the unique property of selectively degrading the phospholipid only at the outer half of the lipid bilayer or vesicle membrane leaflet, leaving the remaining vesicle intact and impermeable to ionic solutes ***(32)***. This unique property of PLA_2 had been extended to demonstrate that only outer membrane phospholipid is involved in the exchange of phosphatidylcholine between small unilamellar liposomes and

human high-density lipoprotein (HDL) ***(33)***. Further studies on the mechanism of activation of PLA_2 confirmed that the structural basis for membrane PLA_2 activation is the consequence of membrane phospholipid (unsaturated phosphatidylethanolamine [PE]) peroxidation which increases the membrane viscosity associated with vesicle instability and enhanced PLA_2 attack ***(34)***. Biphasic substrate dependency of *Agkistrondon piscivorus piscivorus* PLA_2 activation was demonstrated using dipalmitoylphosphatidylcholine (DPPC) vesicles ***(35)***. Dimerization of the enzyme on surface vesicle was proposed previously as an enzyme activation model. This finding had been confirmed here by the observation that the monomeric enzyme, which has a low level of activity toward DPPC vesicles, becomes activated on the vesicle surface by dimerization. This leads to abrupt transition of the vesicle internal structure as observed by fluorescence studies resulting in the fast activation of the enzyme ***(35)***.

Lipid peroxidation contributes to the degree of hydrolysis by PLA_2. Using model membranes consisting of phosphatidylcholine (PC) and PE individual as well as mixed vesicles, the extent of hydrolysis by PLA_2 was measured as a result of induced lipid peroxidation ***(36)***. It has been observed that PC has a much higher preference for lipid peroxidation for all vesicle compositions that resulted in preferential hydrolysis by PLA_2. This effect was proposed to be due to perturbation of membrane structure caused by peroxidation, resulting in a higher PC concentration in the PLA_2 susceptible domain without greatly affecting PE peroxidation and hydrolysis. Lipid peroxidation provides an additional hydrolytic susceptibility of the substrate in addition to vesicle composition. Further studies have indicated that in addition to lipid peroxidation, membrane fusion or vesicle–vesicle interaction provides another cause of higher PLA_2 activation as a result of increased access of surface phospholipid ***(37)***.

Fusion of large unilamellar vesicles containing PC/PE/cholesterol (PC/PE/Chol) in the molar ratio of 2 : 1 : 1 had been shown to be catalytically activated by phospholipase C ***(38)***. This phenomenon is of significant importance in the understanding of membrane fusion processes. Synthetic lipid vesicles of the aforementioned phospholipids containing different concentrations of gangliosides were found to be inhibitory toward phospholipase C activity and other fusion processes including vesicle aggregation ***(39)***. This inhibition was found to increase with increasing oligosaccharide chain of gangliosides, resulting in a decrease in vesicle aggregation and lipid mixing rate. These effects are explained as due to lamellar structure stabilization by gangliosides.

Binding studies with phosphatidylinositol-specific phospholipase C (PI-PLC) from *Bacillus cereus* showed that binding to the micelles and bilayers depends on the ionic nature of the phospholipids and the binding proceeds in two stages in which binding at the interface precedes catalytic turnover at the interface ***(40)***.

Recently activation of phospholipase C δ_1 has been shown to be due to the formation of an enzyme–Ca^{2+}–phosphatidylserine (PS) ternary complex through the C2 domain of the enzyme which increases affinity for the substrate resulting in the activation of the enzyme ***(41)***. Phospholipase C δ had been shown to be inhibited strongly by sphingomyelin and also to some extent by other phospholipids (PC, PS, and PI) irrespective of the presence or absence of spermine, which is an activator of PLC δ ***(42)***.

The physiological relevance of phospholipase D and phosphatidic acid (PA), an anionic lipid, has been proposed using model membrane vesicles. Experimental evidence suggested that human secreted phospholipase A_2 ($sPLA_2$), which accumulates in extracellular fluids during inflammation, has a marked preference for the anionic phospholipid interface. PA present on the surface of the cell membrane can be hydrolyzed by $sPLA_2$ with the formation of lysophosphatidic acid and other lipid intermediates, making the enzyme proinflammatory. Pretreatment of the pure PC vesicle with phospholipase D also resulted in similar observation with enhancement of hydrolysis by $sPLA_2$ ***(43)***.

1.6. Sphingolipid Hydrolases

A large number of sphingolipid hydrolases (aryl sulfatase, ceramidase, and sphingomyelinase) had been purified and their kinetic parameters studied with the use of phospholipid micelles, liposomes, and vesicles by Gatt et al. and described in detail in this book ***(44–46)***. Use of fluorescent sphingolipids originally developed in his laboratory has opened up a new avenue for the study of glycosphingolipid metabolism in vivo ***(45)***.

Among sphingolipid hydrolases, aryl sulfatase, ceramidase, and sphingomyelinase are the most important ones involved in various cellular processes and related to different genetic disorders (Niemann–Pick disease, Gauche's disease). The physiological substrates for all these hydrolases are very hydrophobic in nature and mostly membrane anchored. Thus the presence of detergents is essential for their enzymatic activity. Previous reports, however, indicated the hydrolysis of sulfatide (cerebroside sulfate) by aryl sulfatase A in the presence of an activator protein in the absence of detergent ***(47)***. An investigation using proteoliposomes consisting of nonionic detergent solubilized rat liver and brain microsomes with various phospholipid compositions indicated that phospholipids modulate the kinetic properties of aryl sulfatase and other enzymes ***(48)***. It was concluded that the membrane-bound enzyme activity might be modulated by charged phospholipids due to decreasing or increasing substrate concentration in the unstirred layer.

The uniqueness of the membrane lipid molecule arrangement during phase transition contributes significantly to the sphingomyelinase activity as observed in hydrolysis of sphingomyelin containing different fatty acids ***(49)***. Maximum

hydrolysis by a bacterial sphingomyelinase was achieved at the beginning of the gel to liquid crystalline phase transition compared to much lower activity both below and above those temperatures. Furthermore it was observed that the presence of cholesterol or PE in biomembrane makes the membrane more susceptible to attack by sphingomyelinase ***(50)***. Recent studies with sphingomyelinase and PC showed that these enzymes work independently on their membrane-anchored substrates without major changes in vesicle architecture ***(51)***. It was further observed that the joint hydrolytic activities of these two enzymes gives rise to the leakage-free vesicle aggregation and vesicle fusion in spite of unequal contribution of both enzymes. Induction of a lipid microdomain formation by the action of sphingomyelinase has recently been shown in a fluid PC/sphingomyelin membrane ***(52)***.

The studies on glycosyltransferases involved mainly in glycosphingolipid biosynthesis are discussed in detail in **Subheadings 2.2.–3.6.**

2. Methods

2.1. Preparation of Liposomes

One of the major factors in the preparation of liposomes is the CMC of the individual detergents, and it is a well regarded fact that the efficiency of a detergent to produce micelle depends on its CMC and also on its affinity for the liposomal membranes ***(53)***. A combined method of dilution of the detergent under CMC and dialysis has been used for the preparation of liposomes from mixed micelles ***(54)***. Recently, a new method has been reported for the preparation of hydrophobic peptides and SDS mixed micelles that involves mixing of aqueous detergent solution with an equal volume of the peptide in triflouroethanol. The homogeneous clear solution was then lyophilized, resulting in the formation of dry powder of the protein which could be made to a desirable concentration by suspension ***(55)***. Another new method independent of the CMC of the detergent has been reported recently for the preparation of proteoliposomes of defined lipid/protein ratio from mixed detergent/lipid/protein micelles ***(56)***. The cyclodextrin type inclusion compounds have a higher affinity for detergents than for bilayer forming lipids. Taking advantage of this characteristic, this method results in the production of proteoliposomes and detergent–cyclodextrin complexes that can be easily separated by discontinuous sucrose gradient centrifugation. A recent report also indicates involvement of charged detergents to activate the stable liposomes to produce semipermeable microcompartments ***(57)***. Experimental results established the fact that stable liposomes from 1-palmitoyl-2-oleoyl-*sn*-glycero-3-phosphocholine (POPC) can be used as semipermeable microreactors when

treated with sodium cholate, and this cholate-induced permeability of POPC bilayer allows introduction of enzyme proteins from the outside.

2.2. Glycolipid : Glycosyltransferase Assays Using Various Micelle/Liposomes

2.2.1. Assay of Glycolipid : Glycosyltransferases in Detergent Micelle

All glycolipid : glycosyltransferase assays discussed herein were conducted using our previous protocol ***(58)***. In brief, a chlorofom–methanol (C/M = 2 : 1) solution of specific substrate and detergent solutions in required concentrations is dried in a rotary desiccator under vacuum. Rotary vacuum drying of the substrate and detergent together in C/M solution makes the substrate in the detergent micelle easily accessible to the enzyme. Specific buffer at optimum pH for the particular enzyme was added to the detergent–substrate micelle along with the enzyme protein in the required amount (at saturation concentration) and specific nucleotide sugar donor (^{14}C- or ^{3}H-labeled). All the components were used at constant reaction rate condition. After a linear time of incubation at 37ºC the incubation mixtures were quantitatively spotted on either SG81 or Whatman 3MM chromatography paper and chromatographed in ascending fashion using 1% sodium tetraborate solvent system. The radioactive enzymatic glycolipid product as well as the unreacted glycolipid substrate remained at the origin while the cleaved and unreacted radioactive sugar nucleotide moved with the solvent front. The appropriate areas containing radioactive glycolipid products were quantitated using liquid scintillation ***(58)***. The structures and abbreviations of various glycosphingolipids mentioned in this chapter are listed in **Table 1**. The glycosyltransferases involved in the stepwise in vitro biosynthesis of gangliosides and different glycolipids that have been characterized, purified, and a few of that have been cloned in our laboratory, as well as in others', are shown in **Fig. 1**. **Table 2** is an extension of **Fig. 1**, which summarized the individual glycolipid products formed by each enzyme.

2.2.2. Glycolipid : Glycosyltransferase Assay in Phospholipid Liposomes

Specific phospholipid solutions made in chloroform–methanol (2 : 1) were dried in small reaction tubes (6 × 50 mm) with or without glycolipid substrates using rotary desiccator under vacuum. Phosholipid liposomes were then prepared after addition of appropriate assay buffers by sonication at a constant temperature (37ºC) for 5–15 min in a specially designed water bath fitted with a sonic probe ***(59,60)***. Approximately 25 reaction tubes can be used simultaneously in this apparatus. The enzyme and the other required reaction components were added in the tubes followed by incubation and assay as

Table 1
GLT Nomenclature

Structures of glycolipids	Abbreviation
Galβ1-4Glc-Cer	LacCer (Lc_2)
NeuNAcα2–3Lac-Cer	GM_3
GalNAcβ1–4(NeuNAcα2–3)Lac-Cer	GM_2
Galβ1-3GalNAcGM3	GM_1
GlcNAcβ1-3LacCer	LcOse3Cer (Lc3)
Galβ1-4LcOse3Cer	nLcOse4Cer (nLc4)
Galα1-3nLcOse4Cer	
Galβ1-4LcOse3Cer	nLcOse5Cer (nLc5)
|α1-2	H
Fuc	
NeuAcα2-3nLcOse4Cer	LM1
Galβ1-4GlcNAcβ1-3LacCer	
|α2-3 |α1-3	SA-Le^x
NeuNAc Fuc	
GlcNAcAβ1-3nLcOse4Cer	i-antigen
GlcNAcb1-6(GlcNAcβ1-3)nLcOse4Cer	i/I-antigen
GlcAβ1-3nLcOse4Cer	HNK-1 epitope
Galα1-4LacCer	GbOse3Cer (Gb3)
GalNAcβ1-3GbOse3Cer	Globoside (Gb4)
GalNAcα1-4GalNAcβ1-3GbOse3Cer	Forssman Antigen

described previously. The circular arrangements of the small incubation tubes containing phospholipids around the sonic probe (in the aforementioned specially designed circular sonic water bath) help to distribute the sonic energy equally to all tubes, resulting in the formation of similar types of vesicles in all tubes.

2.2.3. Preparation of Ceramide-Containing Liposomes

A previous report of the preparation of liposome for gluco- or galactocerbroside assay by GlcT or GalT (**Fig. 1** and **Table 2**) is described below ***(61)***. Liposomes containing ceramide substrate with normal or α-hydroxy fatty acid and specific phospholipids were made by evaporating C : M solution of each in specific combinations according the enzymatic requirements under nitrogen, which was then placed under a high vacuum lyophilizer overnight. The dry film was then swollen in EDTA containing Tris buffer of the required pH for 30 min followed by sonication using an ice bath, and the required assay components were added in the tube for enzyme assay.

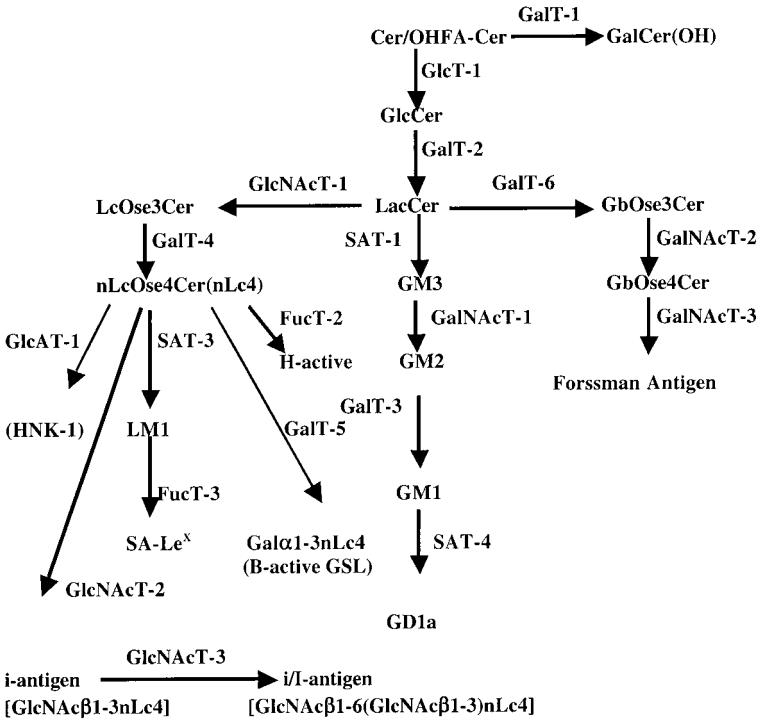

Fig. 1. Proposed pathways for biosynthesis of gangliosides, Forssman, and Blood Group-Related Glycolipids.

2.3. Results and Discussions

The glycolipid:glycosyltransferases (GSL:GLTs) could be classified as CARS (carbohydrate recognizing transferase) and HY-CARS (hydrophobic and carbohydrate recognizing transferases) enzymes according to their substrate specificities (**Table 2**; ***60,62,63***). Our laboratory has been working in the field of GSL:GLTs for the last 30 yr and careful studies with several purified glycosyltransferases have resulted in their classification as CARS and HY-CARS enzymes (**Table 2**; ***60,62,63***). The requirements of the HY-CARS enzymes are very specific as observed in our laboratory, and several different glycosyltransferases fall strictly in that class of enzymes ***(59,60,62–65)***. These HY-CARS transferases are very much dependent on the nature of acyl- or acetylsphingosine in the ceramide moiety of the substrate as discussed later. Various detergents have been used in the solubilization of these glycosyltransferases from Golgi-rich membrane fraction of various tissues. It has been observed that the solubilized enzyme proteins become catalytically inactive very rapidly, most probably due to the removal of an anchoring phospholipid

Table 2
Enzymes/Classification/Linkage in Product

Substrate	Enzyme	Product
Ceramide-OH	GalT-1	Galβ1-1Cer
GlcCer	GalT-2	Galβ1-4Glc-Cer
GM_2	GalT-3	Galβ1-3GalNAcβ1-4GM3
LcOse3Cer (Lc3)	GalT-4	Galβ1-4GlcNAcβ1-3LacCer
nLcOse4Cer	GalT-5	Galα1-3nLcOse4Cer
LacCer	GalT-6	Galα1-4Galβ1-4GlcCer
LacCer	GlcNAcT-1	GlcNAcβ1-3LacCer
LacCer	SAT-1	NeuNAcα2-3Galβ-4GlcCer
nLcOse4Cer (nLc4)	SAT-3	NeuNAcα2-3Galβ1-4LcOse3Cer
GM3	GalNAcT-1	GalNAcβ1-4Gal-Glc-Cer |α2-3 NeuNAc
GbOse3Cer (Gb3)	GalNAcT-2	GalNAcβ1-3Galα1-4LacCer
nLcOse4Cer	FucT-2	Fucα1-2Galβ1-4LcOse3Cer
LM1	FucT-3	NeuNAcα-Galβ1-4 GlcNAcβLacCer |α1-3 Fuc
nLcOse4Cer	GlcAT-1	GlcAβ1-3Galβ1-4LcOse3Cer

in the membrane. It was predicted that there might exist some interactions between hydrophobic domains of these transferases with the lipophilic portions of the membrane phospholipids for stabilization of the membrane-bound phospholipid-anchored enzyme proteins ***(59,60,64)***. Effects of various phospholipid and the sphingolipid metabolites have also been studied with the purified enzymes and are discussed below.

2.3.1. Galactosyltransferases

Several different galactosyltransferases (GalTs) are involved in the biosynthesis of various glycosphingolipids as shown in **Fig. 1** and **Table 2**. These GalTs are classified on the basis of their substrate requirement specificities as CARS or HY-CARS enzymes (**Fig. 1**, **Table 2**; ***59,60,62,63***). The galactosyltransferase GalT-1, which catalyzes the biosynthesis in vitro of galactocerebroside, was reported in the early 1970s from embryonic chicken brains ***(66)***. The effects of various phospholipids have been studied with rat brain galactosyltransferase GalT-1 as well as glucosyltransferase GlcT-1 (**Table 2**) using the specific substrates in phospholipid vesicles ***(67)***. These two enzymes were found to have different phospholipid specificities. Ceramide,

containing normal fatty acid in PC vesicles, was found to be the preferred substrate for GlcT-1 while hydroxy fatty acid containing ceramide in PE or ethanolamine phospholipid vesicles was a better substrate for GalT-1 ***(67)***. From these results it can be anticipated that both GalT-1 and GlcT-1 are HY-CARS enzymes specific for glycolipid biosynthesis. The enzyme protein conformation perhaps plays a specific role in determining such specificities.

Bovine milk galactosyltransferase, the lactose synthetase GT, has been studied in great detail including the effect of phospholipids for stabilization and activation of the purified enzyme. It has been observed that the enzyme activity is modulated not only by phospholipid but the effect is different with different phospholipid head groups. This galactosyltransferase shows a specific preference for PC in a lipid mixture ***(68–70)***. The same galactosyltransferase is also known to catalyze the formation of *N*-acetyllactosamine in the presence of α-lactalbumin. Both these activities has been shown to be stimulated by PC and inhibited by PA ***(70)***. Moreover the inhibitory effect of PA is dominant in a mixture of phospholipids. Mitranic and associates have also reported membrane-perturbing agents such as linoleic acid and benzyl alcohol to affect the activities of various Golgi membrane transferases differently, suggesting the existence of different lipid membrane environments around each enzyme ***(71)***. Experimental results from these studies provided evidence that phospholipid-galactosyltransferase liposomes, containing saturated fatty acyl PC, in particular, prevented inhibition by such agents. Evidence has been presented that indicated that benzyl alcohol increased the fluidity of the membrane as well as increased the specific activity of GalT-2 (UDP-Gal : LacCer GalT; **Table 2**). Investigation on the lipid composition of rat proximal small intestinal Golgi membrane demonstrated that PC, PE, and sphingomyelin are the major phospholipids in Golgi membrane containing C16 or higher fatty acids.

The GalT-4 (UDP-Gal : LcOse3Cer GalT; **Fig. 1**, **Tables 1** and **2**), the galactosyltransferase catalyzing formation of Galβ1–4GlcNAc-R , R (β1–3Galβ1–4Glc-Cer; **Table 2**) being a glycolipid backbone was originally reported from our laboratory ***(72)***. Later, the same GalT-4, which is homologous to the lactose synthetase, was purified and cloned in our laboratory ***(73–76)***. The purified enzyme from both mouse lymphoma and embryonic chicken brain has been stabilized using phopholipid liposomes during enzymatic assay. Both PC and PE exhibited a significant stabilizing effect at moderate concentrations while PS was inhibitory at similar concentration ***(59)*** as was observed in the case of bovine milk galactosyltransferase discussed previously ***(67–70)***. CARS classification of the GalT-4 came from the fact that lyso-Lc3 (**Tables 1** and **2**), in which the *N*-acetyl group of hexosamine as well as fatty acyl chain of sphingosine are removed by hydrazinolysis, failed to show any acceptor activity with the enzyme ***(59)***. Reacetylated Lc3, however, was found to be active with only a

two-fold higher K_m exhibiting similar V_{max} ***(59)***. The inactivity of Lyso-Lc3 as substrate might be due to the loss of *N*-acetyl group of NAcGm. The enzyme-activity-catalyzed transfer of galactose from UDP-gal to p-NO_2-phenyl-β-D-Glc-NAc or a glycoprotein containing terminal GlcNAc moiety (SA^-, Gal^--α_1 glycoprotein) ***(77)***. Two other α-galactosyltransferases **(Fig. 1)**, GalT-5 ***(77)*** and GalT-6 ***(62)***, have been identified, which also require detergents for their optimal activity with the respective glycolipid substrates **(Table 2)**. However, very little is known about the interaction of the transmembrane domains of these glycosyltransferases (native or cloned) with the detergents or liposomes.

The galactosyltransferase GalT-3 (**Fig. 1**, **Table 2**), which catalyzes in vitro biosynthesis of GM_1 was characterized, purified, and cloned in our laboratory from embryonic chicken brains ***(59,76,78–80)***. Experimental evidence suggested this enzyme to be a strictly glycolipid specific enzyme because of the stringent substrate specificities due to strong ceramide moiety recognition in the acceptor and classified as HY-CARS enzyme ***(59,62,63)***. Detailed phospholipid stabilization studies of this enzyme had been conducted in our laboratory with the purified enzyme from embryonic chicken brains ***(59,79,80)***. A specially designed apparatus was used for the preparation of phospholipid liposomes for the assay of enzymatic activity as described previously ***(59)***. Unlike GalT-4, the GalT-3 (**Fig. 1** and **Table 2**) was found to be down-regulated in the presence of all three natural phospholipids—PC, PS, and PI, all of which which play integral roles in membrane functions. PC, which was found to be the best for stabilization of both GalT-4 and lactose synthetase, was found to be inhibitory for GalT-3 ***(59,80)***. However, with changing fatty acid composition of PE to totally saturated (dipalmitoyl) fatty acid moieties, a remarkable stabilization of GalT-3 was observed while unsaturated (dioleyl) fatty acid substitution resulted in inhibition ***(59)***. Phospholipid vesicle structures contribute significantly to the stability of the enzyme. It was proposed from the studies conducted with two different phospholipid vesicles that the purified GalT-3 enzymatic activity was stabilized by hexagonal vesicles containing dipalmitoyl-PE while being inhibited by bilayer vesicles exhibited by dielaidoyl-PE ***(59)***. Studies were also conducted to fully understand the phospholipid effect on GalT-3 in the presence of various concentrations of the substrate GM_2 (**Table 1** and **2**; ***59***). The results indicated this heterotropic modulation of GalT-3 by phospholipid to be noncompetitive in nature. This observation further suggested the phospholipid binding at an allosteric site on the enzyme altering its capacity to react properly with the substrate or the product ***(59)***.

2.3.2. Glucuronyltransferases

The GlcAT-1, the glucuronyltransferase (**Fig. 1**, **Table 2**) that catalyzes the biosynthesis in vitro of HNK-1 precursor epitope, was characterized and

solubilized from 19-d-old embryonic chicken brains (ECBs) in our laboratory ***(81)***. Although the specific activity of the GlcAT-1 was found to be similar between 7- and 21-d embryonic development, the total activity (nmol/g tissue/h) was found to increase gradually to about five-fold between those days ***(81)***. No other embryonic chicken organelles showed the presence of this enzyme under the current assay condition. Both adult guinea pig and rabbit brain homogenate exhibited GlcAT-1 activity approx three-fold lower than observed ECB value. Both neutral and zwitterionic detergent stimulated the membrane-bound GlcAT-1 activity. However, the neutral detergent nonidet P-40 (NP-40) was used to solubilize the enzyme from Golgi-rich membrane ***(81)***. The solubilized enzyme seemed affected when phospholipid liposomes were added in combination with a substrate–detergent mixture for enzyme assay ***(82)***. The phospholipid-substrate-detergent liposomes were prepared according to our protocol using the specially designed apparatus ***(59,60)***. It was observed that at a concentration between 0.25 and 1.0 mg/mL, phosphatidylglycerol (PG) stimulated the solubilized GlcAT-1 activity by almost 50%. The stimulation of GlcAT-1 activity was also observed with both PE and PC at lower concentrations. However, between 0.5 and1.5 mg/mL concentrations, PC was 50–90% inhibitory while only about 10% inhibition was observed with both PE and PG. Sphingosine, a metabolite of the hydrophobic ceramide moiety of the glycolipid substrate, was found to modulate several glycolipid : glycosyltransferases including GlcAT-1 ***(60)***. A gradual inhibition of up to 50% of GlcAT-1 activity was observed with sphingosine concentration between 0.025 and 0.25 mg/mL that follows a sharp decrease in activity (up to 95%) at 0.4 mg/mL. The inhibitory effect of sphingosine is anticipated to be heterotropic in nature, resulting in substrate availability or substrate orientation in the mixture. On the basis of observed inhibition of GlcAT-1 activity by both phospholipids and sphingosine, in addition to the stringent glycolipid substrate specificity, this enzyme could be classified as a HY-CARS enzyme ***(62,63)***.

The bilayer distribution of several enzyme proteins and various phospholipids in the microsomal membranes has been studied in detail after treatment of the membrane with proteases and phospholipases ***(83)***. These membrane proteins behaved differently during solubilization, being activated or inactivated after treatment of protease and trypsin in the absence or presence of detergents. Treatment of the membrane with either trypsin or sodium cholate (used in a concentration to make the membrane permeable without disruption) failed to release membrane-bound glucuronyltransferase. Some of the membrane phospholipids of the intact microsome were hydrolyzed by treatment with phospholipase A (PLA). These phospholipids (PE, PS, and part of PC) were assigned as the components of the outer half of the bilayer membrane while PI, a certain percent of PC, and sphingomyelin were believed to be in the

inner half of the bilayer. From these studies it was concluded that various enzyme proteins and phospholipids of microsomal membrane display an asymmetric distribution in the transverse plane ***(83)***. PLA activation of microsomal membrane sterol:glucuronyltransferase had been reported previously ***(84)***. It might be speculated that perturbation of membrane phospholipids by PLA could activate the membrane-bound sterol:GlcAT, indicating that membrane proteins and phospholipids are very interdependent in the mode of their action. Membrane-to-membrane fusion or the movement of the lipophilic substrates toward an enzyme thus provides an environment for enzyme stabilization. One such example was reported from the study of endoplasmic reticulum glucuronyltransferase and hepatocyte bilirubin in small unilamellar model membranes ***(85)***. Using bilirubin-containing small unilamellar vesicles of egg PC or natural phospholipids in the proportion present in hepatocyte, glucuronidation of bilirubin in rat liver microsomes was measured ***(85)***. These studies suggested that under certain conditions membrane fusion or aggregation might promote the movement of lipophilic substrates in hepatocyte. It was reported that the physical properties of the membrane phospholipids influence the number of functional binding sites of sterol:GlcAT ***(86)***. Reconstitution of glucuronyltransferase in unilamellar vesicles of PC in the gel phase exhibited non-Michaelis–Menten kinetics, which were found to switch to Michaelis–Menten kinetics by the melting of phospholipid gel phase to liquid crystal phase. There are two affinity sites for UDP when GlcAT is reconstituted into the phospholipid bilayer in a gel phase, while during reconstitution of GlcAT into phospholipid bilayer in a liquid crystal phase, there is only one UDP binding site ***(86)***. There is a further report that cholesterol affects the sterol:GlcAT-phospholipid unilamellar bilayer depending on the fatty acid content ***(87)***. Cholesterol had a stabilizing effect on GlcAT in the disteroyl phosphatidylcholine (DSPC) bilayer against thermal inactivation, and stabilization increased with increased concentration of cholesterol in the bilayer. However, under this condition the enzymatic activity decreased. Cholesterol had very little effect if any on the dioleoyl phosphatidylcholine (DOPC) bilayer ***(87)***. From these observations sterol:GlcAT appears to be modulated by membrane phospholipid environments.

2.3.3. Sialyltransferases

Sialyltransferase SAT-1 (**Fig. 1**, **Table 2**), which catalyzes the formation of GM_3 ganglioside from lactosylceramide (**Tables 1** and **2**), had been reported originally from embryonic chicken brain ***(58,79,88,89)***. This SAT-1 has been distinguished from the sialyltransferase, which catalyzes synthesis of sialyllactose ***(90)*** and classified as a HY-CARS enzyme because of its specific requirements for both carbohydrate and hydrophobic moieties of the substrate,

lactosylceramide, for optimal activity ***(60,62–64)***. Sialyltransferase SAT-3 (**Fig. 1**, **Table 2**), which catalyzes biosynthesis of LM1 in vitro (**Table 1**), has been recognized as a CARS enzyme because the rate of the SAT-3-catalyzed reactions was found to be independent of the ceramide composition of the substrate ***(60,62,91,92)***. However, the enzyme was found to be dependent on the oligosaccharide chain of the substrate ***(62,91–93)***.

SAT-1 is believed to be tightly associated with the luminal side of the Golgi membranes like its substrate lactosylceramide. A nonspecific lipid transfer protein that accelerates transfer of phospholipids, cholesterol, and glycolipids has been used to study the kinetic parameters of rat liver SAT-1 ***(94,95)***. In comparison to detergent-solubilized SAT-1, the transfer protein increased the enzymatic activity four- to fivefold. These results suggest that when both the substrate and the enzyme reside in the same membrane, transfer protein can be used to study the kinetics for an membrane-bound enzyme. Rat liver Golgi membrane SAT-1 has been shown to be greatly dependent on the membrane lipid composition, and the lipid environment of the membrane could alter molecular species specificity of SAT-1 toward its substrate LacCer ***(94)***. Extensive studies on the molecular species specificity for SAT-1 have been performed by Kadowski and his associates ***(94,95)***. The lipid composition of the rat Golgi-membrane was changed to resemble that of mouse neuroblastoma Neuro2a cells, a cell line in which SAT-1 does not exhibit any molecular species specificity. This was accomplished by incubating Golgi membrane vesicles with nonspecific lipid transfer protein and a 10-fold excess of liposome prepared with various proportions of purified rat liver lipids. A change in the phospholipid class composition of the Golgi membrane to a composition similar to that of neuroblastoma cells increased rather than decreased the molecular species specificity of rat liver SAT-1 when rat liver lipid containing liposomes was used ***(95)***. Furthermore, molecular species analysis of rat liver Golgi membrane LacCer and GM_3 (**Table 1**) revealed these to be exactly the same, as would be expected on the basis of molecular species specificity of SAT-1 and the molecular species composition of LacCer in the Golgi membrane ***(95)***. From these results it is obvious that SAT-1 activity is very much dependent on the membrane environment and membrane composition as well as on the composition of hydrophobic head group ceramide moiety of the substrate LacCer, confirming further the HY-CARS nature of the enzyme as observed in our laboratory ***(60,62)***.

2.3.4. N-*Acetylglucosaminyltransferases*

The *N*-acetylglucosaminyltransferases (GlcNAcTs) catalyzing the formation of core structure for glycoproteins ***(96)*** and the lacto-series glycolipids ***(97,98)*** are believed to be different gene products (**Fig. 1**, **Table 2**; ***62–64***).

Phospholipid stimulation of GlcNAcT catalyzing the formation of *N*-acetylglucosaminylphosphoryl dolichol (Dol-P-P-GlcNAc) has been shown by Kean ***(99)***. Participation of Dol-P-mannose and phosphatidylglycerol as allosteric activators of GlcNAc-DolP synthesis has been shown. Such phospholipid effects were not studied in detail for glycolipid GlcNAcTs. All the glycolipid : GlcNAcTs have been solubilized using neutral detergent ***(97,98)***. On the basis of the membrane proximity of the oligosaccharide chain of the acceptor glycolipid, Lac-Cer (**Table 1**), the GlcNAcT-1 can be expected to be more affected by membrane structure than the GlcNAcT-2 (**Fig. 1, Table 2**; ***62–64,97,98***) is.

2.3.5. N*-Acetylgalactosaminyltransferases*

GalNAcT-1, the enzyme that catalyzes the formation of GM_2 from GM_3 (**Fig. 1, Tables 1** and **2**), had been shown previously to be a HY-CARS enzyme, as the transferase activity is dependent on the presence of fatty acyl chain of the ceramide moiety of the substrate GM_3 ***(60,62,100,101)***. It was observed that the K_m increased five-fold of normal value when an acetyl group replaced long-chain fatty acid. On the basis of the dependency of the GalNAcT-1 on the hydrophobic part of the substrate structure, modulation of the enzyme by membrane phospholipids can be expected. Stimulation of GalNAcT-1 by phosphatidylglycerol (PG) has been observed in isolated Golgi vesicles in the absence of detergents ***(102)***. This stimulatory effect of PG and also of dolichol phosphate (DP), PE and PS were observed only in intact Golgi vesicles in the absence of detergent . The mechanism of this activation is unclear. Compared to GalNAcT-1, the GalNAcT-2 activity (**Fig. 1**, **Table 2**; ***103,104***) was not affected by any change in the hydrophobic moiety of the substrate ***(60,62)***. Neither K_m nor V_{max} of GalNAcT-2 changed significantly when the activity was tested with the natural substrates GbOse3Cer (Gb3), acetyl-Gb3, or Lyso-Gb3. GalNAcT-2 is thus a CARS enzyme and expected not to be modified significantly by membrane structures or phospholipid compositions.

2.3.6. Fucosyltransferases

Most of the fucosyltransferases are found to be activated by cationic detergents ***(105–108)***. However, for solubilization, neutral detergent was found to be most effective. It has been observed that the nature of FucT-2 and FucT-3 (**Fig. 1**, **Table 2**) differs in regard to substrate structure requirement ***(60,62)***. FucT-3, which catalyzes SA-Lex formation (**Fig. 1**), has been designated as a HY-CARS enzyme because the enzymatic activity is found to be significantly dependent on the ceramide structure. An increased K_m and lower V_{max} were observed when the fatty acid chain of ceramide was replaced by an acetyl group ***(60,62)***. However, the FucT-2 activity (**Fig. 1**) was found to be independent of

substrate hydrophobicity. Based on these findings, FucT-2 and FucT-3 were designated as CARS and HY-CARS enzymes, respectively ***(60,62)***. Phospholipid enhancement of sheep brain microsomal fucosyltransferase (FucT), which catalyzes fucosylation of asialofetuin, had been shown previously ***(109)***. Unsaturated fatty acid containing lyso-phosphatidylcholine (lyso-PC) was shown to activate the FucT. It was concluded that the membrane bilayer structure does not modify the enzymatic activity whereas the micellar structure formed by detergents or lysophospholipids leads to a strong increase in FucT activity. It was also suggested that hydrolysis of PC by PLA_2 leads to enzymatic stimulation.

2.3.7. Conclusion

Most of the glycosyltransferases cloned so far have been shown to contain a short transmembrane domain followed by a long tail (inside Golgi lumen) in which the catalytic activity of the enzyme protein resides ***(110)***. A common peptide motif has also been found near the hydrophobic transmembrane domain in a number of Golgi-localized glycosyltransferases believed to anchor these Golgi-associated transferases to the membrane bilayer ***(111)***. These transmembrane domains of the enzyme proteins are very likely to interact or to be modulated by the membrane composition or bilayer structure in their membrane-bound forms. Detergents are used invariably to solubilize the membrane bound enzyme proteins that somehow alter the membrane fluidity for easier access of the protein ***(62–65)***. The roles of micelle, vesicles, or liposomes are very important for the activation and exposure of the membrane-bound proteins.

References

1. Sood, C. K., Sweet, C., and Zull, J. E. (1972) Interaction of kidney (Na^+, K^+)-ATPase with phospholipid model membrane systems. *Biochim. Biophys. Acta* **282,** 429–434.
2. Gregoriadis, G. and Ryman, B. E. (1972) Lysozomal localization of fructufuranosidase-containing liposomes injected into rats. *Biochem. J.* **129,** 123–133.
3. de Barsy, T., Devos, P., and Van Hoof, F. (1975) The cellular distribution of liposomes in the liver of newborn rats. *Biochem. Soc. Trans.* **3,** 159–160.
4. Hexter, C. S. and Goldman, R. (1973) Interaction of D-hydroxubutyrate dehydrogenase with lecithin vesicles. *Biochim. Biophys. Acta* **307,** 421–427.
5. Toffano, G., Leon, A., Savoini, G., and Orlando, P. (1977) Effect of phospholipid liposomes on the regulation of cerebral metabolism. *Adv. Exp. Med. Biol.* **83,** 407–418.
6. Kaduce, T. L., Schimdt, R. W., and Spector, A. A. (1978) Acylcoenzyme A: cholesterol acyltransferase activity: solubilization and reconstitution in liposomes. *Biochem. Biophys. Res. Commun.* **81,** 462–468.
7. Barzilay, M., de Vries, A., and Condrea, E. (1978) Exposure of human red cell membrane phospholipids to snake venom phospholipase A1: hydrolysis of

substrate by *Vipera palaestinae* phospholipase from within released red cells. *Toxicon* **16,** 145–152.
8. Carroll, R. C. and Racker, E. (1977) Preparation and characterization of cytochrome c oxidase vesicles with high respiratory control. *J. Biol. Chem.* **252,** 6981–6890.
9. Hung, S. C. and Melnykovych, G. (1977) Increase in activity of partially purified alkaline phosphatase after treatment with Mg^{2+}, Zn^{2+} and lysolecithin. *Enzyme* **22,** 28–34.
10. Hall, E. R. and Brodbeck, U. (1978) Human erythrocyte membrane acetylcholinesterase. Incorporation into the lipid bilayer structure of liposomes. *Eur. J. Biochem.* **89,** 159–167.
11. Finkelstein, M. C. and Weissmann, G. (1979) Enzyme replacement via liposomes. Variation in lipid compositions determine liposomal integrity in biological fluids. *Biochim. Biophys. Acta,* **587,** 202–216.
12. Pal, R., Barenholz, Y., and Wagner, R. R. (1980) Effect of cholesterol concentration on organization of viral and vesicle membranes. Probed by accessibility to cholesterol oxidase. *J. Biol. Chem.* **255,** 5802–5806.
13. Frenkel, E. J., Roelofsen, B., Brodbeck, U., vanDeeneen, L. L., and Ott, P. (1980) Lipid:protein interaction in human erythrocyte-membrane acetylcholinesterase. Modulation of enzyme activity by lipids. *Eur. J. Biochem.* **109,** 377–382.
14. Galzina, L., Bertazzon, A., Garbin, L., and Deana, R. (1981) Change of catalytic properties of erythrocyte acetylcholinesterase after binding to lecithin liposomes. *Enzyme* **26,** 8–14.
15. Hebdon, G. M., Levine, H. 3d., Sahyam, N. E., Schmitger, C. J., and Cuatrecasas, P. (1981) Specific phospholipids are required to reconstitute adenylate cyclase solubilized from rat brain. *Proc. Natl. Acad. Sci. USA* **78,** 120–123.
16. Doolittle, G. M. and Chang, T. Y. (1982) Solubilization, partial purification and reconstitution in phosphatidylcholine-cholesterol of acylcoenzyme A:cholesterol acyltransferase. *Biochemistry* **21,** 674–679.
17. Suckling, K. E., Boyd, G. S., and Smellie, C. G. (1982) Properties of a solubilized and reconstituted preparation of acylcoenzyme A:cholesterol acyltransferase from rat liver. *Biochim. Biophys. Acta* **710,** 154–163.
18. Mathur, S. N. and Spector, A. A. (1982) Effect of liposome composition on the activity of detergent solubilized acylcoenzyme A:cholesterol acyltransferase. *J. Lipid Res.* **23,** 692–701.
19. Doolittle, G. M. and Chang, T. Y. (1982) Acylcoenzyme A:cholesterol acyltransferase in chinese hamster ovary cells. Enzyme activity determination after reconstitution in phospholipid/cholesterol liposomes. *Biochim. Biophys. Acta* **713,** 529–537.
20. Jahani, M. and Lacko, A. G. (1982) Study of lecithin:cholesterol acyltransferase reaction with liposome and high density lipoprotein. *Biochim. Biophys. Acta* **713,** 504–511.
21. Forgac, M. and Berne, M. (1986) Structural characterization of ATP-hydrolyzing portion of the coated vesicle pump. Biochemistry ***25,*** 4275–4280.

22. Gould, G. W., McWhirter, J. M., East, J. M., and Lee, A. G. (1987) Uptake of Ca^{2+} mediated by the ($Ca^{2+}Mg^{2+}$)-ATPase in reconstituted vesicles. *Biochim. Biophys. Acta* **904,** 36–44.
23. Holcomb, C. L., Hansen, W. J., Etcheverry, T., and Schekman, R. (1988) Secretory vesicles externalize the major plasma membranes ATPase in yeast. *J. Cell Biol.* **106,** 641–648.
24. Wach, A., Ahlers, J., and Graber, P. (1990) The (H^+)-ATPase of the plasma membrane from yeast. ATP hydrolysis in native, isolated and reconstituted membranes. *Eur. J. Biochem.* **189,** 675–682.
25. Kragh-Hansen, U., Ie Marie, M., and Moller, J. V. (1998) The mechanism of detergent solubilization of liposomes and protein-containing membranes. *Biophys. J.* **75,** 2932–2946.
26. Ohshima, A., Narita, H., and Kito, M. (1983) Phospholipid reverse micelles as a milieu of an enzyme reaction in apolar system. *J. Biochem. (Tokyo)* **93,** 1421–1425.
27. Nametkin, S. N., Kabanov, A. V., and Levashov, A. V. (1993) Alkaline phosphatase from calf intestinal mucosa in reversed micelle system: modulation of enzyme by pH variation. *Biochem. Mol. Biol. Int.* **1,** 103–111.
28. Seetharam, B., Tiruppathi, C., and Alpers, D. H. (1985) Membrane interactions of rat intestinal alkaline phosphatase: role of polar head groups. *Biochemistry* **24,** 6603–6608.
29. Seetharam, B., Tiruppathi, C., and Alpers, D. H. (1987) Hydrophobic interactions of brush border alkaline phosphatases: role of phophatidyl inositol. *Arch. Biochem. Biophys.* **253,** 189–198.
30. Brasitus, T. A., Dahiya, R., Dudeja, P. K., and Bissonnette, B. M. (1988) Cholesterol modulates alkaline phosphatase activity of rat intestinal microvillus membranes. *J. Biol. Chem.* **263,** 8592–8597.
31. Dennis, E. A., Darke, P. L., Deems, R. A., Kensil, C. R., and Pluckthun, A. (1981) Cobra venom phospholipase A2. *Mol. Cell Biochem.* **36,** 37–45.
32. Kupferberg, J. P., Yokoyama, S., and Kezdy, F. J. (1981) The kinetics of PLA_2-catalyzed hydrolysis of egg lecithin in unilamellar vesicles. *J. Biol. Chem.* **256,** 6274–6281.
33. Scherphof, G., Van Leeuwen, B., Wilschut, J., and Damen, J. (1983) Exchange of PC between small unilamellar liposomes and human plasma HDL involves exclusively the PL in the outer monolayer of the liposomal membrane. *Biochim. Biophys. Acta* **732,** 595–599.
34. Sevanian, A., Wratten, M. L., McLeod, L. L., and Kim, E. (1988) Lipid peroxidation and PLA_2 activity in liposomes composed of unsaturated phospholipids. *Biochim. Biophys. Acta.* **961,** 316–327.
35. Bell, J. D. and Biltonen, R. L. (1989) The temporal sequence of events in the activation of PLA_2 by lipid vesicles. *J. Biol. Chem.* **264,** 12194–12200.
36. Salgo, M. G., Corongiu, F. P., and Sevanian, A. (1992) Peroxidation and PLA2 susceptibility of liposomes containing mixed micelles of PC and PE. *Biochim. Biophys. Acta* **1127,** 131–140.

37. Salgo, M. G., Corongiu, F. P., and Sevanian, A. (1993) Enhanced interfacial catalysis and hydrolysis and specificity of PLA2 toward peroxidized PC vesicles. *Arch. Biochem. Biophys.* **304,** 123–132.
38. Nieva, J. L., Goni, F. M., and Alonso, A. (1989) Liposome fusion catalytically induced by phospholipase C. *Biochemistry* **28,** 7364–7367.
39. Basanez, G., Fidelio, G. D., Goni, F. M., Maggio, B., and Alonso, A. (1996) Dual inhibitory effect of gangliosides on phospholipase C-promoted fusion of lipidic vesicles. *Biochemistry* **35,** 7506–7513.
40. Volwerk, J. J., Filthuth, E., Griffith, O. H., and Jain, M. K. (1994) PI-specific PLC from *B. cereus* at the lipid-water interface:interfacial binding, catalysis and activation. *Biochemistry* **33,** 3464–3474.
41. Lomansney, J. W., Cheng, H. F., Roffler, S. R., and King, K. (1999) Activation of PLC delta1 through C2 domain by Ca^{2+}–enzyme–PS ternary complex. *J. Biol. Chem.* **274,** 21995–22001.
42. Pawelczyk, T. and Lowenstein, J. M. (1992) Regulation of PLC delta activity by SM and sphingosine. *Arch. Biochem. Biophys.* **297,** 328–333.
43. Kinkaid, A. R., Othman, R., Voysey, J., and Wilton, D. C. (1998) PLD and PA enhance hydrolysis of phospholipids in vesicles and small membranes by human secreted PLA2. *Biochim. Biophys. Acta* **1390,** 173–185.
44. Gatt, S. and Rapport, M. (1966) Enzymatic hydrolysis of sphingolipids. *Biochem. J.* **101,** 680–686.
45. Gatt, S., Dinur, T., and Dagan, A. (2002) Liposome-mediated, fluorescence-based studies of sphingolipid metabolism in intact cells, in Liposome Methods and Protocols, (Basu, S. and Basu, M, eds.), Humana, Totowa, NJ, Chap. 6, pp. 85–105.
46. Gatt, S., Barenholz, Y., Goldberg, R., Dinur, T., Besley, G., Leibovitz-Ben Gershon, Z., et al. (1981) Assay of enzymes of lipid metabolism with colored and flourescent derivatives of natural lipids. *Methods Enzymol.* **72,** 351–375.
47. Lee-Vaupel, M. and Conzelmann, E. (1987) Assay of sulfatide sulfatase in cultured skin fibroblasts with the natural activator protein. *Clin. Chim. Acta* **168,** 55–68.
48. Nalecz, M. J., Zborowski, J., Famulski, K. S., and Wojtczak, L. (1980) Effect of PL composition on surface potential of liposomes and the activity of enzymes incorporated. *Eur. J. Biochem.* **112,** 75–80.
49. Cohen, R. and Barenholz, Y. (1978) Correlation between thermotropic behavior of SM liposomes and SM hydrolysis by SMase of *S. aureus*. *Biochim. Biophys. Acta* **509,** 181–187.
50. Tomita, M., Sawada, H., Taguchi, R., and Ikezawa, H. (1987) The action of SMase from *B. cereus* on ATP-depleted bovine erythrocyte membranes and different lipid compositions of liposomes. *Arch. Biochem. Biophys.* **255,** 127–135.
51. Ruiz-Arguello, M. B., Goni, F. M., and Alonso, A. (1998) Vesicle membrane fusion induced by concerted activities of SMase and PLC. *J. Biol. Chem.* **273,** 22977–22982.
52. Holopainen, J. M., Subramanian, M., and Kinnunen, P. K. J. (1998) SMase induces lipid microdomain formation in a fluid PC/SM membrane. *Biochemistry* **37,** 17562–17570.

53. Lasch, J., Berdichevsky, V. R., Torchilin, V. P., Koelsch, R., and Kretschmer, K. (1983) A method to measure critical detergent parameters: preparation of liposomes. *Analyt. Biochem.* **33,** 486–491.
54. Jiskoot, W., Teerlink, T., Beuvery, E. C., and Crommelin, D. J. (1986) Preparation of liposomes via detergent removal from mixed micelle by dilution. The effect of bilyer composition and process parameters on liposome characteristics. *Pharm. Weekbl. [Sci.]* **8,** 259–265.
55. Killian, J. A., Trouard, T. P., Greathouse, D. V., Chupin, V., and Lindblom, G. (1994) A general method for the preparation of mixed micelles of hydrophobic peptides and SDS. *FEBS Lett.* **348,** 161–165.
56. Degrip, W. J., Vanoostrum, J., and Bovee-Geurts, P. H. (1998) Selective detergent extraction from mixed detergent/lipid/protein micelles using cyclodextrin inclusion compounds: a novel generic approach for the preparation of proteoliposomes. *Biochem. J.* **330,** 667–674.
57. Oberholzer, T., Meyer, E., Amato, I., Lustig, A., and Monnard, P. A. (1999) Enzymatic reactions in liposomes using the detergent-induced liposome loading method. *Biochim. Biophys. Acta* **141,** 57–68.
58. Basu, M., De, T., Das, K. K., Kyle, J. W., Chon, H. C., Schaeper, R., and Basu, S. (1987) Glycolipid glycosyltransferases. *Methods Enzymol.* **138, 5**95–607.
59. Ghosh, S., Das, K. K., Daussin, F., and Basu, S. (1990) Effect of fatty acid moiety of Pl and ceramide on GalT-3 from embryonic chicken brains. *Ind. J. Biochem. Biophys.* **27,** 379–385.
60. Basu, S., Ghosh, S., Basu, M., Hawes, J. W., Das, K. K., Zhang, B. J., et al. (1990) Carbohydrate and hydrophobic-carbohydrate recognition sites (CARS and HY-CARS) in solubilized glycosyltransferases. *Ind. J. Biochem. Biophys.* **27,** 386–395.
61. Cotantino-Ceccarini, E. and Cestelli, A. (1981) A novel assay method for GlcCer and galcer biosynthesis. *Methods Enzymol.* **72,** 384–391.
62. Basu, S. (1991) Serendipity of ganglioside biosynthesis. *Glycobiology* **1,** 469–475.
63. Basu, S., Basu, M., Dastgheib, S., and Hawes, J. W. (1998) Biosynthesis and regulation of glycosphingolipids in *Comprehensive Natural Products Chemistry*, vol. 3, Carbohydrates (Barton, D. H. R., Nakanishi, K., Meth-Cohn, O., and Pinto, M.) Pergamon Press, New York, pp. 107–128.
64. Basu, S., Basu, M., Das, K. K., Daussin, F., Schaeper, R. J., Banerjee, P., et al. (1988) Solubilized glycosyltransferases and biosynthesis *in vitro* of glycolipids. *Biochimie* **70,** 1551–1563.
65. Basu, S. and Basu, M. (1999) Glycosyltransferases in glycosphingolipid biosynthesis, in *Oligosaccharides in Chemistry and Biology—A Comprehensive Handbook* (Ernst, B., Sinay, P., and Hart, G., eds.), Wiley-VCH Verlag GmbH, Germany, pp. 329–347.
66. Basu, S., Schultz, A., Basu, M., and Roseman, S. (1971) Synthesis of Gal-Cer by GalT from ECB. *J. Biol. Chem.* **243,** 4272–4279.
67. Cestelli, A., White, F. V., and Costantino-Ceccarini, E. (1979) The use of liposomes as acceptors for the assay of lipid glycosyltransferases from rat brain. *Biochim. Biophys. Acta* **572,** 283–292.

68. Mitranic, M. M. and Moscarello, M. A. (1980) The influence of various lipids on the activity of bovine milk galactosyltransferase. *Can. J. Biochem.* **58,** 809–814.
69. Mitranic, M. M., Boggs, J. M., and Moscarello, M. A. (1983) Modulation of bovine milk galactosyltransferase activity by lipids. *J. Biol. Chem.* **258,** 8630–8636.
70. Moscarello, M. A., Mitranic, M. M., and Deber, C. M. (1986) The modulation of bovine milk D-galacosyltransferase by various phosphatidylethanolamines. *Carbohydr. Res.* **149,** 47–58.
71. Mitranic, M. M., Boggs, J. M., and Moscarello, M. A. (1982) The effect of linoleic acid and benzyl alcohol on rat liver Golgi membrane GalT and some soluble glycosyltransferases. *Biochim. Biophys. Acta* **693,** 75–84.
72. Basu, M. and Basu, S. (1972) Biosynthesis *in vitro* of nLcOse4Cer by a GalT from rabbit bone marrow. *J. Biol. Chem.* **247,** 1489–1495.
73. Basu, S., Weng, S. W., Tang, H., Khan, F., Rossi, F., and Basu, S. (1996) Biosynthesis *in vitro* of nLcOse4Cer by a GalT-4 from mouse T-lymphoma. *Glyconjugates J.* **13,** 423–432.
74. Ghosh, S., Basu, S. S., and Basu, S. (1992) Isolation of a cDNA clone for b1-4GalT from ECB and comparison to its mammalian homologs. *Biochem. Biophys. Res. Commun.* **189,** 1215–1222.
75. Basu, S., Ghosh, S., Basu, S. S., Kyle, J. W., Li, Z., and Basu, M. (1993) Regulation of expression of neo-lactoglycolipids and cloning of GalT-4 from ECB. *Ind. J. Biochem. Biophys.* **30,** 315–323.
76. Basu, S. S., Dastgheib, S., Ghosh, S., Basu, M., Kelly, P., and Basu, S. (1998) Purification and characterization of avian glycolipid:β-galactosyl-transferases. *Acta Biochim. Pol.* **45,** 451–467.
77. Basu, M. and Basu, S. (1973) Enzymatic synthesis of a blood-group B-specific pentaglycosylceramide by an α-galactosyltransferase from rabbit bone marrow. *J. Biol. Chem.* **248,** 1700–1706.
78. Basu, S., Kaufman, B. W., and Roseman, S. (1965) Coversion of Tay–Sachs ganglioside to GM1. *J.Biol. Chem.* **240,** PC4115–4118.
79. Kaufman, B. W., Basu, S., and Roseman, S. (1966) Studies on the biosynthesis of gangliosides, in *Inborn Disorders of Sphingolipid Metabolism* (Aronson, S. M. and Volk, B. W., eds.), Pergamon Press, New York, pp. 193–213.
80. Ghosh, S., Kyle, J.W., Dastgheib, S., Daussin, F., Li, Z., and Basu, S. (1995) Purification, properties and immunological characterization of GalT-3 from chicken brain. *Glycoconjugate J.* **12,** 838–847.
81. Das., K. K., Basu, M., Basu, S., Chou, D. K. H., and Jungalwala, F. (1991) Biosynthesis in vitro of HNK-1 epitope by GlcAT-1 from ECB. *J. Biol. Chem.* **266,** 5238–55243.
82. Das, K. K., Basu, M., Li, Z., Basu, S., and Jungalwala, F. (1990) GlcAT-1 from embryonic chicken brain and its inhibition by D-erythro-sphingosine. *Ind. J. Biochem. Biophys.* **27,** 396–401.
83. Nilsson, O. S. and Dallner, G. (1977) Enzyme and phospholipid assymetry in liver microsomal membranes. *J. Cell Biol.* **72,** 568–583.

84. Graham, A. B. and Wood, G. C. (1974) On the activation of microsomal GLcAT by PLA. *Biochim. Biophys. Acta* **370,** 431–440.
85. Whitmer, D. I., Russell, P. E., and Gollan, J. L. (1987) Membrane–membrane interaction associated with rapid transfer of liposomal bilirubin to microsomal UDP-GlcAT. *Biochem. J.* **244,** 41–47.
86. Hochman, Y., Kelley, M., and Zakim, D. (1983) Modulation of number of ligand binding sites of GlcAT by gel to liquid-crystal phase transition of PC. *J. Biol.Chem.* **258,** 6509–6516.
87. Rotenberg, M. and Zakim, D. (1991) Effect of cholesterol on function and thermotropic properties of GlcAT. *J. Biol. Chem.* **266,** 4159–4161.
88. Basu, S. (1966) Biosynthesis of gangliosides. Ph.D. Thesis, University of Michigan, Ann Arbor, Michigan.
89. Kaufman, B., Basu., S., and Roseman, S. (1966). Embryonic chicken brain sialyltransferases. *Meth. Enzymol.* **8,** 365–368.
90. Jourdian, G. W., Carlson, D. M., and Roseman, S. (1963) The enzymatic synthesis of sialyl-lactose. *Biochem. Biophys. Res. Commun.* **10,** 352–358.
91. Basu, M., Basu, S., Stoffyn, A., and Stoffyn, P. (1982) Biosynthesis of GM1b (GlcNAc) by a sialyltransferase from ECB. *J. Biol. Chem.* **257,** 12765–12769.
92. Basu, S. S., Basu, M., Li, Z., and Basu, S. (1996) Sialyltransferases SAT-3 and SAT-4 from Colo-205. *Biochemistry* **35,** 5166–5174.
93. Basu, S., Basu, M., and Basu, S. S. (1995) Biological specificity of sialyltransferases. In: *Biology of the Sialic Acids* (Rosenberg, A., ed.) Plenum, New York, pp. 69–94.
94. Kadowaki, H., Grant, M. A., and Williams, L. A. (1993) Effect of membrane lipids on LacCer molecular species specificity of SAT-1. *J. Lipid Res.* **34,** 905–914.
95. Kadowaki, H. and Grant, M. A. (1995) Relation ship of membrane PL composition, Laccer molecular species and the specificity of SAT-1 to the molecular species composition of GM3. *J. Lipid Res.* **36,** 1274–1282.
96. Schachter, H. and Roseman, S. (1980) Mammalian glycosyltransferases. Their role in synthesis and function of complex carbohydrates and glycolipids, in *The biochemistry of Glycoproteins and Proteoglycans* (Lennarz, W. J., ed.), Plenum Press, New York, pp. 85–160.
97. Basu, M. and Basu, S. (1984) Biosynthesis in vitro of i/I glycolipid in mouse lymphoma. *J. Biol. Chem.* **259,** 12557–12562.
98. Basu, M., Khan, F. A., Das, K. K., and Basu, S. (1991) Biosynthesis in vitro of Lacto-series GSL by GlcNAcTs from human colon carcinoma. *Carbohydr. Res.* **209,** 261–277.
99. Kean, E. L. (1985) Stimulation of GlcNAc-DolP by DolP-Man and PL. *J. Biol. Chem.* **260,** 12561–12571.
100. Steigerwald, J. C., Basu, S., Kaufman, B., and Roseman, S. (1975) *J. Biol. Chem.* **250,** 6727–6734.
101. Schaeper, R.J., Das, K. K., Li, Z., and Basu, S. (1992) Biosynthesis *in vitro* of Gb & GM2 gangliosides by ECB GalNAcTs. *Carbohydr. Res.* **236,** 227–244.

102. Yusuf, H. K., Pohlentz, G., Schwarzmann, G., and Sandhoff, K. (1985) Ganglioside biosynthesis in rat liver Golgi apparatus: stimulation by PG and inhibition by tunicamycin. *Adv. Exp. Med. Biol.* **174,** 227–239.
103. Chein, J. L., Williams, T., and Basu, S. (1973) Biosynthesis of globoside by GalNAcT in ECB. *J. Biol. Chem.* **248,** 1778–1785.
104. Das, K. K., Basu, M., Basu, S., and Evans, C. H. (1986) *Carbohydr. Res.* **149,** 119–137.
105. Basu, S., Chein, J. L., and Basu, M. (1975) Biosynthesis of H glycolipid by FucT-2 from bovine spleen. *J. Biol. Chem.* **250**.
106. Basu, M., Hawes, J. W., Li, Z., Ghosh, S., Khan, F., Zhang, B., and Basu, S. (1991) *Glycobiology* **1,** 527–535.
107. Basu, M., Basu, S. S., Li, Z., Tang, H., and Basu, S. (1993) Biosynthesis and regulation of Lex and SA-Lex glycolipids in metastatic human colon carcinoma cells. *Ind. J. Biochem. Biophys.* **30,** 324–332.
108. Hawes, J. W. (1991) Ph.D. Thesis. University of Notre Dame. Characterization of α-L-fucosyltransferases from neuronal and non-neuronal tissues.
109. Serres-Guillaumond, M., Broquet, P., and Louisot, P. (1985) Involvement of Pl in the modulation of a membrane-bound brain FucT. *Can. J. Biochem. Cell Biol.* **63,** 296–304.
110. Paulson, J. C. and Colley, K. J. (1989) Glycosyltransferases: structure, localization and control of cell type-specific glycosylation. *J. Biol. Chem.* **264,** 17615–17618.
111. Bendiak, B. (1990) A common peptide stretch among enzymes localized in Golgi apparatus. *Biochem. Biophys. Res. Commun.* **170,** 879–882.

8

Liposomes and Phospholipid Binding Proteins in Glycoprotein Biosynthesis

Roger K. Bretthauer and Dennis W. Welsh

1. Introduction

The metabolic process of glycosylation of proteins on the amide nitrogen of specific asparagine residues in proteins, referred to as *N*-linked glycosylation, has common features found in all eucaryotic cells. The distinguishing general features are (1) the preassembly in the endoplasmic reticulum (ER) of the precursor core oligosaccharide on a lipid carrier, dolichol phosphate (dol-P); (2) the transfer of the oligosaccharide from dolichol pyrophosphate to the specific asparagine residue of the protein as a cotranslational event; and (3) the modification of the protein-linked oligosaccharide by removal and addition of sugar residues (processing) as the glycoprotein proceeds through the ER and Golgi complex (*see* **ref.** ***1*** for a comprehensive review of glycoprotein biosynthesis). Preassembly in the ER of the precursor oligosaccharide on dol-P involves the addition of two GlcNAc residues (one of these as GlcNAc-1-P), nine mannose residues, and, in most cases, three glucose residues to generate the dol-P-P-GlcNAc2Man9Glc3 molecule. Fourteen glycosyltransfer steps are involved, presumably catalyzed by 14 specific transferases. Addition of the two GlcNAc residues and five of the mannose residues occurs on the cytosolic side of the ER membrane with sugar nucleotide precursors, whereas the remaining four mannose residues and the three glucose residues are added in the lumen of the ER with dol-P-linked sugar precursors. The numerous enzymes catalyzing glycosyl transfer reactions are thus functionally and topologically located either on the cytosolic side or on the luminal side of the ER membrane; and other proteins involved, such as a translocase or flippase for moving the dol-

From: *Methods in Molecular Biology, vol. 199: Liposome Methods and Protocols*
Edited by: S. Basu and M. Basu © Humana Press Inc., Totowa, NJ

P-P-linked GlcNAc2Man5 from the cytosolic side to the lumen of the ER, have topological features.

Isolation and study of these membrane-associated enzymes in a pure form is difficult because their native phospholipid environment is difficult to mimic, and thus other types of experimental approaches have been taken. For example, where cloning of the gene has been successful, modeling of the higher order structures of the corresponding protein as embedded in a phospholipid bilayer membrane can be done. Solubilization of the membrane with detergents and subsequent studies on catalytic activity of the "solubilized" enzyme, in the presence of phospholipid and detergent, have been carried out. Release of a soluble, surface located domain of the protein by proteolysis has allowed structural and activity studies of the domain to be carried out. Modification of the phospholipid environment surrounding the protein by phospholipid hydrolytic enzymes has allowed observations to be made on the dependence of catalytic activity on the fatty acyl chains or the polar head groups of the neighboring phospholipids.

This chapter describes an approach to studying the dependence of catalytic activity of a dolichol cycle, membrane-embedded enzyme on the phospholipid composition of the membrane. In particular, a nonspecific lipid transfer protein (nsLTP) ***(2)*** is utilized to catalyze exchange of phospholipids of intact membrane vesicles with other types of phospholipids supplied as phospholipid vesicles (liposomes). This method has been utilized successfully by other investigators to explore functions of various membrane-associated proteins ***(3–10)***. In this chapter, the effects of phospholipid alteration of intact ER vesicles on activity of the constituent first enzyme of the dolichol cycle, UDPGlcNAc : dolichol phosphate GlcNAc-1-P transferase (GPT), are presented. Numerous studies have previously been carried out on the biochemical properties, regulation, topology, and gene cloning of this enzyme (results of earlier experiments reviewed in **ref. *11***). Previous studies from this laboratory indicated a requirement for phosphatidylglycerol (PG) to stimulate activity of the enzyme in phospholipase A_2-treated and detergent-disrupted microsomes ***(12)***, a requirement for PG and phosphatidylcholine (PC) to recover activity in lipid-depleted microsomal protein ***(13)***, and a requirement for phosphatidylethanolamine (PE) or diphosphatidylglycerol (DPG) to stimulate the activity in intact microsomal vesicles ***(14)***. As demonstrated by these previous experiments, enhancement or recovery of in vitro transferase activity by any particular membrane phospholipid appears to be a function of membrane integrity and composition. By using the technique of modifying the phospholipid composition of intact membrane vesicles with the nonspecific lipid transfer protein, a relationship of in vitro transferase activity to the PE/PC concentration ratio of intact membrane vesicles can be demonstrated.

2. Materials

1. Cholesterol analysis. Total cholesterol content was determined by using a Cholesterol 20 Sigma Diagnostics® Kit. This kit is based on the enzymatic procedure of Allain et al. ***(26)***.
2. Protein determinations. Protein concentrations were determined by a modified Lowry et al. procedure ***(27)*** using bovine serum albumin as standard.

3. Methods

3.1. Preparation of nsLTP

nsLTP was isolated from *Escherichia coli* cell line W3110 that had been transformed with a pTAC-based expression plasmid containing the DNA fragment encoding human nsLTP ***(15)***. The cells were received as a generous gift from Dr. Jeffrey Billheimer (Dupont Pharmaceutical Company) and stored in 10 m*M* Tris-HCl–5 m*M* EDTA–10% glycerol, pH 8.0 at –70ºC. Thawed cells were resuspended in 10 m*M* potassium phosphate buffer, pH 6.8, containing 0.5 m*M* EDTA and 1 m*M* dithiothreitol (KPED), and 1 mg/L of leupeptin. The following procedures were conducted at 4ºC. The cells were ruptured by passage through a French pressure cell at 10,000 psi and the supernatants were collected after centrifugation at 4000*g* for 30 min. The pH of the supernatant was lowered to pH 5.2 using 6 *N* HCl. After 15 min of mixing, the resulting precipitate was pelleted by centrifuging at 24,000*g* for 20 min, and the pH of the resulting supernatant was adjusted to pH 7.4 by the addition of 8 *M* KOH. Fifty milliliters of this fraction was dialyzed two times against 3 L of KPED. The sample was applied to a HiLoad™ 16/10 Mono-S column (Pharmacia) that was equilibrated with KPED. After extensive washing to remove any nonabsorbed proteins, the nsLTP was eluted with a 0.25 *M* KCl linear gradient in KPED. Fractions eluting at approx 175 m*M* KCl, comprising the lipid exchange activity, were pooled and concentrated over an Amicon YM3 ultrafiltration membrane. The purified protein was shown to be homogeneous by sodium dodecyl sulfate-polyacrylamide (SDS-PAGE). The identity of the protein was further confirmed by Western blotting with a polyclonal antibody received from Dr. Billheimer. Aliquots of the purified nsLTP (0.1–1.0 mL) were stored at –70ºC.

3.2. Preparation of Lipid Vesicles for nsLTP Mitochondrial Assay

Small unilamellar vesicles were prepared by drying 0.27 mg of cholesterol, 0.60 mg of PC, 1.35 µCi of [4-^{14}C]cholesterol (45 mCi/mmol), and 0.70 µCi of [9,10-^{3}H(N)]triolein (4 Ci/mmol, a nonexchangeable marker) under a stream of N_2 and then lyophilizing for 1 h. This mixture was allowed to swell 15 min in 1 mL of SET (0.25 *M* sucrose, 1 m*M* EDTA, 50 m*M* Tris-HCl, pH 7.4), and was then sonicated in a water bath sonicator at 25–30ºC until translucent (approx 20 min). Prior to use in the lipid exchange with the ER, the vesicle

preparation was centrifuged at 35,000 rpm in a Beckman 50-Ti rotor for 45 min, and only vesicles in the supernatant were used. This was done to avoid cosedimentation of ER and phospholipid vesicles after the ER had been modified by incubation with the vesicles and nsLTP.

3.3. Preparation of Mitochondria

Beef heart mitochondria were prepared according to a modified procedure of Smith ***(16)***. In brief, one beef heart was obtained from a local slaughterhouse and immediately placed on ice. Fat and connective tissue were trimmed from the heart and the tissue was cut into small cubes. From this cubed tissue, 400 g was combined with 400 mL of 10 m*M* Tris-Cl, pH 7.8, containing 0.25 *M* sucrose, and the final pH adjusted to 7.5 with 6 *M* KOH. After the mixture was passed through two layers of cheesecloth, 200 g of the filtrate was suspended in 1200 mL of 8.5% sucrose containing 10 m*M* potassium phosphate buffer, pH 7.4 (SP buffer). The suspension was then homogenized in a Waring blender for 30 s. One volume of SP was added to four volumes of the final homogenate and the pH adjusted to 7.4 with 6 *M* KOH. Nonruptured cells and nuclei were removed by centrifugation for 15 min at 1200*g*, and the resulting supernatant centrifuged for 15 min at 9150*g*. The resulting mitochondrial pellet was washed once by centrifugation with SET and then heat treated to inactivate lipases by putting 50 mL of the mitochondrial fraction in SET in a 125-mL Erlenmeyer flask that was placed in a 100ºC water bath. This suspension was heated for 20 min with gentle stirring until the temperature reached 74ºC. After cooling, the mixture was centrifuged for 15 min at 9150*g*, and the mitochondria pellet resuspended in SET and frozen at –20ºC.

3.4. nsLTP Mitochondrial Assay Procedure

Lipid exchange activity of nsLTP was determined by measuring the transfer of [^{14}C]cholesterol from lipid vesicles to mitochondria ***(17)***. Small unilamellar vesicles (60 nmol of total phospholipid) containing [^{14}C]cholesterol and [^{3}H]triolein were incubated with mitochondria (1.2 mg of protein) and nsLTP for 90 min at 37ºC in a total volume of 0.5 mL of SET buffer. Transfer activity was terminated by adding 0.5 mL of cold SET and centrifuging at 5000 rpm for 10 min in a Sorvall GLC-4 centrifuge to pellet the mitochondria. Aliquots of the supernatant were utilized for counting of carbon-14 and tritium in a liquid scintillation counter. Activity of the nsLTP was calculated from the decrease in the ^{14}C/^{3}H ratio resulting from [^{14}C]cholesterol transfer to the mitochondria. This method of determining cholesterol transfer was comparable to measuring the carbon-14 content of the mitochondria with corrections for nonspecific sticking of the [^{3}H]triolein.

3.5. Preparation of Rat Liver Endoplasmic Reticulum

A modified procedure of Carey and Hirschberg ***(18)*** was followed for the isolation of rough endoplasmic reticulum (RER) from rat liver. Sprague–Dawley rats, male and female, 5–18 months of age, were anesthetized intramuscularly with a 2:1 (v/v) ratio of Ketaset (100 mg/mL)/Xylazine (20 mg/mL) (average dose of 1.5 µL/g body weight). After bleeding by aorta puncture, livers were removed, washed in cold 0.25 *M* sucrose, resuspended in five volumes cold 0.25 *M* sucrose, and diced with scissors. Homogenization was carried out with a Brinkman Polytron homogenizer equipped with a PT 10ST generator for 1 min at a power setting of 4. The homogenate was centrifuged at 3500 rpm in a Sorvall SS-34 rotor for 10 min, and the resulting supernatant again centrifuged at 9500 rpm for 10 min. The recovered supernatant was adjusted to 43% sucrose (w/w) with 60% sucrose (w/w) and 18 mL was placed in a 40-mL ultracentrifuge tube. On top of the homogenate solution, 18 mL of 38.7% (w/w) sucrose was layered and the tube then centrifuged at 26,000 rpm in a Beckman SW-28 rotor for 1 h. The middle 43% sucrose portion was collected and diluted five times with cold distilled water. After centrifugation at 30,000 rpm in a Beckman 30 rotor for 75 min, the pellet was collected and resuspended by homogenization in 0.25 *M* sucrose. The ER suspension was stored at –70ºC for up to 1 month with little loss in glucose 6-phosphatase (G-6-Pase) latency. Prior to use, the ER was diluted five times with ST buffer and centrifuged for 45 min at 35,000 rpm in a Beckman 50-Ti rotor. The pellet was resuspended in the noted buffer (typically ST) by multiple passes through a 25-gauge syringe needle. These membrane preparations generally exhibited >80% latency of G-6-Pase activity. Latency decreased to <70% after 1 mo of storage, at which time the membranes were discarded.

3.6. Latency of Glucose 6-Phosphatase in Microsomes

The intactness of rat liver microsome vesicles was monitored by the latency of G-6-Pase with mannose 6-phosphate as substrate ***(19)***. The latency assays were carried out in a total volume of 0.5 mL containing 0.1 mg of microsomal protein, 100 m*M* sodium acetate, 5 m*M* mannose 6-phosphate, 5 mg of bovine serum albumin, and various concentrations of Triton X-100. Reactions were initiated by addition of the mannose 6-phosphate substrate and, after incubation for 15 min at 31ºC, were stopped by the addition of 0.5 mL of 10% trichloroacetic acid. Inorganic phosphate was measured in the supernatant after centrifugation to remove the precipitated protein. The formula $100\ (1 - [G6Pase_{-\ TX\text{-}100}/G6Pase_{+\ 0.5\%\ TX\text{-}100}])$ equals the percent latency and a value of 100% infers fully intact ER. In noted experiments, glucose 6-phosphate was used in the same concentration as mannose 6-phosphate.

3.7. Preparation of Donor Vesicles for nsLTP Modification of ER

A typical vesicle preparation consisted of 10 mg of egg PC, 0.18 mg of egg PA, and 0.15 mg of cholesterol. The organic solvents in the mixture were removed under N_2, further dried overnight in a lyophilizer, and then hydrated with 0.75 mL of ST buffer. The suspension was vortex mixed and then sonicated in a water bath sonicator to clarity in 40 min at 35ºC. The sonicate was centrifuged at 35,000 rpm in a Beckman 50-Ti rotor for 45 min and the supernatant was used for the ER modification assay.

3.8. ER Modification by nsLTP

A typical lipid modification assay contained the following components in a 1.5-mL final volume: 7.5 mg of ER (3.75 µmol of phospholipid); 400 µg of nsLTP; donor vesicles (4.62 µmol of phospholipid); 0.2 *M* sucrose, 8 m*M* Tris-Cl, pH 7.4; 2 m*M* potassium phosphate, pH 6.8; 36.5 m*M* KCl; 0.1 m*M* EDTA, and 0.2 mM dithiothreitol. The assay was initiated by the addition of the vesicles. After 30 min of incubation at 31ºC, the lipid exchange was terminated by the addition of 4 mL of cold ST buffer. The mixture was centrifuged at 35,000 rpm for 45 min to pellet the ER and for removal of nsLTP and vesicles in the supernatant. The ER pellet was resuspended in ST by multiple passes through a 25-gauge syringe needle, and then analyzed for G-6-Pase latency, GPT activity, phospholipid content and composition, and cholesterol content.

3.8.1. GlcNAc 1-Phosphate Transferase Assay

Synthesis of dol-P-P-GlcNAc was measured with the tritiated substrate, UDP-[^{3}H]GlcNAc ***(14)***. The assay mixture contained the following components (added in the order shown) in 0.1 mL total volume: 0.1 mg of microsomal protein; 75 µ*M*/0.3 µCi UDP-[^{3}H]GlcNAc; a mixture composed of 5 µg of dol-P in Triton X-100; 10 m*M* $MgCl_2$; 200 m*M* KCl; 5 m*M* 5′-AMP; and 50 m*M* Tris-HCl, pH 7.5. The dol-P was prepared by evaporating the organic solvent in which it was suspended, adding Triton X-100 and H_2O, and sonicating until clear. Final Triton X-100 concentrations were either 0.005% or 0.5% (w/w). In experiments in which exogenous phospholipids were added, the lipid solutions in organic solvents were dried under nitrogen and resuspended in H_2O by sonication (PE did not form a clear solution). After incubation of the assay mixture for 10 min at 31ºC, the reaction was stopped with 0.7 mL of chloroform–methanol (2:1). Following mixing and separation of phases, the upper aqueous phase was removed, added to 50 µL of water, and extracted again with 0.7 mL of chloroform–methanol (2:1). The pooled organic layers were back extracted with 0.2 mL of 50% aqueous methanol. The organic phase was collected, solvents were removed by evaporation, and the remaining

residue dissolved in 250 µL of 1% SDS and 3.5 mL of liquid scintillation cocktail for counting of radioactivity.

3.9. Product Analysis of GPT

With these GPT assay conditions, substrates are available for the production of two [3H]GlcNAc-containing lipids, dol-P-P-[^{3}H]GlcNAc and dol-P-P-[^{3}H]GlcNAc$_2$. To analyze the percentage of each product in a given assay, the sugars were first released by mild acid hydrolysis (in 0.2 mL of 0.1 *N* HCl in 50% propanol at 80ºC for 30 min). After cooling, the HCl was neutralized by the addition of 0.1 mL of 0.2 *N* NaOH, and 0.6 mL of chloroform and 0.2 mL of methanol were added. The solution was mixed and centrifuged to clarify the two phases. The water phase was collected and deionized with Dowex 50W × 8 (H^+) and Dowex AG1 × 8 (OH^-). Separation of the neutral radioactive sugars was carried out by descending chromatography on Whatman 3 MM paper with butanol–pyridine–water (6:4:3 by vol) for 24 h. The paper was dried, cut into 2-cm strips, and counted for radioactivity. Standard GlcNAc and glucosamine (similar mobility as GlcNAc2) were run in a separate lane and located with periodate–silver nitrate stain ***(20)***.

3.10. Total Phospholipid Analysis

Lipids were extracted from the membranes in CHCl3 and MeOH by the procedure of Bligh and Dyer ***(21)***. Aliquots were analyzed for phospholipid content by total phosphate analysis ***(22)***.

3.11. Phospholipid Composition Analysis

Individual phospholipids were separated by a two-dimensional thin-layer chromatography system developed by using modifications of two previously used methods ***(23,24)***. K6 Silica Gel 60 Å chromatography plates (20 cm^2) were activated for 1 h at 110ºC and total lipid extracts were applied to the origin immediately after the plates had cooled to room temperature. Normally 400–500 nmol of phospholipid were applied. Developing tanks, lined with Whatman 3MM filter paper, were allowed to equilibrate with developing solvent for 1 h before chromatography. The solvent for the first dimension was $CHCl_3$–MeOH–H_2O–NH_4OH (70:30:3:2 by vol). After development in the first dimension, the plates were placed in a 70ºC oven for 2 min and then in a fume hood for 15 min. Once no trace of NH_4OH could be detected, the plates were turned 90 degrees and developed in the second solvent of $CHCl_3$–MeOH–Skelley F–acetic acid–H_3BO_3 (40:20:30:10:1.8 by vol). The boric acid was dissolved in MeOH before addition of the other components. Chromatograms were developed to within 2 cm of the top of the plate and after drying for

15 min in a fume hood the lipids were visualized by brief exposure to iodine vapor. Phospholipids were identified by comparison to pure reference compounds. The areas of silica representing desired phospholipids were scraped by razor blade into tubes and extracted three times with CHCl3–MeOH (2 : 1 v/v). The extracts were analyzed for total phosphate.

3.12. Fatty Acid Analysis

A modified method of Lipsky and Landowne *(25)* was used to analyze the fatty acid content of phospholipids. To the dried sample of phospholipid was added 1 mL of 1 *M* H_2SO_4 in methanol and 50 µL of benzene. After incubation for 20 h at 60ºC, 2 mL of Skelly B and 1 mL of water were added. The solvents were thoroughly mixed and the resulting petroleum ether layer containing the fatty acid methy esters removed. The remaining aqueous layer was extracted two more times with petroleum ether and the pooled petroleum ether extracts were then back-extracted with 1 mL of water until the water was neutral to pH paper. Gas chromatography on a 10% Silar 10C column was then utilized, with appropriate standards, to analyze the fatty acid methyl ester content.

3.13. Results and Discussion

Table 1 shows the effects on ER phospholipid content after exposure to the nsLTP and phospholipid vesicles. For these experiments the phospholipid vesicles contained PC–PA–cholesterol (1 : 0.02 : 0.1 by mol). The results shown are an average of 11 experiments using identical assay conditions as described in **Subheading 3.** The single variable was the batch of ER, this being from eight different animals on eight different dates of preparation. The results show that when ER was incubated with both nsLTP and phospholipid vesicles, the PC/PE ratio was increased to 3.89 from 1.78 in untreated ER. With vesicles alone, the ratio was not significantly changed (from 1.78 to 2.10). A 25% increase in total lipid content (from 475 to 597 nmol/mg) occurred also, but this was dependent on the presence of transfer protein (483 nmol/mg with vesicles but without nsLTP) and may result from some nsLTP-dependent fusion of vesicles with ER *(unpublished data)*. Actual exchange of phospholipid is indicated by the increase in PC content (from 243 to 338 nmol/mg) and decrease in PE content (from 136 to 87 nmol/mg) of the ER. Other results (data not shown) verified the phospholipid exchange process by showing that the PE content increased (from 13 to 39 nmol), in a nsLTP-dependent manner, in the phospholipid vesicles remaining in the supernatant fluid after removing the ER by centrifugation. A decrease in the PC/PE ratio from 9.5 to 3.2 thus occurred in the donor/acceptor vesicles. It should be noted that all the lipids in this system are presumably fully exchangeable, not just the PC and PE that are being discussed. The PA and cholesterol levels in the ER did not change (data

Table 1
Phospholipid Content and Latency of ER Vesicles Before and After Exposure to Phospholipid Vesicles (PLV) in the Presence or Absence of 400 μg of nsLTP

		Phospholipid Content of ER (nmol/mg)				
PLV	nsLTP	Total PL	PC	PE	PC/PE	% Latency
–	–	475 ± 37	243 ± 19	136 ± 26	1.78 ± 0.33	82 ± 6
+	–	483 ± 41	260 ± 5	124 ± 17	2.10 ± 0.40	78 ± 6
+	+	597 ± 44	338 ± 51	87 ± 15	3.89 ± 0.91	78 ± 7

Numbers shown represent the averages and the standard deviations calculated from 11 experiments with eight different ER preparations as described in **Subheading 3.**

not shown) because the levels of these lipids in the phospholipid vesicles were formulated to be the same as that of the ER. Fatty acid analyses of the ER before and after treatment with phospholipid vesicles and nsLTP revealed an increase (data not shown) in total unsaturated fatty acids (mainly oleic acid) and a decrease in total saturated fatty acids (mainly stearic acid), resulting in an overall change of 60% saturated fatty acids in the native ER to 50% saturated fatty acids in the treated ER. This could result in altered fluidity of the ER membranes.

The observed effect of the ER phospholipid changes on GPT activity is presented in **Fig. 1**. The variation in the physiological levels of lipids in the ER made it difficult to compare results between ER preparations from different rats. Using ratios of GPT activity and lipid content aided in minimizing this variation. The GPT activities are shown on the vertical axis as ratios of GPT activity in ER pretreated with both synthetic phospholipid vesicles and nsLTP (ER++), to GPT activity in ER pretreated with synthetic phospholipid vesicles but not with nsLTP (ER+–). Emphasis is thus placed on GPT activity changes resulting only from effects of the exogenous nsLTP in the presence of ER and phospholipid vesicles. The lipid content data are presented on the horizontal axis also as ratios. Since the PE and PC were the only lipid levels to significantly change, the results are expressed by relating the changes in ratios of PE/(PC + PE) in ER++ (phospholipid vesicles and nsLTP) to ER+–) (phospholipid vesicles only). The results of all the experiments show that as the PE/(PC + PE) ratio decreased, the GPT activity ratio also decreased.

Table 1 also shows that latency of G-6-Pase was retained in the ER vesicles after exposure to phospholipid vesicles with or without nsLTP. This indicates the changes in PC and PE content did not result in physical disruption of the

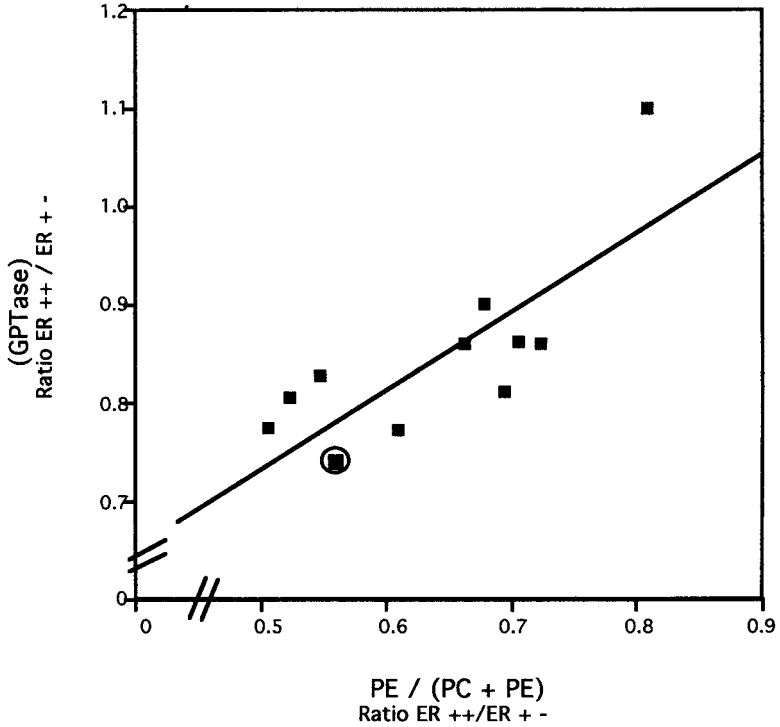

Fig. 1. Effects of nsLTP modification of ER phospholipids on GPT (GTPase) activity. Results for GPT activity are presented as the ratio of activity in ER treated with nsLTP and phospholipid vesicles (ER++) to the activity in ER treated with only phospholipid vesicles (ER+–). Phospholipids are shown as the ratio of PE content to (PE + PC) content in ER treated with nsLTP and phospholipid vesicles (ER++) to that in ER treated with only phospholipid vesicles (ER+–).

ER vesicles, and shows the changes therefore occurred in the outer leaflet of the vesicle membrane. The low concentration of Triton X-100 in the GPT assay has also been shown not to disrupt the ER vescicles as indicated by no loss in latency of the G-6-Pase ***(14)***. Considering all of these results, the observed alteration in outer leaflet PC and PE can potentially have a direct effect on the GPT-catalyzed reaction also occuring on the outer cytosolic side of the ER vesicle.

Several previous studies by other investigators have demonstrated effects of PE on activities of enzymes that utilize dolichol-containing substrates (reviewed in **refs.** ***28*** and ***29***). The ability of PE to adopt the hexagonal H_{II} phase that is bilayer disrupting ***(30)*** may be significant in anchoring

the hydrophobic dolichol molecule in the membrane, in providing a proper environment for the enzymes utilizing dolichol-linked substrates, or in other functions. Phospholipid exchange with the nsLTP affords a way of enriching or depleting PE from biological membranes without physical disruption of the membrane vesicle, thus allowing for further studies on particular functions of PE and other lipids in biological membranes ***(31)***.

References

1. Montreuil, J., Vliegenthart, J. F. G., and Schachter, H., eds. (1995) *Glycoproteins*. Elsevier, New York.
2. Wirtz, K. W. A. (1991) Phospholipid transfer proteins. *Annu. Rev. Biochem.* **60,** 73–99.
3. Dyatlovitskays, E. V., Lemenovskaya, A. F., and Bergelson. L. C. (1979) Use of protein-mediated lipid exhange in the study of membrane-bound enzymes. The lipid dependence of glucose-6-phosphatase. *Eur. J. Biochem.* **99,** 605–612.
4. Crain, R. C. and Zilversmit, D. B. (1981) Lipid dependence of glucose-6-phosphate phosphohydrolase: a study with purified phospholipid transfer proteins and phosphatidylinositol-specific phospholipase C. *Biochemistry* **20,** 5320–5326.
5. North, P. and Fleischer, S. (1983) Alteration of synaptic membrane cholesterol/phospholipid ratio using a lipid transfer protein. Effect on γ-aminobutyric acid uptake. *J. Biol. Chem.* **258,** 1242–1253.
6. McOsker, C. C., Weiland, G. A., and Zilversmit, D. B. (1983) Inhibition of hormone-stimulated adenylate cyclase activity after altering turkey erythrocyte phospholipid composition with a nonspecific lipid transfer protein. Phosphatidylinositol uncouples catecholamine binding from adenylate cyclase activation. *J. Biol. Chem.* **258,** 13017–13026.
7. Lunardi, J., DeFoor, P., and Fleischer, S. (1988) Modification of phospholipid environment in sarcoplasmic reticulum using nonspecific phospolipid transfer protein. *Methods Enzymol.* **157,** 369–377.
8. Gumbhir, K., Sanyal, S. N., Minocha, R., Wali, A., and Majumdar, S., (1989) Glucose-6-phosphate phosphohydrolase activity in guinea pig liver microsomes is influenced by phosphatidylcholine. Interaction with cholesterol-enriched membranes. *Biochim. Biophys. Acta* **981,** 77–84.
9. Kadowaki, H., Grant, M. A., and Seyfried, T. N. (1994) Effect of Golgi membrane phospholipid composition on the molecular species of GM3 gangliosides synthesized by rat liver sialytransferase. *J. Lipid. Res.* **35,** 1956–1964.
10. Bayon, Y., Croset, M., Guerbette, F., Daveloose, D., Chirouze, V., Viret, J., et al. (1995) Selective modifications of the phospholipid fatty acid composition in human platelet membranes using nonspecific and specific lipid transfer proteins. *Analyt. Biochem.* **230,** 75–84.
11. Lehrman, M. A. (1991) Biosynthesis of *N*-acetylglucosamine-P-P-dolichol, the step of asparagine-linked oligosaccharide assembly. *Glycobiology* **1,** 553–562.

12. Plouhar, P. L. and Bretthauer, R. K. (1982) A phospholipid requirement for dolichol pyrophosphate *N*-acetylglucosamine synthesis in phospholipase A_2-treated rat lung microsomes. *J. Biol. Chem.* **257,** 8907–8911.
13. Plouhar, P. L., and Bretthauer, R. K. (1983) Restoration by phospholipids of pyrophosphate *N*-acetylglucosamine synthesis in delipidated rat lung microsomes. *J. Biol. Chem.* **258,** 12988–12993.
14. Chandra, N. C., Doody, M. B., and Bretthauer, R. K. (1991) Specific lipids enhance the activity of UDP-GlcNAc : dolichol phosphate GlcNAc-1-phosphate transferase in rat liver endoplasmic reticulum membrane vesicles. *Arch. Biochem. Biophys.* **290,** 345–354.
15. Matsuura, E. J., George, H. J., Ramachandran, N., Alverez, J. G., Strauss, J. F. III, and Billheimer, J. T. (1993) Expression of the mature and pro-form of human sterol carrier protein 2 in *Escherichia coli* alters bacterial lipids. *Biochemistry* **32,** 567–572.
16. Smith, A. L. (1967) Preparation, properties, and conditions for assay of mitochondria: slaughterhouse material, small-scale. *Methods Enzymol.* **10,** 81–86.
17. Zilversmit, D. B. and Johnson, L. W. (1975) Purification of phospholipid exchange proteins from beef heart. *Methods Enzymol.* **35,** 262–269.
18. Carey, S., and Hirschberg, C. B. (1980) Kinetics of glycosylation and intracellular transport of sialoglycoproteins in mouse liver. *J. Biol. Chem.* **255,** 4348–4354.
19. Burchell, A. (1990) The molecular pathology of glucose-6-phosphatase. *FASEB J.* **4,** 2978–2988.
20. Trevelyan, W. E., Procter, D. P., and Harrison, J. S. (1950) Detection of sugars on paper chromatography. *Nature* **166,** 444–448.
21. Bligh, E. G., and Dyer, W. J. (1959) A rapid method of total lipid extraction and purification. *Can. J. Biochem. Physiol.* **37,** 911–917.
22. Ames, B. N. (1966) Assay of inorganic phosphate, total phosphate, and phosphatases. *Methods Enzymol.* **8,** 115–118.
23. Poorthuis, B. J. H. M., Yazki, P. J., and Hostetler, K. Y. (1976) An improved two dimensional thin-layer chromatography system for the separation of phosphatidylglycerol and its derivatives. *J. Lipid Res.* **17,** 433–437.
24. Gilfillan, A. M., Chu, A. J., Smart, D. A., and Rooney, S. A. (1983) Single plate separation of lung phospholipids including disaturated phosphatidylcholine. *J. Lipid Res.* **24,** 1651–1656.
25. Lipsky, S. R. and Landowne, R. A. (1963) The identification of fatty acids by gas chromatography. *Methods Enzymol.* **6,** 513–537.
26. Allain, C. A., Poon, L. S., Chan, C. S. G., Richmond, W., and Fu, P. C. (1974) Enzymatic determination of total serum cholesterol. *Clin. Chem.* **20,** 470–476.
27. Lowry, O. H., Rosebrough, N. J., Farr, A. L., and Randall, R. J. (1951) Protein measurement with the Folin phenol reagent. *J. Biol. Chem.* **193,** 265–275.
28. Schutzbach, J. S. (1997) The role of the lipid matrix in the biosynthesis of dolichyl-linked oligosaccharides. *Glycoconjugate J.* **2,** 175–182.
29. Chojnacki, T., and Dallner, G. (1988) The biological role of dolichol. *Biochem J.* **251,** 1–9.

30. Cullis, P. R., Hope, M. J., and Tilcock, C. P. S. (1986) Lipid polymorphism and roles of lipids in membranes. *Chem. Phys. Lipids* **40,** 127-144.
31. Dowhan, W. (1997) Molecular basis for membrane phospholipid diversity: Why are there so many lipids? *Annu. Rev. Biochem.* **66,** 199–232.

9

Therapeutic Uses of Antioxidant Liposomes

William L. Stone, Shyamali Mukherjee, Milton Smith, and Salil K. Das

1. Introduction

This chapter focuses on the use of antioxidant liposomes in the general area of free radical biology and medicine. The term *antioxidant liposome* is relatively new and refers to liposomes containing lipid-soluble chemical antioxidants, water-soluble chemical antioxidants, enzymatic antioxidants, or combinations of these various antioxidants. The role of antioxidants in health and disease has been extensively discussed, and many excellent reviews and books are available ***(1–3)***. Antioxidant liposomes hold great promise in the treatment of many diseases in which oxidative stress plays a prominent role. Oxidative stress is a physiological condition in which the production of damaging free radicals exceeds the in vivo capacity of antioxidant protection mechanisms to prevent pathophysiology. Free radicals are molecules with unpaired electrons, often highly reactive and damaging to biological systems. The biological membranes of subcellular organelles are a major site of free radical damage but proteins and DNA are also significant targets. Moreover, free radicals can alter cellular signal transduction pathways and stimulate the synthesis of inflammatory cytokines. Oxygen radicals and other reactive oxygen species (ROS) arise from the single electron reductions of oxygen.

$$O_2 + e^- \rightarrow O_2^{\bullet -} \quad (1)$$

$$O_2^{\bullet -} + e^- + 2H^+ \rightarrow H_2O_2 \quad (2)$$

$$H_2O_2 + e^- + H^+ \rightarrow H_2O + OH^{\bullet} \quad (3)$$

$$OH^{\bullet} + e^- + H^+ \rightarrow H_2O \quad (4)$$

$$O_2^{\bullet -} + NO \rightarrow ONOO^- \quad (5)$$

From: *Methods in Molecular Biology, vol. 199: Liposome Methods and Protocols*
Edited by: S. Basu and M. Basu © Humana Press Inc., Totowa, NJ

In addition, the superoxide radical ($O_2^{\bullet -}$) can react rapidly with nitric oxide to yield peroxynitrite ($ONOO^-$) as shown in **Eq. 5**. Peroxynitrite is a reactive nitrogen oxide species (RNOS) that can also cause damage to DNA, proteins, and membranes. Moreover, $ONOO^-$ is likely to be generated during inflammation and the killing of bacteria. Free radicals are generated in both the aqueous and lipid compartments of cells and, to minimize their damaging effects, requires both lipid- and water-soluble antioxidants. Nevertheless, the potential clinical use of such bifunctional liposomes has been extremely limited ***(4)***.

A primary use of antioxidant liposomes has been to define the molecular mechanism of action for various antioxidants ***(5–13)***. Antioxidants such as butylated hydroxytoluene (BHT) and α-tocopherol have also been used to prevent the oxidation of unsaturated fatty acid moieties in the phospholipids of liposomes during storage ***(14)*** or sonication ***(15)***. This chapter, however, focuses on the potential therapeutic uses of antioxidant liposomes. This is a rapidly evolving area of medical research not extensively reviewed. Most of the research to date has been accomplished using in vitro cell culture systems or animal models. Very few clinical trials have been attempted, yet obvious medical situations exist (as discussed later) in which antioxidant liposomes have enormous health-related significance. The preparation of antioxidant liposomes that can be targeted to specific sites in the body is also a promising area but awaits further research. Most chemical antioxidants are phytoceuticals whose properties have already been extensively studied and are generally regarded as nontoxic and safe for human consumption ***(1)***. In the following subheadings, we first review the varieties of antioxidants that have either been used in antioxidant liposomes or hold the promise of such utilization. We then focus on issues relating to the modes of administration and lastly describe the clinical uses of antioxidant liposomes for diseases in which oxidative stress plays a major role. Major emphasis is placed on the use of antioxidant liposomes for pulmonary diseases.

2. Lipid-Soluble Antioxidants

The lipid-soluble antioxidants that can be incorporated into liposomes include vitamin E (tocopherols and tocotrienols) ***(16)***, ubiquinones ***(17)***, retinoids ***(18–20)***, carotenoids ***(21,22)***, lipid-soluble flavonoids (e.g., quercetin, hesperetin, naringenin) ***(23)***, tamoxifen ***(24,25)***, as well as synthetic lipid-soluble antioxidants such as BHT, tertiary butylhydroquinone (TBHQ), and probucol. Tocopherols can readily be incorporated into both monolayers of unilamellar liposomes in a monomeric form ***(16)***. Furthermore, tocopherol in liposomes can undergo spontaneous intermembrane transfer to an acceptor membrane without the fusion of the tocopherol liposome ***(16)***. This intermembrane transfer is more pronounced when the tocopherol liposome contains

polyunsaturated fatty acids ***(16)***. *R,R,R*-α-tocopherol and *R,R,R*-α-tocotrienol are forms of vitamin E that have the same aromatic chromanol head group but differ in the structure of their hydrocarbon tails. *R,R,R*-α-tocotrienol is, however, a better peroxyl radical scavenger than *R,R,R*-α-tocopherol in phosphatidylcholine liposomes ***(26)***.

β-Carotene (a carotinoid) can be incorporated into liposomes to a maximum of about 0.5 mol% (based on phospholipid) whereas tocopherol can be incorporated at levels as high as 30 mol%. The ability of β-carotene in liposomes to inhibit free radical mediated lipid peroxidation appears, however, to be much lower than that of α-tocopherol ***(27)***. β-Carotene at 0.45 mol% (of phospholipid) is, however, a more powerful inhibitor of singlet oxygen mediated lipid peroxidation than α-tocopherol at 0.45 mol% ***(28)***. α-Tocopherol at 4.5 mol% is, however, also effective at inhibiting both free radical lipid peroxidation as well as singlet oxygen mediated lipid peroxidation ***(28)***. Singlet oxygen can be generated by photosensitization and this reactive oxygen species may contribute to light-induced skin toxicity as well as the aging of skin.

The lipids used in the preparation of antioxidant liposomes also provide an opportunity to introduce antioxidant capacity into liposomes. For example, plasmalogens (1-alkenyl, 2-acyl-) phospholipids are thought to have antioxidant properties ***(29,30)***. Liposomes constructed with ethanolamine plasmalogen inhibit both iron- and copper-dependent peroxidation in the presence of preformed lipid hydroperoxides ***(31)***. Koga et al. have synthesized a novel phospholipid containing a chromanol structure as its polar head group ***(12,32)***. This phosphatidyl derivative of vitamin E is almost as effective an antioxidant as α-tocopherol in unilamellar liposomes subjected to free radicals generated in the lipid phase. The potential therapeutic value of liposomes with antioxidant phospholipids has not been explored but this is an obvious area for future research.

A major advantage of antioxidant liposomes is their ability to simultaneously contain (and deliver) both water- and lipid-soluble antioxidants. This is particularly important in the case of liposomes with both tocopherol (TOH) and ascorbate (Asc), as it has been demonstrated that ascorbate can regenerate tocopherol from the tocopheroxyl radical ($TO^{\bullet}$) ***(33)***.

$$TO^{\bullet} + Asc \rightarrow TOH + Asc^{\bullet} \quad (6)$$

3. Water-Soluble Antioxidants

The water-soluble antioxidants that can be used in antioxidant liposomes include ascorbate (vitamin C), urate, glutathione, *N*-acetylcysteine (NAC), lipoic acid (or dihydrolipoic acid which is its reduced form), pro-cysteine, and water-soluble flavonoids (as in pycnogenol). Dihydrolipoic acid is somewhat

unique because it can quench peroxyl radicals generated both in the aqueous phase and in membranes ***(34)***. Chemical antioxidants generally act by donating an electron to a free radical (thereby quenching the free radical) or by serving as a substrate for an antioxidant enzyme. Glutathione, for example, is itself an antioxidant ***(6)*** and can also function as a substrate for glutathione peroxidase, a key (selenium containing) antioxidant enzyme that converts lipid hydroperoxides (LOOH) or H_2O_2 into the corresponding lipid alcohols (LOHs) or H_2O. Chemical antioxidants can also be chelators of transition metal ions that catalyze lipid peroxidation reactions. Urate, which is present at very high concentrations in human plasma, is an excellent antioxidant that can both chelate transition metal ions and also quench aqueous free radicals ***(35)***. Recently, we have observed 50–60% protection by *N*-acetylcysteine in the generation of free radicals in lungs by mustard gas induced lung injury in guinea pigs (Das and coworkers unpublished observations).

4. Entrapped Antioxidant Enzymes

The application of antioxidant liposomes to problems of medical interest has primarily been with liposomes containing entrapped antioxidant enzymes. Recombinant biotechnology has provided the means to obtain large (i.e., commercial) quantities of human antioxidant enzyme but these enzymes do not normally penetrate the plasma membrane of cells and have a short half-life when introduced into the body by intravenous injection. Turrens has reviewed the potential of antioxidant enzymes as in vivo pharmacological agents ***(36)***. The attachment of polyethylene glycol (PEG) to antioxidant enzymes increases their in vivo half-lives and their effectiveness in preventing pulmonary oxygen toxicity in rats ***(37)***. The various procedures for preparing liposomes with entrapped antioxidant enzymes have been evaluated by Aoki et al. ***(38)***. This group and others ***(39)*** have found that positively charged liposomes have a superior trapping efficiency for superoxide dismutase (which has a negative charge).

Early work by Freeman et al. ***(40)*** has shown that porcine aortic endothelial cells treated with liposomes with entrapped superoxide dismutase (SOD liposomes) can dramatically increase their cellular SOD levels and thereby protect the cells from oxygen-induced injury. In a key paper, Beckman et al. ***(41)*** found that endothelial cells treated with liposomes containing entrapped superoxide dismutase and catalase (SOD+CAT liposomes) can increase the cellular specific activity of these enzymes by at least 40-fold within 2 h. These results are particularly important because endothelial cells are a major site for oxidative damage. Moreover, intravenous antioxidant liposomes would certainly make contact with vascular endothelial cells under in vivo conditions.

5. Modes of Administration

Antioxidant liposomes can be administered topically, intratracheally, intravenously, by inhalation in an aerosol form, or by intramuscular injection. Topical administration can certainly be long term and is of considerable interest to the cosmetic industry in treating specific skin disorders such as psoriasis. α-Tocopheryl acetate in liposomes has been found to have a better dermal absorption than free α-tocopheryl acetate ***(42)***. Topical administration of antioxidant liposomes could also be useful in situations where individuals were exposed to toxic substances (e.g., chemical warfare agents) causing skin damage by free radical mechanisms. Inhalation and intratracheal administration can be useful for those situations in which pulmonary tissues are subjected to oxidative stress such as with influenza infection or inhalation of toxic substances such as paraquat ***(4)***.

Intravenous administration would primarily be limited to situations in which oxidative stress is a component of an acute trauma or disease. The intravenous use of antioxidant liposomes has the potential for rapidly increasing the plasma and tissue concentration of antioxidants far beyond what oral administration could achieve. Moreover, the proteolytic and bioselective processes of the gastrointestinal tract do not limit the types of antioxidants that can be administered via intravenous antioxidant liposomes. For example, it is known that plasma levels of α-tocopherol are about 10 times higher than the levels of γ-tocopherol despite the fact that dietary levels of γ-tocopherol are at least two times that of α-tocopherol. Nevertheless, γ-tocopherol has a unique chemical ability to detoxify peroxynitrite that is not shared with α-tocopherol ***(43)***. Peroxynitrite is a powerful oxidant formed by the reaction of nitric oxide with superoxide radicals (*see* **Eq. 5**) and may be an important mediator of acute oxidant tissue damage. It is reasonable to suspect, therefore, that medical situations could arise in which it would be desirable to rapidly increase plasma (and tissue) levels of γ-tocopherol. The poor bioavailability of orally administered γ-tocopherol makes this very difficult to accomplish. This limitation could, however, be overcome by the intravenous administration of liposomes containing γ-tocopherol.

Vitamin E used in oral supplements is often in the form of a tocopheryl ester such as tocopheryl acetate or tocopheryl succinate. Tocopheryl esters are not, however, absorbed and must first be acted upon by intestinal esterases to liberate the unesterified tocopherol. It is interesting, therefore, that α-tocopheryl succinate but not α-tocopherol has been found to inhibit the activation of nuclear factor κB (NFκB) in cultured macrophages ***(44)***. NFκB is a key transcription factor that regulates the expression of many inflammatory cytokines. α-Tocopheryl succinate can be incorporated into liposomes, and intravenous injection would deliver this form of vitamin E to phagocytic cells

(45). Oral administration of tocopheryl succinate would not, however, be expected to deliver this form of vitamin E to cells.

It is very significant that Cu,ZnSOD liposomes administered by intravenous injection can penetrate the blood–brain barrier and significantly elevate brain levels of SOD activity within 24 h *(46,47)*. Moreover, the intravenous administration of Cu,ZnSOD liposomes to rats can reduce cerebral infarction caused by ischemia *(47)* and also inhibit learning dysfunction caused by a low dose of total body irradiation *(48)*. Surprisingly, intraperitoneal injection of SOD liposomes has also been found to increase the brain levels of SOD in gerbils and to inhibit ischemia/reperfusion oxidative stress *(49)*.

A major problem with conventional liposomes is that they are recognized by the immune system as foreign substances and are rapidly removed from circulation by the phagocytic cells of the reticuloendothelial system. The Kupffer cells of the liver are the most abundant population of phagocytic cells in the body. In some circumstances, however, the uptake of conventional liposomes by hepatic Kupffer cells can actually be an advantage. Carbon tetrachloride (CCl_4), for example, is known to induce hepatotoxicity by a free radical mediated mechanism. Yao et al. *(45)* found that intravenous administration of liposomes containing vitamin E (TOH liposomes) was very effective in decreasing mortality in mice given a lethal dose of CCl4. The TOH liposomes were found to primarily accumulate in the Kupffer cells of the liver.

In recent years considerable advances have been made in the design of stealth liposomes that are not well recognized by the immune system and therefore have a much longer half-life in circulation than conventional liposomes. Stealth technology employs liposomes with a polymer coating of polyethylene glycol–phosphatidylethanolamine (PEG–PE). Recently, the preparation of pH-sensitive stealth liposomes has been described *(50)*. These liposomes have a prolonged circulation in vivo and destabilize at mildly acidic pH, thereby being particularly efficient at delivering a water-soluble compound into a cell's cytoplasm. The use of stealth antioxidant liposomes is very new with an increasing commercial interest in their potential therapeutic applications.

6. Antioxidant Liposomes and Oxidative Stress

Increasing evidence suggests that oxidative stress is an important factor in the aging process and in the etiology of many chronic diseases such as atherosclerosis, ischemic heart disease *(51)*, and cancer *(52,53)*. Schwartz et al. *(54)* at the Harvard School of Dental Medicine have used the hamster cheek pouch tumor model to explore the potential anticancer use of various antioxidants. This group found that β-carotene liposomes injected into the oral squamous cell carcinoma of the hamster caused a lysis of the tumor cells but not of normal cells *(54)*. Retinoids have also been shown to be clinically

effective in treating diverse premalignant and malignant conditions such as cutaneous T-cell lymphomas, leukoplakia, squamous cell carcinomas of the skin, and basal cell carcinomas ***(55,56)***. Several investigators have documented dramatic improvement in patients with acute promyelocytic leukemia after treatment with all-*trans*-retinoic acid ***(57–59)***. However, the side effects of oral all-*trans*-retinoic acid therapy are similar to effects seen with vitamin A: headaches, other central nervous system problems, and dryness of mucosal tissues, erythema, and desquamation of skin. When incorporated in liposomes, all-*trans*-retinoic acid-associated toxicity is markedly reduced whereas antitumor properties, that is, growth inhibition and differentiation induction of all-*trans*-retinoic acid are maintained or even enhanced ***(60,61)***. Phase I and phase II clinical studies found that plasma levels of all-*trans*-retinoic acid were maintained at high concentrations even after prolonged treatment of patients with all-*trans*-retinoic acid-liposomes ***(62)***. In general, the use of retinoids is safe and induces complete remission in 80–90% of acute promyelocytic leukemia patients. However, chronic oral administration results in reduced plasma levels associated with disease relapse in the majority of patients; this can be circumvented by using all-*trans*-retinoic acid liposomes.

Oxidative stress also contributes to the pathology observed in acute medical problems such as heart attack ***(51,63–66)***, respiratory distress syndrome ***(67)***, trauma ***(3)***, irradiation ***(48)***, cold injury ***(68)***, and certain types of infectious diseases such as influenza and human immunodeficiency virus (HIV) infection. Evidence suggests that trauma to the brain results in the overproduction of superoxide radicals that may contribute to edema ***(69,70)***. Antioxidant liposomes containing SOD have been used effectively to treat posttraumatic brain edema ***(69,70)*** and neurological dysfunctions in rats ***(71)***.

Retinopathy of prematurity is a leading cause of blindness in premature and low birth weight infants who are often treated with high levels of oxygen due to surfactant deficiency. Considerable evidence ***(72)*** indicates that oxidative stress is a major contributor to this disease. In an animal model, Niesman et al. ***(73)*** found that intraperitoneal administration of SOD encapsulated in PEG-modified liposomes resulted in a significant increase in retinal SOD activity and an improved tolerance to high oxygen levels. Despite the enormous health-related significance, there are no clinical trials testing the efficacy of antioxidant liposomes to treat retinopathy of prematurity.

7. Pulmonary Applications of Antioxidant Liposomes

7.1. Potential Clinical Applications

Premature children often suffer from respiratory distress syndrome because they lack the capacity to synthesize pulmonary surfactant ***(74)***. Surfactant is

necessary to maintain proper expansion of the small air sacs in the lung. If surfactant levels are low, the small air sacs in the lungs collapse resulting in poor oxygen delivery (hypoxia) to tissues. Infants deficient in surfactant therefore require treatment with high levels of oxygen to prevent damage to their vital organs. Unfortunately, premature infants are often deficient in antioxidants that are necessary to protect organs from injury caused by high concentrations of oxygen. The combination of surfactant deficiency and the presence of oxygen free radicals promote the development of chronic lung disease (bronchopulmonary dysplasia or BPD). BPD is a major cause of morbidity and mortality in premature infants. An estimated 50% of all neonatal deaths result from BPD or its complications. In the adult form of respiratory distress syndrome (ARDS), antioxidants such as *N*-acetylcysteine are recognized for their role in reducing the duration of acute lung injury ***(75,76)***. The rationale for using antioxidant liposomes to treat respiratory distress in premature infants or adults is certainly compelling and supported by the animal models detailed below. However, almost no clinical trials have been initiated.

7.2 Animal Models

Shek et al. ***(77)*** have discussed the general application of liposomes for improved drug delivery to pulmonary tissues. These authors point out that the delivery of drugs to the lung via liposomes is particularly useful because it can minimize extrapulmonary side effects and potentially result in increased drug retention time. In addition (as discussed previously), liposomes for delivery by inhalation or instillation can encapsulate enzyme and/or chemical substances that cannot be delivered by an oral route. Smith and Anderson ***(78)*** demonstrated that intratracheally administered liposomes (with phosphatidylcholine, cholesterol, and stearylamine) have a long retention time (> 5 d) in the mouse lung. Liposomes with entrapped Cu,Zn superoxide dismutase and catalase (Cu,ZnSOD+CAT liposomes) were intratracheally instilled in rabbits and the alveolar distribution of the antioxidants measured after 4 and 24 hours ***(79)***. The results indicate that Cu,ZnSOD+CAT liposomes could increase both SOD and CAT activities in distal lung cells, including alveolar type I, alveolar type II cells, and macrophages. More recent studies by Walther et al. ***(80)*** have shown that intratracheal administration of CuZn-CAT liposomes to premature rabbits can increase the lung SOD activity and protect against hyperoxic lung injury. Moreover, intratracheal delivery of SOD liposomes or CAT liposomes does not down-regulate mRNA synthesis of these enzymes in the premature rabbit lung ***(81)***.

Archer et al. ***(82)*** have made effective use of the isolated perfused rat lung to study the role of oxygen radicals in modulating pulmonary vascular tone. This group showed that the generation of oxygen radicals (from xanthine–xanthine

oxidase) decreased pulmonary vascular presser response to alveolar hypoxia. Either pretreatment of the lung with desferrioxamine or a mixture of superoxide and catalase liposomes inhibited decreases in pulmonary vascular reactivity. Superoxide dismutase administered free in solution or combined with catalase in liposomes, increased the normoxic pulmonary arterial pressure, and enhanced vascular reactivity to angiotensin II and hypoxia ***(82)***.

In a rat model, Freeman et al. ***(83)*** have shown that intravenous injection of SOD liposomes or CAT liposomes can increase (two- to fourfold) the lung-associated specific activity of these antioxidant enzymes and also provide resistance to oxygen injury. Intravenous injection of non-entrapped (i.e., free) SOD or CAT (in the absence or presence of control liposomes) neither increased the specific lung activities of these enzymes nor provided resistance to oxygen toxicity. Similarly, intratracheal administration of SOD liposomes or CAT liposomes (negatively charged and multilamellar) to rats resulted in a significant elevation of lung SOD or CAT activity as well as resistance to pulmonary oxygen toxicity ***(84)***.

Barnard et al. ***(85)*** have demonstrated that instillation of cationic SOD+CAT liposomes in a rabbit model was effective in preventing the increase in pulmonary filtration coefficient (a sensitive index of microvascular permeability) owing to free radical initiated lung injury. Repair of lung injury was inhibited by inhalation of elevated oxygen concentrations. This is of particular importance to the preterm human infant who may be exposed to elevated oxygen concentrations for weeks or months that could result in the chronic pneumopathy known as bronchopulmonary dysplasia. Treatment with liposome-encapsulated SOD and catalase conferred protection against the cytotoxic effects of 50% and 95% oxygen ***(86,87)*** and also protect against cell death ***(88)***.

Briscoe et al. ***(89)*** have evaluated the delivery of SOD to cultured fetal rat pulmonary epithelial cells via pH-sensitive liposomes. A fivefold increase in cellular SOD activity was observed after the culture cells were incubated with the pH-sensitive SOD liposomes ***(89)***. Fetal pulmonary epithelial cells express a high affinity receptor for surfactant protein A (SP-A). This receptor can be used to target liposome delivery to these cells by incorporating SP-A during the preparation of the SOD liposomes ***(89,90)***. The presence of SP-A in the SOD liposomes facilitates their uptake by pulmonary epithelial cells ***(89,90)***.

Considerable evidence suggests that oxidative injury to lung tissues can be mediated by neutrophils ***(91)***. Phorbol myristate acetate (PMA) has often been used to induce neutrophil-mediated lung injury in animal models. It is significant, therefore, that liposomes (dipalmitoylphosphatidylcholine) with α-tocopherol are able to counteract some PMA-induced lung injury in a rat model ***(91)***. In contrast, rats pretreated with blank liposomes (no α-tocopherol) showed no protection from PMA-induced lung injury ***(91)***.

Paraquat has also been used to induce oxidative lung injuries in animal models ***(4)***. Suntres and Shek ***(4)*** have compared the ability of α-tocopherol liposomes (TOH liposome) or liposomes with both α-tocopherol and glutathione (TOH+GSH liposome) to inhibit paraquat-induced lung damage in a rat model. Lung damage was assessed by increases in lung weight (caused by edema) and decreases in lung activities of angiotensin converting enzyme (ACE) that reflects damage to endothelial and alveolar type II epithelial cells. These investigators found that both TOH liposomes and TOH+GSH liposomes were equally effective in preventing loss of lung ACE activity but that TOH+GSH liposomes were more effective in preventing injury to alveolar type II epithelial cells ***(4)***. Interestingly, neither antioxidant liposome was effective in preventing lung edema ***(4)***.

Liposomes encapsulated with catalase (CAT liposomes) have also been found to be efficacious in preventing chronic pulmonary oxygen toxicity in young rats ***(92)***. In this work, rats were treated with 100% oxygen for 8 d and also given daily intratracheal injections of the CAT liposomes (with 160 U of CAT) that prevented chronic lung toxicity. Liposomes encapsulated with superoxide dismutase (SOD liposomes) or with lower levels of CAT (50 U or 70 U) did not prevent the chronic lung changes. SOD+CAT liposomes are also effective in protecting lung tissues from bleomycin-induced injury as evidenced by decreased levels of lipid peroxidation products ***(93)***.

Acknowledgments

This work was supported in part by grants from the Department of Defense (DOD; DAMD17-99-9550 to W. L. S., M. S., and S. K. D.), USDA National Research Initiative Competitive Grants Program (Proposal no. 9600976 to W. L. S.), Natural Source Vitamin E Association (to W. L. S.), and NIH grant 2S06GM0837 (to S. K. D.)

References

1. Papas, A. M. (1999) *Contemporary Food Science. Antioxidant Status, Diet, Nutrition and Health* (Clydesdale, F. M., ed.), CRC Press, Boca Raton, FL.
2. Krinsky, N. I. (1998) The antioxidant and biological properties of the carotenoids. *Ann. NY Acad. Sci.* **854,** 443–447.
3. Oldham, K. M. and Bowen, P. E. (1998) Oxidative stress in critical care: Is antioxidant supplementation beneficial? *J. Am. Diet. Assoc.* **98,** 1001–1008.
4. Suntres, Z. and Shek, P. (1996) Alleviation of paraquat-induced lung injury by pretreatment with bifunctional liposomes containing alpha-tocopherol and glutathione. *Biochem. Pharmacol.* **52,** 1515–1520.
5. Barclay, L., Bailey, A., and Kong, D. (1985) The antioxidant activity of alpha-tocopherol-bovine serum albumin complex in micellar and liposome autoxidations. *J. Biol. Chem.* **260,** 15809–15814.

6. Barclay, L. (1988) The cooperative antioxidant role of glutathione with a lipid-soluble and a water-soluble antioxidant during peroxidation of liposomes initiated in the aqueous phase and in the lipid phase. *J. Biol. Chem.* **263,** 16138–16142.
7. Barclay, L. and Vinqvist, M. (1994) Membrane peroxidation: inhibiting effects of water-soluble antioxidants on phospholipids of different charge types. *Free Radic. Biol. Med.* **16,** 779–788.
8. Barclay, L., Antunes, F., Egawa, Y., McAllister, K., Mukai, K., Nishi, T., and Vinqvist, M. (1997) The efficiency of antioxidants delivered by liposomal transfer. *Biochim. Biophys. Acta* **1328,** 1–12.
9. Di Giulio, A., Saletti, A., Oratore, A., and Bozzi, A. (1996) Monitoring by *cis*-parinaric fluorescence of free radical induced lipid peroxidation in aqueous liposome suspensions. *J. Microencapsul.* **13,** 435–445.
10. Doba, T., Burton, G., and Ingold, K. (1985) Antioxidant and co-antioxidant activity of vitamin C. The effect of vitamin C, either alone or in the presence of vitamin E or a water-soluble vitamin E analogue, upon the peroxidation of aqueous multilamellar phospholipid liposomes. *Biochim. Biophys. Acta* **835,** 298–303.
11. Hayashi, K., Noguchi, N., and Niki, E. (1995) Action of nitric oxide as an antioxidant against oxidation of soybean phosphatidylcholine liposomal membranes. *FEBS Lett.* **370,** 37–40.
12. Koga, T. and Terao, J. (1996) Antioxidant behaviors of vitamin E analogues in unilamellar vesicles. *Biosci. Biotechnol. Biochem.* **60,** 1043–1045.
13. Takahashi, M., Tsuchiya, J., Niki, E., and Urano, S. (1988) Action of vitamin E as antioxidant in phospholipid liposomal membranes as studied by spin label technique. *J. Nutr. Sci. Vitaminol. (Tokyo)* **34,** 25–34.
14. Chow, C. and Heath, T. (1995) Rapid diffusion of the lipid phosphorus of phosphatidylglycerol liposomes through polycarbonate membranes is caused by the oxidation of the unsaturated fatty acids. *Biochim. Biophys. Acta* **1239,** 168–176.
15. Gabrielska, J., Sarapuk, J., and Przestalski, S. (1995) Antioxidant protection of egg lecithin liposomes during sonication. *Z. Naturforsch. [C]* **50,** 561–564.
16. Kagan, V., Bakalova, R., Zhelev, Z., Rangelova, D., Serbinova, E., Tyurin, V., et al. (1990) Intermembrane transfer and antioxidant action of alpha-tocopherol in liposomes. *Arch. Biochem. Biophys.* **280,** 147–152.
17. Yamamoto, Y., Komuro, E., and Niki, E. (1990) Antioxidant activity of ubiquinol in solution and phosphatidylcholine liposome. *J. Nutr. Sci. Vitaminol. (Tokyo)* **36,** 505–511.
18. Tesoriere, L., Bongiorno, A., Pintaudi, A., DqAnna, R., DqArpa, D., and Livrea, M. (1996) Synergistic interactions between vitamin A and vitamin E against lipid peroxidation in phosphatidylcholine liposomes. *Arch. Biochem. Biophys.* **326,** 57–63.
19. Tesoriere, L., Ciaccio, M., Bongiorno, A., Riccio, A., Pintaudi, A., and Livrea, M. (1993) Antioxidant activity of all-*trans*-retinol in homogeneous solution and in phosphatidylcholine liposomes. *Arch. Biochem. Biophys.* **307,** 217–223.

20. Tesoriere, L., DqArpa, D., Re, R., and Livrea, M. (1997) Antioxidant reactions of all-*trans* retinol in phospholipid bilayers: effect of oxygen partial pressure, radical fluxes, and retinol concentration. *Arch. Biochem. Biophys.* **343,** 13–18.
21. Stahl, W., Junghans, A., de Boer, B., Driomina, E., Briviba, K., and Sies, H. (1998) Carotenoid mixtures protect multilamellar liposomes against oxidative damage: synergistic effects of lycopene and lutein. *FEBS Lett.* **427,** 305–308.
22. Woodall, A., Britton, G., and Jackson, M. (1995) Antioxidant activity of carotenoids in phosphatidylcholine vesicles: chemical and structural considerations. *Biochem. Soc. Trans.* **23,** 133S.
23. Saija, A., Scalese, M., Lanza, M., Marzullo, D., Bonina, F., and Castelli, F. (1995) Flavonoids as antioxidant agents: importance of their interaction with biomembranes. *Free Radic. Biol. Med.* **19,** 481–486.
24. Wiseman, H., Laughton, M., Arnstein, H., Cannon, M., and Halliwell, B. (1990) The antioxidant action of tamoxifen and its metabolites. Inhibition of lipid peroxidation. *FEBS Lett.* **263,** 192–194.
25. Wiseman, H. (1994) Tamoxifen and estrogens as membrane antioxidants: comparison with cholesterol. *Methods Enzymol.* **234,** 590–602.
26. Suzuki, Y., Tsuchiya, M., Wassall, S., Choo, Y., Govil, G., Kagan, V., and Packer, L. (1993) Structural and dynamic membrane properties of alpha-tocopherol and alpha-tocotrienol: implication to the molecular mechanism of their antioxidant potency. *Biochemistry* **32,** 10692–10699.
27. Liebler, D., Stratton, S., and Kaysen, K. (1997) Antioxidant actions of beta-carotene in liposomal and microsomal membranes: role of carotenoid-membrane incorporation and alpha-tocopherol. *Arch. Biochem. Biophys.* **338,** 244–250.
28. Stratton, S. P. and Liebler, D. C. (1997) Determination of singlet oxygen-specific versus radical-mediated lipid peroxidation in photosensitized oxidation of lipid bilayers: effect of beta-carotene and alpha-tocopherol. *Biochemistry* **36,** 12911–12920.
29. Engelmann, B., Bräutigam, C., and Thiery, J. (1994) Plasmalogen phospholipids as potential protectors against lipid peroxidation of low density lipoproteins. *Biochem. Biophys. Res. Commun.* **204,** 1235–1242.
30. Vance, J. E. (1990) Lipoproteins secreted by cultured rat hepatocytes contain the antioxidant 1-alk-1-enyl-2-acylglycerophosphoethanolamine. *Biochim. Biophys. Acta* **1045,** 128–134.
31. Zommara, M., Tachibana, N., Mitsui, K., Nakatani, N., Sakono, M., Ikeda, I., and Imaizumi, K. (1995) Inhibitory effect of ethanolamine plasmalogen on iron- and copper-dependent lipid peroxidation. *Free Radic. Biol. Med.* **18,** 599–602.
32. Koga, T., Nagao, A., Terao, J., Sawada, K., and Mukai, K. (1994) Synthesis of a phosphatidyl derivative of vitamin E and its antioxidant activity in phospholipid bilayers. *Lipids* **29,** 83–89.
33. Thomas, C., McLean, L., Parker, R., and Ohlweiler, D. (1992) Ascorbate and phenolic antioxidant interactions in prevention of liposomal oxidation. *Lipids* **27,** 543–550.

34. Kagan, V., Shvedova, A., Serbinova, E., Khan, S., Swanson, C., Powell, R., and Packer, L. (1992) Dihydrolipoic acid—a universal antioxidant both in the membrane and in the aqueous phase. Reduction of peroxyl, ascorbyl and chromanoxyl radicals. *Biochem. Pharmacol.* **44,** 1637–1649.
35. Ma, Y. S., Stone, W. L., and LeClair, I. O. (1994) The effects of vitamin C and urate on the oxidation kinetics of human low-density lipoprotein. *Proc. Soc. Exp. Biol. Med.* **206,** 53–59.
36. Turrens, J. (1991) The potential of antioxidant enzymes as pharmacological agents in vivo. *Xenobiotica* **21,** 1033–1040.
37. White, C., Jackson, J., Abuchowski, A., Kazo, G., Mimmack, R., Berger, E., et al. (1989) Polyethylene glycol-attached antioxidant enzymes decrease pulmonary oxygen toxicity in rats. *J. Appl. Physiol.* **66,** 584–590.
38. Aoki, H., Fujita, M., Sun, C., Fuji, K., and Miyajima, K. (1997) High-efficiency entrapment of superoxide dismutase into cationic liposomes containing synthetic aminoglycolipid. *Chem. Pharmaceut. Bull. (Tokyo)* **45,** 1327–1331.
39. Miyajima, K., Komatsu, H., Sun, C., Aoki, H., Handa, T., Xu, H., et al. (1993) Effects of cholesterol on the miscibility of synthetic glucosamine diesters in lipid bilayers and the entrapment of superoxide dismutase into the positively charged liposomes. *Chem. Pharmaceut. Bull. (Tokyo)* **41,** 1889–1894.
40. Freeman, B. A., Young, S. L., and Crapo, J. D. (1983) Liposome-mediated augmentation of superoxide dismutase in endothelial cells prevents oxygen injury. *J. Biol. Chem.* **258,** 12534–12542.
41. Beckman, J., Minor, R. L, Jr., and Freeman, B. (1986) Augmentation of antioxidant enzymes in vascular endothelium. *J. Free Radic. Biol. Med.* **2,** 359–365.
42. Natsuki, R., Morita, Y., Osawa, S., and Takeda, Y. (1996) Effects of liposome size on penetration of dl-tocopherol acetate into skin. *Biol. Pharmaceut. Bull.* **19,** 758–761.
43. Christen, S., Woodall, A., Shigenaga, M., Southwell-Keely, P., Duncan, M., and Ames, B. (1997) Gamma-tocopherol traps mutagenic electrophiles such as NO(X) and complements alpha-tocopherol: physiological implications. *Proc. Natl. Acad. Sci. USA* **94,** 3217–3222.
44. Nakamura, T., Goto, M., Matsumoto, A., and Tanaka, I. (1998) Inhibition of NF-kappa B transcriptional activity by alpha-tocopheryl succinate. *Biofactors* **7,** 21–30.
45. Yao, T., Degli Esposti, S., Huang, L., Arnon, R., Spangenberger, A., and Zern, M. (1994) Inhibition of carbon tetrachloride-induced liver injury by liposomes containing vitamin E. *Am. J. Physiol.* **267,** G476–484
46. Imaizumi, S., Woolworth, V., Kinouchi, H., Chen, S. F., Fishman, R. A., and Chan, P. H. (1990) Liposome-entrapped superoxide dismutase ameliorates infarct volume in focal cerebral ischaemia. *Acta Neurochir. Suppl. (Wien)* **51,** 236–238.
47. Imaizumi, S., Woolworth, V., Fishman, R. A., and Chan, P. H. (1990) Liposome-entrapped superoxide dismutase reduces cerebral infarction in cerebral ischemia in rats. *Stroke* **21,** 1312–1317.

48. Lamproglou, I., Magdelenat, H., Boisserie, G., Baillet, F., Mayo, W., Fessi, H., et al. J. Y. (1998) An experimental model of acute encephalopathy after total body irradiation in the rat: effect of liposome-entrapped Cu/Zn superoxide dismutase. *Int. J. Radiat. Oncol. Biol. Phys.* **42,** 179–184.
49. Stanimirovic, D. B., Markovic, M., Micic, D. V., Spatz, M., and Mrsulja, B. B. (1994) Liposome-entrapped superoxide dismutase reduces ischemia/reperfusion 'oxidative stress' in gerbil brain. *Neurochem. Res.* **19,** 1473–1478.
50. Slepushkin, V. A., Simões, S., Dazin, P., Newman, M. S., Guo, L. S., Pedroso de Lima, M. C., and Duzgunes, N. (1997) Sterically stabilized pH-sensitive liposomes. Intracellular delivery of aqueous contents and prolonged circulation in vivo. *J. Biol. Chem.* **272,** 2382–2388.
51. Tang, C. S., Su, J. Y., Li, Z. P., Zhang, L. Z., Yang, J., Qi, M., et al. (1993) Possibility of targeting treatment for ischemic heart disease with liposome (II). *Sci. China B.* **36,** 809–816.
52. Demopoulos, H., Pietronigro, D., Flamm, E., and Seligman, M. (1980) The possible role of free radical reactions in carcinogenesis. *J. Environ. Pathol. Toxicol.* **3,** 273–303.
53. Stone, W. L. and Papas, A. M. (1997) Tocopherols and the etiology of colon cancer. *J. Natl. Cancer Inst.* **89,** 1006–1014.
54. Schwartz, J., Shklar, G., Flynn, E., and Trickler, D. (1990) The administration of beta carotene to prevent and regress oral carcinoma in the hamster cheek pouch and the associated enhancement of the immune response. *Adv. Exp. Med. Biol.* **262,** 77–93.
55. Lippman, S. M., Kessler, J. F., and Meyskens, F. L. J. (1987) Retinoids as preventive and therapeutic anticancer agents (Part II). *Cancer Treat. Rep.* **71,** 493–515.
56. Smith, M. A., Parkinson, D. R., Cheson, B. D., and Friedman, M. A. (1992) Retinoids in cancer therapy. *J. Clin. Oncol.* **10,** 839–864.
57. Chomienne, C., Ballerini, P., Balitrand, N., Huang, M. E., Krawice, I., Castaigne, S., et al., (1990) The retinoic acid receptor alpha gene is rearranged in retinoic acid-sensitive promyelocytic leukemias. *Leukemia* **4,** 802–807.
58. Castaigne, S., Chomienne, C., Daniel, M. T., Berger, R., Miclea, J. M., Ballerini, P., and Degos, L. (1990) Retinoic acids in the treatment of acute promyelocytic leukemia. *Nouv. Rev. Fr. Hematol.* **32,** 36–38.
59. Chomienne, C., Ballerini, P., Balitrand, N., Daniel, M. T., Fenaux, P., Castaigne, S., and Degos, L. (1990) All-trans retinoic acid in acute promyelocytic leukemias. II. In vitro studies: structure–function relationship. *Blood* **76,** 1710–1717.
60. Sacks, P. G., Oke, V., and Mehta, K. (1992) Antiproliferative effects of free and liposome-encapsulated retinoic acid in a squamous carcinoma model: monolayer cells and multicellular tumor spheroids. *J. Cancer Res. Clin. Oncol.* **118,** 490–496.
61. Parthasarathy, R., Sacks, P. G., Harris, D., Brock, H., and Mehta, K. (1994) Interaction of liposome-associated all-*trans*-retinoic acid with squamous carcinoma cells. *Cancer Chemother. Pharmacol.* **34,** 527–534.

62. Fiorentini, D., Cabrini, L., and Landi, L. (1993) Ubiquinol-3 and ubiquinol-7 exhibit similar antioxidant activity in model membranes. *Free Radic. Res. Commun.* **18,** 201–209.
63. Bilenko, M., Morgunov, A., Churakova, T., Bulgakov, V., and Komarov, P. (1989) Disorders of cardiac contractile function in ischemic shock; the protective effect of antioxidants and liposomes made from egg phospholipids. *Bull. Eksp. Biol. Med.* **108,** 660–663.
64. Ferrari, R., Agnoletti, L., Comini, L., Gaia, G., Bachetti, T., Cargnoni, A., et al. (1998) Oxidative stress during myocardial ischaemia and heart failure. *Eur. Heart J.* **19** (Suppl B), B2–11.
65. Janero, D. and Burghardt, B. (1989) Oxidative injury to myocardial membrane: direct modulation by endogenous alpha-tocopherol. *J. Mol. Cell Cardiol.* **21,** 1111–1124.
66. Sjogren, K., Hjalmarson, A., and Ek, B. (1992) Antioxidants protect against reoxygenation-induced cell damage in ventricular myocytes. *Biochem. Soc. Trans.* **20,** 233S.
67. Gupta, A., Majumdar, S., and Sanyal, S. (1996) Effect of lung surfactant liposomes on the rabbit fetal lung type II cell antioxidant enzymes following prenatal dexamethasone treatment. *Res. Exp. Med. (Berl.)* **196,** 67–76.
68. Das, D. K., Russell, J. C., and Jones, R. M. (1991) Reduction of cold injury by superoxide dismutase and catalase. *Free Radic. Res. Commun.* **12–13** (Pt 2), 653–662.
69. Chan, P. H., Longar, S., and Fishman, R. A. (1987) Protective effects of liposome-entrapped superoxide dismutase on posttraumatic brain edema. *Ann. Neurol.* **21,** 540–547.
70. Chan, P. H. (1992) Antioxidant-dependent amelioration of brain injury: role of CuZn-superoxide dismutase. *J. Neurotrauma* **9** (Suppl 2), 417–423.
71. Michelson, A. M., Jadot, G., and Puget, K. (1988) Treatment of brain trauma with liposomal superoxide dismutase. *Free Radic. Res. Commun.* **4,** 209–224.
72. Papp, A., Németh, I., Pelle, Z., and Tekulics, P. (1997) Prospective biochemical study of the antioxidant defense capacity in retinopathy of prematurity. *Orv. Hetil.* **138,** 201–205.
73. Niesman, M., Johnson, K., and Penn, J. (1997) Therapeutic effect of liposomal superoxide dismutase in an animal model of retinopathy of prematurity. *Neurochem. Res.* **22,** 597–605.
74. Stone, W. L. (1999). Oxidative stress and antioxidants in premature infants, in *Antioxidant Status, Diet, Nutrition, and Health* (Papas, A. M., ed.), CRC Press, Boca Raton, FL, pp. 277–297.
75. Bernard, G. R. (1991) *N*-Acetylcysteine in experimental and clinical acute lung injury. *Am. J. Med.* **91,** 54S.
76. Bernard, G. R., Wheeler, A. P., Arons, M. M., Morris, P. E., Paz, H. L., Russell, J. A., and Wright, P. E. (1997) A trial of antioxidants *N*-acetylcysteine and procysteine in ARDS. The Antioxidant in ARDS Study Group. *Chest,* **112,** 164–172.

77. Shek, P., Suntres, Z., and Brooks, J. (1994) Liposomes in pulmonary applications: physicochemical considerations, pulmonary distribution and antioxidant delivery. *J. Drug Target* **2,** 431–442.
78. Smith, L. and Anderson, J. (1993) Lung retention of phosphatidylcholine and cholesterol from liposomes: effects of oxygen exposure and fasting. *J. Appl. Physiol.* **74,** 1899–1904.
79. Baker, R. R., Czopf, L., Jilling, T., Freeman, B. A., Kirk, K. L., and Matalon, S. (1992) Quantitation of alveolar distribution of liposome-entrapped antioxidant enzymes. *Am. J. Physiol.* **263,** 585–594.
80. Walther, F. J., David-Cu, R., and Lopez, S. L. (1995) Antioxidant-surfactant liposomes mitigate hyperoxic lung injury in premature rabbits. *Am. J. Physiol.* **269,** 613–617.
81. Walther, F., Mehta, E., and Padbury, J. (1996) Lung CuZn-superoxide dismutase and catalase gene expression in premature rabbits treated intratracheally with antioxidant-surfactant liposomes. *Biochem. Mol. Med.* **59,** 169–173.
82. Archer, S. L., Peterson, D., Nelson, D. P., DeMaster, E. G., Kelly, B., Eaton, J. W., and Weir, E. K. (1989) Oxygen radicals and antioxidant enzymes alter pulmonary vascular reactivity in the rat lung. *J. Appl. Physiol.* **66,** 102–111.
83. Freeman, B. A., Turrens, J. F., Mirza, Z., Crapo, J. D., and Young, S. L. (1985) Modulation of oxidant lung injury by using liposome-entrapped superoxide dismutase and catalase. *Fed. Proc.* **44,** 2591–2595.
84. Padmanabhan, R. V., Gudapaty, R., Liener, I. E., Schwartz, B. A., and Hoidal, J. R. (1985) Protection against pulmonary oxygen toxicity in rats by the intratracheal administration of liposome-encapsulated superoxide dismutase or catalase. *Am. Rev. Respir. Dis.* **132,** 164–167.
85. Barnard, M. L., Baker, R. R., and Matalon, S. (1993) Mitigation of oxidant injury to lung microvasculature by intratracheal instillation of antioxidant enzymes. *Am. J. Physiol.* **265,** L340–L345.
86. Tanswell, A. K. and Freeman, B. A. (1987) Liposome-entrapped antioxidant enzymes prevent lethal O_2 toxicity in the newborn rat. *J. Appl. Physiol.* **63,** 347–352.
87. Tanswell, A. K., Olson, D. M., and Freeman, B. A. (1990) Liposome-mediated augmentation of antioxidant defenses in fetal rat pneumocytes. *Am. J. Physiol.* **258,** L165–L172.
88. Tanswell, A. K., Olson, D. M., and Freeman, B. A. (1990) Response of fetal rat lung fibroblasts to elevated oxygen concentrations after liposome-mediated augmentation of antioxidant enzymes. *Biochim. Biophys. Acta* **1044,** 269–274.
89. Briscoe, P., Caniggia, I., Graves, A., Benson, B., Huang, L., Tanswell, A. K., and Freeman, B. A. (1995) Delivery of superoxide dismutase to pulmonary epithelium via pH-sensitive liposomes. *Am. J. Physiol.* **268,** 374–380.
90. Walther, F., David-Cu, R., Supnet, M., Longo, M., Fan, B., and Bruni, R. (1993) Uptake of antioxidants in surfactant liposomes by cultured alveolar type II cells is enhanced by SP-A. *Am. J. Physiol.* **265,** L330–339.

91. Suntres, Z. and Shek, P. (1995) Prevention of phorbol myristate acetate-induced acute lung injury by alpha-tocopherol liposomes. *J. Drug Target* **3,** 201–208.
92. Thibeault, D., Rezaiekhaligh, M., Mabry, S., and Beringer, T. (1991) Prevention of chronic pulmonary oxygen toxicity in young rats with liposome-encapsulated catalase administered intratracheally. *Pediatr. Pulmonol.* **11,** 318–327.
93. Ledwozyw, A. (1991) Protective effect of liposome-entrapped superoxide dismutase and catalase on bleomycin-induced lung injury in rats. I. Antioxidant enzyme activities and lipid peroxidation. *Acta Vet. Hung.* **39,** 215–224.

10

Targeted Gene Delivery by Virosomes*

Debi P. Sarkar, Komal Ramani, and Sandeep K. Tyagi

1. Introduction

In 1990, the first federally approved clinical trials for treatment of a genetic disorder by gene therapy began under the leadership of R. Michael Blease, W. French Anderson, and their colleagues at the National Institutes of Health. This technique involves the identification of required DNA sequences and cell types followed by appropriate ways of DNA delivery to the diseased cells. The therapeutic potential ranges from treating of genetic defects and slowing the progression of tumors to fighting viral infections and curing neurodegenerative disorders. A unique set of problems, such as the lack of efficient delivery systems, lack of sustained expression, and host immune reactions still put forward formidable challenges. It has been almost unanimously pointed out that the major constraint in the field of gene therapy is to devise ideal "vehicles" to target appropriate cells and achieve physiological levels of the desired gene product ***(1)***. Several new strategies have been presented in the recent past for correction of genetic diseases of muscle and skin. Encouraging reports have been published in delivering genes encoding liver-derived factor IX to correct hemophilia B and fumarylacetoacetate hydrolase to cure hereditary tyrosinemia type I. Serious attempts to target genes to precise locations (such as airway epithelial cells of the respiratory tract) in diseases such as cystic fibrosis have so far proved to be difficult and exemplify the need for new delivery methods. Newer viral and nonviral vectors/vehicles, which hold promise to facilitate target-specific vector uptake and retention and are able to evade

*US Patent No. 5,683,866.

From: *Methods in Molecular Biology, vol. 199: Liposome Methods and Protocols*
Edited by: S. Basu and M. Basu © Humana Press Inc., Totowa, NJ

unwanted immune responses, constitute the major demanding criteria for durable and successful gene therapy for genetic diseases ***(2)***.

It is understood that improving the accuracy of a vehicle often compromises its efficiency and vice versa. Nevertheless, it is important to note that the technology now available for specific targeting encompasses most of the currently available delivery systems. The choice is either at the level of (a) target cell surface recognition, by exploiting the strong ligand–receptor interaction of viruses and liposomes, or (b) by incorporating transcriptional elements into plasmid (expression vectors) or viral genomes in such a way so as to trigger the expression of the therapeutic gene only in target cell types of interest. In a nutshell, this may require an appropriate amalgamation of the most opted features of a variety of viral and nonviral vectors into a single "hybrid" carrier selectively custom-made for each individual therapeutic condition ***(3)***. Technical detail of such a hybrid vector as we have developed in our laboratory for liver-directed gene transfer in vivo is presented here.

A major problem in the delivery of DNA and other biological macromolecules into cells is the crossing of the permeability barrier imposed by the plasma membrane. Various methods have been employed to generate effective gene delivery vehicles needed for therapeutic application. In the past few years, various delivery vehicles such as adenoviral vectors, retroviral vectors, and nonviral vectors such as liposomes and DNA–polylysine complexes have been extensively used for the transfer and expression of reporter genes as well as therapeutic genes both in vitro and in vivo ***(4,5)***. These methods have been modified to generate high efficiency vehicles, but they suffer from many other drawbacks that limit their use for in vivo application. In spite of all recent developments in gene therapy since 1989, the formulation of a targeted gene delivery vector is still far from ideal.

Reconstituted Sendai viral envelopes (F, HN-virosomes) containing two glycoproteins, F (fusion)-protein and HN (hemagglutinin-neuraminidase), are known to fuse efficiently with the plasma membrane of target cells and are excellent carriers for fusion-mediated microinjection of biologically active macromolecules in vitro ***(6)***. This delivery system utilizes the binding of HN to the sialic acid residues of the membrane, followed by the F-protein-mediated fusion of the viral envelopes with the host cell plasma membrane at neutral pH. However, this promising system of gene delivery lacks cell-type specificity because of the presence of HN protein known to bind to various cell types through the sialic acid moiety of cell surface glycoconjugates. It has been recently demonstrated in our laboratory that F-virosomes (devoid of HN protein) can specifically bind and fuse with HepG2 cells ***(6)***. The target specificity of F-virosomes has been ensured by the strong interaction between the terminal β-galactose moiety of F protein and the asialoglycoprotein

receptor (ASGP-R) on the membrane of HepG2 cells. In further studies, F-virosomes have been successfully used for the delivery of biologically active macromolecules into the cytoplasm of liver cells both in vitro and in vivo ***(6–9)***. Liver is known to be a model organ for somatic gene therapy. Hence, F-virosomes by virtue of their specific interaction and fusion with liver cells should be an ideal vector for gene delivery both in vitro and in vivo. We have reported for the first time the F-virosome-mediated delivery of CAT gene and its expression in HepG2 cells in a systematic and quantitative fashion ***(8)***. Our findings of the specific interaction of Sendai viral fusion glycoprotein (F) with the human asialoglycoprotein receptor (ASGP-R) is of considerable importance for the development of safe and efficient hepatotropic vectors coveted for in vivo liver gene therapy applications. Based on interaction with ASGP-R, viral and nonviral hepatotropic gene transfer systems have been employed both in vitro and in vivo. While partial targeting to hepatocytes was achieved, the efficiency of these vectors was found to be severely impeded because of the lysosomal degradation of endocytosed ligands ***(10)***. Interestingly, in case of F-virosomes, the F-protein acts in a bifunctional way, that is, binding to hepatocytes followed by membrane fusion mediated direct release of the virosomal aqueous contents to the cytoplasm of target cells ***(6)***. Having established F-virosome-mediated efficient delivery of foreign genes specifically into human hepatoblastoma cells in culture, we assessed the ability of DNA-loaded F-virosomes to affect targeted gene expression in mice following tail vein injection.

2. Materials

1. 150 m*M* NaCl, 20 m*M* Tris-HCl, pH 8.4, containing 3 m*M* dithiothreitol (DTT).
2. 150 m*M* NaCl, 10 m*M* Tris-HCl, pH 7.4, 2 m*M* Ca^{2+}, 2 m*M* Mg^{2+}.
3. 0.01 *M* Tris-HCl, pH 7.4, containing 0.25 *M* sucrose.
4. TE buffer: 10 m*M* Tris-HCl, pH 8.0, 1 m*M* EDTA.

3. Methods

3.1. Construction and Isolation of Eukaryotic Expression Vectors: pCIS3CAT

A 1.55-kb *Xho*I–*Sma*I fragment from plasmid pTKCAT containing CAT gene and SV40 polyadenylation signal was cloned into the plasmid pCIS2, downstream of the cytomegalovirus promoter-enhancer element. Ligation mixture was used to transform *E. coli* DH5α following a standard protocol ***(11)***. A putative clone was identified and confirmed by restriction mapping and Southern hybridization using ^{32}P-labeled CAT gene fragment as a probe. This putative clone was designated as pCIS3CAT. Plasmid, pBVluc (6.38 Kb), containing the firefly luciferase gene under control of CMV promoter, was

derived from pCEP4-X2 luc (Stratagene, La Jolla, CA). In pBVluc, the luciferase coding sequence is followed by SV40 polyadenylation sequence. These plasmids were isolated and purified using Qiagen Megaprep columns. DNA concentration was determined by measuring the absorbance at 260 nm.

3.2. Preparation of F-Virosomes Loaded with pCIS3CAT and pBVluc DNA

Reconstituted Sendai viral envelopes containing the F protein (F-virosomes) were prepared following the procedure standardized in our laboratory ***(12)***. A suspension of 20 mg of Sendai virus (Z strain, grown in 10-d-old embryonated chicken eggs) in phosphate-buffered saline (PBS) was centrifuged, and the pellet obtained was resuspended in 4 mL of buffer A. The suspension was incubated at 37ºC for 2 h and then dialyzed at 4–10ºC for 16 h against three changes of 2 L of buffer B. The viral particles were centrifuged, and the pellet obtained was resuspended in 2 mL of buffer B containing 40 mg of Triton X-100. After incubation at 20ºC for 1 h, the suspension obtained was centrifuged (100,000*g* for 1 h at 4ºC) to remove the detergent-insoluble substances which presumably contain reduced HN and nuleocapsid. From the clear supernatant, the detergent was removed by stepwise addition of SM2 Bio-Beads. In brief, 320 mg of methanol-washed SM2 Bio-Beads was added to 2 mL of supernatant and incubated at 4ºC with gentle rocking. After 2 h, an additional 320 mg of SM2 Bio-Beads was added, and incubation continued at 20ºC for 2 h. Incubation was further continued for 2 h at 20ºC with an additional 640 mg of SM2 Bio-Beads. The turbid suspension was separated from the Bio-Beads with a 26-gauge needle and centrifuged as described previously. The pellet containing F-virosomes was resuspended (0.5–1 mg of protein) in 1 mL of buffer B and stored at 4ºC. For preparation of F-virosomes containing DNA, the Triton X-100 solubilized fraction of virus was mixed with plasmid DNA (75 µg of DNA per milligram of viral protein) and reconstituted as described previously. The unentrapped DNA adsorbed on the outer surface of the virosomal membrane was removed by treatment of virosomes with DNase I (60 µg of DNase I per milligram of F-protein) at 37ºC for 30 min. The presence of entrapped DNA was checked by lysing virosomes with 2% sodium dodecyl sulfate (SDS), loading on 0.8% agarose gel, and subsequently staining with ethidium bromide. The amount of DNA entrapped in F-virosomes was calculated using 32P-labeled plasmid DNA as a tracer. Membrane fusion activity of loaded F-virosomes was ascertained by their ability to bring about lysis of mouse red blood cells (RBCs) in the presence of wheat germ agglutinin (WGA) ***(12)***. Structural integrity of loaded F-virosomes was checked by leakage of entrapped DNA during incubation with PBS (150 m*M* NaCl, 10 m*M* phosphate, pH 7.4), with fresh mouse plasma, with 10% fetal calf serum (FCS)

containing Dulbecco's modified Eagle medium (DMEM) at 37ºC for 16 h and after heat treatment at 56ºC for 30 min. F-virosome preparations were examined for purity by SDS-polyacrylamide gel electrophoresis SDS-PAGE in the presence of β-mercaptoethanol ***(12)*** and were found to be free from any detectable contamination of other proteins. Membrane fusion activity of these virosomal preparations was checked by their ability to lyse mouse RBCs in the presence of WGA. F-virosome associated plasmid DNA was DNase I resistant, indicating it was entrapped rather than adsorbed on the virosomal membrane. No detectable leakage of DNA was observed from F-virosomes incubated with PBS or plasma/FCS and heat-treated F-virosomes. Two to five microgram of intact DNA was found to be encapsulated in 1 mg of F-virosomes.

3.3. Administration of Loaded F-Virosomes and Gene Expression In Vivo

Twelve-week-old female Balb/c mice (~18 g) were injected intravenously into the tail vein with DNA-loaded F-virosomes (0.4 mg of F protein containing 2 μg of DNA) in a final volume of 0.2 mL of Tris-buffered saline ***(9)*** containing 2 m*M* Ca^{2+}. Antibody response against F protein was checked as described earlier ***(9)***.

3.3.1. Reverse Transcriptase-Polymerase Chain Reaction (RT-PCR) Amplification of CAT-Specific Transcripts

One hundred micrograms of total RNA isolated ***(9)*** from liver was incubated with 10 U of DNase I (Sigma) at 37ºC for 15 min and 1 μg of this RNA was reverse-transcribed with 200 U of MMLV-reverse transcriptase (Gibco-BRL, USA). CAT-specific transcripts were amplified by 35 cycles of RT-PCR (1 min at 94ºC, 1 min at 60ºC, 1 min at 72ºC and final extension, 1 min at 72ºC) using the antisense primer 5′ TTA CGC CCC GCC CTG CCA 3′ from the 3′ end of CAT and the sense strand primer, 5′ ACC GTT GAT ATA TCC CAA TGG 3′ from a sequence 27 nucleotides downstream of the 5′ end of CAT. The RT-PCR products were electrophoresed on 1.2% agarose gel and transferred to nylon membrane. A 1.5 Kb *Xho*I/*Sma*I CAT gene fragment derived from the plasmid pCIS3CAT was labeled with [α-^{32}P]dCTP using a random primer labeling technique. The aforementioned blots were subsequently hybridized with this probe.

3.3.2. Detection of CAT Protein by Enzyme-Linked Immunosorbent Assay (ELISA)

Subcellular fractionation of various organs was carried out as described earlier ***(6)***. In brief, the organs were placed in isotonic homogenizing buffer and then dispersed in Potter–Elvehjem type homogenizer at 4ºC. The cytosolic

fraction was purified after differential centrifugation of the homogenate. The amount of CAT protein expressed in the cytosolic fraction was quantitated using the CAT ELISA kit (Boehringer Mannheim, Germany).

3.4. Detection of CAT Gene in Liver Parenchymal Cells by PCR

Parenchymal cell (hepatocyte) separation was carried out following a standard procedure ***(13)***. To summarize, the perfused liver was excised from the animal, cut into small pieces, and washed thoroughly. The liver pieces were incubated at 37ºC for 15 min in buffer containing collagenase A (Boehringer Mannheim, Germany). The resulting liver mass was filtered through a nylon mesh, and the filtrate was centrifuged at 400 rpm for 10 min at 4ºC to obtain the pellet containing hepatocytes. The supernatant containing nonhepatocytes was treated with 0.2% pronase E (Sigma, St. Louis, USA) to digest the contaminating hepatocytes completely ***(14)***. The nonhepatocyte pellet was obtained by centrifuging the pronase-treated supernatant at 1300 rpm for 10 min at 4ºC. Both these cell types were washed three times with ice-cold PBS containing 5 m*M* EDTA, and the cell pellets were processed for subcellular fractionation as described previously. One microgram of total DNA isolated from each subcellular fraction was subjected to PCR using 1.25 U of AmpliTaq® DNA polymerase (Perkin Elmer-Cetus, USA). A 633 basepair fragment of CAT gene was amplified by 35 cycles of PCR (using the conditions mentioned previously). The PCR products were visualized on a 1.2% agarose gel.

3.5. Measurement of Luciferase Activity in Parenchymal and Nonparenchymal Liver Cells 24 h Post-Injection of pBVluc-Loaded F-Virosomes

Following separation, these cells were washed twice with Tricine-buffered saline and suspended in the same. For luciferase assay, the Triton X-100 solubilized cell lysate (from 1 × 107 cells) was mixed with luciferase assay buffer containing 1 m*M* luciferin (Boehringer Mannheim). Luciferase activity (in mV) was measured in a 1250 Luminometer (BIO-Orbit, Finland).

3.6. State of Targeted DNA Associated with Persistent Gene Expression

Total DNA was extracted from parenchymal cells at 1, 15, 30, and 60 d post-injection. The chromosomal DNA was separated from episomal DNA by gel filtration using Sephacryl S-1000 beads. Both the DNA fractions were ethanol precipitated and finally dissolved in TE buffer. The chromosomal DNA was made free of any contaminating episomal DNA by electrophoresis on a 1% low melting point agarose (LMP) gel. Following electrophoresis of the chromosomal DNA (undigested) on 0.7% agarose gel, the blots were

hybridized with 1.5 Kb-CAT gene fragment. Purified chromosomal DNA digested with various restriction enzymes (New England Biolabs, Inc. USA) was hybridized as described previously. The chromosomal and episomal fractions were analyzed by PCR using CAT-specific primers. The PCR cycles were as follows: initial denaturation, 94ºC for 10 min; denaturation, 94ºC for 1 min; annealing, 60ºC for 1 min; extension, 72ºC for 1 min; final extension, 72ºC for 10 min. After 35 cycles, the products were electrophoresed on 1.2% agarose gel, transferred to nylon membrane, and the blot was hybridized with 1.5 Kb-CAT gene fragment.

3.7. Future of Gene Therapy

The real challenge in the field of gene therapy for human diseases lies in translating many vibrant ideas into reality, which could be finally applied in the clinic. The major hurdle is restricted to the poor efficiency of the gene delivery process in vivo with the presently available technology. The following properties of both viral and synthetic systems in conjunction may constitute an ideal gene courier:

- High titre viral particles allowing many cells to be infected.
- Ease and reproducibility of production.
- Targeting of the desired cell type.
- Possession of a transcriptional unit capable of manipulation by regulatory elements.
- Site-specific integration of the transgene in the host chromosome or of its maintenance as a stable episome.
- Components should be nonimmunogenic.

No such kind of vector is available so far. However, we hope this will be overcome by further engineering of viral vectors and synthetic systems and by combining the best elements of these carriers (**Fig. 1**). The focus will be to understand the mechanism controlling of gene expression in target cells so as to approach long-term therapy. With the advent of advanced information on gene promoters and enhancers combined with our understanding of chromatin structure and function emanating from the Human Genome Project, we should eventually design and control the coveted vector for lifetime use.

4. Notes

The present findings constitute a rational and quantitative approach to targeted delivery and expression of a foreign reporter gene (CAT) in liver cells using a novel vehicle derived from Sendai viral envelopes (F-virosomes) with the added novelty of avoiding the degradation of the entrapped DNA caused by the endocytotic pathway. The target specificity of F-virosomes has been

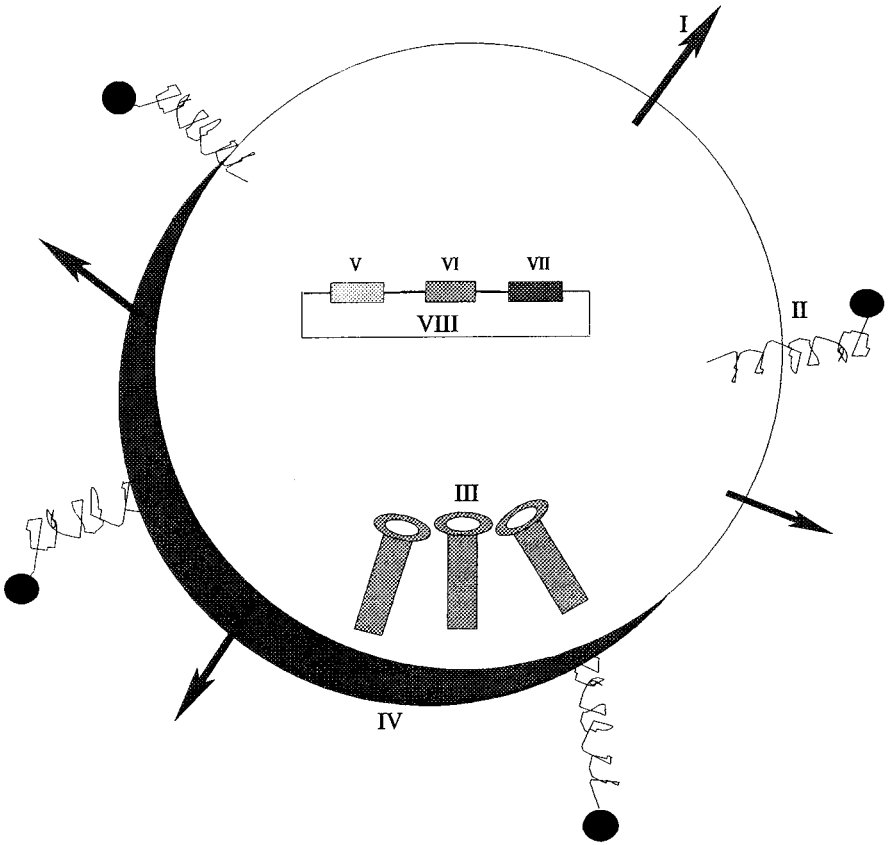

Fig. 1. Hypothetical targeted gene courier. (I) Specific ligands; (II) membrane fusogen; (III) factor for directed integration of vector DNA (site-specific recombinanse); (IV) membranous envelope; (V) sequence for specific homologous recombination; (VI) tissue-specific promoter; (VII) therapeutic gene; (VIII) cDNA vector.

ensured by the strong interaction between terminal β-galactose moiety of F-protein and asialoglycoprotein receptor (ASGP-R) on the membrane of HepG2 cells ***(6)***. We have recently established in our laboratory that F-protein behaves both as a ligand and membrane fusogen for targeting of virosomal aqueous contents to the cytosolic compartment of liver cells both in vitro and in vivo ***(6–9)***. It was shown previously that heat treatment of F-protein in F-virosomes completely abrogates its fusogenic potential without significantly affecting the galactose-mediated specific recognition of ASGP-R ***(6)***. This has suggested the use of heat-treated F-virosomes loaded with DNA, as liganded proteoliposomes which may be efficiently endocytosed by HepG2 cells. The art of natural ligand-receptor interaction and Sendai viral F-glycoprotein-catalyzed

membrane fusion has been exploited in the construction of a safe and efficient vehicle (F-virosome) for site-specific gene delivery to mouse liver cells in vivo. The F-glycoprotein is known to possess Le^x (Galβ1–4[Fucα1–3]GlcNAc-) terminated biantennary oligosaccharides ***(15)***. The Le^x moiety possesses much higher affinity for ASGP-R present on hepatocytes. This property is considered to be a prerequisite of targeted delivery systems. The liver is an ideal organ for transfection of a gene whose product is secreted into the circulation and is important for systemic gene therapy for several inherited diseases. Moreover, the nonpathogenicity of Sendai virus to humans and its little immunogenicity have together increased the prospects of F-virosomes in gene therapy ***(16)***. It has been shown earlier that heat-treated loaded F-virosomes deliver genes to the lysosomal compartment of the cell following the receptor-mediated route of entry ***(8)***. The higher efficiency of fusion-mediated delivery over receptor-mediated entry is very much pronounced below 3 μg of a DNA dose. The hepatotropic nature of this gene carrier is clearly revealed both in terms of mRNA and protein levels. More striking is the sustained nature of gene expression. These features represent a novel instance of targeted and stable gene expression in vivo with no detectable adverse immune effects. Recently, attempts have been made to use liganded cationic liposomes for transgene expression in vivo. Besides the known risk of toxicity of cationic lipids and the transient expression of CAT gene, the efficiency of this system is about 10–12 times less ***(17)*** than that of the F-virosomal delivery. In spite of a sustained insulin gene expression through Sendai virus–liposome complex, this system lacks cell-type specificity and may have undesirable side effects because of the presence of the sialic acid binding protein (HN) of viral origin ***(16)***. The known Le^x type of ligand present on F-virosomes confers it with the added novelty of selective targeting to specific cell types in vivo over the existing modes of DNA targeting.

The F-virosome mediated targeted cytosolic gene delivery in vivo to liver parenchymal cells is apprehended from the cytosolic localization of plasmid DNA at 2 h post-injection and from its absolute nuclear localization 6 h post-injection onward. This is additionally substantiated from the lysosomal localization of plasmid when delivered through heat-treated F-virosomes ***(8)***. The overall efficiency of this delivery mode is also reflected from the absence of any detectable PCR signal on intravenous administration of free DNA. This is probably the first systematic demonstration of intracellular trafficking of a foreign gene administered in vivo. Another strong evidence of this membrane fusion-mediated targeted gene delivery is the preferential expression of luciferase gene in the parenchymal cell types of mouse liver.

The persistent nature of transgene expression in hepatocytes may be explained from the stable integration of CAT gene in the mouse chromosome. It is

pertinent to note that sustained gene expression does not appear to be affected by the random nature of integration of pCIS3CAT DNA. The F-virosomes, being at the interface of viral and nonviral vectors, are adequately safe in comparison to their nonhybrid counterparts ***(1)***. These attributes altogether highlight the potential of this gene carrier for targeted delivery of therapeutic genes both in vitro and in vivo.

References

1. Verma, I. M. and Somia, N. (1997) Gene therapy—promises, problems and prospects. *Nature* **389,** 239–242.
2. Blau, H. and Khavari, P. (1997) Gene therapy: progress, problems, prospects. *Nat. Med.* **3,** 612–613.
3. Miller, N. and Vile, R. (1995) Targeted vectors for gene therapy. *FASEB J.* **9,** 190–199.
4. Harris, J. D. and Lemoine, N. R. (1996) Strategies for targeted gene therapy. *Trends Genet.* **12,** 400–405.
5. Wu, G. Y., Zhan, P., Sze, L. L., Rosenberg, A. R., and Wu, C. H. (1994) Incorporation of adenovirus into a ligand-based DNA carrier system results in retention of original receptor specificity and enhances target gene expression. *J. Biol. Chem.* **269,** 11542–11546.
6. Bagai, S. and Sarkar, D. P. (1994) Fusion-mediated microinjection of lysozyme into HepG2 cells through hemagglutinin-neuraminidase depleted Sendai viral envelopes. *J. Biol. Chem.* **269,** 1966–1972.
7. Bagai, S. and Sarkar, D. P. (1993) Targeted delivery of hygromycin B using reconstituted Sendai viral envelopes lacking hemagglutinin-neuraminidase. *FEBS Lett.* **326,** 183–188.
8. Ramani, K., Bora, R. S., Kumar, M., Tyagi, S. K., and Sarkar, D. P. (1997) Novel gene delivery to liver cells using engineered virosomes. *FEBS Lett.* **404,** 164–168.
9. Ramani, K., Hassan, M. Q., Venkaiah, B., Hasnain, S. E., and Sarkar, D. P. (1998) Site-specific gene delivery *in vivo* through engineered Sendai viral envelopes. *Proc. Natl. Acad. Sci. USA* **95,** 11886–11890.
10. Wu, G. Y., Zhan, P., Sze, L. L., Rosenberg, A. R., and Wu, C. H. (1994) Incorporation of adenovirus into a ligand-based DNA carrier system results in retention of original receptor specificity and enhanced target gene expression. *J. Biol. Chem.* **269,** 11542–11546.
11. Sambrook, J., Fritsch, E. F., and Maniatis, T. (1989) *Molecular Cloning: A Laboratory Manual*, 2nd edit., Cold Spring Harbor Laboratory, Cold Spring Harbor, NY.
12. Bagai, S., Puri, A., Blumenthal, R., and Sarkar, D.P. (1993) Hemagglutinin-neuraminidase enhances F protein-mediated membrane fusion of reconstituted Sendai virus envelopes with cells. *J. Virol.* **67,** 3312–3318.
13. Celis, J. E. (1994) *Cell Biology: A Laboratory Handbook*, vol. 1., Academic Press, San Diego, pp. 96–102.

14. Soriano, P., Dijkstra, J., Legrand, A., Spanjer, H., Londos-Gagliardi, D., Roerdink, F., Scherphof, G., and Nicolau, C. (1983) Targeted and non-targeted liposomes for *in vivo* transfer to rat liver cells of a plasmid containing the preproinsulin I gene. *Proc. Natl. Acad. Sci. USA* **80,** 7128–7131.
15. Yoshima, H., Nakanishi, M., Okada, Y., and Kobata, A. (1981) Carbohydrate structure of HVJ (Sendai virus) glycoproteins. *J. Biol. Chem.* **256,** 5355–5361.
16. Tomita, N., Morishita, R., Higaki, J., Tomita, S., Aoki, M., Ogihara, T., and Kaneda, Y. (1996) *In vivo* gene transfer of insulin gene into neonatal rats by the HVJ-liposome method resulted in sustained transgene expression. *Gene Ther.* **3,** 477–482.
17. Templeton, N. S., Lasic, D. D., Frederik, P. M., Strey, H. H., Roberts, D. D., and Pavlakis, G. N. (1997) Improved DNA:liposome complexes for increased systemic delivery and gene expression. *Nat. Biotech.* 15, 647–652.

11

Liposomes Containing Ligands

Binding Specificity to Selectins

Sriram Neelamegham and Khushi L. Matta

1. Introduction

Carbohydrate-binding proteins have attracted much attention as they are often considered to be mediators of specific cell adhesion ***(1–5)***. It has been suggested that the neutrophils utilize at least three types of adhesion molecules for homing to the sites of inflammation. These are members of the lectin-epidermal growth factor-complement related-cell adhesion molecule (LEC-CAM), integrin, and Ig gene superfamilies ***(6,7)***. The LEC-CAM family of adhesion molecules has recently been recognized to play a central role in mediating leukocyte–endothelial cell interaction. The term selectin is now commonly used to represent three members of this LEC-CAM family: L-, E-, and P-selectin. The lectin character of these cell adhesion molecules (CAMs) makes the selectin family unique among all the known CAM families ***(8–10)***.

One of the landmark events in the area of selectin studies occurred when various groups independently reported that selectins recognize carbohydrate ligands containing the sialyl Le^x (SLe^x) and sialyl Le^a (SLe^a) (structures given in **Fig. 1**) functional moieties ***(11–13)***. These findings stimulated interest in the synthesis of these SLe^x and SLe^a structures along with their sulfated and other related modified analogues. Various review articles have appeared on this subject ***(8–10,14)***. The mechanism of selectin-mediated cell adhesion has also been implicated to play a role in regulating the progress of ischemia–reperfusion injury and cancer metastasis ***(15,16)***. These findings provide added incentive and encouragement for the procurement of carbohydrate derivatives as future drugs, not only for the treatment of inflammatory diseases but also

From: *Methods in Molecular Biology, vol. 199: Liposome Methods and Protocols*
Edited by: S. Basu and M. Basu

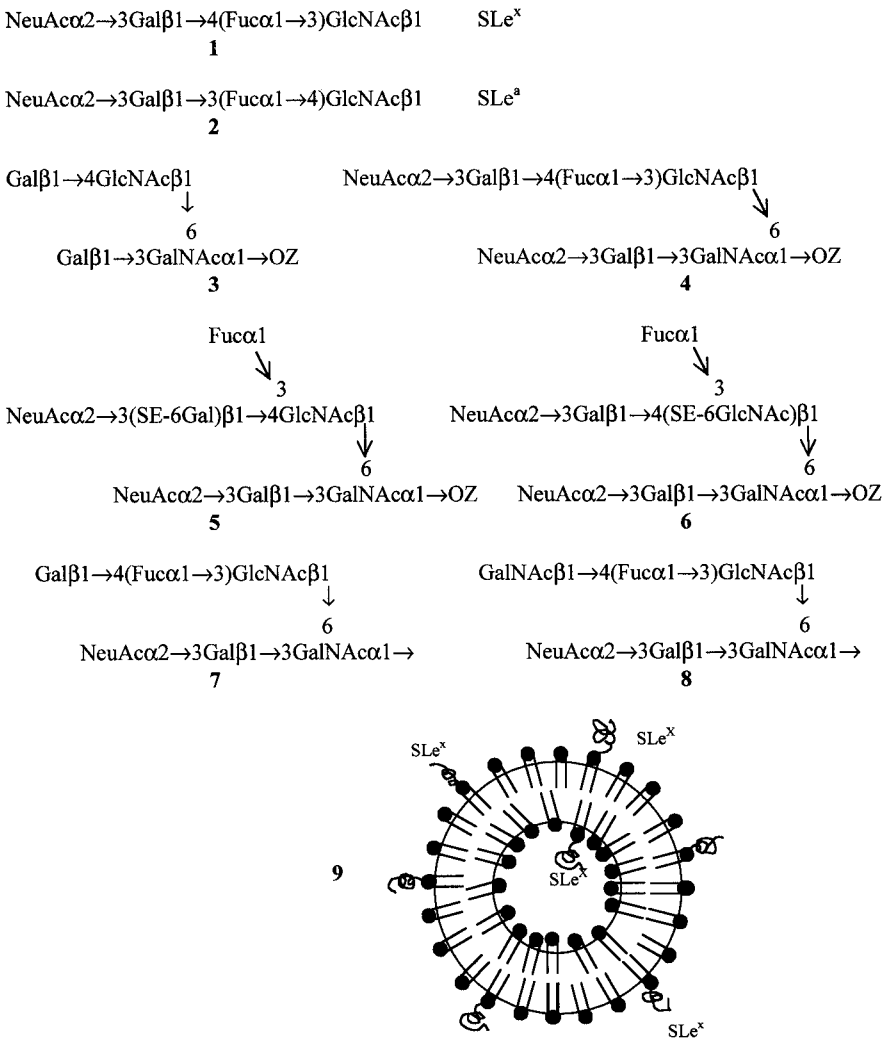

Fig. 1. Structure of oligosaccharides with core 2 structure and liposomes. NeuAc = sialic acid; Gal = galactose; Fuc = fucose; GlcNac = *N*-acetylglucoasamine; GalNac = *N*-acetylgalatosamine; SE = sulfate ester.

for cancer chemotherapy. Inhibitors of L-selectin may also be of therapeutic value in treating septic shock ***(17)***.

1.1. Core 2 Branched Structures as Ligands for Selectins, Especially for L- and P-Selectins

The complex chains of *O*-linked glycoproteins consist of three distinct regions: core, backbone, and nonreducing terminus ***(18–21)***.

Nonreducing terminus→Backbone→Core α→Ser/Thr

Among the known core structures (now more than six), four designated as Galβ1→3GalNAcα-, *core 1*; Galβ1→3(GlcNAcβ1→6)GalNAcα-, *core 2*; GlcNAcβ1→3GalNAcα-, *core 3*; and GlcNAcβ1→3(GlcNAcβ1→6)GalNAcα-, *core 4* are more common. Of these, the *core 2* structure appears to be the most prominent. These core structures are unique to *O*-linked glycoproteins, while the backbone and nonreducing terminal sugar residues can be found in glycolipids, and also as a part of *N*-glycans. *N*-Acetylglucosamine and galactose are key β-linked sugars found in the backbone region, while Galα→, Fucα→, NeuAcα2→, and GalNAcα→ are generally located at the nonreducing terminus of a glycoprotein. The sulfate groups of glycoproteins are important functionalities that are gaining much attention. Some *O*-linked glycoproteins can lack a backbone region. In this case, either the core structure alone or the core structure followed by the galactosylation of GlcNAc present therein may contain the nonreducing terminus residue(s). The core 2 structure on galactosylation leads to the Galβ1→4GlcNAcβ1→6(Galβ1→3)GalNAcα1→sequence, **3** (**Fig. 1**) which can be further branched by sulfate, sialic acid, or fucose residues at the nonreducing terminus by their respective transferases, depending on enzyme specificity and biosynthetic pathway. Biosynthesis of tumor-associated glycoproteins, especially *O*-linked mucins containing fucose, sialic acid, and sulfate, is getting increased attention in recent years. Moreover, it is now well established that natural selectin ligands are mucin glycoproteins, for example, CD34, MAdCAM-1, GlyCAM-1, and P-selectin glycoprotein (PSGL-1) ***(8–11)***. Information on the structure of the carbohydrate moieties of the latter two ligands has become available. The core 2-branched SLe^x- containing structure ***(4)*** has been reported as a significant component of both PSGL-1 ***(22,23)*** and GlyCAM-1 ***(24)***. However, according to Hemmerich ***(24)***, sulfate was reported to be present at the C-6 position of galactose or 6 position of GlcNAc of the SLe^x moiety linked to the C-6 position of GalNAc (**5** and **6**).

The NeuAcα2→3Galβ1→3GalNAc sequence is part of the *O*-linked structure of GlyCAM-I (**5** and **6**) and PSGL-I (**4**). To the best of our knowledge, K. L. Matta's group was the first to demonstrate the importance of this sequence in core 2 structures for binding with L- and P-selectin ***(25,26)***. For example, synthetic compound Galβ1→4(Fucα1→3) GlcNAcβ1→6(Neu Acα2→3Galβ1→3)GalNAcα1→OB **7** was found to be an inhibitor for L- and P-selectin (threefold better than SLe^x) ***(26)***. Interestingly, this compound contains only Le^x moiety linked to C-6 of GalNAc and yet it acts as an inhibitor for selectin. Grinnell et al. ***(27)*** demonstrated that this uncommon sequence, GalNAcβ1→4(Fucα1→3)GlcNAc (GalNAc Le^x), occurs as a terminal structure in certain human C-glycoproteins and it was a better inhibitor than SLe^x for E-selectin. Thomas et al. have also prepared a series of GalNAc Le^x compounds

for similar studies *(28)*. Synthetic GalNAcβ1→4(Fucα1→3)GlcNAcβ1→OMe also binds with selectin *(26)*. Combining this with the knowledge of core 2 branched structures, Matta et al. have synthesized structure **8** which is a five- to sixfold better ligand *(26)*. In fact, a series of synthetic core 2 branched structures have been examined as selectin ligands *(25,26)*. These studies were carried out in collaboration with A. Varki (University of California, San Diego). These findings clearly demonstrated the importance of core 2 structures in the ligands for selectins. It is noteworthy that Ellies et al. *(29)* reported on the function of core 2 *O*-glycans in selectin ligand formation at the recent (Nov '98) meeting of The Society of Glycobiology. To investigate the physiologic role of core 2 *O*-glycans, these investigators deleted the β1,6-GlcNAc transferase gene (a key enzyme for the formation of core 2) from a mouse germ line and observed a deficiency of core 2 *O*-glycans concurrent with a reduction in the biosynthesis of selectin ligands.

1.2. Role of Multivalency in Binding with Selectins, Multivalent SLe^x Peptides, and SLe^x Bearing Liposomes

Most of the efforts toward the procurement of small molecule inhibitory ligands for selectins have been centered on the synthesis of SLe^x type structures *(14)*. Of note, the affinity for selectins for all of these synthetic analogs appears to be poorer than those of the above-mentioned natural mucin ligands *(14,25,30)*. Currently several theories explain the disparity between the high affinity of selectin for the natural ligands and the poor affinity of monomeric synthetic analogs *(25)*. In one respect, it has been hypothesized that the superiority of natural ligands may be due to the presence of clustered arrays of sugar determinants *(30)*. Based on this rationale, synthesis of various multivalent ligands containing SLe^x has been performed in various laboratories *(14,30)*. Thus, according to Renkonen et al. *(31)*, synthetic compounds containing multiple SLe^x determinants at the polylactosamine backbone had higher affinities for L-selectin as compared to SLe^x. Thomas et al. *(30)* have reported that bientennary and trientennary and *N*-linked oligosaccharides are ligands for E-selectin. Synthesis of sialyl SLe^x and glycopeptides as effective ligands for E-selectin have also been reported *(32)*. DeFrees and co-workers *(33)* have synthesized sialyl SLe^x liposome as multiple ligand for E-selectin (structure **9** in **Fig. 1**). Very recently, Stahn et al. *(34)* have also examined both di- and trivalent SLe^x peptides and SLe^x-bearing liposomes as ligands for selectin. For example, for the preparation of glycoliposomes, glycylamine derivatives of SLe^x were coupled to dimyristoyl phosphatidylethanolamine applying disuccinimidyl suberate as a homobifunctional spacer.

1.3. Binding Assay Techniques for Selectins

The ability of liposomes to inhibit selectin-mediated cell adhesion has been typically studied in competitive assays under static conditions. In one set of studies, E-selectin was immobilized on a tissue culture plate surface or expressed on human umbilical vein endothelial cells (HUVECs), and the ability of liposomes to inhibit HepG2 cell binding to the E-selectin-expressing substrate was monitored ***(34)***. A similar protocol has been used in other studies that examined the ability of liposomes to inhibit either HL-60 cell binding to E-selectin-coated substrates ***(33)***, or P-selectin IgG chimera binding to HL-60 cells in suspension ***(35)***. A few recent publications have also measured the ability of glycolipids to mimic cell rolling behavior exhibited by physiological selectin ligands. In one study, the ability of SLe^x and SLe^a glycolipds to support the tethering and rolling of E-selectin and L-selectin-mediated adhesion was demonstrated in a flow chamber apparatus ***(36)***. In a more recent investigation, it was demonstrated that SLe^x glycolipid coated microspheres can roll on E-selectin-IgG chimera-coated substrates in a cell-free assay ***(37)***.

The research efforts in our laboratories focus on the chemical synthesis of carbohydrate selectin–ligand mimics that can be used as specific antagonists to treat a wide variety of vascular ailments. The testing of these antagonists as inhibitors of selectin-mediated adhesion is conducted under linear shear field conditions in a cone-plate viscometer device. Flow cytometry is used for data acquisition and analysis. The protocol used is distinct from the static assays described earlier. Here, we measure the function of isolated blood cells as opposed to soluble molecules or cell lines. Further, these studies are carried out under physiological temperature, pH, and hydrodynamic shear conditions. This contribution of shear in modulating selectin function is ignored in the static assays. However, as recently demonstrated, selectin–ligand bond formation is not only dependent on the intrinsic affinities of adhesion molecules, but it also depends on the applied hydrodynamic shear forces which may alter their binding properties ***(38–40)***. The protocol described here also has a major advantage over the more conventional parallel plate flow chamber assay used to study cell adhesion under shear conditions ***(41)***. In our assay, the sample volume is small (~100 μL/run) and therefore the amount of carbohydrate analogue required for each run is also small. Further, the application of flow cytometry for data analysis enables us to average cell adhesion measurements over thousands of collisions. This is unlike the flow chamber experiments where observations are limited to the area under the microscope's field of view.

In this chapter, we discuss the application of cone-plate viscometry to quantify the ability of carbohydrates and liposomes to inhibit L-selectin-

mediated adhesion. As discussed, this protocol can be suitably modified to study P- and E-selectin-mediated cell adhesion also (*see* **Note 7**). As an example, experimental data are presented from recent studies that quantified the ability of SLe^a to block L-selectin-mediated neutrophil homotypic aggregation (*see* **Note 6**).

2. Materials

1. *N*-(2-Hydroxyethyl)+piperazine-*N*-(2-ethanesulfonic acid) (HEPES) buffer: 110 m*M* NaCl, 10 m*M* KCl, 10 m*M* glucose, 1 m*M* $MgCl_2$, and 30 m*M* HEPES at pH 7.35. All chemicals are tissue-culture grade from Sigma and endotoxin free (*see* **Note 1**). Normal HEPES buffer as described here is Ca^{2+} free. When supplemented with 1.5 m*M* Ca^{2+} just prior to the experiment, the buffer is referred to as "HEPES with Ca^{2+}". Have both types of buffers ready during the experiment.
2. 2% Prosil-28 solution in distilled water (Lancaster Synthesis, Pelham, NH).
3. 100 µg/mL of acridine orange stock solution in HEPES buffer with Ca^{2+} (*see* **Note 5**).
4. 1% Paraformaldehyde solution in HEPES buffer containing 10 ng/mL of acridine orange for sample fixation. Aliquot 200 µL of this paraformaldehyde solution into regular flow cytometry analysis tubes for sample collection (*see* **Note 2**). Separate flow cytometric tubes are required for each sampling point.
5. Extra long pipet tips (PGC Scientific, Gaithersburg, MD) to withdraw sample from viscometer.
6. Isolated cells in HEPES buffer without Ca2+ at a concentration of 10^7 cells/mL or greater.
7. Formyl peptide (FMLP) or other neutrophil stimulus.
8. Oligosaccharide or liposome to be tested.
9. Flow cytometer with standard 488-nm argon laser and fluorescein isothiocyanate (FITC) detector.
10. Cone-plate viscometer that can apply constant shear rate to cell suspension (manufactured by Brookfield, Haake, Paar-Physica, Bohlin Instruments, etc.) (*see* **Note 3**).

3. Methods

3.1. Basic Principle

Cell adhesion experiments are performed in a cone-plate viscometer followed by flow cytometric analysis. The cone-plate viscometer consists of an inverted cone placed over a flat plate surface that is maintained at 37ºC (**Fig. 2**). In the results presented here, a cone angle of 2º was used, and the gap between the cone and plate was set to vary from <10 µm at the center to 870 µm at the outside edge. The cell suspension is placed between the cone and the plate surface prior to the application of shear. In this device the distance between

the cone and the plate surface increases linearly with radial distance from the center. This unique design feature of the viscometer, in comparison to other shear-producing devices, enables the application of a uniform and linear shear rate to the entire cell suspension. The shear rate (G, in unit/s) for a viscometer with cone angle θ (in unit radians or º), varies linearly with angular velocity ω (in unit radians/s) as: $G = \omega/\tan(\theta)$. For example, if the angular velocity of the cone is 52.4 radians/s and the cone angle θ is 2º, then the shear rate *(G)* applied to the entire cell suspension is 1500 s^{-1}. For newtonian fluids such as isolated or dilute cell suspensions, the applied shear stress (τ) varies linearly with fluid viscosity (ν) and applied shear rate: $\tau = \nu \times G$. At 37ºC, the fluid viscosity of typical buffers is ~0.7 centipoise.

In the cone-plate viscometer, the fluid velocity is zero on the plate surface and it increases linearly in the vertical direction. Consequently, following cell stimulation and application of shear, the cells closer to the rotating cone surface move faster than those near the plate surface. This difference in velocities results in cell–cell collision. The frequency of collision is dependent on the radius of the colliding species, their individual concentrations, and the applied shear rate. Mathematically, the collision frequency per unit volume per unit time is given by $f_{ij} = 16/3\ r_i^3\ GC_i$ ***(42)***, where r_i and r_j are the radii of the i^{th} and j^{th} colliding species, C_i and C_j are the concentrations of the two species, and G is the applied shear rate. A fraction of these collisions may result in adhesion of the two colliding particles. This fraction or probability of a successful collision is termed as adhesion efficiency, E.

During the course of the experiment, a flow cytometry methodology described in **Subheading 3.2.2.** is used to determine the distribution of particle sizes, ranging from singlets to quadruplets and larger aggregates, at each time point of the experiment. Following this, we estimate two measures of cell adhesion kinetics.

3.1.1. Percent Aggregation

This parameter quantifies the fraction of singlets recruited into aggregates. Mathematically,

$$\% \text{ Aggregation} = \left(1 - \frac{S}{S + 2D + 3T + 4Q + 5(> Q)}\right) \times 100 \qquad (1)$$

where the neutrophil aggregate sizes are given by S (singlets), D (doublets), T (triplets), Q (quadruplets), and $> Q$ (aggregates larger than quadruplets). This parameter depends not only on the biological adhesivity of the stimulated neutrophils, but also on the physical parameters of the system that alter the cell collision frequency. For example, increasing cell concentration and cell

size increases the number of cell–cell collisions and this results in an increase in percent aggregation. Therefore, percent aggregation depends both on the physical parameters of the system and the biological adhesivity of the cells.

3.1.2. Cell Adhesion Efficiency

Adhesion efficiency is defined as the fraction of intercellular collisions that result in firm adhesion and it is always less than or equal to 1. This parameter is estimated by fitting the data from the aggregation experiments over the first 30–60 s after the application of shear, with a mathematical model based on Smoluchowski's linear two-body collision theory ***(42)***. The simplest way to quantify this parameter is based on measuring the rate of change of the total particle concentrations (including isolated cells and aggregates) during the experiment. In homotypic neutrophil aggregation experiments, if $n(t)$ and $n(0)$ are the total particle concentrations at times t and 0 respectively, then the adhesion efficiency E of neutrophils with radius r being sheared at a rate G can be estimated:

$$n(t) = n(0) \bullet \exp\left(-16\, n(0)\, r^3\, GEt/3\right) \tag{2}$$

This equation is valid in experiments during the first 10–30 s after the application of shear, in the absence of aggregate breakup, and when large multicellular aggregates are not formed. At these short times most of the aggregates are either singlets or doublets, and percent aggregation is typically < 30%.

For systems in which a number of large aggregates are formed rapidly, the analysis of cell aggregation data and the quantification of adhesion efficiency requires the application of a more complex mathematical model as outlined elsewhere ***(43)*** along with appropriate corrections ***(44)***. The adhesion efficiency evaluated by this methodology is solely a function of the intrinsic biological properties of the cell that determine its adhesivity including, but not limited to, the number, affinity, and distribution of adhesive receptors expressed on the cell surface, and their response to applied shear, inhibitors, and the time after stimulation.

3.2. Homotypic Neutrophil Aggregation

3.2.1. Cone-Plate Viscometry

1. Place 2% Prosil-28 solution in the gap between the cone and plate surface of the viscometer for at least 10 min at 37ºC. Prosil-28 should cover the entire cone and plate surface. Over 10 min, Prosil will coat the viscometer so that cells do not attach to its surface.
2. Dilute the isolated neutrophils in HEPES buffer (with calcium) at appropriate concentrations (typically between 5×10^5 and 5×10^6 cells/mL) (*see* **Note 4**). Incubate this cell suspension with acridine orange at 10 ng/mL, and liposome/

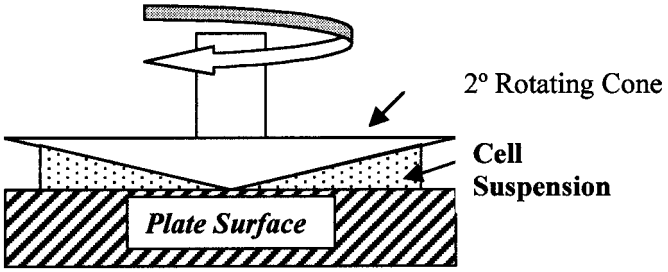

Fig. 2. Schematic of a cone and plate viscometer. The cone-plate viscometer consists of a rotating cone placed over a stationary plate. The cell suspension is placed in the narrow gap between the cone and plate surface prior to stimulation and application of shear.

oligosaccharide at room temperature for 10 min, followed by 37ºC for 5 min. The acridine orange will stain the cell's nucleus for subsequent flow cytometric detection. The total volume of the suspension can range between 100 and 1000 µL. Smaller volumes are normally preferred because the quantity of liposome required is less. Maintain constant sample volume, shear rate, and cone angle in all experiments that compare the inhibitory role of liposomes so as to simplify subsequent comparisons.

3. Take the initial sample at $t = 0$ (20 µL volume) and fix it in cold 1% paraformaldehyde solution containing 10 ng/mL of acridine orange.
4. Now place the remaining suspension in the viscometer, stimulate it with FMLP or other agonists, and begin application of shear. FMLP concentration used may be 1 µ*M* or lower, and the applied shear rate may typically vary from 50 to 3000/s.
5. At each sampling time point, stop the viscometer for 3–4 s, insert the extra-long pipet tip to withdraw a 20-µL sample, and fix the withdrawn cell suspension in aliquots containing 200 µL of 1% cold paraformaldehyde suspension. These samples will be subsequently analyzed using flow cytometry to determine the changes in aggregate size distribution with time.

3.2.2. Flow Cytometric Analysis of Particle Distribution

1. Perform flow cytometric analysis by gating the cell suspension on its characteristic forward and side scatter profile to identify the neutrophils (**Fig. 3A**,**E**). A threshold may be set on the green fluorescent channel to eliminate the red blood cell impurities in the isolated neutrophil preparation.
2. Adjust the gain and attenuation of the green fluorescence so that single neutrophils have a fluorescence that is approximately equal to 1/8 of the maximum possible value allowed by the instrument (**Fig. 3B**,**F**).
3. The histogram distribution of the green acridine orange fluorescence is obtained for each time point, allowing distinction between singlet neutrophils and

aggregates consisting of more than one neutrophils (**Fig. 3C**,**G**). As seen, the green fluorescence of neutrophil aggregates are integral multiples of singlet fluorescence. The number and fraction of particles which are singlets *(S)*, doublets *(D)*, triplets *(T)*, quadruplets *(Q)*, and larger than quadruplets (> *Q*) can be measured from the histogram. Their statistics for a representative experiment is presented in a table form at time $t = 0$ and 60 s (**Fig. 3D**,**H**).

4. Analyze these data in terms of two parameters: (a) percent aggregation and (b) adhesion efficiency as described in **Subheadings 3.1.1.** and **3.1.2.**

Sample experimental results from our laboratory are illustrated in **Fig. 4**. The results demonstrate that increasing SLe^a concentration inhibits neutrophil homotypic aggregation in a dose-dependent fashion (**Fig. 4A**). Up to 90% inhibition was observed on addition of 2 m*M* SLe^a. The experimental results in the form of adhesion efficiency are presented in **Fig. 4B**. These calculations were obtained by using the more complex mathematical model ***(43,44)*** as opposed to the simple equation (**Eq. 2**) for adhesion efficiency in **Subheading 3.1.2.** This is because, at the chosen cell concentration and shear rate, the percent aggregation was large (up to 60%) within 10 s of application of shear.

4. Notes

1. All buffers and reagents are stored at 4ºC and are used within 4 wk of preparation. Neutrophils are sensitive to endotoxins and are easily activated.
2. It is best to complete all experiments within 2–3 h of blood cell isolation. Paraformaldehyde fixed samples should be analyzed on the same day if possible, or at least within 2–4 d after fixation.
3. Any cone angle in the range between 1/3 and 4º is acceptable for biological cell aggregation studies. The smaller cone angles are better, as this allows the application of a wider range of shear for a given instrument. Further, we have recently demonstrated, both theoretically and experimentally, that large cone angles and high shear rates may result in significant secondary flow in the viscometer ***(45)***. Conventional analysis (or primary analysis) as described in the preceding sections assumes that flow in the viscometer takes place only in the radial direction and that it is purely linear. While this is valid for low shear rates, at high shear rates centrifugal forces cause an outward radial motion of the fluid near the rotating cone surface and an inward radial flow near the plate. This additional radial motion of the liquid is called "secondary flow" and it causes nonlinear fluid flow. Recently, we have observed that this nonlinear flow results in positional variations in the nature and kinetics of cell adhesion in the viscometer. For neutrophil homotypic aggregation experiments, this secondary flow can cause up to a 25% reduction in the cell adhesion kinetics at a shear rate of 1500/s, sample volume of 1 mL, and cone angle of 2º, as compared to primary flow alone.

   Secondary flow is a limitation of this instrument, and it is unavoidable especially at high shear rates greater than 1500/s. To ensure that all experiments

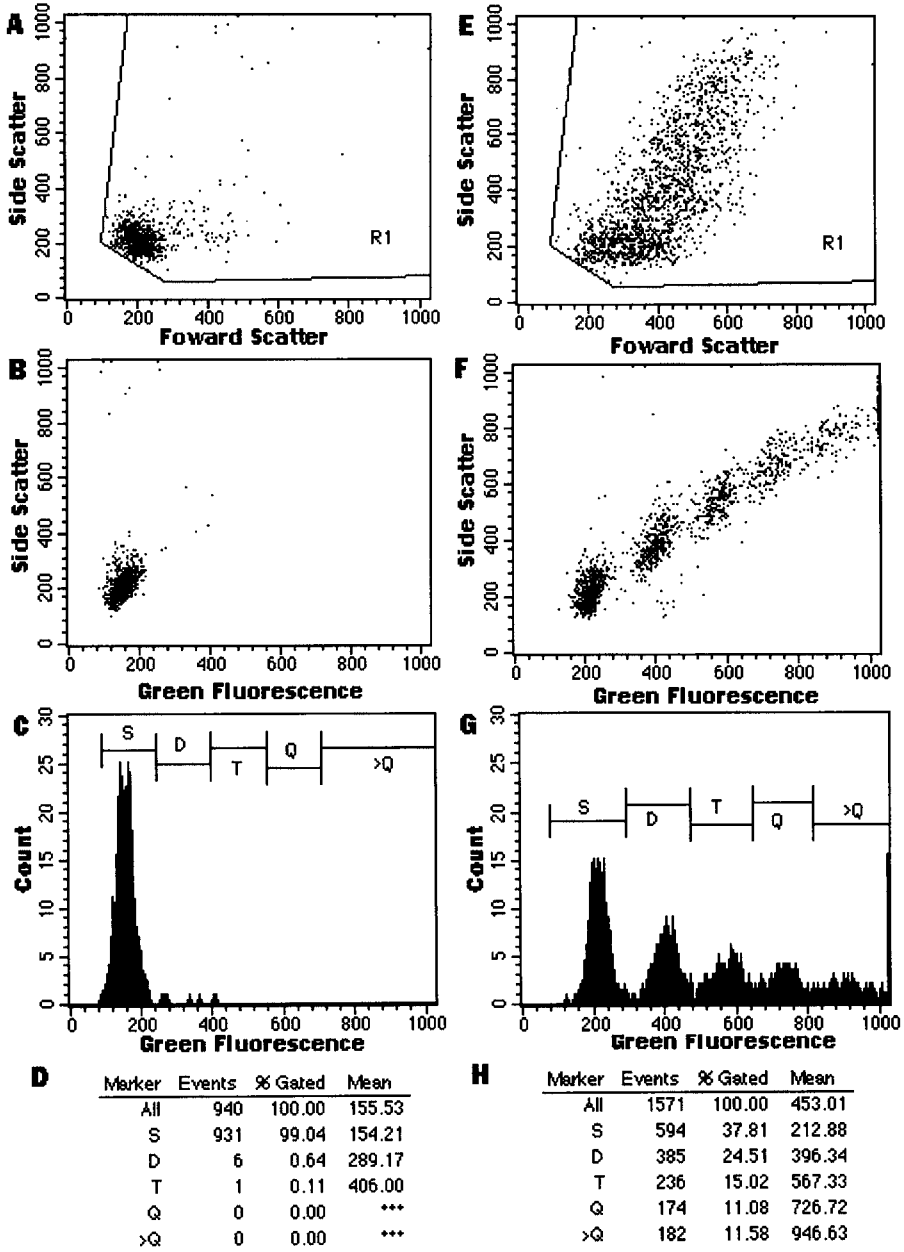

D

Marker	Events	% Gated	Mean
All	940	100.00	155.53
S	931	99.04	154.21
D	6	0.64	289.17
T	1	0.11	406.00
Q	0	0.00	***
>Q	0	0.00	***

H

Marker	Events	% Gated	Mean
All	1571	100.00	453.01
S	594	37.81	212.88
D	385	24.51	396.34
T	236	15.02	567.33
Q	174	11.08	726.72
>Q	182	11.58	946.63

Fig. 3. Flow cytometric detection of neutrophil homotypic aggregation at $t = 0$ s **(A–D)** and 60 s **(E–H)**. Neutrophils are detected in the flow cytometer by gating on their characteristic forward vs side scatter **(A,E)**. The distribution of the singlets *(S)*, doublets *(D)*, triplets *(T)*, quadruplets *(Q)*, and larger aggregates (> *Q*) is then measured using green fluorescence due to acridine orange staining of neutrophils **(B,F)**. The histogram plots of green fluorescence **(C,G)**, and the corresponding histogram statistics **(D,H)** are used to quantify the aggregate size distribution.

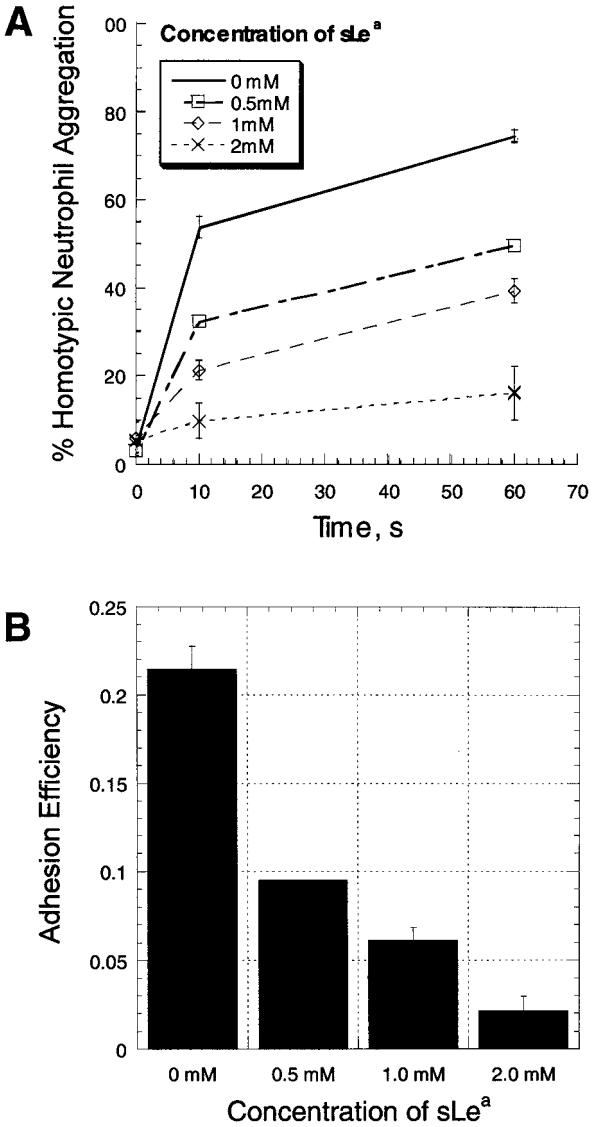

Fig. 4. Dose-dependent inhibition of L-selectin-mediated aggregation by SLe^a. One hundred microliters of acridine orange labeled neutrophils at 5×10^5 cells/mL were preincubated with SLe^a at varying dosages, stimulated with 1 μ*M* FMLP and sheared in a 2° cone-plate viscometer at 1500/s. **(A)** Percent aggregation varies with time after stimulation. **(B)** Adhesion efficiency ± SEM plotted as a function of SLe^a dosage.

that quantify liposome/oligosaccharide inhibition have equal contribution of secondary flow, the sample volume, cone angle, and applied shear rate should not be changed between individual runs comparing selectin-inhibition function. Experiments with smaller sample volumes are preferred as they minimize the secondary flow phenomenon and use lesser carbohydrate.

4. The cell concentration used in the experiment typically varies from 5×10^5 to 5×10^6 cells/mL. Lower concentration (as low as 2×10^5 cells/mL) may also be used by the experimenter. Over a range of shear rates this may result in slower depletion of singlets and may allow the simple application of the Eq. 2 to quantify cell adhesion efficiency.
5. Besides detection of neutrophils with acridine orange, other nuclear dyes such as LDS-751 and fluorescent monoclonal antibodies to receptors on the neutrophil surface such as CD45-FITC can also be used. In these cases, control experiments should be performed to ensure that addition of the dye/antibody does not itself cause neutrophil activation. Neutrophil aggregate distribution can also be measured by fixing the cell samples with glutaraldehyde, which emits autofluorescence. This autofluorescence can be detected using flow cytometry and thus used to quantify cell aggregation kinetics ***(43)***.
6. Homotypic neutrophil aggregation is mediated via two receptors, L-selectin and β_2-integrin ***(38,46)***. A detailed discussion of the role of selectins and integrins in this process as a function of hydrodynamic shear is provided elsewhere ***(45)***. In brief, in this two-receptor system, L-selectin is apparently necessary to tether the two colliding neutrophil species, and thus form transient neutrophil aggregates. If these aggregates are held together in the hydrodynamic shear field of the viscometer for a sufficient period of time, the β_2-integrin subunits lymphocyte function associated antigen-1 (LFA-1) and macrophage antigen-1 (MAC-1) engage their counter-ligands on adjacent neutrophils resulting in the formation of firm aggregates. Blocking L-selectin at a shear rate > 400/s in this system can abolish neutrophil aggregation ***(38)***. However, at lower shear rates it is possible that β_2-integrins may themselves, in the absence of L-selectin, mediate neutrophil aggregation in a selectin independent fashion. Therefore the ability of liposomes/carbohydrates to block selectin mediated adhesion should be studied at moderate or high shear rate, G greater than 400/s. The choice of shear rates for a given experiment depends on the desired objective. Typically, at the higher shear rates the amount of oligosaccharide/liposome required to inhibit neutrophil aggregation is lower.
7. This assay can be adapted to study cell adhesion via P-selectin and E-selectin also, as neutrophils constitutively express the ligands for these selectins. P-selectin-mediated adhesion can be studied by quantifying the rate at which neutrophils heterotypically bind cotransfected cell expressing P-selectin and ICAM-1. Similarly E-selectin mediated adhesion can be studied by quantifying the rate at which neutrophils bind E-selectin/ICAM-1 cotransfectants. The extension of the current methodology to measure heterotypic cell adhesion rates has been described recently ***(47)***.

Acknowledgment

The cone-plate viscometry and flow cytometry was first developed by SN in collaboration with S. I. Simon and A. D. Taylor. This work was supported by grants from the United Engineering Foundation, Whitaker Foundation (S. N.) and NIH (HL63014 (S.N.), CA35329 (K. L. M.), and CA63218 (K. L. M.)).

References

1. Roseman, S. (1970) The synthesis of complex carbohydrates by mltiglycosyltransferase systems and their potential function in intercellular adhesion. *Chem. Phys. Lipids* **5,** 270–297.
2. Sharon, N. and Lis., H. (1993) Carbohydrates in cell recognition. *Sci. Am.* **82,** 89.
3. Kemler, R. (1992) Introduction: cell adhesion. *Semin. Cell Biol.* **3,** 147–148.
4. Drikamer, K. (1988) Two distinct classes of carbohydrate-recognition domains in animal lectin. *J. Biol. Chem.* **263,** 9557–9560.
5. Marx, J. L. (1989) A new family of adhesion proteins discovered. *Science* **243,** 1144.
6. Kishimoto, T. K. (1991) A dynamic model for neutrophil localization to inflammatory sites. *J. NIH Res.* **3,** 75–77.
7. Springer, T. A. (1995) Traffic signals on endothelium for lymphocyte recirculation and leukocyte emigration. *Annu. Rev. Physiol.* **57,** 827–872.
8. Varki, A. (1997) Selectin ligands: Will the real ones please stand up? *J. Clin. Investi.* **99,** 158–162.
9. Rosen, S. D., and Bertozzi, C. R. (1994) The selectins and their ligands. *Cur. Opin. in Cell Biol.* **6,** 663–673.
10. Vestweber, D. and Blanks, J. E. (1999) Mechanisms that regulate the function of the selectins and their ligands. *Physiol. Rev.* **79,** 181–213.
11. Phillips, M. L., Nudelman, E., Gaeta, F. C. A., Perez, M., Singhal, A. K., Hakomori, S. I. and Paulson, J. C. (1990) ELAM-1 mediates cell adhesion by recognition of a carbohydrate ligand, sialyl-Lex. *Science* **250,** 1130–1132.
12. Walz, G., Aruffo, A., Kolanus, W. , Bevilacqua, M. and Seed, B. (1990) Recognition by ELAM-1 of the sialyl-Lex determinant on myeloid and tumor cells. *Science* **250,** 1132–1135.
13. Lowe, J. B., Stoolman, L. M., Nair, R. P., Larsen, R. D., Berhend, T. L. and Marks, R. M. (1990) ELAM-1-dependent cell adhesion to vascular endothelium determined by a transfected human fucosyltransferase cDNA. *Cell* **63,** 475–484.
14. Simanek, E. E., McGarvey, G. J., Jablonwski, J. A. and Wong, C.-H. (1998) Selectin–carbohydrate interactions: from natural ligands to designed mimics. *Chem. Rev.* **98,** 833–862.
15. Thiagarajan, R. R., Winn, R. K. and Harlan, J. M. (1997) The role of leukocyte and endothelial adhesion molecules in ischemia-reperfusion injury. *Thromb. Haemostas.* **78,** 310–314.

16. Meyer, T., and Hart, I. R. (1998) Mechanisms of tumor metastasis. *Eur. J. Cancer* **97,** 214–221.
17. Malhotra, R., Priest, R. and Bird, M. I. (1996) Role for L-selectin in lipopolysaccharide-induced activation of neutrophils. *Biochem. J.* **320,** 589–593.
18. Schachter, H. (1986) Biosynthetic controls that determine the branching and microheterogeneity of protein-bound oligosaccharides. *Biochem. Cell Biol.* **64,** 163–181.
19. Varki, A., and Marth, J. (1995) Oligosaccharides in vertebrate development. *Semin. Dev. Biol.* **6,** 127–138.
20. Matta, K. L. (1996) Synthetic glycosyltransferase acceptors and inhibitors; useful tools in glycobiology, in *Modern Methods in Carbohydrate Synthesis* (Khan, S. H. and O'Neill, R. A., eds.) Perkin Elmer, Harwood Academic Publishers, New York, pp. 437–466.
21. Reuter, G., and Gabius, H. J. (1999) Eukaryotic glycosylation: whim of nature or multipurpose tool? (Review). *Cell. Mol. Life Sci.* **55,** 368–422.
22. Wilkins, P. P., McEver, R. P. and Cummings, R. D. (1996) Structures of the *O*-glycans on P-selectin glycoprotein ligand-1 from HL-60 cells. *J. Biol. Chem.* **271,** 18732–18742.
23. McEver, R. P. and Cummings, R. D. (1997) Role of PSGL-1 binding to selectins in leukocyte recruitment. *J. Clin. Invest.* **100,** 485–492.
24. Hemmerich, S., Leffler, H. and Rosen, S. D. (1995) Structure of the *O*-glycans in GlyCAM-1, an endothelial-derived ligand for L-selectin. *J. Biol. Chem.* **270,** 12035–12047.
25. Koenig, A., Jain, R., Vig, R., Norgard-Sumnicht, K. E., Matta, K. L. and Varki, A. (1997) Selectin inhibition: synthesis and evaluation of novel sialylated, sulfated and fucosylated oligosaccharides, including the major capping group of GlyCAM-1. *Glycobiology* **7,** 79–93.
26. Jain, R. K., Piskorz, C. F., Huang, B. G., Locke, R. D., Han, H. L., Koenig, A., et al. (1998) Inhibition of L- and P-selectin by a rationally synthesized novel core 2-like branched structure containing GalNAc-Lewisx and Neu5Acalpha2-3Galbeta1-3GalNAc sequences. *Glycobiology* **8,** 707–717.
27. Grinnell, W. B., Hermann, R. B., and Yan, S. B. (1994) Human protein C inhibits selectin-mediated cell adhesion: role of unique fucosylated oligosaccharide. *Glycobiology* **4,** 221–225.
28. Thomas, V. H., Elhalabi, J., and Rice, K. G. (1998) Enzymatic of *N*-linked oligosaccharides terminating in multiple sialyl-Lewisx and GalNAc-Lewisx determinants: clustered glycosides for studying selectin interactions. *Carbohydr. Res.* **306,** 387–400.
29. Ellies, L. G., Tsuboi, S., Petryniak, B., Lowe, J. B., Fukuda, M., and Marth, J. D. (1998) The function of core 2 *O*-glycans in selectin ligand formation and leukocyte trafficking, in *Glycobiology '98, 3rd Annual Conference of the Society for Glycobiology*, Baltimore, MD. Abstract 49.

30. Thomas, V. H., Yang, Y., and Rice, K. G. (1999) *In vivo* ligand specificity of E-selectin binding to multivalent sialyl Lewisx *N*-linked oligosaccharides. *J. Biol. Chem.* **274,** 19035–19040.
31. Renkonen, O., Toppila, S., Penttila, L., Salminen, H., Helin, J., Maaheimo, H., et al. (1997) Synthesis of a new nanomolar sacharide inhibitor of lymphocyte adhesion: different polylactosamine backbones present multiple sialyl Lewis x determinants to L-selectin in high-affinity mode. *Glycobiology* **7,** 453–461.
32. Sprengard, U., Schudok, M., Schmidt, W., Kretzschmar, G., and Kunz, H. (1996) Multiple sialyl Lewisx *N*-glycopeptides: effective ligands for E-selectin. *Angew. Chem. Int. Ed. Engl.* **35,** 321.
33. DeFrees, S. A., Phillips, L, Guo, L., and Zalipsky, S. (1996) Sialyl lewis x liposomes as a multivalent ligand and inhibitor of E-selectin mediated cellular adhesion. *J. Am. Chem. Soc.* **118,** 6101–6104.
34. Stahn, R., Schäfer, H., Kernchen, F., and Schreiber, J.. (1998) Multivalent sialyl Lewis x ligands of definite structures as inhibitors of E-selectin mediated cell adhesion. *Glycobiology* **8,** 311–319.
35. Spevak, W., Foxall, C., Charych, D. H., Dasgupta, F., and Nagy, J. O. (1996) Carbohydrate in an acidic multivalent assembly: Nanomolar P-selectin inhibitors. *J. Med. Chem.* **39,** 1018–1020.
36. Alon, R., Feizi, T., Yuen, C., Fuhlbrigge, R. C., and Springer, T. A. (1995) Glycolipid ligands for selectins support leukocyte tethering and rolling undr physiologic flow conditions. *J. Immunol.* **154,** 5356–5366.
37. Brunk, D. K. and Hammer, D. A. (1997) Quantifying rolling adhesion with a cell-free assay: E-selectin and its carbohydrate ligands. *Biophys. J.* **72,** 2820–2833.
38. Taylor, A. D., Neelamegham, S., Hellums, J. D., Smith, C. W., and Simon, S. I. (1996) Molecular dynamics of the transition from L-selectin- to beta 2-integrin-dependent neutrophil adhesion under defined hydrodynamic shear. *Biophys. J.* **71,** 3488–3500.
39. Finger, E. B., Puri, K., Alon, R., Lawrence, M. B., von Andrian, U. H., and Springer, T. A. (1996) Adhesion through L-selectin requires a threshold hydrodynamic shear. *Nature* **379,** 266–269.
40. Alon, R., Chen, S., Puri, K. D., Finger, E. B., and Springer, T. A. (1997) The kinetics of L-selectin tethers and the mechanics of selectin-mediated rolling. *J. Cell Biol.* **138,** 1169–1180.
41. Sanders, W. J., Gordon, E. J., Dwir, O., Beck, P. J., Alon, R., and Kiessling, L. L. (1999) Inhibition of L-selectin-mediated leukocyte rolling by synthetic glycoprotein mimics. *J. Biol. Chem.* **274,** 5271–5278.
42. Smoluchowski, M. V. (1917) Versuch einer mathematischen theorie der koagulationskinetik kolloider losungen. *Zeitschr. Physik. Chem.* **92,** 129–168.
43. Neelamegham, S., Taylor, A. D., Hellums, J. D., Dembo, M., Smith C. W., and Simon, S. I. (1997) Modeling the reversible kinetics of neutrophil aggregation under hydrodynamic shear. *Biophys. J.* **72,** 1527–1540.
44. Hentzen, E. R., Neelamegham, S., Kansas, G. S., Benanti, J. A., McIntire, L. V., Smith, C. W., and Simon, S. I. (2000) Sequential binding of CD11a/CD18 and

CD11b/CD18 define neutrophil capture and stable adhesion to ICAM-1. *Blood* **95,** 911–920.
45. Shankaran, H., and Neelamegham, S. (2001) Non-linear flow affects hydrodynamic forces and neutrophil adhesion rates in cone-plate viscometers. *Biophys. J.* **80,** 2631–2648.
46. Simon, S. I., Rochon, Y. P., Lynam, E. B., Smith, C. W., Anderson, D. C., and Sklar, L. A. (1993) β2-Integrin and L-selectin are obligatory receptors in neutrophil aggregation. *Blood* **82,** 1097–1106.
47. Neelamegham, S., Taylor, A. D., Burns, A. B., Smith, C. W., and Simon, S. I. (1998) Hydrodynamics shear reveals distinct roles for LFA-1 and Mac-1 in neutrophil adhesion to ICAM-1. *Blood* **92,** 1626–1638.

12

Preparation and Characterization of Glycolipid-Bearing Multilamellar and Unilamellar Liposomes

P. R. Satish and A. Surolia

1. Introduction

The carbohydrate residues of glycosphingolipids were implicated in many biologic processes such as cell-to-cell interactions; and as receptors for some viruses, bacterial and plant toxins, hormones, and so forth, and invariably for all the lectins ***(1)***. However, their receptor functions remained poorly defined for a long time as they form micelles even at very low concentrations in aqueous medium. In micelles, the oligosaccharide chains are not expected to have a well defined orientation suitable for recognition by macromolecular ligands. This problem was overcome by incorporating them in model membranes, namely, the liposomes. The demonstration of lectin–glycolipid interaction using liposomal model membranes was a crucial development that established glycolipids as biological receptors. Moreover, glycolipid-bearing liposomes provide a convenient system for investigating the role of glycolipid density, orientation, and exposure of their oligosaccharide chains at the membrane interface relevant to their receptor function ***(2–4)***.

Although the methods for preparing liposomes are well described and have been extensively and lucidly dealt with elsewhere ***(5–8)***, the preparation of glycosphingolipid-bearing liposomes, and especially their characterization in practice, entails several subtle modifications to these procedures ***(9)***. The following description allows for a reproducible preparation of glycosphingolipid-containing liposomes with well defined properties.

From: *Methods in Molecular Biology, vol. 199: Liposome Methods and Protocols*
Edited by: S. Basu and M. Basu © Humana Press Inc., Totowa, NJ

2. Materials (*See* Note 1)

1. Egg yolk lecithin, synthetic phospholipids such as dipalmitoyl phosphatidylcholine or dimirystoyl phosphatidylcholine, cholesterol, purified glycosphingosipids such as GM_1, GD_{1a}, lactosyl ceramide, ceramide trihexoside, lactotetrosyl ceramide, and galactocerebroside are all available from Biocarb.
2. *Vibrio cholerae* neuraminidase, castor bean agglutinnin, octyl glucoside, sodium deoxycholate, Sepharose 4B, Tris, and so forth, are available from Sigma Chemical Co. (USA).
3. Other chemicals such as 1-amino-2-naphthol-4-sulfonic acid, sodium bisulfite, ammonium molybdate, sodium and potassium phosphate (both monohydrogen and dihydrogen), sodium chloride, calcium chloride, and solvents such as chloroform, methanol, ethanol, acetic acid, and so forth, should be of analytical grade.

3. Methods

In this section, we describe the preparation of liposomes and their subsequent characterization. Currently, several methods for the preparation of both the multilamellar and unilamellar liposomes bearing glycosphingolipids are in use in our laboratory. They are presented as described in the following subheadings.

3.1. Preparation of Multilamellar Liposomes (See Notes 2–4*)*

1. A desired molar ratio of glycolipid and phospholipid is dissolved in a suitable volume of 2:1 (v/v) chloroform–methanol and evaporated in a round-bottom flask (RBF) under reduced pressure in a rotory flash evaporator so that a thin film of the lipids is deposited on the inner wall of the RBF. Once the lipid is completely evaporated, the RBF is transferred into a vacuum desiccator and allowed to stand for 4–10 h. (*See* **Notes 5–7**.)
2. An appropriate volume of the buffer of choice (any buffer can be chosen from a compendium of buffers, such as phosphate-buffered saline (PBS), Tris-buffered saline, or Tris-HCl, etc.) is added to the flask so the amount of the total lipid per milliliter of the buffer does not exceed 2% by weight. (*See* **Note 8**.)
3. A few glass beads are introduced into the RBF and it is then vortex-mixed for 15 min or longer so that the lipid film adsorbed onto the RBF surface is easily dislodged.
4. The sample in the RBF is flushed with nitrogen during vortex-mixing if phospholipids containing unsaturated fatty acids are used in the preparation of the liposomes.
5. The contents of the RBF are then transferred into a beaker and a short pulse (5 s) of sonication using a probe sonicator is given. The resultant suspension is centrifuged at 1000 rpm for 10 min to facilitate the removal of any particulate material. The milky suspension in the supernatant essentially consists of a multilamellar liposomal preparation. (*See* **Note 9**.)

3.2. Preparation of the Unilamellar Vesicles

Four different methods for preparation of unilamellar vesicles are described in the following subheadings, plus one modification method.

3.2.1. The Sonication Method

1. The multilamellar liposome preparation obtained as described previously is sonicated for 15 min in a probe sonicator until the suspension is almost clear with a light bluish tinge. Alternatively, the suspension can be put in a bath sonicator again, until the suspension is nearly clear with a light bluish tinge.
2. The liposome prepared by probe sonication requires an additional centrifugation (5000*g*, 30 min) step to remove titanium particles.
3. The unilamellar liposome preparation should now be centrifuged at 105,000*g* for 1 h at 4°C to remove any large multilamellar liposomal fraction.
4. The supernatant from the above centrifugation is then collected and passed through a column of Sepharose 4B (2 cm × 40 cm, at a flow rate of 20 mL/h). Typically, 2–4 mL of the supernatant obtained after the high-speed centrifugation is loaded. Usually the column is equilibrated and eluted with PBS, and the elution of liposomes is monitored by light scattering at 330 nm.
5. The sonicated liposomes generally elute in two major fractions, one of which comes in the void volume (35% of the bed volume, ~42 mL in this case). The fraction coming in the void volume is mostly made up of multilamellar vesicles. It elutes, as expected, as a sharp peak. The unilamellar liposome preparation on the other hand comes in the inner volume of the column and in general elutes as a broad peak.

3.2.2. Extrusion Method

In this method, the multilamellar liposomal suspension is extruded through a porous polycarbonate membrane held between two gas tight syringes, which are used to force the solution back and forth.

It is possible to obtain the liposomes of defined size by using polycarbonate membranes of defined pore sizes. The commercial version of this device is also available (Sigma Chemical Co.), and the back and forth extrusion of liposomes through the porous membrane prevents the clogging of the membrane. In this method, the liposomes are actually forced back and forth 19 times.

It is also possible to make unilamellar liposomes by using a porous polycarbonate membrane and a single gas tight syringe. The multilamellar liposome suspension is taken in the gas tight syringe and forced through the polycarbonate filter into a suitable container. The syringe is then disconnected from the filter.

The once-filtered solution is collected into the syringe, and the filter is inverted and fitted back onto the syringe (i.e., in an opposite direction with respect to the initial orientation). The solution in the syringe is then forced through the filter.

The cycle of steps from the passage of the multilamellar liposome suspension through the polycarbonate filter using a single gas tight syringe and the inversion of the filter with respect to the initial orientation is repeated 10 times.

3.2.3. Rapid Dilution of Solvent by Aqueous Phase Method (See **Notes 10** *and* **11***)*

1. The glycosphingolipid–phospholipid mixture (10 µmol each) is dissolved in 1 mL of ethanol.
2. The ethanol-solubilized glycosphingolipid–phospholipid mixture is then rapidly injected into 20 mL of PBS, pH 7.4, through a syringe.
3. The suspension is then concentrated to 1–2 mL using an XM-100A membrane (Amicon ultrafiltration device) by using nitrogen at a pressure of 10 lb/in^2.

3.2.4. Detergent-Dialysis Method (See **Note 12***)*

1. Octyl glucoside from a stock solution of 400 m*M* is added to multilamellar vesicles prepared as described in **Subheading 3.1.** The solution is gently and continuously mixed until it is very clear.
2. After clarification of the sample, it is held at 25°C for 30 min.
3. Alternatively, when unilamellar liposomes of smaller dimensions are required, sodium cholate from a stock solution of 200 m*M* is used in the place of octyl glucoside.
4. The lipid–detergent mixture is transferred into a dialysis bag (Spectrapore ~12,000 Da cutoff). A thick-walled tubing is advisable so the equilibrium with the solvent occurs at a slower rate. Dialysis of the sample is carried out by placing the dialysis bag in 50 volumes of buffer for 6 h.
5. After two more changes of 500 volumes of fresh buffer, once in 6 h and once at the end of dialysis, the vesicles can be collected from the dialysis bag.

3.2.5. Improved Detergent-Dialysis Method (See **Note 13***)*

1. An improved version of the detergent-dialysis method is called the defined dialysis of lipid/detergent mixed micelles ***(9)***. In this method, the dried lipid film obtained (as mentioned previously) from the methanolic/ethanolic solutions is dispersed in appropriate buffer and subsequently mixed with variable amounts of detergent to obtain lipid/detergent molar ratios in the range of 0.2–1.15.
2. The mixture is then gently stirred at room temperature for 12 h.
3. This preparation (6 mL) is then introduced into the middle cell (of a triple-cell dialyzer) that is in contact with two cellulose membranes of high permeability (~10,000 Da cutoff). Each of these cellulose membranes separates the middle cell (MC) from a flow-through cell (FC) containing the buffer of choice. The diffusion of detergent from MC to FC is facilitated by having the FC contents continually stirred against the high permeability cellulose membranes by a stirrer set at 100 rpm.

4. Simultaneously, the contents of FC are subjected to continuous draining at a flow rate of 0.3–3.0 mL/min for 22 h. (*See* **Note 14**.)
5. After the designated period, the formed liposomes are taken out from the middle cell and are used for further experiments.

3.3. Characterization of the Liposomes

Some of the important parameters for characterizing the liposomes prepared as described earlier are:

1. The size of the liposomes.
2. The ratio of the glycosphingolipids and the phospholipids incorporated into the liposomes.
3. The amount of the glycosphingolipids exposed (expressed) on the liposome surface.

Each is discussed in detail below.

3.3.1. Determination of Size of the Liposomes

1. The size of the liposomes can be determined using a gel filtration column in which latex beads of defined diameter are used as standards. A standard curve of the elution profile of latex beads of average diameters of 0.1, 0.3, 0.4, 0.6, 0.8, 1.1, and 3.0 μm (Sigma Chemical Co., USA) loaded onto a Sepharose 4B column is constructed.
2. The indicated column is equilibrated and eluted with PBS. The elution of the latex beads is monitored by light scattering at 330 nm. The sizes of the liposomes prepared using various methods are determined by their position in the elution profile.
3. Based on these experiments the average diameter of the liposomes prepared using sonication is found to be in the range of 220–260 Å. On the other hand, the solvent dilution in buffer yields liposomes that generally have a diameter of 250–280 Å. Liposomes prepared using detergent dialysis method have an average diameter of 560–630 Å when octyl glucoside is used, and an average diameter of 270–330 Å when sodium cholate is used. The defined dialysis of lipid/detergent mixed micelles method yields liposomes in the range of 600–1600 Å.
4. The size of the liposomes can also be measured by using the calculations of turbidity that employ the expression of Kerker ***(10)*** for hollow spheres.

   The molar absorbance (turbidity per mole of lipid, denoted below as ϵ) of a dispersion of vesicles of a given composition increases linearly with the hydrodynamic radius (R_h) of the vesicles. The value of ϵ is, therefore, a measure of the vesicle size.

   For vesicles made of phosphatidylcholine and cholate, R_h in angstroms can be estimated from the empirical relationship

$$R_h = 8.33\ \epsilon_{450} + 64 \quad (1)$$

or

$$R_h = 2.63\ \epsilon_{330} + 45 \quad (2)$$

for molar absorbance measured at 450 and 330 nm, respectively ***(11)***.

3.3.2. Determination of Glycosphingolipid-to-Phospholipid Ratio

The glycosphingolipid/phospholipid ratio can be determined by estimating the neutral sugar ***(12)*** and total phosphorus ***(13)***. Gangliosides are quantitated at much higher sensitivity by using Warren's method of the thiobarbituric acid assay of sialic acids ***(14)***.

3.3.2.1. Dubois Method for Estimating the Neutral Sugar ***(12)***

1. Phenol, 80% (w/v), is prepared by adding 20 g of glass-distilled water to 80 g of redistilled reagent grade phenol. This mixture forms a water-white liquid that is readily pipetted.
2. Sugar solution (2.0 mL) containing between 10 and 70 µg of sugar is pipetted into a colorimetric tube, and 0.05 mL of 80% phenol is added to each of the tubes.
3. Chilled concentrated sulfuric acid (specific gravity 1.84, reagent grade, 95.5% purity, 5.0 mL volume) is added rapidly into each tube, the stream of acid being directed against the liquid surface rather than against the side of the test tube to obtain good mixing. The tubes are allowed to stand for 10 min.
4. The tubes are then shaken and placed for 20 min in a water bath at 30°C, and the absorbance at 490 nm of the characteristic yellow-orange color is measured against a suitable blank. The amount of sugar is then determined by reference to the standard curve previously constructed, using a known amount of sugars. All solutions are prepared in triplicate to minimize errors.

3.3.2.2. Bartlett's Procedure for Total Phosphorus Analysis ***(13)***

1. Purified 1-amino-2-naphthol-4-sulfonic acid (0.5 g) is added with continuous mechanical stirring to 200 mL of freshly prepared 15% sodium bisulfite (anhydrous), followed by 1.0 g of sodium sulfite. The solution, called the Fiske–SubbaRow reagent ***(13)***, is filtered, stored in a dark bottle, and prepared fresh weekly.
2. Each of the samples (2.0 mL volume) to be analyzed is taken in 12-mL conical centrifuge tubes and 0.5 mL of 10 *N* H_2SO_4 is added to each. The tubes are then placed in an oven and heated at 150–160°C for 3 h.
3. The tubes are removed from the oven, and two drops (amounting to ~ 100 µL) of 30% phosphorus-free hydrogen peroxide are added, and the tubes subsequently returned to the oven. A further 1.5 h heat treatment at 150–160°C completes the combustion and decomposes all the peroxide.
4. The tubes are taken out, 4.6 mL of 0.22% ammonium molybdate and 0.2 mL of Fiske–SubbaRow reagent are added and mixed thoroughly. The tubes are then heated for 7 min in a boiling water bath. The optical density of 1-cm pathlength of the samples at 830 nm is recorded against a suitable blank. The amount of

total phosphorus is then determined by reference to the standard curve previously constructed. All solutions are prepared in triplicate to minimize errors.

3.3.2.3. Warren's Thiobarbituric Acid Assay Method for Estimation of Sialic Acids ***(14)***

The following solutions were used for the procedure in its final form: 0.2 *M* sodium periodate (meta) in 9.0 *M* phosphoric acid; 10% sodium arsenite in a solution of 0.5 *M* sodium sulfate and 0.1 *N* H_2SO_4; and 0.6% thiobarbituric acid in 0.5 *M* sodium sulfate. All these solutions were prepared with warming, stored at room temperature, and were stable for more than a month.

1. Periodate solution (0.1 mL) is added to a sample containing up to 0.05 μmol of *N*-acetylneuraminic acid in a volume of 0.2 mL. The tubes are shaken and allowed to stand at room temperature for 20 min.
2. Arsenite solution (1.0 mL) is then added to each of the tubes and the tubes are shaken until the yellow-brown color disappears.
3. Thiobarbituric acid solution (3.0 mL) is added to each tube, and the tubes are shaken, capped with glass beads, and heated in a vigorously boiling water bath for 15 min. The tubes are then removed from the boiling water bath and placed in cold water for 5 min. During cooling, the red color fades and the solution often becomes cloudy, but this does not affect the final reading.
4. After cooling, 1.0 mL of the contents from any one or all of the triplicates is transferred to different tube(s) containing 1.0 mL of cyclohexanone for organic extraction. If desired, the entire 4.3 mL of aqueous solution can be extracted with 4.3 mL of cyclohexanone.
5. Subsequently, the tubes are shaken twice and centrifuged for 3 min in a clinical centrifuge. The clear upper cyclohexanone phase is red, the color being more intense than when in water. The optical density of the organic phase is determined at 549 nm using cuvettes with a capacity of 0.6 mL and a 1.0-cm long light path. The procedure is also carried out in 0.2 mL of water for the blank vessel, and readings are made against this solution. Color production varies linearly with concentration of *N*-acetylneuraminic acid over the range usually used, 0.01–0.06 μmol. The molecular extinction is 57,000. The amount of *N*-acetylneuraminic acid (NANA) present in a given sample is determined from the following equation:

$$\mu M \text{ NANA} = V \times A_{549} / 57 = 4.3 \times A_{549} / 57 = 0.075 \times A_{549} \quad (3)$$

where *V* is the final volume of the test solution.
All solutions are prepared in triplicate to minimize errors.

3.3.3. Estimation of the Glycosphingolipids Present on the Liposome Surfaces

The amount of incorporated glycosphingolipids present at the surface of these liposomes is usually determined by treating the liposomes with neuraminidase.

1. The typical reaction mixture consists of liposomes containing 30 nmol of glycosphingolipid, 2.5 U of *Vibrio cholerae* neuraminidase, 0.9% (w/v) NaCl, 0.1% (w/v) $CaCl_2$ in 0.1 m*M* sodium acetate buffer, pH 5.5, in a final reaction volume of 0.5 mL at 28°C. (*See* **Note 15**.)
2. Aliquots are drawn out at the end of 5, 15, and 30 min and 1 h, after the commencement of the reaction by addition of the enzyme. The liberated NANA in these aliquots is then estimated according to the method of Warren ***(14)*** as explained previously.
3. The percentage of total glycosphingolipids available to neuraminidase at the liposomal surface is computed from the amount of NANA released from these liposomes.
4. Alternatively, the amount of *Ricinus communis* Agglutinin-1 (RCA_1) bound per μmol of glycosphingolipids such as GM_1, asialo GM_1, triosyl ceramide, by taking into account the saturation value of RCA_1 binding to these glycosphingolipids and considering RCA_1 as bivalent, is calculated.
5. The amount of phospholipid per liposome is calculated by considering the molecular weight of the liposomes (see the following example) which is a known quantity, whereas the area occupied by one micromole of phospholipid is obtained by considering another known quantity, namely the diameter of the liposome.

   From the preceding data, the number of RCA_1 binding sites per square micrometer of the liposomal surface is obtained. For example, for a unilamellar liposome whose molecular mass and diameter are respectively 2000 kDa and 300 Å, and whose composition is 10 μmol/mL of dimirystoyl lecithin and 0.185 μmol/mL of GM_1, the glycosphingolipid to phospholipid ratio is 1:55, the amount of RCA_1 bound is found to be 635.0 μg/μmol of dimirystoyl lecithin, the percentage of GM_1 available for RCA_1 binding is 56–63%, and the value of RCA_1 binding sites/μm^2 is 4.1×10^3. (*See* **Notes 16** and **17**.)

4. Notes

1. Generally, dimirystoyl phosphatidylcholine is preferred to dipalmitoyl phosphatidylcholine while preparing the liposomes, as the latter exhibit a tendency to aggregate upon keeping, within several hours (*see* **Subheading 2.**).
2. Care should be taken so that the concentration of glycosphingolipids under any circumstance does not exceed 25 mol%, because at such concentrations, the glycosphingolipids exhibit a tendency to form nonbilayer structures and destabilize the liposomes (*see* **Subheading 3.1.**).
3. About 93% of the phospholipid and 95% of the glycosphingolipid become incorporated into the liposomes (*see* **Subheading 3.1.**).
4. When the aim of the preparation of multilamellar liposomes is to incorporate a water-soluble drug or protein, then the so desired drug or protein is dissolved in the buffer as mentioned in **Subheading 3.1., step 2**, and subsequent steps are carried out accordingly.
5. When phospholipids containing unsaturated fatty acids are used for the preparation of the liposomes, it is essential to flush the sample with nitrogen during

hydration and subsequent procedures, especially sonication, to prevent oxidation of the fatty acid chains.

6. For preparations with phospholipids containing the unsaturated fatty acids, it is advisable to determine the extent of oxidation by monitoring the ratio of absorbance at 233 nm and absorbance at 215 nm ***(15)***.
7. When the aim of the preparation of multilamellar liposomes is to incorporate a water-insoluble molecule, such molecule is added to the organic solvents along with the lipids as mentioned in **Subheading 3.1., step 1**, and subsequent steps are carried out accordingly.
8. When a buffer is chosen as the medium for dispersal of chloroform–methanol solubilized and dried lipids, facts about subsequent experiments should be borne in mind. For example, if some experiments involving calcium are planned for the liposomes bearing the glycosphingolipids, then the phosphate buffer or the PBS are to be scrupulously avoided since, later, calcium phosphate precipitation would interfere with the monitoring of light scattering at 330 nm.
9. Both the unilamellar and the multilamellar liposomes can be stored at 4°C in the presence of 1% (w/v) sodium azide, without losing their properties up to a period of 1 wk.
10. The solvent dilution in aqueous medium method of preparation of liposomes imparts the limitation that only those glycosphingolipids that are ethanol soluble can be used to prepare the liposomes.
11. Some amount of ethanol always remains in the liposomes when prepared using the solvent dilution in aqueous medium method.
12. Liposomes prepared using detergent dialysis retain small amounts of the detergent in the bilayer.
13. In the early stages of the defined dialysis of lipid/detergent mixed micelles method for the preparation of liposomes, transformation of the micelles into homogeneous bilayer liposomes takes place. This transformation is characterized by an intermediate state in which mixed micelles and liposomes are at equilibrium, which in turn is a function of the rate of removal of the detergent. Thus, constant kinetics of detergent removal is essential to prevent the formation of heterogenous liposomal systems. Rigorous control of conditions as described earlier for detergent removal is therefore of primary importance.
14. The rate at which detergent is removed by dialysis influences the vesicle size. For example, a 500% decrease of the rate at which the detergent is removed leads to an increase of the mean vesicle radius of about 40% over the initial value.
15. Estimation of the extent of the exposure of GM_1 ganglioside with the *V. cholerae* neuraminidase is not possible as this enzyme does not hydrolyze the GM_1 ganglioside. Exposure of neutral glycosphingolipids can be monitored using the specific lectin-binding assays, as has been described with RCA_1 for the GM_1 ganglioside-containing liposomes.
16. By incorporating glycosphingolipids that contain oligosaccharides of different chain lengths, that is, lactotetrosyl ceramide, trihexosyl ceramide, lactosyl ceramide, and galactocerebroside, it should be possible to study the effect of

the distance of the terminal sugar from the bilayer interface on the receptor properties of such glycosphingolipids using binding studies with an appropriate lectin such as RCA_1 ***(4)***.

17. Likewise, the effect of incorporation of cholesterol on the receptor properties of glycosphingolipid incorporated in the liposome can be studied.

References

1. Sharon, N. and Lis, H. (1972) Lectins: cell-agglutinating and sugar-specific proteins. *Science* **177,** 949–959.
2. Surolia, A., Bachhawat, B. K., and Podder, S. K. (1975) Interaction between lectin from *Ricinus communis* and liposome containing gangliosides. *Nature* **257,** 802–804
3. Ketis, N. V. and Grant, C. W. M. (1982) Co-operative binding of concanavalin A to a glycoprotein in lipid bilaters. *Biochim. Biophys. Acta* **689,** 194–197.
4. Surolia, A. and Bachhawat, B. K. (1978) The effect of lipid composition on liposome–lectin interaction. *Biochem. Biophys. Res. Commun.* **83,** 779–785.
5. Huang, C. H. (1969) Studies on phosphatidylcholine vesicles. Formation and physical characteristics. *Biochemistry* **8,** 344–352.
6. Johnson, S. M., Bangham, A. D., Hill, M. W., and Korn, E. D. (1971) Single bilayer liposomes. *Biochim. Biophys. Acta* **233,** 820–826.
7. Batzri, S. and Korn, E. D. (1973) Single bilayer liposomes prepared without sonication. *Biochim. Biophys. Acta* **298,** 1015–1019.
8. MacDonald, R. C., MacDonald, R. I., Menco, B. Ph.M., Takeshita, K., Subbarao, N. K., and Hu, L. R. (1991) Small-volume extrusion apparatus for preparation of large, unilamellar vesicles. *Biochim. Biophys. Acta* **1061,** 297–303.
9. Zumbuehl, O. and Weder, H. G. (1981) Liposomes of controllable size in the range of 40 to 180 nm by defined dialysis of lipid/detergent mixed micelles. *Biochim. Biophys. Acta* **640,** 252–262.
10. Kerker, M. (1969) Hollow spheres: turbidity measurements; scattering by a sphere. In: *The Scattering of Light and Other Electromagnetic Radiation*, Academic Press, New York, pp. 27–90, 411.
11. Almog, S., Kushnir, T., Nir, S., and Lichtenberg, D. (1986) Kinetic and structural aspects of reconstitution of phosphatidylcholine vesicles by dilution of phosphatidylcholine-sodium cholate mixed micelles. *Biochemistry* **25,** 2597–2605.
12. Dubois, M., Gilles, K. A., Hamilton, J. K., Rebers, P. R., and Smith, F. (1956) Colorimetric method for determination of sugars and related substances. *Analyt. Chem.* **28,** 350–356.
13. Bartlett, G. R. (1959) Phosphorus assay in column chromatography. *J. Biol. Chem.* **234,** 466–468.
14. Warren, L. (1959) The thiobarbituric acid assay of sialic acids. *J. Biol. Chem.* **234,** 1971–1975.
15. Klein, R. A. (1970) The detection of oxidation in liposome preparations. *Biochim. Biophys. Acta* **210,** 486–489.

13

Use of Liposomes Containing Carbohydrates for Production of Monoclonal Antibodies

Reiji Kannagi

1. Introduction

Monoclonal anticarbohydrate antibodies have been widely utilized for the study of expression, distribution, and function of carbohydrate determinants on a variety of cells and tissues **(Table 1)** ***(1)***. Functional analysis of glycolipids and glycoproteins has been greatly facilitated by the application of monoclonal antibodies. Monoclonal anticarbohydrate antibodies have been also utilized for expression cloning of glycosyltransferases and related genes ***(2,3)***.

A recently developed field for the application of anticarbohydrate monoclonal antibodies is the study of cell adhesion, which was not covered in our earlier review ***(1)***. Selectins, the family of cell adhesion molecules that have a C-type lectin domain at the outer terminus of each molecule, have been shown to recognize sialyl Lewis x (Le^x) ***(4–6)*** and sialyl Lewis a (Le^a) ***(7–9)*** as specific carbohydrate ligands. The cell adhesion mediated by E- or P-selectin and these carbohydrate determinants has been proposed to be implicated in the recruitment of leukocytes in inflammation ***(10,11)***, hematogenous metastasis of cancer cells ***(7,9,12)***, and tissue infiltration of leukemic cells ***(13,14)***. More recently, sialyl 6-sulfo-Le^x was identified as an L-selectin ligand on high endothelial venules of human lymph nodes ***(15–18)***. The binding of L-selectin and sialyl 6-sulfo-Le^x is involved in the homing of lymphocytes to peripheral lymph nodes. Monoclonal anti-carbohydrate antibodies were utilized as very effective tools during the course of these studies.

Another recently developing area is the study of subtle intramolecular modifications of carbohydrate determinants. A classical example of this is cancer-associated *O*-acetylation of sialic acid in human melanoma cells.

From: *Methods in Molecular Biology, vol. 199: Liposome Methods and Protocols*
Edited by: S. Basu and M. Basu © Humana Press Inc., Totowa, NJ

Table 1
Applications of Anticarbohydrate Antibodies in Cell Biology, Biochemistry, and Medicine

1. Study of expression and distribution of carbohydrate determinant in various cells and tissues, including semiquantitative analysis by immunoassay and flow cytometry.
   (i) Analysis of glycoproteins by Western blot and/or immunoprecipitation.
   (ii) Analysis of glycolipid pattern by TLC-immunostaining.
   (iii) Structural analysis of carbohydrate determination by a combination of multiple monoclonal antibodies and enzymatic degradation.
2. Separation of specific glycoproteins and cell populations.
   (i) Isolation of glycoproteins by affinity chromatography.
   (ii) Separation of a specific type of cells having a specific cell-surface carbohydrate marker by flow cytometric and/or immunomagnetic bead method.
3. Expression cloning of glycosyltransferases
4. Study of function of cell surface carbohydrate determinants such as cell adhesive activity by cell-adhesion inhibition experiments.
5. Clinical applications.
   (i) Diagnosis of cancer using serum levels of cancer-associated carbohydrate markers.
   (ii) Imaging and treatment of cancer using antibodies directed to cancer-associated carbohydrate determinants by targeting of drugs with drug antibody complex.

O-Acetylation of sialic acid moiety is known to affect its binding capacity to the cell adhesion molecules of the sialoadhesin family (Siglecs) ***(19)***. Besides *O*-acetylation, lactone formation, and de-*N*-acetylation of sialic acid moiety are reported to occur in cells and tissues, and some of these changes are proposed to be related to signal transduction phenomena ***(20–27)***. Recently, lactam formation of sialic acid moiety was found to occur by the 12-*O*-tetradecanoylphorbol 13-acetate (TPA) stimulation of cells ***(28,29)***. For these studies, antibodies were generated to discriminate these subtle changes in the sialic acid moiety in the given carbohydrate determinants and were utilized for the detection of these alterations at the cell surface.

1.1. Generation of Anticarbohydrate Antibodies

Carbohydrate antigens in higher animals are carried by two classes of membrane molecules, glycolipids and glycoproteins. Glycolipids, but not glycoproteins, have been favored as immunogen for generation of anticarbohydrate monoclonal antibodies. Carbohydrate antigens carried by glycolipids can be extracted and purified to a single component by established methods. In contrast, carbohydrate antigens carried by glycoproteins are heterogeneous,

and separation of a single determinant is only possible after extensive digestion of the carrier proteins by proteases. Because a single protein carries a number of different determinants, structural information on carbohydrate determinants bound to proteins is much more difficult to elucidate than those on glycolipids. For this reason, structural information on many carbohydrate determinants in membranes is based primarily on those bound to lipids rather than those bound to proteins.

It is not easy to obtain anticarbohydrate antibody using glycoproteins as immunization antigen. When animals are immunized with xenogeneic or allogeneic glycoproteins, they produce antibodies specific to the protein portion, but the carbohydrate moiety is not strongly immunogenic. When animals are immunized with syngeneic glycoproteins, they usually do not produce antibodies to either the protein portion or carbohydrate determinant. A few exceptions include carbohydrate determinants, which are very short and linked directly to the polypeptide core, such as Tn, sialyl Tn, and T determinants in *O*-linked glycans ***(30–32)*** or Fucα1→6GlcNAc sequence in *N*-linked glycans ***(33)***. In contrast, a significant antibody response has long been reported to occur against the carbohydrate portion of glycolipids when animals are immunized with a glycolipid included in a lipid bilayer liposome or cell membrane.

In particular, glycolipids noncovalently adsorbed onto acid-treated *Salmonella minnesota* provided effective immunization in mice against a number of glycolipids. Immunization with liposomes containing lipid A, such as monophosphoryl lipid A (MPL) + trehalose (TDM) emulsion ***(34)***, can be used as an alternative for acid-treated *S. minnesota*. Because both glycolipids and glycoproteins frequently carry the same carbohydrate determinant, the monoclonal antibodies obtained by the immunization of glycolipids are useful for the analysis of glycoproteins as well. Some carbohydrate determinants are specific to glycoproteins and not found in glycolipids. To obtain antibodies specific to such determinants, artificial glycolipids carrying the determinants are organochemically synthesized and sometimes used as immunogens (***16***,***35***; *see* **Note 1**).

1.2. Solid-Phase Radioimmunoassay and Enzymoimmunoassay

Glycolipids or glycoproteins are adsorbed to the plastic surface when an aqueous suspension of these antigens is incubated in a plastic well. Glycolipids can be more efficiently immobilized and form a stable lipid film on a plastic surface when an ethanol solution of glycolipid is added to a plastic well and the ethanol is evaporated. In this method, the plastic well with immobilized glycolipids or glycoproteins is utilized as a solid-phase for detection of the antigen–antibody reaction.

1.3. Thin-Layer Chromatography (TLC)-Immunostaining Using Anticarbohydrate Antibodies

To establish the specificity of the obtained monoclonal antibodies, the 96-well solid-phase immunoassay is sometimes not adequate, especially when the antigen used in the solid-phase immunoassay is a mixture of several carbohydrate determinants. The TLC-immunostaining method *(36)* frequently applied in such cases specifically visualizes the bands of antigenic glycolipids reactive to the antibody on TLC plates.

2. Materials

2.1. Generation of Anticarbohydrate Antibodies

1. Antigens: Ethanol solution of antigen glycolipids (200 µg/ 200 µL).
2. Acid-treated *S. minnesota* (*see* **Note 2**): *S. minnesota* strain R595 (ATCC No.: 49284) obtained by culturing in 2 L of bouillon for 16 h are centrifuged (5000*g*, 20 min), and washed twice with 1% acetic acid. The bacteria are then suspended in 1% acetic acid (1 g/50 mL) and heated at 100°C for 2 h. The acid-treated bacteria are washed with distilled water and lyophilized.

2.2. Solid-Phase Radioimmunoassay and Enzymoimmunoassay

1. Antigens: Glycolipids having relatively short carbohydrate chains (fewer than five sugar residues) can easily be adsorbed to the well without addition of phosphatidylcholine–cholesterol. An ethanol solution of glycolipid (1 µg/mL) can be used. However, glycolipids having relatively long carbohydrate chains, or gangliosides, tend to detach from the wells during washings, and the addition of phosphatidylcholine–cholesterol greatly stabilizes the lipid film. In this case, an ethanol solution of glycolipid (1 µg/mL), phosphatidylcholine (5 µg/mL), and cholesterol (2.5 µg/mL) is used. Glycoprotein antigen solution is prepared at a concentration of 5–25 µg/mL in phosphate-buffered saline (PBS).
2. Antibodies: Culture supernatants of hybridoma are used as first antibody. The second antibody is usually polyclonal antimurine Ig antibody when mice are used for immunization and generation of monoclonal antibody. ^{125}I-labeled protein A solution (5×10^4 cpm/50 µL) is used in a solid-phase radioimmunoassay, and substrate solution for peroxidase (50 mL of 0.05 *M* citrate–0.1 *M* Na_2HPO_4 buffer, pH 5.0, containing 20 mg of *O*-phenylenediamine and 10 µL of 30% H_2O_2) is used in a solid-phase enzymoimmunoassay. The second antibody should be labeled with peroxidase in a solid-phase enzymoimmunoassay.
3. Blocking and washing buffers (*see* **Note 3**): 5% bovine serum albumin (BSA)–PBS, (PBS, pH 7.4, with 5% BSA) is used for blocking, and 0.5% BSA–PBS, (PBS, pH 7.4, with 0.5% BSA) is used for washings.

2.3. TLC-Immunostaining Using Anticarbohydrate Antibodies

1. TLC: HPTLC plate (SiHPF, Baker Chemical Co.) and appropriate solvent system for developing antigenic glycolipids on TLC. Any TLC plates that endure

repeated soakings in PBS can be used, but high-performance (HPTLC) plates are recommended from the standpoint of high resolution.

2. Antigens: Because glycolipids will be separated on TLC in this method, the starting antigen can be a mixture of glycolipids. The sensitivity of this method is very high and eventually < 1 ng of glycolipid antigen can be detected under the best conditions. However, it is recommended to develop two TLC plates, one for immunostaining and the other for chemical coloring reaction, such as orcinol–H_2SO_4 staining, to visualize all glycolipids in the sample; the latter requires material on the order of micrograms.
3. Antibodies: Culture supernatants of hybridoma is used as first antibody. The second antibody is usually polyclonal rabbit antimurine Ig antibody when mice are used for generation of monoclonal antibody. ^{125}I-labeled protein A solution (5×10^6 cpm/25 µL) is used for radioimmunostaining. The second antibody should be labeled with peroxidase in enzymoimmunostaining. ECL Western blotting detection reagents (Amersham Life Science Ltd., Buckinghamshire, UK), originally developed for Western blotting, can be used for TLC-enzymoimmunostaining.
4. Blocking and washing buffers: 5% BSA–PBS (PBS, pH 7.4, with 5% BSA) is used for blocking, and 0.5% BSA–PBS (PBS, pH 7.4, with 0.5% BSA), is used as washing buffer.

3. Methods

3.1. Generation of Anticarbohydrate Antibodies

3.1.1. Coating S. minnesota *with Glycolipids*

Glycolipids are adsorbed to the bacteria according to the procedure described by Galanos et al. ***(37)***. Two milliliters of distilled water is heated to 50°C in a tube, and 30 µg of glycolipid dissolved in ~30 µL of ethanol is injected with a Hamilton syringe. The solution is then vortex mixed. The concentration of ethanol in water should not exceed 5%. Dry powder of acid-treated *S. minnesota* (120 µg) is added to the tube, which is again vortex mixed. The glycolipid/bacteria ratio is usually 1:4 (w/w). The mixture is incubated for 10 min at 50°C, then aliquotted to the desired amount, lyophilized, and stored in a freezer.

3.1.2. Immunization Protocols

The aliquots of lyophilized glycolipid–bacteria complex are resuspended in PBS and injected into mice intravenously or intraperitoneally. The standard immunization schedule is 5 µg of glycolipid on day 0, 10 µg on day 4, 15 µg on day 8, 20 µg on day 12, and 25 µg on d 16. After a rest of at least 2 wk, the mice receive a final booster injection with 25 µg of glycolipid. Three days after the final injection, the spleen cells are harvested and fused with hypoxanthine-

aminopterin-thymidine (HAT)-sensitive mouse myeloma cells. The procedure for generating hybridoma is essentially the same as that described for non-carbohydrate antigens ***(38)***. A solid-phase radioimmunoassay or enzymoimmunoassay as described in the following subheading is used for screening positive hybridoma clones.

3.2. Solid-Phase Radioimmunoassay and Enzymoimmunoassay

3.2.1. Immobilization of the Antigen and Blocking

1. In the assay using glycolipid antigens, 10–20 μL of antigen solution in ethanol as described in **Subheading 2.2.1.** are added to each well of the 96-flat bottom-well assay plates. The amount of antigen will be 10–20 ng per well in the assay with constant antigen concentration. In the assay with variable antigen concentration, the antigen solution is serially diluted with ethanol.
2. The 96-well plates are incubated at room temperature or at 37°C for a few hours to evaporate the ethanol. A glycolipid–phosphatidylcholine–cholesterol film is formed at the bottom of each well. In the assay using glycolipid antigens, 50-μL aliquots of antigen solution in PBS are placed in each well, incubated for 18 h, and washed with PBS.
3. Blocking: To each well, 100 μL of 5% BSA–PBS is added and incubated for 2 h at room temperature to block the nonspecific binding of antibody to the wells. Each well is then washed twice with 0.5% BSA–PBS.

3.2.2. First and Second Antibody Reactions

1. First antibody reaction: An appropriately diluted first antibody solution in 0.5% BSA–PBS is added to each well and incubated at 4°C for 1 h. In the assay with a constant antigen concentration, the antibody is serially diluted over 12 wells. The same concentration of antibody is added to each well receiving a serially diluted antigen. Wells are washed with 0.5% BSA–PBS three times to remove the unreacted antibody.
2. Second antibody reaction: The second antibody solution is added to each well and incubated at 4°C for 1 h, followed by washing three times with 0.5% BSA–PBS. In a solid-phase radioimmunoassay, 50 μL of ^{125}I-labeled protein A solution is added and incubated at 4°C for 45 min. The wells are washed three times with 0.5% BSA–PBS to remove unreacted protein A. The radioactivity in each well is measured with a gamma-scintillation counter. In an enzymoimmunoassay, peroxidase-labeled antibody is used as a second antibody and incubated at 4°C for 1 h. After washing three times with 0.5% BSA–PBS, 50 μL of substrate solution is added and incubated at room temperature for 10 min. The absorbance of each well is determined with an appropriate 96-well plate reader. (*See* **Note 4**).

3.2.3. Examples

Sialyl Lewis x and related determinants have recently attracted special attention since they serve as ligands for well known cell adhesion molecules,

selectins. Monoclonal anti-sialyl Lewis x antibodies are frequently utilized to detect the selectin ligands in cells and tissues, and ensure their binding activity to selectins in cell adhesion inhibition assays. However, sialyl Le^x determinants are acknowledged to be heterogeneous, and the specificity of anti-sialyl Le^x antibodies is not homogeneous. **Figure 1** indicates the results of the specificity of hitherto-known 6 anti-sialyl Le^x antibodies against various molecular species of sialyl Le^x antigens, ascertained by solid-phase enzymoimmunoassay using a panel of synthetic carbohydrate determinants. All anti-sialyl Le^x antibodies significantly reacted with conventional sialyl Le^x as indicated in **Fig. 1a**. All antibodies also reacted with the sialyl Le^x determinant on the GlcNAcβ1→Galβ branch, as well as with the sialyl dimeric Le^x determinant (**Fig. 1b**, **c**). However, these antibodies exhibited various cross-reactivity to other sialyl Le^x-related structures. The antibodies 2F3, HECA-452, and 2H5 significantly cross-reacted with sialyl Le^x, whereas other antibodies did not (**Fig. 1d**). On the other hand, the antibodies SNH-3 and FH-6 were found to be heavily cross-reactive to the VIM-2 ganglioside (**Fig. 1e**).

These findings indicate that these antibodies can be classified into two groups as schematically shown in **Fig. 2** ***(39)***. One group (group A) includes the antibodies CSLEX-1, SNH-3, and FH-6, which recognize the type 2 chain core, Galβ1→GlcNAcβ, and therefore never cross-react with sialyl Le^a having the type 1 chain core, Galβ1→3GlcNAcβ. Among these antibodies, CSLEX-1 seems to be relatively specific to sialyl Lex, while the other two antibodies do not seem to recognize the Fucα moiety strongly, judging from their heavy cross-reactivity against VIM-2 ganglioside. The other group (group B) includes the antibodies 2F3, HECA-452, and 2H5, which do not recognize the type 2 chain core, Galβ1→4GlcNAcβ, while they recognize terminal Fucα as well as NeuAcα moieties and never cross-react to the structure devoid of Fucα moiety on the penultimate GlcNAcβ.

When tested against sialyl 6-sulfo Le^x Lewis x antigen (**Fig. 1f**), only the antibodies belonging to Group B (2F3, HECA-452, 2H5) were reactive, while all antibodies in group A (CSLEX-1, SNH-3, FH-6) were devoid of any activity ***(15,16)***. It is quite natural that the group A antibodies, which strictly recognize the Galβ1→4GlcNAcβ core, were all very sensitive to the modification at the core GlcNAcβ, whereas the reactivity of the group B antibodies that do not recognize the Galβ1→4GlcNAcβ core was not affected by the modification.

These antibodies also showed variable reactivity against the sialyl Le^x determinant carrying *N*-glycolyl sialic acid (NeuGcα). The antibody 2H5 was strongly reactive to the *N*-glycolyl sialyl Le^x. CSLEX-1, SNH-3, and HECA-452 reacted only weakly to the antigen, while 2F3 and FH-6 were virtually nonreactive. These findings should be noted when applying these antibodies to cells and tissues of mice and rats, which are known to express

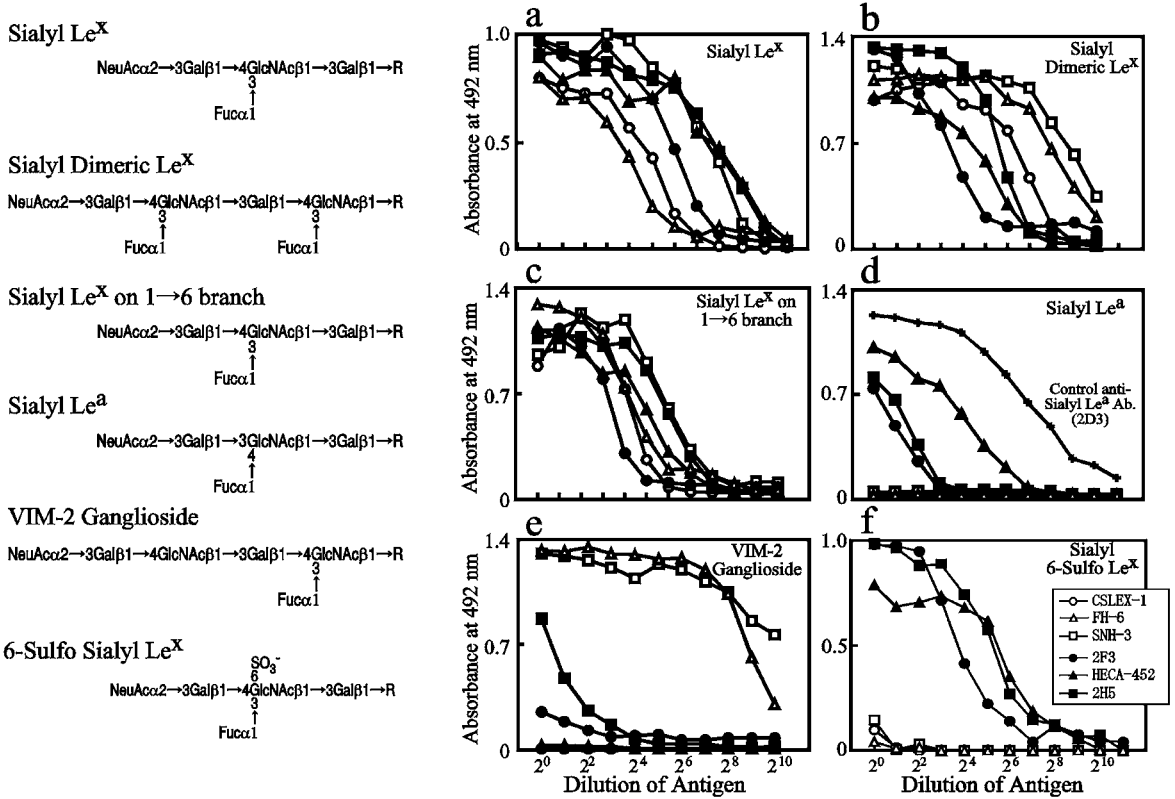

Fig. 1. Specificity of 6 anti-sialyl Lewis x antibodies towards pure carbohydrate determinants as ascertained by solid-phase enzymoimmunoassays.

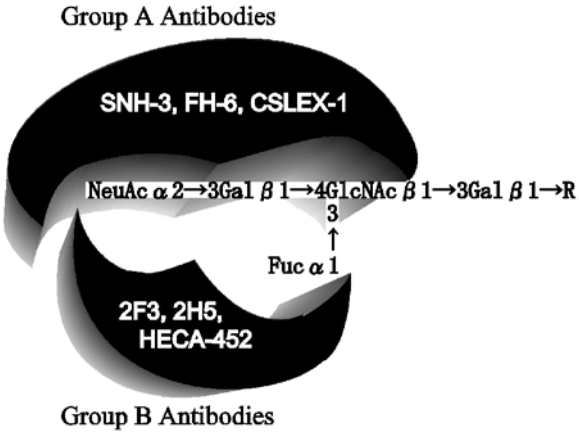

Fig. 2. Schematic illustration of reactivity of two groups of anti-sialyl Lewis x antibodies.

carbohydrate determinants containing *N*-glycolylneuraminic acid. The results indicate that the anti-sialyl Le^x antibodies show different reactivity to an antigen that contains *N*-acetyl or *N*-glycolyl neuraminic acid, eventually limiting the use of some antibodies in animal experiments. **Table 2** summarizes the reactivity of known anti-sialyl Le^x antibodies against sialyl Le^x-related structures.

3.3. TLC-Immunostaining Using Anticarbohydrate Antibodies

3.3.1. TLC and Blocking with BSA Solution

1. The sample glycolipid is first chromatographed on two HPTLC plates (SiHPF, Baker Chemical Co.) with an appropriate solvent.
2. After drying at room temperature, one of the TLC plates is soaked in 5% BSA–PBS in a tissue culture dish of appropriate size for 2 h at room temperature to block nonspecific absorption of antibodies.
3. The TLC plate is soaked and gently washed in 0.5% BSA–PBS with two changes of buffer.

3.3.2. First Antibody Reaction

1. The TLC plate is then soaked in the first antibody solution and incubated for 2 h at 4°C. The plate is then gently washed with 0.5% BSA–PBS with three changes of the buffer.

3.3.3. Second Antibody Reaction and Visualization

1. In radioimmunostaining, the plate is soaked in the second antibody solution, incubated at 4°C for 1 h, and washed with 0.5% BSA–PBS with three changes of the buffer.

Table 2
Summary of Reactivity of Anti-Sialyl Lewis x Antibodies Against Pure Carbohydrate Determinants as Ascertained by Solid-Phase Enzymoimmunoassay

Name of MoAb	Sialyl Le^x	Sialyl Le^x on 1→6 branch	Sialyl dimeric Le^x	Sialyl Le^a	VIM-2 Ganglioside	Sialyl 6-sulfo Le^x	*N*-Glycolyl sialyl Le^x
Group A							
CSLEX-1	++	+	+	–	–	–	+
SNH-3	++	++	++	–	++	–	+
FH-6	++	+	++	–	++	–	–
Group B							
2F3	++	+	+	+	–	++	–
HECA-452	++	++	+	++	–	++	–
2H5	++	++	+	+	±	++	++

2. The plate is soaked in ^{125}I-labeled protein A solution (5×10^6 cpm/25 μL diluted in 25 mL of 0.5% BSA–PBS), incubated at 4°C for 1 h, and washed with 0.5% BSA–PBS with two changes of the buffer, followed by PBS with two changes of the buffer.
3. The TLC plate is allowed to dry at room temperature overnight, and the radioactive spot on the TLC plate is detected by overnight autoradiography of the plate on X-ray film.
4. In enzymoimmunostaining, the plate is soaked in the peroxidase-labeled second antibody solution, incubated at 4°C for 1 h, and washed with 0.5% BSA–PBS in the same way. A positive reaction is visualized using ECL Western blotting detection reagents. The other TLC plate is developed with orcinol–H_2SO_4 or other appropriate chemical reaction, and the mobility of positive bands is compared with those in the immunostained TLC plate.
5. This method has a very high sensitivity, but sometimes cross-reactive glycolipid bands are strongly detected as well as the real antigenic glycolipid (false-positive reaction). It is advisable to prepare several TLC plates and to stain them with serially diluted antibody solutions. It is also recommended to interpret the result of TLC-immunostaining by comparing it with the results of solid-phase enzymoimmunoassay with serially diluted antigens. Fully acetylated glycolipids can be chromatographed first on TLC, and stained by antibodies after deacetylation by soaking the plate in sodium methoxide solution, when a better resolution on TLC is obtained in the acetylated form. Glycolipids chromatographed on TLC are known to be successfully cleaved by soaking the plate in a solution of neuraminidase.

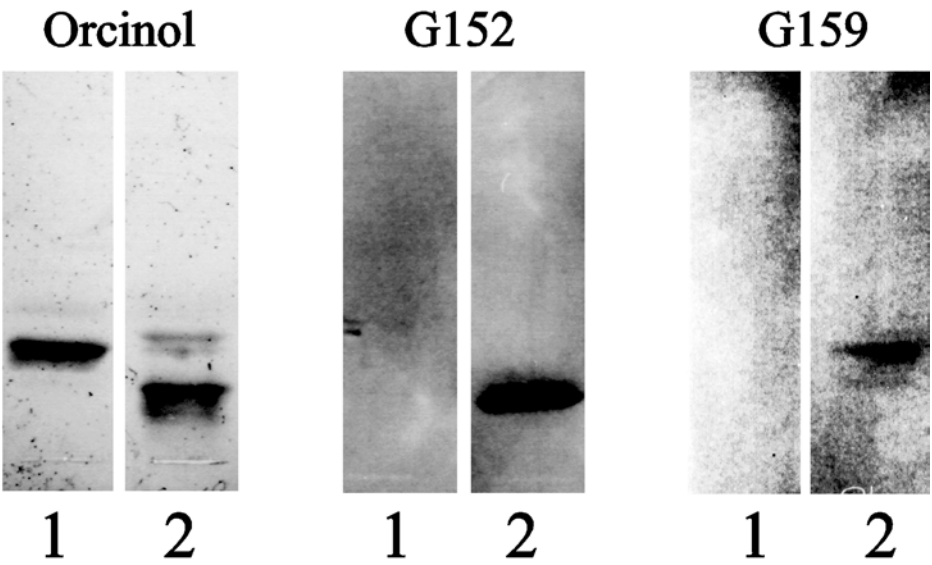

Fig. 3. Reactivity of anti-6-sulfo-sialyl Lewis x antibodies G152 and G159 in TLC-immunostaining. From left, orcinol–H_2SO_4 staining which visualizes all glycolipids; immunostaining patterns of the same TLC plates with the G152 and G159 antibodies. *Lane 1*, genuine sialyl Lewis x serving as a negative control; *lane 2*, synthetic sialyl 6-sulfo-Lewis x, which contains minor impurities.

3.3.4. Examples

When the glycolipid antigen preparation used as the immunogen contains impurities, monoclonal antibodies directed to very minor contaminants are occasionally obtained. For instance, **Fig. 3** indicates the TLC-immunostaining pattern of sialyl 6-sulfo-Le^x glycolipid by the antibody G152 and G159, the two monoclonal antibodies obtained from the same fusion. It is clear from this pattern that the G152 antibody is specific to the original sialyl 6-sulfo-Le^x glycolipid, while the G159 antibody is reactive to a very minor contaminant that has a higher TLC mobility than the authentic sialyl 6-sulfo-Le^x glycolipid. More precisely, the sialyl 6-sulfo-Le^x glycolipid used as an immunogen contained three minor contaminants which migrated faster than the authentic substance, and the G159 antibody was reactive to the second fast-migrating component. This was not noticed when a solid-phase immunoassay on 96-well plates was employed for the characterization of these two antibodies. Later it turned out that the minor contaminant detected by the G159 antibody is

the sialyl 6-sulfo-Le^x glycolipid carrying lactamized sialic acid. The G159 antibody became a useful tool to detect this new modification of sialic acid in cells and tissues which may play a role in the regulation of the selectin ligand activity of the sialyl 6-sulfo-Le^x determinant ***(28,29)***.

4. Notes

1. Variable regions of some anticarbohydrate antibodies are well characterized, and anticarbohydrate antibodies are known to be encoded by a limited set of V_H and V_L genes in mice ***(40)*** and humans ***(41,42)***. Anticarbohydrate antibodies with a high affinity can be obtained by genetic manipulation using a phage display library ***(43,44)***.
2. So far, the use of *S. minnesota* is the best method for obtaining the antiglycolipid antibodies. However, it is still difficult to obtain specific antibodies to some glycolipids even with this method. In such cases, the whole cells that express the target antigen can be used as immunogen, and then the obtained hybridomas are screened against the target antigen by solid-phase immunoassay using purified glycolipids. Immunization of mice with whole cells or tissues is sometimes more effective than immunization with glycolipids absorbed on *S. minnesota*. Synthetic glycolipids are utilized as immunogen when the target antigen is a very minor component, and it is difficult to obtain enough antigen for immunization from a natural source. At least 200 μg of glycolipid is necessary to immunize a mouse and screen the hybridomas.
3. Blocking solutions prepared from bovine milk are commercially available for 96-well plate assay. These can be used in the assays for protein antigens, but are not recommended for carbohydrate antigens, as they seem to contain oligosaccharides which eventually interfere with the reaction of the antibody with the cognate carbohydrate determinants. Similarly, use of buffers containing surface active substances such as Tween or Triton is sometimes recommended as washing solutions in protocols for the solid-phase immunoassays of protein antigens; their use, however, is not recommended for glycolipid antigens, as they substantially wash away the glycolipid determinants immobilized at the bottom of the wells. A BSA–PBS solution as indicated previously is recommended for glycolipid determinants.
4. Wells incubated without first antibody will serve as negative controls. In addition to this, wells to which only phosphatidylcholine–cholesterol is adsorbed are necessary as negative controls, when gangliosides or glycolipids having relatively long carbohydrate chains are used as antigens. Antibodies recognizing phosphorylcholine are frequently obtained when stronger immunization protocols for mice are applied. Sulfated carbohydrate determinants such as sulfatides sometimes nonspecifically absorb antibodies, and in this case the use of positional isomer of the cognate determinants is preferable to serve as negative control to obtain specific monoclonal antibodies.

   The method is useful, convenient, and highly sensitive. As little as 1–2 ng of antigen can be detected. However, when the antigenic glycolipid preparation used

in the assay is contaminated with other glycolipids having longer carbohydrate chains than the antigen glycolipid, the reactivity of the antigen is sometimes masked and false-negative results can be obtained ***(45)***.

References

1. Kannagi, R. and Hakomori, S. (1986) Monoclonal antibodies directed to carbohydrate antigens, in *Handbook of Experimental Immunology*, vol.4, *Applications of Immunological Methods in Biomedical Sciences* (Weir, D. M., Herzenberg, L., Blackwell, C., and Herzenberg, L. A. eds.), Blackwell Scientific, Boston, pp. 117.1–117.20.
2. Nagata, Y., Yamashiro, S., Yodoi, J., Lloyd, K. O., Shiku, H., and Furukawa, K. (1992) Expression cloning of β-1,4 *N*-acetylgalactosaminyltransferase cDNAs that determine the expression of G_{M2} and G_{D2} gangliosides. *J. Biol. Chem.* **267,** 12082–12089.
3. Kanamori, A., Nakayama, J., Fukuda, M. N., Stallcup, W. B., Sasaki, K., Fukuda, M., and Hirabayashi, Y. (1997) Expression cloning and characterization of a cDNA encoding a novel membrane protein required for the formation of *O*-acetylated ganglioside: a putative acetyl-CoA transporter. *Proc. Natl. Acad. Sci. USA* **94,** 2897–2902.
4. Lowe, J. B., Stoolman, L. M., Nair, R. P., Larsen, R. D., Berhend, T. L., and Marks, R. M. (1990) ELAM-1-dependent cell adhesion to vascular endothelium determined by a transfected human fucosyltransferase cDNA. *Cell* **63,** 475–484.
5. Phillips, M. L., Nudelman, E., Gaeta, F. C. A., Perez, M., Singhal, A. K., Hakomori, S., and Paulson, J. C. (1990) ELAM-1 mediates cell adhesion by recognition of a carbohydrate ligand, sialyl-Le^x. *Science* **250,** 1130–1132.
6. Walz, G., Aruffo, A., Kolanus, W., Bevilacqua, M., and Seed, B. (1990) Recognition by ELAM-1 of the sialyl-Le^x determinant on myeloid and tumor cells. *Science* **250,** 1132–1135.
7. Takada, A., Ohmori, K., Takahashi, N., Tsuyuoka, K., Yago, K., Zenita, K., et al. (1991) Adhesion of human cancer cells to vascular endothelium mediated by a carbohydrate antigen, sialyl Lewis A. *Biochem. Biophys. Res. Commun.* **179,** 713–719.
8. Berg, E. L., Robinson, M. K., Mansson, O., Butcher, E. C., and Magnani, J. L. (1991) A carbohydrate domain common to both sialyl Le^a and sialyl Le^x is recognized by the endothelial cell leukocyte adhesion molecule ELAM-1. *J. Biol. Chem.* **266,** 14869–14872.
9. Takada, A., Ohmori, K., Yoneda, T., Tsuyuoka, K., Hasegawa, A., Kiso, M., and Kannagi, R. (1993) Contribution of carbohydrate antigens sialyl Lewis A and sialyl Lewis X to adhesion of human cancer cells to vascular endothelium. *Cancer Res.* **53,** 354–361.
10. Springer, T. A. (1995) Traffic signals on endothelium for lymphocyte recirculation and leukocyte emigration. *Annu. Rev. Physiol.* **57,** 827–872.
11. Rosen, S. D. and Bertozzi, C. R. (1994) The selectins and their ligands. *Curr. Opin. Cell Biol.* **6,** 663–673.

12. Kannagi, R. (1997) Carbohydrate-mediated cell adhesion involved in hematogenous metastasis of cancer. *Glycoconjugate J.* **14,** 577–584.
13. Ohmori, K., Takada, A., Ohwaki, I., Takahashi, N., Furukawa, Y., Maeda, M., et al. (1993) A distinct type of sialyl Lewis X antigen defined by a novel monoclonal antibody is selectively expressed on helper memory T cells. *Blood* **82,** 2797–2805.
14. Furukawa, Y., Tara, M., Ohmori, K., and Kannagi, R. (1994) Variant type of sialyl Lewis X antigen expressed on adult T cell leukemia cells is associated with skin involvement. *Cancer Res.* **54,** 6533–6538.
15. Mitsuoka, C., Kawakami-Kimura, N., Kasugai-Sawada, M., Hiraiwa, N., Toda, K., Ishida, H., et al. (1997) Sulfated sialyl Lewis X, the putative L-selectin ligand, detected on endothelial cells of high endothelial venules by a distinct set of anti-sialyl Lewis X antibodies. *Biochem. Biophys. Res. Commun.* **230,** 546–551.
16. Mitsuoka, C., Sawada-Kasugai, M., Ando-Furui, K., Izawa, M., Nakanishi, H., Nakamura, S., et al. (1998) Identification of a major carbohydrate capping group of the L-selectin ligand on high endothelial venules in human lymph nodes as 6-sulfo sialyl Lewis x. *J. Biol. Chem.* **273,** 11225–11233.
17. Kimura, N., Mitsuoka, C., Kanamori, A., Hiraiwa, N., Uchimura, K., Muramatsu, T., et al. (1999) Reconstitution of functional L-selectin ligands on a cultured human endothelial cell line by co-transfection of $\alpha 1 \rightarrow 3$ fucosyltransferase VII and newly cloned GlcNAcβ: 6-sulfotransferase cDNA. *Proc. Natl. Acad. Sci. USA* **96,** 4530–4535.
18. Bistrup, A., Bhakta, S., Lee, J. K., Belov, Y. Y., Gunn, M. D., Zuo, F. -R., et al. (1999) Sulfotransferases of two specificities function in the reconstitution of high-endothelial-cell ligands for L-selectin. *J. Cell Biol.* **145,** 899–910.
19. Kelm, S., Brossmer, R., Isecke, R., Gross, H. J., Strenge, K., and Schauer, R. (1998) Functional groups of sialic acids involved in binding to siglecs (sialoadhesins) deduced from interactions with synthetic analogues. *Eur. J. Biochem.* **255,** 663–672.
20. Ding, K., Rosen, A., Ray, A. K., and Magnusson, G. (1992) Anti-G_{M3}-lactam monoclonal antibodies of the IgG type recognize natural G_{M3}-ganglioside lactone but not G_{M3}-ganglioside. *Glycoconjugate J.* **9,** 303–306.
21. Chammas, R., Sonnenburg, J. L., Watson, N. E., Tai, T., Farquhar, M. G., Varki, N. M., and Varki, A. (1999) De-*N*-acetyl-gangliosides in humans: unusual subcellular distribution of a novel tumor antigen. *Cancer Res.* **59,** 1337–1346.
22. Sjoberg, E. R., Chammas, R., Ozawa, H., Kawashima, I., Khoo, K. H., Morris, H. R., et al. (1995) Expression of de-*N*-acetyl-gangliosides in human melanoma cells is induced by genistein or nocodazole. *J. Biol. Chem.* **270,** 2921–2930.
23. Varki, A. (1997) Sialic acids as ligands in recognition phenomena. *FASEB J.* **11,** 248–255.
24. Hanai, N., Dohi, T., Nores, G. A., and Hakomori, S. (1988) A novel ganglioside, de-*N*-acetyl-G_{M3} ($II^3NeuNH_2LacCer$), acting as a strong promoter for epidermal growth factor receptor kinase and as a stimulator for cell growth. *J. Biol. Chem.* **263,** 6296–6301.

25. Bouchon, B., Levery, S. B., Clausen, H., and Hakomori, S. (1992) Production and characterization of a monoclonal antibody (BBH5) directed to ganglioside lactone. *Glycoconjugate J.* **9,** 27–38.
26. Chou, D. K., Flores, S., and Jungalwala, F. B. (1990) Identification of disialosyl paragloboside and *O*-acetyldisialosyl paragloboside in cerebellum and embryonic cerebrum. *J. Neurochem.* **54,** 1598–1607.
27. Zhang, G., Ji, L., Kurono, S., Fujita, S. C., Furuya, S., and Hirabayashi, Y. (1997) Developmentally regulated *O*-acetylated sialoglycans in the central nervous system revealed by a new monoclonal antibody 493D4 recognizing a wide range of O-acetylated glycoconjugates. *Glycoconjugate J.* **14,** 847–857.
28. Mitsuoka, C., Ohmori, K., Kimura, N., Kanamori, A., Komba, S., Ishida, H., et al. (1999) Regulation of selectin binding activity by cyclization of sialic acid moiety of carbohydrate ligands on human leukocytes. *Proc. Natl. Acad. Sci. USA* **96,** 1597–1602.
29. Kannagi, R., Mitsuoka, C., Ohmori, K., Kanamori, A., Khoo, K. -H., and Inoue, Y. (1999) Cyclic sialic acid: a new regulatory mechanism of selectin ligand activity, in *Sialobiology and Other Novel Forms of Glycosylation* (Inoue, Y., Lee, Y. C., and Troy, F. A., eds.), Gakushin, Osaka, Japan, pp. 37–43.
30. Karsten, U., Butschak, G., Cao, Y., Goletz, S., and Hanisch, F. G. (1995) A new monoclonal antibody (A78-G/A7) to the Thomsen-Friedenreich pan-tumor antigen. *Hybridoma* **14,** 37–44.
31. Hanisch, F. G., Stadie, T., and Bosslet, K. (1995) Monoclonal antibody BW835 defines a site-specific Thomsen–Friedenreich disaccharide linked to threonine within the VTSA motif of MUC1 tandem repeats. *Cancer Res.* **55,** 4036–4040.
32. Thurnher, M., Clausen, H., Sharon, N., and Berger, E. G. (1993) Use of *O*-glycosylation-defective human lymphoid cell lines and flow cytometry to delineate the specificity of *Moluccella laevis* lectin and monoclonal antibody 5F4 for the Tn antigen (GalNAc-alpha-1-O-Ser/Thr). *Immunol. Lett.* **36,** 239–244.
33. Srikrishna, G., Varki, N. M., Newell, P. C., Varki, A., and Freeze, H. H. (1997) An IgG monoclonal antibody against *Dictyostelium discoideum* glycoproteins specifically recognizes Fucα1,6GlcNAcβ in the core of *N*-linked glycans—localized expression of core-fucosylated glycoconjugates in human tissues. *J. Biol. Chem.* **272,** 25743–25752.
34. Miyake, M., Ito, M., Hitomi, S., Ikeda, S., Taki, T., Kurata, M., et al. (1988) Generation of two monoclonal antibodies that can discriminate *N*-glycolyl and *N*-acetyl neuraminic acid residues of G_{M2} gangliosides and distribution of the antigens in human lung cancer. *Cancer Res.* **48,** 6154–6160.
35. Yamashita, Y., Chung, Y. S., Murayama, K., Kannagi, R., and Sowa, M. (1995) Alterations in gastric mucin with malignant transformation: novel pathway of mucin synthesis. *J. Natl. Cancer Inst.* **87,** 441–446.
36. Magnani, J. L., Brockhaus, M., Smith, D. F., and Ginsburg, V. (1982) Detection of glycolipid ligands by direct binding of carbohydrate- binding proteins to thin-layer chromatograms. *Methods Enzymol.* **83,** 235–241.

37. Galanos, C., Luderitz, O., and Westphal, O. (1971) Preparation and properties of antisera against the lipid-A component of bacterial lipopolysaccharides. *Eur. J. Biochem.* **24,** 116–122.
38. Köhler, G. and Milstein, C. (1975) Continuous culture of fused cells secreting antibody of predefined specificity. *Nature* **256,** 495–497.
39. Kannagi, R. (1998) CD15s cluster report, in *Leukocyte Typing VI* (Kishimoto, T., Kikutani, H., von dem Borne, E. G. Jr., Goyert, S. M., Mason, D. Y., Miyasaka, M., et al., eds.), Garland, New York, pp. 352–355.
40. Snyder, J. G., Dinh, Q., Morrison, S. L., Padlan, E. A., Mitchell, M., Yu-Lee, L. -Y., and Marcus, D. M. (1994) Structure–function studies of anti-3-fucosyllactosamine (Le^x) and galactosylgloboside antibodies. *J. Immunol.* **153,** 1161–1170.
41. Jefferies, L. C., Carchidi, C. M., and Silberstein, L. E. (1995) Immunoglobulin gene use by naturally occurring cold agglutinins. *Ann. NY Acad. Sci.* **764,** 433–435.
42. Thorpe, S. J., Turner, C. E., Stevenson, F. K., Spellerberg, M. B., Thorpe, R., Natvig, J. B., and Thompson, K. M. (1998) Human monoclonal antibodies encoded by the V4-34 gene segment show cold agglutinin activity and variable multireactivity which correlates with the predicted charge of the heavy-chain variable region. *Immunology* **93,** 129–136.
43. Dinh, Q., Weng, N. P., Kiso, M., Ishida, H., Hasegawa, A., and Marcus, D. M. (1996) High affinity antibodies against Le^x and sialyl Le^x from a phage display library. *J. Immunol.* **157,** 732–738.
44. Mao, S. L., Gao, C. S., Lo, C. H. L., Wirsching, P., Wong, C. H., and Janda, K. D. (1999) Phage-display library selection of high-affinity human single-chain antibodies to tumor-associated carbohydrate antigens sialyl $Lewis^x$ and $Lewis^x$. *Proc. Natl. Acad. Sci. USA* **96,** 6953–6958.
45. Kannagi, R., Stroup, R., Cochran, N. A., Urdal, D. L., Young, W. W., Jr., and Hakomori, S. (1983) Factors affecting expression of glycolipid tumor antigens: influence of ceramide composition and coexisting glycolipid on the antigenicity of gangliotriaosylceramide in murine lymphoma cells. *Cancer Res.* **43,** 4997–5005.

14

Inhibition of Tumor Metastasis by Liposomes Containing Glyco-Replica Peptides

Takao Taki and Naoto Oku

1. Introduction

Liposomes can be used as ideal drug carriers, and many previous studies have demonstrated the prolonged circulation time, enhanced efficacy, and reduced toxicity of encapsulated drugs ***(1–3)***. If liposomes could be delivered only to the target site, liposomal drugs would overcome most of the diseases including tumor as their "magic bullet," since one could use an appropriate amount of drugs without considering side effects. For such a purpose, specific antibody-modified liposomes, so called immunoliposomes, have been widely attempted. Conventional liposomes, however, have limitations: They are recognized as foreigners by the immune defense system and removed by the reticuloendothelial system (RES). Many attempts have been made to reduce the RES-trapping of liposomes, and long-circulating liposomes were developed by a modification of liposomes with glucuronide derivative ***(4,5)*** or polyethylene glycol (PEG) ***(6–8)***. Rigid, small-sized liposomes are also known to have long-circulating character. Antibody modification for active targeting of liposomes, however, enhances RES-trapping even though long-circulating liposomes are used. On the contrary, small molecule ligands may be more desirable for active targeting of liposomes because RES recognizes them less than antibodies. If we could easily prepare small molecule ligands, liposomes could be easily modified. However, in many cases, cell surface molecules or their ligands are glycoconjugates and difficult to prepare in large amount.

Incidentally antibodies can generated against most existing molecules, such as peptides, carbohydrates, nucleic acids, lipids, vitamins, drugs, chemical

From: *Methods in Molecular Biology, vol. 199: Liposome Methods and Protocols*
Edited by: S. Basu and M. Basu © Humana Press Inc., Totowa, NJ

compounds, and so on. As peptides can recognize most existing molecules, peptides are also able to mimic structurally most of existing molecules.

In this chapter, we propose a new strategy for preparing actively targeted liposomes or liposomes specifically bound to certain ligands or receptor molecules including glycoconjugates by using the small molecule peptidic ligands. The strategy is as follows:

1. A specific peptides recognizing or mimicking some specific molecule is selected by biopanning from phage display random peptide library originally developed by Scott and Smith ***(9)***.
2. Epitope amino acid sequence is determined by using fragment peptides from the mother peptide.
3. An epitope fragment peptide is alkylated peptide and incorporated into liposomes.

This strategy has many advantages. For example, the strategy is applicable to any kind of molecules including carbohydrates, and also applicable to unknown ligands or unknown receptors.

In this chapter, we present an example applied to the strategy. RAW117-H10 cells are highly liver metastatic subline of RAW117 murine large cell lymphoma, and RAW117-P cells are the low metastatic parental line. We first examined the ganglioside pattern of both kinds of cells and observed that ganglioside GD1α was highly expressed on RAW117-H10 cells. Furthermore, GD1α suppressed the binding of RAW117-H10 cells to hepatic sinusoidal microvessel endothelial (HSE) cells ***(10)***. Therefore, we selected GD1α replica peptide-expressing phage from 15-mer phage-displayed peptide library ***(11)***. Biopanning was done by using GD1α specific monoclonal antibody which can neutralize the binding of RAW117-H10 cells to HSE cells. Four kinds of GD1α replica peptide-expressing phage clones were selected. A replica peptide from one phage clone, which showed the strongest inhibitory activity against RAW117-H10 cell binding to HSE cells, actually inhibited metastasis of RAW117-H10 cells to the liver of injected mice. Then the epitope of the replica peptide was determined to be WHW tripeptide. Finally WHW-modified liposomes were applied as the antimetastatic agent of RAW117-H10 cells. In the present case, the receptor molecule against GD1α on the HSE cell surface is still unknown.

2. Materials

1. Phage-displayed random peptide library: A phage-displayed random peptide library expressing a pentadecamer (15-mer) at the N-terminus of pIII phage coat protein of filamentous phage (fd phage) was constructed, through a kind donation by Dr. Saya at Kumamoto University ***(12)***. In brief, 15 repeats of NNK nucleotides sequence were inserted into N-terminal of pIII protein after

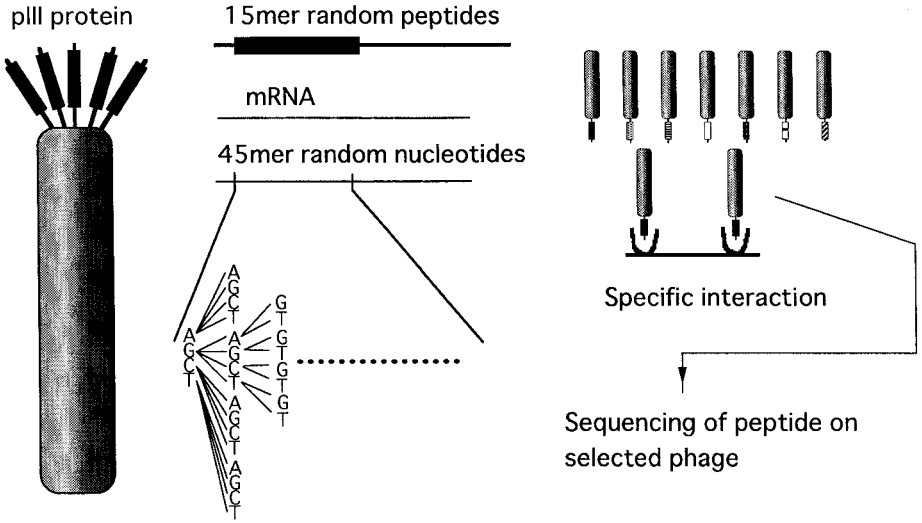

Fig. 1. Scheme of phage display random peptide library.

an ADGA amino acid sequence, where N was constructed from the equimolar mixture of A, T, G, and C, and K was constructed from the equimolar mixture of G and T. Therefore, NNK covered all 20 kinds of amino acids. The scheme of a phage-displayed random peptide library is shown in **Fig. 1**. Next, the gene library encoding pIII with insertion of 45 nucleotides was ligated into phage DNA and the obrained phage DNA was transfected to *E. coli* for producing phages. This method could essentially be used to construct a phage library displaying an appropriate number of amino acids.

2. Cells: Low metastatic RAW117-P mouse lymphoma cells and highly liver metastatic RAW117-H10 variant cells were maintained in suspension culture high-glucose Dulbecco's modified Eagle medium (hG-DMEM, DMEM containing additional 4.5 g/L of D-glucose) supplemented with 5% heat-inactivated fetal bovine serum (FBS) at 37°C under a humidified atmosphere of 5% CO_2 in air. The sizes of RAW117-P and RAW117-H10 cells were 13.4 ± 1.4 μm and 13.8 ± 1.4 μm, respectively, and doubling time of these cells under the condition was 9.2 h and 9.5 h, respectively. HSE cells established from liver cells were cultured in DMEM: Ham's F-12 (D-MEM/F12 1 : 1 mixture) supplemented with 10% FBS, 10 U/mL of heparin sodium, and 50 μg/mL of endothelial mitogen (Biomedical Technologies, Inc.) in a humidified CO_2 incubator.
3. Peptides and hydrophobized peptides: Various peptides were synthesized in the from of amide at the c-termini. For the modification of liposomes, a palmitoyl group was bound to WHW peptide at the following carbon chain: CH_3 $(CH_2)_{16}$ CO-NH-WHW-CO-NH_2.
4. Lipids: Dipalmitoylphosphatidylcholine (DPPC) and distearoylphosphatidylcholine (DSPC) were gifts from Nippon Fine Chemicals, and cholesterol was

obtained from Sigma. Lipids were dissolved in chloroform and stored at –20°C until use.

5. Antibodies: The monoclonal antibody (mAb) directed against GD1α (clone KA17) was kindly donated by Dr. Hirabayashi at RIKEN ***(13)***. Biotinylated antibody was prepared as follows: KA17 in 50 m*M* $NaHCO_3$, pH 8.8, were incubated with sulfo-NHS-biotin (Pierce) in dimethyl sulfoxide overnight at 4°C. The reaction mixture was dialyzed at 4°C against Tris-buffered saline (TBS), pH 7.2, and concentrated with a Centricon-30 (Amicon). Horseradish peroxidase (HRP)-cojugated $F(ab')_2$ fragment of goat anti-mouse IgG + IgM antibody was purchased from Jackson Immuno Research Laboratories, Inc.
6. Blocking solution: 100 m*M* $NaHCO_3$, 5 mg/mL of bovine serum albumin (BSA), 0.1 μg/mL of streptavidin, and 0.02% NaN_3.
7. Elution buffer: 0.1 *N* HCl containing 1 mg/mL of BSA, the pH of which was adjusted to 2.2 with glycine.

3. Methods

3.1. Selection of GD1α-Replica Peptide Displaying Phage Clones from a Phage-Displayed Random Peptide Library (Biopanning) (11)

The scheme of biopanning is shown in **Fig. 2**.

1. For isolation of GD1α-replica peptide displaying phage clones, each well of a 96-well plate was covered with 10 μg of streptavidin in 100 μL of 100 m*M* $NaHCO_3$ overnight at 4°C and treated with a blocking solution for 1 h at room temperature.
2. The biotinylated KA17 (1 μg) was adsorbed onto the streptavidin-coated well, and the library was added to each well.
3. After having been washed 10 times with TBS, pH 9.1, the affinity-bound phages were eluted with elution buffer for 10 min at room temperature.
4. The eluted phages were concentrated with Centricon-30 after dilution with TBS (final volume of 0.2 mL).
6. Then the aliquot was used for titration and the rest was used for amplification. The phages obtained from a biopanning were transfected to 5×10^8 *E. coli* K91KAN for 15 min and incubated in NZY medium containing tetracycline. Generated phages were purified with polyethylene glycol (PEG 6000) and used for the next cycle of biopanning.
7. Biopanning was usually performed several times. In the present study, we applied four cycles of biopanning to obtain the GD1α-replica peptide displaying phage clones by use of anti-GD1α antibody, KA17. (*See* **Note 1**.)

3.2. DNA Sequencing

Phages selected from the library were purified with PGE 6000 and their single strand DNA was prepared by phenol extraction. DNA was sequenced

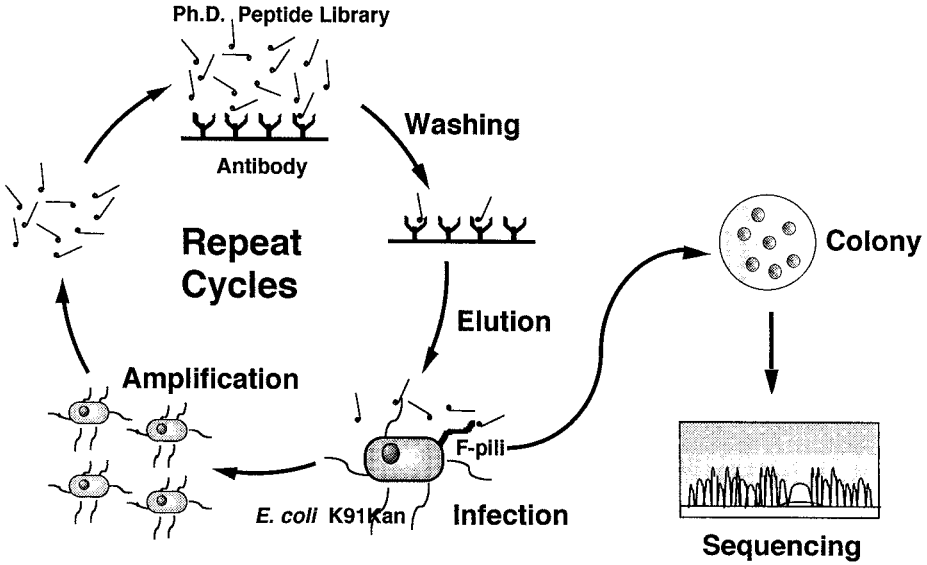

Fig. 2. Procedure of biopanning.

by the protocol of Pharmacia Cy5 dye-primer system. A Cy5-conjugated oligonucleotide 5′-TAACAATGAGTTTCGTCACCAGTC was used as an antisense primer.

In the present study, after four cycles of biopanning, 24 bacterial clones were randomly picked up, and inserted DNA sequence of isolated phages was determined. As shown in **Table 1**, the phages obrained were classified four clones, and two of them possessed the WHW tripeptide domain in the pentadecapeptides.

3.3. Affinity of the Isolated Phage Clones to the Specific Antibody

1. Each well of microtiter plates was coated with isolated phage clones (10^9–10^{14} particles) in 100 µL of 100 m*M* $NaHCO_3$ by incubation overnight at 4°C.
2. The coated plates were washed three times with TBS, pH 7.4, blocked with TBS/1% bovine serum albumin (BSA) for 1 h at room temperature, washed three times with TBS, and KA17 in 100 µL of TBS/1% BSA was added to each well. Then the plates were incubated overnight at 4°C.
3. After the well was washed with TBS, the bound KA17 was detected with HRP-conjugated anti-mouse IgM, for 2 h at room temperature. The bound antibody was monitored by peroxidase activity using *o*-phenylenediamine, and the color developed was determined at 490 nm.

As shown in **Fig. 3** all four clones isolated in the present study showed high affinity to KA17, especially the phage displaying WHWRHRIPLQLAAGR

Table 1
Inserted Amino Acid Sequences of Selected Phage Clones

Phage	Sequence	Clones
GD1αPR-Φ1	FRSDVRFWHWSTPFM	11
GD1αPR-Φ2	VRVYFGFGPPPYFFGG	9
GD1αPR-Φ3	WHWRHRIPLQLAAGR	2
GD1αPR-Φ4	RYWLYGDPASFPVNH	2

Amino acid sequences were deduced from DNA of the inserted 45 nucleotides.

sequence, which had the highest affinity among isolated phage clones. (*See* **Note 2**.)

3.4. Cell Adhesion Assay

1. RAW117 cells were labeled either with 2′, 7′-*bis*(2-carboxyethyl)-5(and 6)-carboxyfluorescein, acetoxymethylester (BCECF-AM, Dojindo Laboratories) or with [^{35}S] methionine.
2. BCECF-labeling was performed as follows ***(14)***: RAW117 cells (1.2×10^6 cells/mL) were incubated with 3 m*M* BCECF-AM (final 0.3% dimethyl sulfoxide) in hG-DMEM containing 5% heat-inactivated FBS for 30 min at 37°C. After washing twice with PBS, the labeled cells were suspended in hG-DMEM/1% BSA.
3. HSE cells were seeded on 96-microwell plates precoated with 0.1% gelatin in PBS, and culture overnight.
4. After washing with PBS, 25 µL of BCECF-labeled cells (4×10^5 cells/mL) and 25 µL of various peptides or liposomes were added onto HSE monolayer cells. After an incubation for 20 min at 37°C and washing of nonadherent cells, adherent cells were solubilized in 100 µL of 10% Triton X-100. RAW117-H10 cells bound to HES were determined fluorometrically with excitation at 490 nm and emission at 526 mn.
5. The inhibition of adhesion of RAW117-H10 cell to HSE cells was also determined by use of [^{35}S]methionine-labeled cells. In this case, preseeded HSE cells were incubated with the isolated phage clones or synthesized peptides for 30 min at 37°C. Then the labeled RAW117-H10 cells were added to the culture and incubated for 30 min at 37°C. The adherent cells were solubilized with 50 µL of 1 *N* NaOH containing 1% sodium dodecyl sulfate (SDS). After neutralization with 2 *N* HCl, the radioactivity of the solution was measured.

This method was applied for determining inhibitory activity of selected phages or GD1α-replica peptides against adhesion of RAW117-H10 cells to HSE cells. Since KA17 anti-GD1α antibody blocked adhesion of RAW117-H10 cells to HSE cells ***(10)***, GD1α might be involved in the adhesion. Thus,

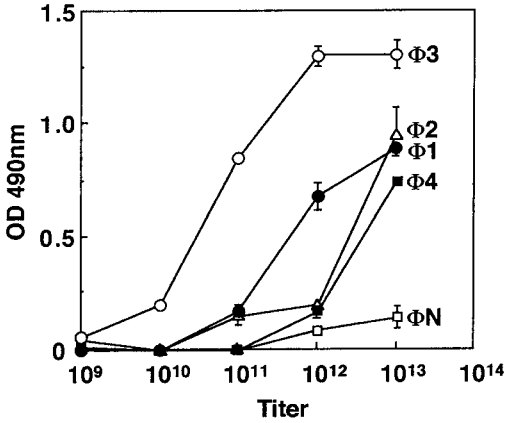

Fig. 3. Affinity of selected phage clones against GD1α-mAb KA 17.

selected phages or GD1α-replica peptides may also inhibit the adhesion, if the displayed peptide mimic GD1α structurally and/or functionally. In fact, all four isolated phages or peptides derived from these phages inhibited the adhesion of RAW117-H10 cells to HSE cells in a dose-dependent manner (**Fig. 4**). Among them, the phage clone displayed the WHWRHRIPLQLAAGR sequence, and WHWRHRIPLQLAAGR peptide showed the highest inhibitory activity, respectively.

Next, we determined the epitope sequence for mimicking GD1α. To examine the importance of the WHW sequence for mimicking GD1α function, a mutated peptide in which WHW was substituted by trialanine was synthesized. As a result, AAARHRIPLQLAAGR did not inhibit the adhesion of RAW117-H10 cells to HSE cells, suggesting the importance of WHW moiety for mimicking GD1α (data not shown). To dissect the role of the WHW domain in GD1α-mediated cell adhesion, we prepared various deletion mutants of WHWRHRIPLQLAAGR. As shown in **Fig. 5**, WHW tripeptide is revealed to be a minimal sequence exerted comparable inhibitory activity toward adhesion of RAW117-H10 cells to HSE cells.

3.5. Confirmation of Epitope Peptides as a Recognition Site by the Specific Antibody

To confirm the WHW sequence as epitope mimetic of GD1α recognized by KA17, we performed a competitive binding assay for measuring the binding of KA17 to GD1α-coated plates in the presence of various peptides.

1. GD1α in methanol (3.2 μg/well) was applied to each well of microtiter plates (polysope, NUNC) and methanol was evaporated.

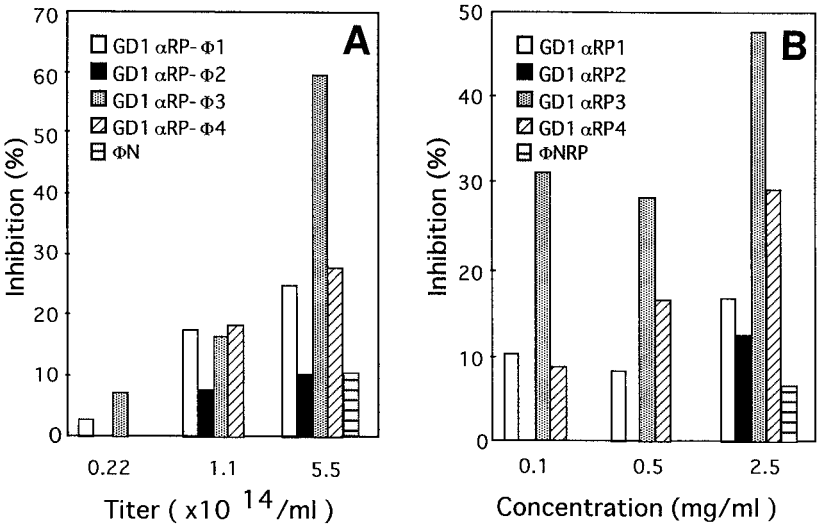

Fig. 4. Inhibitory effect of the selected phage clones and synthetic peptides against adhesion of RAW117-H10 cells to HSE cells. ^{35}S-labeled RAW117-H10 cells were incubated with HSE cells preseeded on a plate for 30 min the presence of various titers of phages **(a)**, or synthetic peptides derived from the selected phages **(b)**. ΦN shows negative clone and ΦNRP (ΦN replica peptide) is peptide corresponding to ΦN.

2. The coated plates were washed three times with TBS, and blocked with TBS/1% BSA.
3. After washing with TBS, 25 µL of the anti-GD1α mAb KA17 in TBS/0.1% BSA and 25 µL of various peptides or buffer alone were added into each well and incubated for 2 h at 4°C.
4. After washing, bound mAb KA17 was detected by further incubation with HRP-conjugated goat anti-mouse IgG + IgM for 2 h at 4°C. The bound antibody was detected by monitoring peroxidase activity.

As a result, WHW tripeptide as well as WHW-containing hepta- and pentadeca-peptides inhibited the binding of mAb KA17 to GD1α, suggesting that the WHW domain is a minimal sequence mimicking the GD1α epitope recognized by mAb KA17 (**Fig. 6**). (*See* **Note 3**.)

3.6. Preparation of GD1α-Replica Peptide-Modified Liposomes

Liposomes modified with specific peptides are useful for active targeting to specific molecules or organs that express receptors for the peptides. Therefore, WHW was hydrophobized and incorporated into liposomal membrane. Liposomes were prepared as follows: DPPC or DSPC, cholesterol, and alkylated WHW (10:5:1 or 4:2:1 as molar ratio) dissolved in chloroform were dried

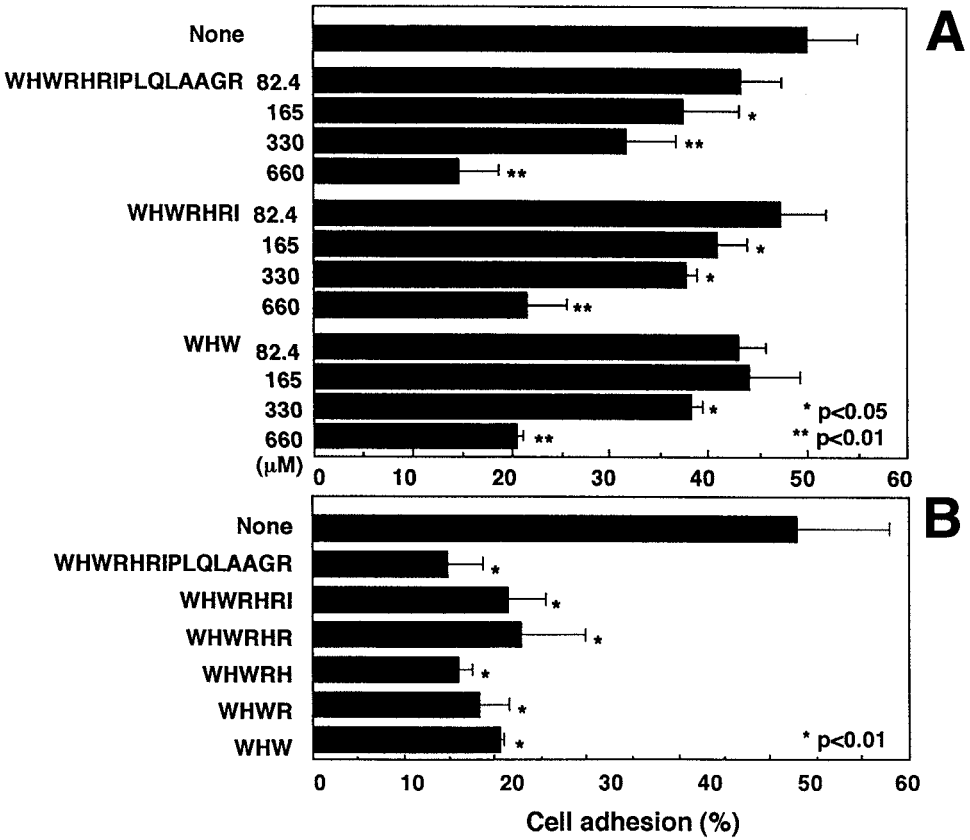

Fig. 5. Adhesion of RAW117 cells to HSE cells in the presence of GD1α-replica peptide fragments. BCECF-labeled RAW117-H10 cells were incubated with HSE for 20 min in the presence or absence of fragment peptides derived from GD1α-replica RP3 (WHWRHRIPLQLAAGR). **(A)** Dose dependence of 3-, 7-, and 15-mer peptides including WHW sequence was examined. **(B)** Three- to seven-mer sequential peptides as well as 15-mer peptides at the concentration of 660 μ*M* were used.

under reduced pressure to prepare thin lipid film, and stored *in vacuo* for at least 1 h. Then the thin lipid film was hydrated with 0.3 *M* glucose, frozen, and thawed for three cycles using liquid nitrogen, and sonicated to prepare liposomes.

As shown **Fig. 7**, WHW-liposomes could efficiently inhibit adhesion of RAW117-H10 cells to HSE cells that express hypothetical GD1α receptors. Furthermore, the inhibitory activity of WHW peptide increased approx twofold in case of liposomalization, compared with the result using soluble peptides shown in **Fig. 5**. (*See* **Note 4**.)

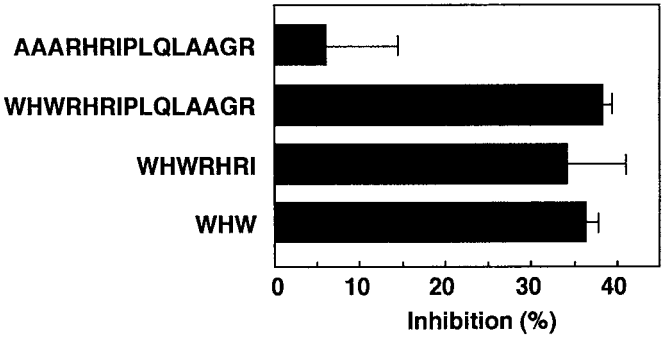

Fig. 6. Effect of WHW peptides on the binding of anti-GD1α mAb to GD1α. Anti-GD1α mAb KA17 was added to ELISA plates precoated with GD1α in the presence or absence of indicated peptides (1.32 m*M*), and incubated for 2 h at 4°C. The binding of anti-GD1α mAb to GD1α was measured by ELISA assay.

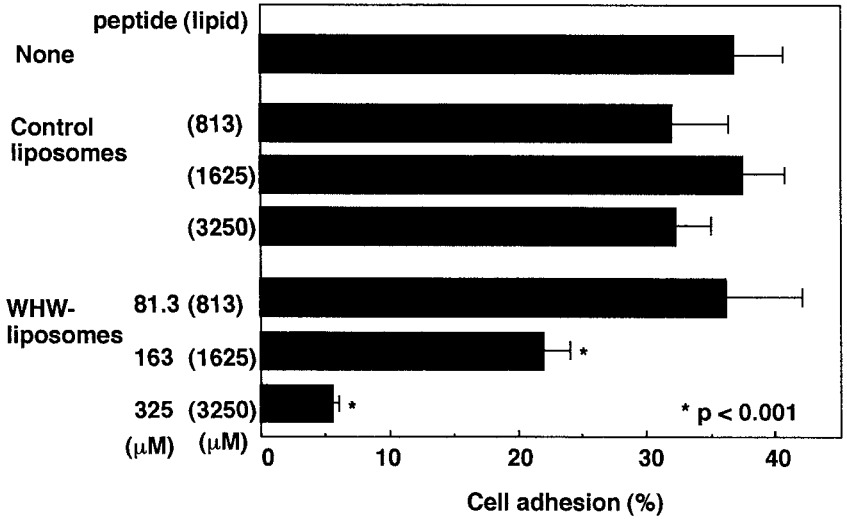

Fig. 7. Effect of WHW-liposomes on adhesion of RAW117-H10 cells to HSE cells. Adhesion of RAW117-H10 cells was analyzed in the presence or absence of WHW peptide-modified liposomes. Liposomes composed of DPPC, cholesterol, and palmitoyl WHW (10:5:1 as a molar ratio) were used. Control liposomes were prepared without palymitoyl WHW. Liposomal concentration was shown as DPPC concentrations in parentheses.

Table 2
Suppression of RAW117-H10 Metastasis by Liposomal GD1α-Replica Peptide

Group	Liver weight (mg ± SD)	Weight gain (mg)	Inhibition (%)
Sham	861 ± 14		
RAW117-H10 cells	1363 ± 195	502	0
RAW117-H10 cells +control liposomes	1305 ± 110	444	11.6
RAW117-H10 cells +WHW-liposomes	1137 ± 40[a]	276	45.0

RAW117-H10 cells (1×10^5 cells/0.2 mL/mouse) were injected into mice ($n = 5$) via portal vein with or without liposome (1.25 m*M* as a peptide). After 7 d, liver weight was measured for evaluating experimental metastasis in liver. Control and WHW-liposomes were composed of DSPC/cholesterol (2 : 1) and DSPC/cholesterol/peptide (4 : 2 : 1), respectively.

[a] $p < 0.05$ against RAW117-H10 infected group without liposome.

3.7. Animal Experiment

To ascertain whether WHW-liposomes could inhibit the adhesion of RAW117-H10 cells to HSE cells in vivo, we examined experimental metastasis of RAW117-H10 cells in the liver. Seven-week-old female Balb/c mice (five per group, SLC, Inc., Shizuoka, Japan) were anesthetized with sodium pentobarbital (0.05 mg/g body weight). Mice were cared for according to the guidelines of the University of Shizuoka. RAW117-H10 cells (1×10^5 cells/0.1 mL) were mixed with either an equal volume of liposome solution or the medium alone, and injected into mice via the portal vein after an incision was made along the midline of abdomen to expose the mesentery. At d 7 after injection, the animals were killed and livers were removed for weighing.

The liver weight at 7 d after injection of RAW117-H10 cells into mice via the portal vein increased due to liver metastasis (**Table 2**). The liver weight gain due to metastasis was drastically inhibited when the WHW-liposomes were coinjected, suggesting WHW-liposomes inhibited the binding of RAW117-H10 cells with hepatic endothelium through blocking GD1α-mediated interaction in the early steps of metastatic processes ***(13)***.

4. Notes

1. Recovery of phage titier in each biopanning is an important indicator whether biopanning is successful or not. If recovery is increased in each biopanning, it is successful. If not, other methods are worth trying for example antibody was immobilized on beads instead of plates.

2. Each phage clone is amplified individually, titrated, and screened by enzyme-linked immunosorbent assay (ELISA).
3. Not only fragment peptides derived only from insertion sequences, but also sequences having franking region should be tested.
4. Peptides grafting short chain acyl groups are sometimes easily detached from liposomes. Palmitoyl or stearoyl peptides might be more stable in liposomal membrane than lauroyl or shorter acylated peptides. Liposomal phospholipids are also important for the stability of acylated peptides, especially in the presence of serum.

References

1. Oku, N. (1999) Anticancer therapy using glucuronate modified long-circulating liposomes. *Adv. Drug. Delivery Rev.* **40,** 63–73.
2. Oku, N., Koike, C., Tokudome, Y., Okada, S., Nishikawa, N., Tsukada, H., et al. (1997) Application of liposomes for cancer metastasis. *Adv. Drug. Delivery Rev.* **24,** 215–223.
3. Woodle, M. and Storm, G., eds. (1998) *Long Circulating Liposome*. Springer-Verlag, Berlin.
4. Namba, Y., Sakakibara, T., Masada, M., Ito, F., and Oku, N. (1990) Glucuronate-modified liposomes with prolonged circulation time. *Chem. Pharmaceut. Bull.* **38,** 1663–1666.
5. Oku, N., Namba, Y, and Okada, S. (1992) Tumor accumulation of novel RES-avoiding liposomes. *Biochim. Biophys. Acta* **1126,** 255–260.
6. Blume, G. and Cevc, G. (1990) Liposomes for the sustained drug release *in vivo*. *Biochim. Biophys. Acta* **1029,** 91–97.
7. Klibanov, A. L., Maruyama, K., Torchilin, V. P., and Huang, L. (1990) Amphiphathic polyethyleneglycols effectively prolong the circulation time of liposomes. *FEBS Lett.* **268,** 235–237.
8. Allen, T. M., Hansen, C., Martin, F., Redemann, C., and Yan-Young, A. (1991) Liposomes containing synthetic lipid derivatives of poly(ethylene glycol) show prolonged circulation half-lives *in vivo*. *Biochim. Biophys. Acta* **1066,** 29–36.
9. Scott, J. K. and Smith, G. P. (1990) Searching for peptide ligands with an epitope library. *Science* **249,** 386–390.
10. Taki, T., Ishikawa, D., Ogura, M., Nakajima, M., and Handa, S. (1997) Ganglioside GD1α functions in the adhesion of metastatic tumor cells to endothelial cells of the target tissue. *Cancer Res.* **57,** 1882–1888.
11. Ishikawa, D., Kikkawa, H., Ogino, K., Hirabayashi, Y., Oku, N, and Taki, T. (1998) GD1α-replica peptides functionally mimic GD1α, and adhesion molecule of metastatic tumor cells, and suppress the tumor metastasis. *FEBS Lett.* **441,** 20–24.
12. Nishi, T., Budde, R. J. A., McMurray, J. S., Obeyesekere, N. U., Safdar, N., Levin, V. A, and Saya, H. (1996) Tight-binding inhibitory sequences against pp60 (c-src) identified using a random 15-amino-acid peptide library. *FEBS Lett.* **399,** 237–240.

13. Furuya, S., Irie, F., Hashikawa, T., Nakazawa, K., Kozakai, A., Hasegawa, A., et al. (1994) Ganglioside GD1α in cerebellar Purkinje cells: Its specific absence in mouse mutants with Purkinje cell abnormality and altered immunoreactivity in response to conjunctive stimuli causing long term desensitization. *J. Biol. Chem.* **269,** 32418–32425.
14. Kikkawa, H., Miyamoto, D., Imafuku, H., Koike, C., Suzuki, Y., Okada, S., et al. (1998) Role of sialylglycoconjugate(s) in the initial phase of metastasis of liver-metastatic RAW117 lymphoma cells. *Jpn. J. Cancer Res.* **89,** 1296–1305.
15. Takikawa, M., Kikkawa, H., Asai, T., et al. (2000) Suppression of GD1α ganglioside-mediated tumor metastasis by liposomalized WHW-peptide. *FEBS Lett.* **466,** 381–384.

15

Use of Phospholipid Bilayers and Monolayers in Binding Studies of Vitamin K-Dependent Blood Coagulation Proteins

Francis J. Castellino and Eric H. Ellison

1. Introduction

The vitamin K-dependent coagulation plasma proteins possess from 9 to 12 residues of γ-carboxyglutamic acid (Gla) distributed in an approx 40 amino acid peptide sequence, that is, the Gla domain, which encompasses the N-terminal region. In the presence of Ca^{2+} and negatively charged phospholipids (PLs), the Gla domain functions as the site of protein attachment to membranes. Strong evidence exists that the adsorption of these proteins to membranes is driven by a Ca^{2+}-mediated bridging interaction between negatively charged PL (e.g., phosphatidylserine) and the Gla residues of proteins (for a review, *see* **ref. *1***). More recent studies demonstrated that adsorption to PL membranes of Gla-containing coagulation proteins, such as VII, factor IXa, factor X, prothrombin, and protein C (PC), also possessed a significant hydrophobic determinant ***(2–6)***. Adsorption of the Gla-containing coagulation proteins to membranes is critical to proper function of the blood coagulation system.

One special feature of the Gla domain is the high degree of sequence homology found among the various Gla-containing coagulation proteins. However, the affinity of these proteins for equivalent model membranes can vary by as much as two orders of magnitude. A topic of current interest is whether these varied affinities are related to differences in the Gla domains of these proteins. For example, it is unclear whether proteins with a larger number of Gla residues make additional contacts with the membrane, or, more generally, if actual protein attachment to membranes is related to more subtle differences in the Gla domain sequences between proteins. This type

From: *Methods in Molecular Biology, vol. 199: Liposome Methods and Protocols*
Edited by: S. Basu and M. Basu © Humana Press Inc., Totowa, NJ

of information is important in developing future strategies for understanding and/or mimicking protein-membrane contact.

Studies of blood coagulation protein–membrane interactions have been conducted with mixed lipid vesicle bilayer systems. This strategy has provided valuable results, but is complicated by the fact that changes in bulk lipid compositions in these types of systems also have significant effects on biophysical properties of the bilayer, such as its radius of curvature and its inner–outer membrane compositional symmetry. In addition, such work is limited by the fact that certain PLs do not assume a bilayer structure and/or, in fact, might disrupt an existing bilayer. Protein binding is affected not only by membrane composition but also by these types of biophysical properties of the bilayer. Because of these potential problems with bilayer-based investigations, we have studied the binding of these types of proteins to PL monolayers spread at the air–water interface below their collapse pressures. This approach has been successfully employed in the past in systems of importance to this work ***(7)***. Some advantages of this approach exist, for example, (a) the packing densities of spread monolayers can be varied at constant area; (b) a full range of PL compositional effects can be examined without concern for their abilities to form bilayers and/or to influence the inner–outer membrane composition of a bilayer; and/or (c) measurements of the influence of adsorbed proteins on the surface tension of the monolayer at the lipid–air interface can yield unique information regarding the binding energies. Regarding this latter point, measurements of the surface tensions of bilayers and the effects of proteins thereon are not directly possible with bilayer systems since the surface tension of bilayer membranes is zero ***(8,9)***. In this review, methods for studying the binding of proteins to PL bilayers and monolayers are described, and representative examples of the types of data obtained are presented.

2. Materials

2.1. Proteins

Bovine prothrombin (bPt) was obtained from the Enzyme Research Corp. (South Bend, IN). The generation and purification of wild-type (wt)-recombinant (r) human protein C (wtr-PC) has been described in detail ***(10)***. The r-PC mutants described in this article were obtained as described ***(5)***. Prior to use, all proteins were dialyzed against the desired buffer at 4°C. The protein concentrations were determined by absorption spectroscopy utilizing an ε_{280}, 1% = 1.44 for bPt and 1.45 mL mg^{-1} cm^{-1} for wtr-PC as well as the r-PC mutants.

2.2. Lipids

1. Egg phosphatidylcholine (ePhC) and bovine brain phosphatidylserine (bPhS) were purchased from the Sigma Chemical Co. (St. Louis, MO).

2. Stock solutions of 1-palmitoyl-2-oleoyl-*sn*-glycero-3-phosphocholine (POPhC) and 1-palmitoyl-2-oleoyl-*sn*-glycero-3-phospho-L-serine (POPhS) were purchased from Avanti Polar Lipids (Alabaster, AL) and used as received.
3. The concentration of PL in the stock solutions was determined by weighing a known volume of lipid to the nearest 0.01 mg following evaporation of the solvent *in vacuo*. The standard buffer contained 10 m*M* Tris-HCl, 100 m*M* NaCl, 0.5 m*M* EDTA, pH 7.4. $CaCl_2$ was added to the buffer when required.
4. High purity water (TOC < 3 ppb) was obtained in-house from a Barnstead Easypure-UV system.

2.3. Preparation of PL Bilayers

PL vesicles containing 60/40 (w/w) PhC/PhS are prepared as follows.

1. A volume of 72 µL of ePhC (100 mg/mL) and 480 µL of bPhS (10 mg/mL) are mixed in a 10-mL beaker and kept on ice. The $CHCl_3$ in the stock solution is removed by flushing with N_2.
2. The PL mixture is then suspended in 5 mL of a buffer (pretreated with Chelex-100) containing 25 m*M* Na^+–*N*-(2-hydroxyethyl)piperazine-*N*′-(2-ethanesulfonic acid (HEPES)–0.1 *M* NaCl, pH 7.4, and the suspension subjected to vigorous vortex-mixing. The suspension is sonicated at 5°C with a Heat Systems Ultrasonics sonicator (Model W200R) containing a standard microchip probe adjusted to deliver a power output of 75 W on a 50% duty cycle. An atmosphere of N_2 is maintained to prevent air oxidation of the PL.
3. The PL vesicle preparation is obtained after centrifugation at 40,000 rpm for 90 min at 4° C using a Beckman SW50 rotor.
4. The precipitate is discarded and the supernatant passed over a Chelex-100 column, which has been preequilibrated and developed with a solution of 25 m*M* Na^+-HEPES, 0.1 *M* NaCl, pH 7.4. This procedure allows isolation of the smallest unilamellar bilayer vesicles. This phospholipid dispersion is stable on ice for approx 10 h.
5. The concentration of PL in the suspension can be conveniently determined by the Lowry assay ***(11)***.

2.4. Preparation of PL Monolayers

1. Monolayers for protein-binding analysis are prepared by carefully spreading one drop (4–5 µL) of lipid solution in $CHCl_3$ on the buffer surface. Spreading and stabilization of the surface pressure is achieved equally well using either $CHCl_3$ or CH_3OH/C_6H_{14} (10:90, v/v) as the spreading solvent.

3. Methods

3.1. Measurement of Protein Binding to PL Bilayers

These measurements are accomplished by quasielastic light-scattering measurements ***(12–14)***. Two types of experiments are usually performed. In

the first, the dependency of a fixed protein concentration on varying Ca^{2+} levels is determined, and, in the second, the efficiency of protein binding is evaluated at fixed levels of Ca^{2+}. For these studies, a SLM-Aminco 8000C spectrofluorimeter is used with excitation and emission wavelengths of 320 nm., along with 4-nm slit widths. Using the example of titrations with human r-PC, the procedure employed is as follows.

1. A 1.5-mL solution containing 93 µg of protein and 9 µg of ePhC/bPhS in Chelex-100-treated 20 m*M* Tris-HCl–100 m*M* NaCl, pH 7.4, is employed.
2. After stirring for 15 min, a stable baseline is observed. Additions of $CaCl_2$ are made in 2-µL amounts from stock solutions (100–2500 m*M*) followed by stirring for at least 10 min, or until a stable baseline is observed. Following the titration, 150 m*M* EDTA is added to examine the extent of reversibility of the Ca^{2+} effects.
3. The data are analyzed by determination of the total concentration of Ca^{2+} or protein that allows for 50% saturation of the increase in scattering. The data are plotted as M_2/M_1 vs [Ca^{2+}] or [protein]. This molecular weight ratio is calculated using the equation:

$$\frac{KC}{I_s/I_{so}} = 1/M + 2BC$$

where I_s/I_{so} is the ratio of scattered to incident light intensities, C is the concentration (g/mL) of scattering component, K is an instrument constant, M is the molecular weight of the scattering component, and B refers to the second virial coefficient. At the protein and PL concentrations used in these experiments, the term $2BC$ can be neglected.

Assuming that $2BC$ is neglected, the equation describing the scattering of PL becomes:

$$I_{s2}/I_{s1} = \frac{(\partial n_2/\partial C_2)^2 M_2 C_2}{(\partial n_2/\partial C_2)^2 M_2 C_2}$$

where I_{s2} and I_{s1} are the ratio of light-scattering intensities for the protein–PL complex and PL vesicles, alone, respectively. The quantities $\partial n_2/C_2$ and $\partial n_1/C_1$ are the changes in refractive indices with concentration of the protein-PL and PL vesicles alone, respectively. In our case, the concentration of light-scattering particles is unchanged ($C_1/M_1 = C_2/M_2$). Thus,

$$I_{s2}/I_{s1} = \frac{(\partial n_2/\partial C_2)^2 M_2^2}{(\partial n_1/\partial C_1)^2 M_1^2}$$

This equation can be further simplified by assuming that $n_2/C_2 = n_1/C_1$. This would be the case if the free protein light scattering contributed negligibly to the total scattering, as compared to the PL. Therefore, to determine M_2/M_1, the following reduced equation is used:

$$M_2/M_1 = \sqrt{\frac{I_{s2}}{I_{s1}}}$$

3.2. Measurement of Protein Binding to PL Monolayers

The binding of proteins to spread PL monolayers is determined by measurements of the changes in surface pressure ($\Delta\pi$) of the PL. The Wilhemly technique is employed to monitor π; using filter paper as the Wilhemly plate. Correspondingly, the free protein concentration in the titrations is determined by fluorescence measurements of the aqueous subphase ***(15,16)***. The example used herein is the adsorption of prothrombin to spread monolayers. Surface pressures (π) are measured with use of a Cahn 2000 electrobalance. For this, a 1.2 $cm^2 \times 10$ cm^2 section of Whatman no. 50 filter paper is employed as the Wilhemly plate ***(17)***. The approach developed to evaluate protein adsorption to spread PL monolayers involves the use of a 32-mL quartz trough filled with buffer solution. This circular trough with a surface area of 20 cm^2 has been constructed locally from commercial quartz. A capillary tube is fused to the quartz trough to allow for the injection of solutions into the subphase. The quartz trough is cleansed with a mild detergent solution and rinsed with copious amounts of ethanol and water between experiments. The trough is housed in a plexiglass chamber to control the atmosphere. One drop of lipid solution is carefully spread at the air–water interface and following stabilization of π, the protein was injected into subphase. With stirring, π and the subphase fluorescence intensity (I_f) are continuously and simultaneously monitored as the protein adsorbed to the monolayer.

Measurements of the subphase fluorescence intensity are made using an SLM-8000 spectrofluorometer with a 450-W xenon arc lamp. To monitor fluctuations in lamp energy, a portion of the excitation beam is reflected, using a quartz slide, into a reference PMT. Hamamatsu R928 photomultiplier tubes are used to monitor emission and reference signals. An air-driven stirrer, located external to the Plexiglas chamber, is used to stir the subphase at a constant rate of 90 rpm during the course of all measurements. The use of an air-driven stirrer is necessary because electric-powered stirrers produced heat which interfered with temperature control of the system. These measurements provide ΔC_b (λ_{ex} = 280 nm, λ_{em} = 335 nm).

The change in subphase fluorescence intensity due to adsorption varied between 5% and 15%. To determine ΔC_b, accurate values of the initial fluorescence intensity were required. With stirring of the subphase, the fluorescence intensity stabilized within 2–3 min of injection. Following this mixing period, the intensity decreased depending on the nature of the film and C_b. At $C_b < 0.05$ μM, the drop in intensity is sufficiently slow so that the initial fluorescence intensity

can be determined by extrapolation to zero time. Since the fluorescence intensity is observed to be proportional to C_b (at the low protein concentrations), and the background fluorescence is negligible, the protein concentration at the monolayer surface (C_s) can be determined from the percentage change in fluorescence intensity with aid of standard curves of fluorescence intensity vs bPt concentrations. Fluorescence and electrobalance readings are collected simultaneously at a rate of 0.1Hz. The output from the electrobalance is analog-filtered and subsequently digitized using a DAS-801 (Omega) data acquisition board controlled by standard computer software.

The chamber is purged with a flowing stream of compressed purified air (in-house laboratory air supply) that is bubbled through water immediately prior to entering the chamber. This atmosphere is sufficient to maintain a stable pressure reading of all monolayers tested. When unsaturated hydrocarbon monolayers were exposed to room air, the pressure reading increased rapidly with time. This was the result of ozone, which reacts with unsaturated hydrocarbon monolayers and that is not present in the in-house air supply.

3.3. Results and Discussion

3.3.1. Binding of PC Variants to Acidic Phospholipid Bilayers

The ability of Ca^{2+} to induce binding of PC and several of its variants to acidic PL vesicles has been examined by titrations with Ca^{2+} of the protein/PL interaction at constant protein concentrations (**Fig. 1**). It can be observed that the concentration of Ca^{2+} required for 50% of the maximal scattering (M_2/M_1) change ($C_{50,Ca}$–PL) obtained for the [F^4Q]r-PC–PL interaction (1.2 m*M*) is nearly the same as that for wtr-PC (1.7 m*M*), but this same value for the [L^8Q]r-PC–PL interaction (7.1 m*M*) was considerably higher. This shows a more defective overall interaction with PL of [L^8Q]r-PC than of [F^4Q]r-PC, with the characteristics of the former in this regard being more similar than the latter to that of [L^5Q]r-PC >18 m*M*) ***(4)***.

The data of **Fig. 1** also indicate the maximal M_2/M_1 values for [F^4Q]r-PC and [L^8Q]r-PC are smaller than for their wild-type counterpart, suggesting the Ca^{2+}–mutant protein complexes interacted more weakly with PL than did wtr-PC, or these variants bound differently to PL as compared to the wild-type protein. This is also the case for [L^5Q]r-PC–PL binding to these types of vesicles ***(4)***. To probe this point more rigorously, titrations of PL with the mutant proteins were conducted at a constant concentration of Ca^{2+}. At a concentration of 2 m*M* Ca^{2+} (**Fig. 1**), the value of the concentration of PC required for a 50% of maximum increase in the light scattering ($C_{50,PC}$–PL) for [L^8Q]r-PC–PL binding is approx 15-fold higher than that same parameter

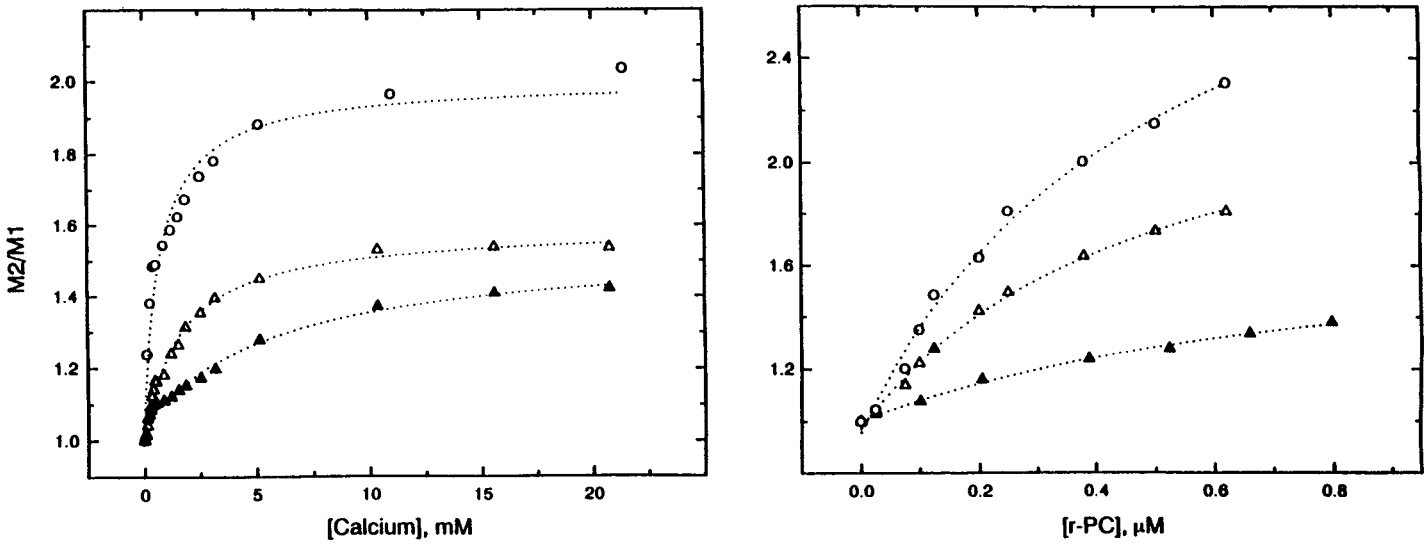

Fig. 1. **(Left)** The effect of Ca^{2+} on the binding of wtr-PC to acidic PL (60%:40% w/w ePhC/bPhS). The molecular weights of the protein–PL complexes were determined by 90° relative light scattering. The concentration of Ca^{2+} required for a 50% increase in the M_2/M_1 value ($C_{50,Ca}$–PL) was calculated by nonlinear least-squares minimization of the data, allowing both $C_{50,Ca}$–PL and the maximum attainable M_2/M_1 to float during the iterations. Solutions of Ca^{2+} were titrated into a protein (1 μ*M*)/PL (6 μg/mL in phosphate)–vesicle suspension. The buffer for these experiments was 20 m*M* Tris-Cl–100 m*M* NaCl, pH 7.4, 20°C. Excitation and emission wavelengths of 320 nm and slit widths of 4 nm were used. (○) PC; (△), [F^4Q]r-PC; (▲), [L^8Q]r-PC. **(Right)** Measurement of the binding of r-PC to acidic PL (60%:40% w/w chicken ePhC/bPhS) in the presence of Ca^{2+}. The dependence on protein concentrations of the interaction of r-PC mutants with PL (6 μg/mL) in the presence of 2 m*M* $CaCl_2$. The molecular weights of the protein–PL complexes were determined by 90° light scattering after subtraction of the scattering of the nonbound protein. The concentration of PC required for a 50% increase in M_2/M_1 ($C_{50,PC}$–PL) was calculated by nonlinear least-squares minimization of the data allowing both $C_{50,PC}$–PL and the maximum attainable M_2/M_1 to float during the iterations. The buffer for these experiments was 20 m*M* Tris-Cl–100 m*M* NaCl–2 m*M* $CaCl_2$, pH 7.4, 20° C. (○) r-PC; (△), [F^4Q]r-PC; (▲), [L^8Q]r-PC. These illustrations were taken from **ref. *5***.

for the same binding to wtr-PC (0.4 μ*M*), whereas that for [F^4Q]r-PC binding (0.5 μ*M*) is nearly the same as that for the wtr-PC–PL interaction. This indicates defective binding of [L^8Q]r-PC to PL under these conditions of Ca^{2+}.

3.3.2. Binding of Vitamin K-Dependent Coagulation Proteins to Phospholipid Monolayers

Adsorption isotherms and K_d values of bPt to PhS-containing monolayers were determined from measurements of Δπ against C ***(15)***. A representative plot of these data is provided in **Fig. 2**. In **Fig. 2A**, a rapid increase in π is observed immediately following the injection of protein into the subphase. This is more obvious at higher C_b. A slower increase in π is also observed due to nonspecific protein–monolayer interactions ***(15)***. The fast rise in π is the result of Ca^{2+}-specific adsorption. As expected, the equilibration time for Ca^{2+}-specific adsorption is shorter at higher C_b. Plots of Δπ vs C_b are illustrated in **Fig. 2B**. Here, the values of Δπ are those from the rapid increase in π. The slow Δπ is ignored. The Langmuir model was applied to assess values of K_d from the data in **Fig. 2B**. The corresponding double-reciprocal plots of these data are illustrated in **Fig. 2C**, from which K_d values could be obtained.

The measurement of Δπ resulting from protein adsorption to monolayers can also provide information not attainable by the use of bilayer systems as model membranes. For example, combined measurements of Δπ and the corresponding increase in surface protein concentration have provided direct information regarding protein–membrane contact ***(16)***. We have discovered that five Gla proteins with largely different binding affinities for model membranes exhibit similar values of $d\Gamma/d\pi$ where $d\Gamma$ and $d\pi$ are defined as the change in surface protein excess concentration and surface pressure, respectively, due to Ca^{2+}-specific adsorption to PhS monolayers ***(16)***. Therefore, the Gla-containing proteins examined were similar in the way they perturbed the surface pressure. This implies a common mode of Gla protein attachment to negatively charged membranes, a result heretofore not realizable using bilayer systems.

3.4. Conclusions

Methods are described herein that allow quantitative assessment of the nature of the binding of proteins involved in blood coagulation to PL vesicles or to spread monolayers. Simple extrapolations of these methods will allow similar examination of the binding of other proteins to PL. Employing the monolayer system described allows examination of a variety of PL systems which may not form appropriate bilayers, but additional specialized equipment is required. Such equipment is described in the original references ***(15,16)*** and is not difficult to manufacture.

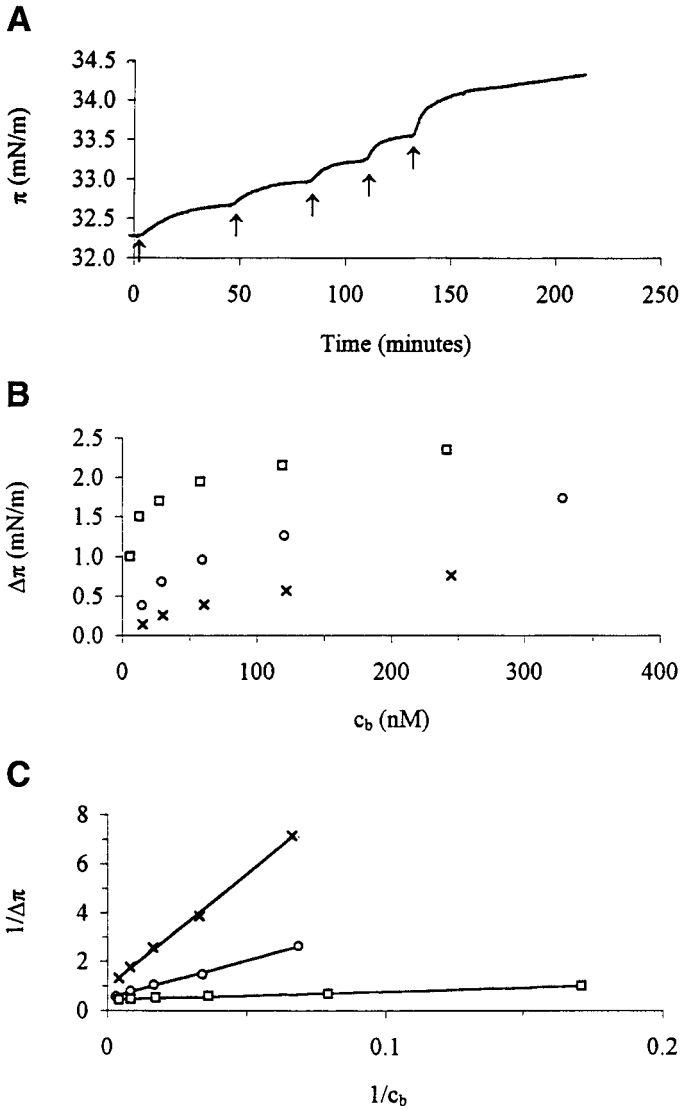

Fig. 2. Dependence on initial surface pressure (π_i) and PhS content of the adsorption of bovine prothrombin to POPhC/POPhS liquid expanded (LE) monolayers at 25°C. **(A)** Representative plot of the change in monolayer surface pressure ($\Delta\pi$) from successive additions (↓, injection points) of prothrombin in the aqueous subphase of a 2:1 (mol/mol) POPC/POPS monolayer. **(B)** Adsorption isotherms of the binding (C_b = prothrombin concentration). **(C)** Double-reciprocal plots of the adsorption isotherms. (○), 1:2 (mol/mol) POPhC/POPhS film at π_i = 37 mN/mol; (○) 2:1 (mol/mol) POPhC/POPhS film at 32 mN/m; (×) 2:1 (mol/mol) POPhC/POPhS film at 38 mN/m. The buffer was 10 m*M* borate/100 m*M* NaCl/10 m*M* $CaCl_2$, pH 8.0. These illustrations were taken from **ref. *15***.

References

1. Mann, K. G., Neshiem, M. E., Church, W. R., Haley, P., and Krishnaswamy, S. (1990) Surface-dependent reactions of the vitamin K-dependent enzyme complexes. *Blood* **76,** 1–16.
2. Atkins, J. S. and Ganz, P. R. (1992) The association of human coagulation factor VIII, factor IXa and factor X with phospholipid vesicles involves both electrostatic and hydrophobic interactions. *Mol. Cell. Biochem.* **112,** 61–71.
3. Lecompte, M. F. and Dode, C. (1992) Embedding of prethrombin domains of human prothrombin into phospholipid membranes. *Bioelectrochem. Bioenerg.* **29,** 149–157.
4. Zhang, L. and Castellino, F. J. (1994) The binding energy of human coagulation protein C to acidic phospholipid vesicles contains a major contribution from leucine-5 in the gamma-carboxyglutamic acid domain. *J. Biol. Chem.* **269,** 3590–3595.
5. Christiansen, W. T., Jalbert, L. R., Robertson, R. M., Jhingan, A., Prorok, M., and Castellino, F. J. (1995) Hydrophobic amino acid residues of human anticoagulation protein C that contribute to its functional binding to phospholipid vesicles. *Biochemistry* **34,** 10376–10382.
6. Jalbert, L. R., Chan, J. C. Y., Christiansen, W. T., and Castellino, F. J. (1996) The hydrophobic nature of residue-5 of human protein C is a major determinant of its functional interactions with acidic phospholipid vesicles. *Biochemistry* **35,** 7093–7099.
7. Mayer, L. D., Nelsestuen, G. L., and Brockman, H. L. (1983) Prothrombin association with phospholipid monolayers. *Biochemistry* **22,** 316–321.
8. Israelachvili, J. N., Mitchell, D. J., and Ninham, B. W. (1977) Theory of self-assembly of lipid bilayers and vesicles. *Biochim. Biophys. Acta* **470,** 185–200.
9. Jahnig, F. (1996) What is the surface tension of a lipid bilayer membrane. *Biophys. J.* **71,** 1348–1349.
10. Zhang, L. and Castellino, F. J. (1990) A γ-carboxyglutamic acid variant (γ^6D, γ^7D) of human activated protein C displays greatly reduced activity as an anticoagulant. *Biochemistry* **29,** 10828–10834.
11. Lowry, D. H. and Lopez, J. A. (1946) The determination of inorganic phosphate in the presence of labile phosphate esters. *J. Biol. Chem.* **162,** 421–428.
12. Nelsestuen, G. L. and Lim, T. K. (1977) Equilibria involved in prothrombin- and blood clotting factor X-membrane binding. *Biochemistry* **16,** 4164–4171.
13. Nelsestuen, G. L. and Broderius M. (1977) Interaction of prothrombin and blood-clotting factor X with membranes of varying composition. *Biochemistry* **16,** 4172–4177.
14. Lim, T. K., Bloomfield, V. A., and Nelsestuen, G. L. (1977) Structure of the prothrombin- and blood clotting factor X-membrane complexes. *Biochemistry* **16,** 4177–4181.
15. Ellison, E. H. and Castellino, F. J. (1997) Adsorption of bovine prothrombin to spread phospholipid monolayers. *Biophys. J.* **72,** 2605–2615.

16. Ellison, E. H. and Castellino, F. J. (1998) Adsorption of vitamin k-dependent blood coagulation proteins to spread phospholipid monolayers as determined from combined measurements of the surface pressure and surface protein concentration. *Biochemistry* **37,** 7997–8003.
17. Gaines, G. L. (1977) On the use of filter paper Wilhelmy plates with insoluble monolayers. *J. Colloid Sur.* **62,** 191–192.